# Power system state estimation using an on-line time domain electro-mechanical transient simulator

Bennett, A. C.

*Award date:*
2000

*Awarding institution:*
University of Bath


# POWER SYSTEM STATE ESTIMATION USING AN ON-LINE TIME DOMAIN ELECTRO-MECHANICAL TRANSIENT SIMULATOR

Submitted by
A. C. Bennett, BEng(Hons),AMIEE,MIEEE
for the degree of
Doctor of Philosophy
of the University of Bath
1999



Andrew Bennett

Bath, November 30th, 1999





ProQuest LLC
789 East Eisenhower Parkway
P.O. Box 1346
Ann Arbor, MI 48106-1346

# Summary

Data from an Electrical Power System is transmitted via a Supervisory Control and Data Acquisition (SCADA) network to be stored at the electrical utility's Control Centre in an Energy Management System (EMS) database. The data is used directly by control engineers or transformed into more useful information by the EMS Real Time Network Analysis (RTNA) functions.

The raw power system data cannot be used directly in RTNA functions because it could contain errors and inconsistencies which would cause the RTNA software to fail. State Estimation is the process which transforms the SCADA data set into an error minimised consistent data set which may then be used as the starting point for RTNA functions.

This thesis presents work which harnesses the capabilities of a time domain electro-mechanical transient simulator and applies these capabilities to form a new type of State Estimation. This approach is termed Dynamic On-Line State Estimation, (DOLSE). It incorporates a state synchronised time domain model state estimator, a time domain topology determinator and a time domain power system stiffness calculation engine. These features combine to provide accurate system information using a different methodology to any which has previously been implemented.

The author presents analysis of conventional Static State Estimation (SSE) giving practical results obtained. Full details of the need for the various components of DOLSE in addition to the overall DOLSE methodology are presented. Results are presented showing the advantages of this new approach using a full model of the grid system of England and Wales.

Keywords

*State Estimation, Time Domain Simulation, Supervisory Control And Data Acquisition, Energy Management Systems, Real Time Network Analysis*

# Dynamic On-Line State Estimation

*Electric power industry deregulation has transformed state estimation from an important application into a critical one.*

Brian Stott, 1999
PCA Corporation
Mesa,Arizona,USA

# Acknowledgements

Thank you to my supervisor Dr R.W. Dunn, for his patience, help and gentle encouragement over the past three years.

Thanks are also due to Mr A.R. Daniels, for his good humour, friendly banter and ever frank advice.

Thank you Mr T.E. Harrison for nurturing my initial interest in Electrical Power Systems.

I would also like to thank my colleagues and friends, Dr K.W. Chan, Dr K. Bell, Dr J. Grzejewski, Dr J.E. Hodgson, Dr B.A. Nicholson, Mr D.P. Brook, Mr G.H. Benson, and Mr J.D. Pilgrim, for providing a lively and intellectually stimulating environment in which to work.

I would like to gratefully acknowledge the continued technical and financial support of the National Grid Company. Thanks go to my industrial supervisor, Dr M.E. Bradley, for reassurance, and help beyond the call of duty. Also thank you to those who have provided technical advice about typical State Estimators and Energy Management Systems - Mr Ron Brady and Mrs Bridget Kanner.

Thanks to Mr V. Gott and Mr B. Ross for software and hardware support.

Thanks to Reginald, Samuel and to my Mum, for all her support over what seems like many years. Thanks J.C.

This report was prepared using the LaTeX type-setting package.

# Contents


**1 Introduction** 1

1.1 Motivation . . . . . 4

1.2 Thesis Overview . . . . . 8

1.3 Contributions from this research . . . . . 11

**2 Power System Operation and Data Processing** 12

2.1 Supervisory Control And Data Acquisition . . . . . 13

2.1.1 The Need for Information and Control . . . . . 15

2.1.2 Data Errors within SCADA system . . . . . 16

2.1.3 SCADA systems in Practice . . . . . 18

2.1.4 Quasi-SCADA Emulation . . . . . 20

2.2 Energy Management Systems . . . . . 21

2.2.1 Functions of the EMS . . . . . 21

2.2.2 Real Time Network Analysis . . . . . 21

2.2.3 Conventional RTNA facilities . . . . . 22

2.2.4 Extended RTNA facilities . . . . . 23

2.3 Proposed Enhancement to EMS . . . . . 25

2.3.1 Development of Data Availability . . . . . 25

2.3.2 Development of RTNA capability . . . . . 26

2.4 Summary . . . . . 27

**3 Review of State Estimation** 28

3.0.1 Concept of State . . . . . 28

3.1 Conventional State Estimation Models . . . . . 29

3.1.1 Direct Current Analysis . . . . . 30

3.1.2 Alternating Current Analysis . . . . . 31

3.2 Static State Estimation . . . . . 32
3.2.1 Normal Equations . . . . . 34
3.2.2 Other Approaches . . . . . 35
3.3 Dynamic State Estimation . . . . . 36
3.3.1 Tracking Estimators . . . . . 37
3.3.2 Dynamic Estimators . . . . . 37
3.3.3 Practical Experience . . . . . 39
3.3.4 Implementation . . . . . 40
3.4 Error Visualisation . . . . . 42
3.4.1 Results . . . . . 43
3.4.2 Discussion . . . . . 47
3.5 Summary . . . . . 48
3.5.1 Similarities and Differences . . . . . 49

**4 Review of Power System Simulation** **50**
4.1 Algorithms and conventional Applications . . . . . 51
4.1.1 Electro-mechanical Transient Stability Simulation . . . . 53
4.2 Detail of Component Models . . . . . 54
4.2.1 Network Elements . . . . . 55
4.2.2 Synchronous Machine Model . . . . . 55
4.2.3 Machine Saturation . . . . . 55
4.2.4 Control System Models . . . . . 56
4.2.5 Solution Method . . . . . 56
4.3 Requirements for DOLSE and Enhancements Implemented . . . 57
4.3.1 Controller Model Synchronisation . . . . . 58
4.3.2 Extended Convergence Information . . . . . 58
4.4 Summary . . . . . 59

**5 Topology Determination** **61**
5.0.1 Concept of Topology . . . . . 61
5.1 Present Approaches . . . . . 62
5.1.1 Artificial Intelligence Approaches . . . . . 63

5.2 Dynamic Topology Determination . . . . . 64
5.2.1 Time Domain Simulation Approach and Benefits . . . . 64
5.2.2 Details of Implementation . . . . . 65
5.3 Topology Determination Results . . . . . 72
5.4 Summary . . . . . 74

**6 Power System Stiffness** **75**
6.0.1 Concept of Stiffness . . . . . 75
6.1 Real Power Relationship ($\Delta P/\Delta f$) . . . . . 78
6.1.1 Power System Transitory Real Stiffness . . . . . 79
6.1.2 Real Stiffness in event of System Split . . . . . 81
6.2 Reactive Power Relationship ($\Delta Q/\Delta V$) . . . . . 81
6.2.1 Power System Transient Reactive Stiffness . . . . . 84
6.3 Software to Calculate Real and Reactive Stiffness . . . . . 85
6.3.1 Details of Implementation . . . . . 86
6.3.2 Results . . . . . 86
6.4 Stiffness Calculations within DOLSE . . . . . 87
6.4.1 Interpretation . . . . . 87
6.4.2 Limitations . . . . . 88
6.5 Summary . . . . . 89

**7 Total Dynamic On-Line State Estimation Implementation** **90**
7.1 Overview . . . . . 90
7.2 Hardware . . . . . 91
7.3 Software Techniques . . . . . 93
7.3.1 Network Sockets . . . . . 93
7.3.2 POSIX Threads . . . . . 93
7.4 Methods Proposed . . . . . 94
7.4.1 Database . . . . . 97
7.5 Software Implementation . . . . . 98
7.6 Summary . . . . . 103

**8 Dynamic On-Line State Estimation Results** **104**

8.1 Dynamic On-Line State Estimation Test Bed . . . . . 104

8.2 Results from Dynamic On-Line State Estimator . . . . . 106

8.2.1 Line Outage and Delayed Auto Re-closure . . . . . 107

8.3 Discussion of Results . . . . . 117

**9 Conclusions** **118**

**10 Suggestions for Further Work** **122**

10.1 Continuation of System Stiffness Analysis . . . . . 123

10.2 Oscillatory Mode Identification . . . . . 123

10.3 Operation in Event of System Split . . . . . 124

10.4 Global Positioning System . . . . . 124

10.5 Small Substation Synchronisation . . . . . 125

10.6 Parameter Estimation . . . . . 126

10.7 Comprehensive Validation . . . . . 127

10.8 Voltage Collapse Prediction . . . . . 128

10.9 Deployed Models . . . . . 128

10.10 Limitations . . . . . 129

10.11 Summary . . . . . 130

**A Schematic Diagram of the Electrical Power System of England and Wales** **132**

**B Dynamic Security Assessment Ranking for Test System** **134**

**C Topology Determination Data Output Example** **146**

C.1 Contingency File . . . . . 146

C.2 Information Request . . . . . 147

C.3 Completed Information Request . . . . . 148

C.4 Output Information . . . . . 148

C.5 Output Information Analysed . . . . . 151

**D Power System Stiffness Characteristic Output Data** **154**

**E DOLSE State Vector Output Example** **163**

**F Global Positioning System** **183**

F.1 Background . . . . . 183

F.1.1 Tolerances . . . . . 183

F.1.2 Implementation in Power Systems . . . . . 185

F.2 A Planning Tool to Aid Initial Placement of GPS Facilities . . . . 186

F.3 Modes of DOLSE operation with GPS . . . . . 186

**G Published Work** **187**

**References** **198**

# List of Figures


1.1 Horizontally partitioned electricity supply industry . . . . . 2

2.1 Degree of freedom available to control engineers . . . . . 13
2.2 Diagram of RTU and communications . . . . . 14
2.3 Possible SCADA RTU configurations . . . . . 17
2.4 A diagrammatic representation of typical RTNA processes . . . 23

3.1 Direct current model of line . . . . . 30
3.2 Alternating current model of line . . . . . 31
3.3 Static state estimation . . . . . 33
3.4 Dynamic state estimation . . . . . 38
3.5 Error visualisation graph . . . . . 43
3.6 State estimated versus real time MW loads . . . . . 45
3.7 State estimated versus real time MVAr loads . . . . . 46

4.1 Power system dynamic phenomena time frames . . . . . 51
4.2 A diagrammatic representation of PowSim solution method . . 57

5.1 Occurrence of power system islands during topology determination . . . . . 66
5.2 Diamond envelope around busbar voltage oscillation . . . . . 69
5.3 Box envelope around power flow oscillation . . . . . 70

6.1 Governor speed/load characteristic exhibiting droop . . . . . 77
6.2 Change in frequency for a change in real power post-transient . 78
6.3 Peak of change in frequency for a change in real power . . . . . 79
6.4 System frequency following loss of load at SIZE81 . . . . . 80
6.5 Mean system voltage following loss of load at SIZE81 . . . . . 82

6.6 Change in mean system voltage for a change in reactive power post-transient . . . . . 83
6.7 Peak change in mean system voltage for a change in reactive power . . . . . 85

7.1 Diagram of Dynamic On-Line State Estimation implementation 91
7.2 Diagram of state synchronised power system simulator implementation . . . . . 98
7.3 Diagram of topology determinator implementation . . . . . 100
7.4 Diagram of power system stiffness calculation engine implementation . . . . . 101

8.1 Actual system/DOLSE voltage magnitude error distribution, frequency versus per unit error . . . . . 107
8.2 Metered data/DOLSE voltage magnitude error distribution, frequency versus per unit error . . . . . 108
8.3 Voltage magnitude error distribution, frequency versus per unit error . . . . . 108
8.4 Voltage magnitude and angle error distributions - pre LACK2-GRST2B:1:2 fault, frequency versus per unit error . . . . . 110
8.5 Voltage magnitude and angle error distributions - post fault no analogue update, frequency versus per unit error . . . . . 112
8.6 Voltage magnitude and angle error distributions - post fault after analogue update, frequency versus per unit error . . . . . 114
8.7 Voltage magnitude and angle error distributions - DAR no analogue update, frequency versus per unit error . . . . . 115
8.8 Voltage magnitude and angle error distributions - DAR after analogue update, frequency versus per unit error . . . . . 116

B.1 DSA output screen for worst contingency . . . . . 145

F.1 System-wide GPS sources of error . . . . . 184
F.2 Sine curve peak showing GPS resolution . . . . . 185

# List of Tables

2.1 Typical SCADA analogue transducer variances . . . . . 16
2.2 Typical SCADA analogue to digital conversion quanta resolutions 18
2.3 Typical cycle times for DC and AC processes . . . . . 22

7.1 Secondary variables and the information they yield . . . . . 102

8.1 On-line data sets and the operations which they represent . . . 109

# List of Abbreviations

| | |
|---|---|
| AC | Alternating Current |
| DC | Direct Current |
| ANN | Artificial Neural Network |
| AVR | Automatic Voltage Regulator |
| PSS | Power System Statibiliser |
| C | C programming language |
| DSA | Dynamic Security Assessor |
| EPSRC | Engineering and Physical Sciences Research Council |
| IEE | Institute of Electrical Engineers, UK |
| IEEE | Institute of Electrical and Electronics Engineers, USA |
| | |
| V | Volts |
| kV | kilo-Volts |
| W | Watts |
| MW | Mega-Watts |
| GW | Giga-Watts |
| VAr | Volt-Ampere reactive |
| MVAr | Mega-Volt-Ampere reactive |
| | |
| PQ | Load-flow node with constant real power and constant reactive power, normally used to represent loads |
| PV | Load-flow node with constant real power and constant voltage, normally used to represent a generator or reactive compensator |

| | |
|---|---|
| PVM | Parallel Virtual Machine |
| SVC | Static VAr Compensator |
| QB | Quadrature Booster |
| NGC | National Grid Company plc., UK |
| REC | Regional Electricity Company |
| LV | Low Voltage, (up to 66kV) |
| HV | High Voltage, (above 66kV) |
| VT | Voltage Transformer |
| CVT | Capacitor Voltage Transformer |
| WVT | Wound Voltage Transformer |
| CT | Current Transformer |
| RTU | Remote Terminal Unit |
| GSP | Grid Supply Point |
| FACTS | Flexible Alternating Current Transmission Systems |
| SCADA | Supervisory Control And Data Aquisition |
| EMS | Energy Management System |
| RTNA | Real-Time Network Analysis |
| SE | State Estimation |
| SSE | Static State Estimation |
| TSE | Tracking State Estimation |
| DSE | Dynamic State Estimation |
| DOLSE | Dynamic On-Line State Estimation |

# List of Symbols

| | |
|---|---|
| $z$ | vector of measurements |
| $x$ | vector of states |
| $H$ | state to measurement linear transform |
| $h(x)$ | state to measurement non-linear function |
| $e$ | vector of errors |
| $r$ | vector of residuals |
| | |
| $f$ | Frequency, (Hertz, Hz) |
| $\omega$ | Angular Frequency, (radians per second, rad/s) |
| | |
| $j$ | complex imaginary operator, $\sqrt{-1}$ |
| | |
| $V$ | Voltage, (kilo-Volt, kV) |
| $I$ | Current, (kilo-Ampere, kA) |
| $\phi$ | Phase angle, (rad) |
| $\cos\phi$ | Power factor |
| | |
| $R$ | Resistance, (Ohm, $\Omega$) |
| $L$ | Inductance, (Henry, H) |
| $C$ | Capacitance, (Farad, F) |
| | |
| $X$ | Reactance, (Ohm, $\Omega$) |
| $Z$ | Impedance $= (R + jX)$, (Ohm, $\Omega$) |

$G$ Conductance, (Siemen, $\Omega^{-1}$)

$B$ Susceptance, (Siemen, $\Omega^{-1}$)

$Y$ Admittance $= (G + jB) = 1/Z$, (Siemen, $\Omega^{-1}$)

$P$ Real Power, (Mega-Watt, MW)

$Q$ Reactive Power, (Mega-Volt-Ampere reactive, MVAr)

$S$ Apparent Power, (Mega-Volt-Ampere, MVA)

Chapter One

# Introduction

Technological advance breeds technological advance. Energy realised from combustion of fuel, or by harnessing renewable sources, is converted into convenient *electricity*. It is used in many different ways in our lives today - without an understanding of electricity or without its proper application, our quality of life would be very different.

Electricity is the life blood of industrial processes and modern technology. On an atomic level, energy is used to move electrons from one atom to another. On a larger scale this process may be harnessed to provide heat and light which is clean at the point of use. It is electricity which has made developments such as the computer feasible, the modelling capabilities of which in turn aid our understanding of how the world works. For example, until recently it was not possible to model digitally the electrical power system in real time without the loss of a great deal of accuracy. However this is now possible - helping us to evaluate better how the system behaves.

It was Thomas Edison who first instigated the mass generation of electricity in 1882. The first generating station in the UK produced *Direct Current* (DC) at Holborn Viaduct. The first *Alternating Current* (AC) plant was installed later at Deptford. Since then the electrical power system in the UK has evolved to increase reliability and reduce costs. It has been transformed from de-centralised local generating plant, through an integrated nationalised generation and transmission utility, to its present state as a horizontally

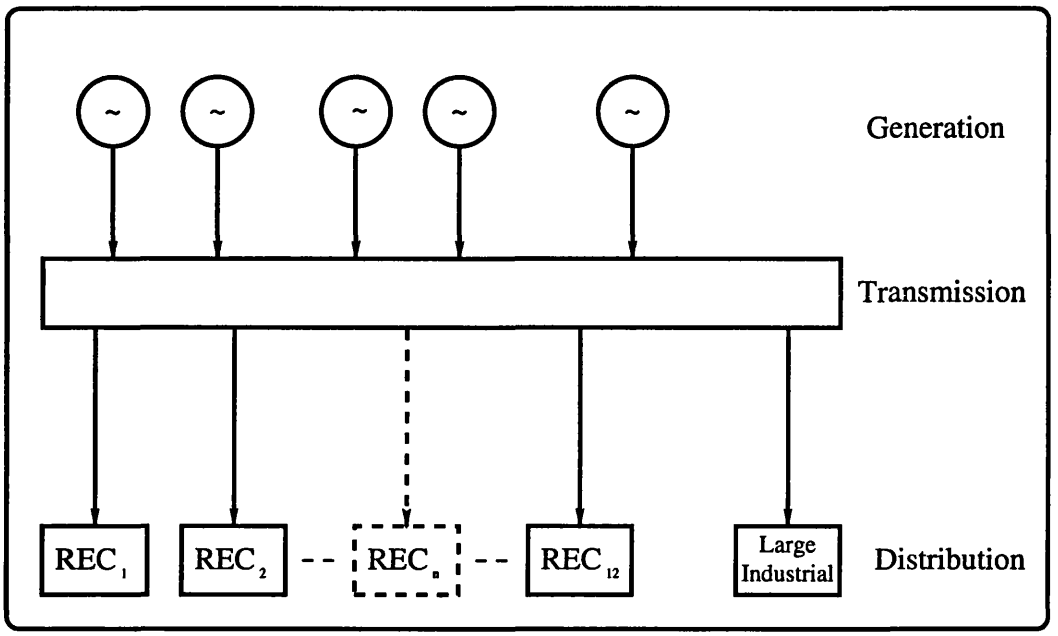


Figure 1.1: Horizontally partitioned electricity supply industry

partitioned re-privatised set of electrical utilities (see figure 1.1).

Since the inception of the use of electricity it has been measured. Originally, for scientific research, measurement was important in order to quantify the phenomena which were observed. In today's interconnected electrical power systems metering is necessary so that costs may be apportioned between users and so the system may be adequately controlled. Reliable system data is crucial to power system operation. In order to minimise system losses and utilise the cheapest sources of electrical energy, thus reducing the cost to the end user, it is necessary to operate the network as close to its limits as is possible without compromising the secure operation of the system.

These limits are imposed by the physical nature of the network. Switchgear must not be operated so as to impair its ability to break current, lines must not be subjected to carrying more electrical power than their thermal capacity. All components must be run at a voltage level commensurate with their insulation capability. Generators must be operated so that they are not likely to move to an unstable, oscillatory or transient mode of operation. Many constraints need to be met to ensure safe, secure, economic operation. These constraints must

be imposed on a real time, second by second basis.

A model of a system has a structure, parameters and variables. Firstly a suitable structure for the model must be chosen. Parameters are then selected so that the model accurately represents the system to be studied. Variables define the point of operation of this model. Real time metered values represent the variables of the model, but variables of any model are related by the model structure and its parameters.

In an over determined system of equations there exists a set of variables which contains all variables within the model. Due to the interaction of the variables via the model's equations there are one or more subsets of variables which contain the minimum information necessary to enable all other variables within the model to be uniquely calculated. Any such subset of variables is a set of *states*. This set of states is termed the *state vector*, and uniquely identifies the actual operating point of the system.

In electrical power systems more variables are metered than are necessary to calculate the system states. If all the metered values are available the system is completely observable and forms an over determined problem. Conventionally, an electrical power system state vector contains all busbar voltage magnitudes and busbar voltage angles.

State Estimation is necessary as the metering on the power network is subject to error. Errors in the data need to be found and minimised. The State Estimation process of the power utility's *Energy Management System* (EMS) seeks to do this.

Data from an electrical power system is transmitted via a Supervisory Control And Data Acquisition (SCADA) network to be stored at the control centre. The raw telemetered data is held in the EMS database, and is passed to the State Estimation function on a regular basis. Given this data and a model of the power system network, the State Estimator performs an error minimisation on the data, to obtain the best estimate of the actual state vector of the power

system.

System data is used by the control engineers to enable them to make informed decisions on how to operate the power system within the physical limitations of the system. Voltage and thermal limits are monitored by the Energy Management System and dynamic stability limits are ascertained by programs such as a Dynamic Security Assessor and other *Real Time Network Analysis,* (RTNA) processes.

## 1.1 Motivation

The first published journal papers regarding Power System Static State Estimation [1, 2, 3, 4, 5] will be thirty years old in January 2000. Despite the large number of published papers during that period (for a summary of papers from 1968 to 1989 see [6]), the field continues to remain open to new and innovative techniques. An example of disagreement over differing approaches is typified by the interesting debate which took place in the 1970s as to the best methodologies of Power System State Estimation and where these techniques had been conceived. The camps of Massachusetts Institute of Technology, and Systems Control Incorporated (Palo Alto, California) formerly Wolf Management Services, were firmly pitted against one another. SCI was the first to conceive the idea in internal documents ([7] versus [8]), whereas MIT was the first to publish them in IEEE transactions.

Due to the complexity of a problem involving metered variables with data errors, quantisation error, drop out, un-observability and time-skew of data there are an abundance of papers presenting many different techniques designed to reduce the computational overhead and the time needed to determine the vector of system states. Over the years both conventional algorithmic approaches and artificial intelligence techniques have been suggested. These include the use of genetic algorithms for network partitioning [9], expert systems for topology determination [10], and even artificial neural networks for state estimation in its entirety [11].

Conventional State Estimators perform their function in a batch mode of operation. Due to limited computational resource, generally the EMS has a time frame within which complete analysis of one point of system operation is performed. The frequency of this cycle for a given EMS system is determined by the computational power available, but is also limited by the batch processing approach. State Estimators are run at the beginning of the energy management system cycle. This can mean they are executed once every 5 minutes on state-of-the-art systems or once every 15 minutes on older systems.

Load-flow analysis involves calculation of the real and reactive electrical power flows on the electrical power system when the system is in steady-state. In order to calculate the state of the system more quickly it is insufficient to take only the load-flow analysis into account. The dynamic response of the system also needs to be known so SCADA data can be correctly interpreted as soon as it is available. Power systems, as with any system, may be modelled in varying levels of detail. Models are crucial to aid understanding and once formed they may be refined in structure and parameters to become more like the system they represent.

As State Estimation techniques have been designed and used, they have invariably been tested on real systems, and on models of systems. The models incorporated into conventional static state estimation formulation are generally load-flow models. Conventional state estimators use a combination of load-flow ([12]) and probabilistic techniques. This represents only a small sub-section of power system models which are available. With the advent of fast time domain electro-mechanical power system simulators it has become possible to run electro-mechanical power system models at a time step of 10ms in real time or faster. This gives us the opportunity to use these models as the basis for state estimation. This is the approach termed *Dynamic On-Line State Estimation* or *DOLSE* for short, explored within this thesis.

Conventional State Estimation utilises basic models in order to achieve estimation of power system states. However, more detailed models from the area

of transient simulation are available which allow the time response of the system to be simulated. Using these more complex models should enable a more accurate analysis of the power system over time as opposed to only at one time instant. This thesis sets out to find ways to use the more detailed models available in order to achieve a better state estimation implementation.

The main advantage of the DOLSE methodology is the use of a time domain model executed at real time speed. This matches its variables to those of the real system using SCADA telemetered data. Its effective aim is to synchronise its states to those of the real system. These states are then available at any instant to processes within the EMS or to control engineers who need to refer to a corrected power system consistent model set.

To achieve an implementation which incorporates transient simulation models into the formation of a state estimator necessitates the development of other tools which are able to increase the speed of data processing. If more detailed models are used to form the models for state estimation these should also be incorporated into the other data processing tools.

An important part of achieving a reliable state estimate is the correct identification of the power network's topology. The correct model is needed before the parameters of the model and subsequently the states can be of any use. Simply using a matched power system simulator which has been aligned to the actual system via SCADA data without some means of topology determination would be pointless, so a topology determinator has been incorporated into this work.

Conventional State Estimators assume that the generation exactly matches the demand and therefore that the power system frequency is at its nominal value (in the UK this is 50 Hertz - in the USA 60 Hertz). Power system frequency information is a variable which is continually available at an Electricity Control Centre. Until the present time this information has been used by the control engineers as a convenient guide to the real power imbalance at any given time on the system and within *Automatic Generation Control* (AGC).

The time domain models available from the field of transient simulation have been used to calculate real and reactive stiffness characteristics in an off-line mode. The results from these off-line calculations are then used within the database which controls the state synchronised simulator in order to determine the real and reactive power imbalances. These are then applied to the state synchronised model.

As power system frequency relates to the real power balance of the power system, so busbar voltages are a good indication of the reactive power imbalances. This real and reactive stiffness has never previously been incorporated into a state estimation methodology. In the DOLSE approach the power system frequency information has been used in order to decrease the time from the raw data being available to the solution being computed. It is not possible to state synchronise the transient simulator to the power system without taking account of the fact that the frequency is seldom at its nominal value.

Although separate chapters deal with the various topics detailed above, it is important to remember that it is the combination of these methodologies which constitute Dynamic On-Line State Estimation. It is the combined aspects of a database encapsulated power system simulator with topology determination and stiffness calculations performed by a contingency analysis engine which are of prime importance. In order to quickly obtain the system states all of the techniques are necessary. These are tightly integrated within DOLSE because the electrical power system is a fast changing dynamic system and therefore needs to be modelled as such within the State Estimation formulation.

This work is an investigation into an alternative method. It uses transient simulation in place of load-flow to more quickly obtain the states of the system. The benefits of this approach are its speed and the opportunity afforded for a complete redesign of Real Time Network Analysis methodologies. In addition it offers the chance to deploy new techniques for closed loop power system control. These are discussed within the chapter of further work (chapter 10).

## 1.2 Thesis Overview

**Chapter 2** looks in detail at power system data processing and operation. The Supervisory Control And Data Acquisition (SCADA) system is examined from transducer to database. The data types, communications channels, and protocols are discussed. Of particular relevance to the work in this thesis are the qualification and quantification of errors in the SCADA data. As modern power system operation is characterised by the use of an Energy Management System (EMS), and the location of State Estimation lies with the EMS, the methodology and functionality of currently available EMS suites are presented. This analysis provides the background necessary to appreciate the novel aspects of this work. Finally the available packages for a conventional Real Time Network Analysis (RTNA) suite with several enhanced RTNA functions are catalogued, providing the background for a clear understanding of future RTNA capabilities using the work documented in this thesis.

**Chapter 3** reviews the nature of state, and conventional techniques for state estimation of an electrical power system. Methods previously developed are discussed chronologically, thus showing the development of state estimation over time. The techniques presented include static, tracking and dynamic methodologies. As it is important to see these techniques in a practical light as well as a theoretical one, careful attention has been paid to a discussion and presentation of the benefits, advantages, practicalities and problems of each method in their actual deployment. Experience gained and the results from a commercial state estimator installed on a live EMS suite are presented.

**Chapter 4** starts with an overview of power system simulation reviewing algorithms and conventional applications. The models used in this work are presented. The specific functionality which has been incorporated

into the simulator in order to give the state synchronised simulation capability is also shown.

**Chapter 5** places topology determination in context in the field of electrical power systems. The advantages and disadvantages of present conventional techniques, and techniques such as expert systems and neural networks, are discussed. The chapter continues to present the advances made by this work in the area of power system topology determination. This new method involving the time domain electro-mechanical transient simulator is detailed. It represents a significant improvement over conventional techniques by applying possible contingencies to a full time domain model of the system, enabling the envelope of transient oscillations to be found on a variable by variable basis. Results of the deployment of this approach are presented and discussed.

**Chapter 6** shows the extra data which may be obtained from simple processing of SCADA data if the real and reactive phenomena are assumed to be decoupled. Due to the strong relationship between the power system frequency and real power, and the voltage magnitudes and reactive power, these two relationships are discussed separately within this chapter. The motivation for this work and the investigation completed into these stiffness characteristics are presented. It was found that quicker utilisation of the power system data was possible by exploiting features observed in the sets of data collected. Results from this analysis are also presented and implementation of these techniques within DOLSE placed in context.

**Chapter 7** summarises the work completed for this thesis. The complete DOLSE framework incorporating the functions of the previous chapters is constructed for the reader. The design methodology adhered to and the techniques used are presented. The interconnections between the different elements of DOLSE are clearly shown.

**Chapter 8** presents the results obtained from the performance of DOLSE when it was attached to the SCADA test bed implemented for this project.

If connected to a real power system comparison could only be made between the SCADA data set and the data set produced using the estimated state vector in conjunction with the system model. However, when using the SCADA emulator the state vector of the underlying system emulator is available before the errors of the SCADA process are combined with it. It is this pure state vector which is used to calculate the error distribution of DOLSE's output. The strengths and weaknesses of the DOLSE implementation are discussed, and attention is drawn to how the DOLSE method could be best utilised.

**Chapter 9** concludes the research undertaken.

**Chapter 10** describes areas identified for further work. The possible implementations of truly parallelisable RTNA capabilities are presented, fully illuminating the impact that this could have on present conventional Transient and Dynamic Security Assessment and other RTNA functions.

## 1.3 Contributions from this research

In order for the submission for the degree of PhD. to be considered, it is realised that the work must be novel and indeed provide a significant new contribution to a field of study. This work meets that criteria in these specific ways:

- novel application of time domain power system simulation to determine network topology.
- account taken of the power system frequency data in State Estimation. This has only ever previously been used as a manual guide to the control engineers or in Automatic Generation Control.
- state synchronisation of a time domain simulator connected to incoming SCADA data, minimising errors, and allowing data errors to be monitored and corrected over time. Previously only batch processed state estimated data sets have been used as the initialisation point for RTNA.
- the speed with which a solution is achieved post transient using these novel techniques.
- development of a truly on-line, parallelisable real time network analysis suite which harnesses the power of DOLSE.

Chapter Two

# Power System Operation and Data Processing

This is the Power System Operation chapter. However what is different about *this* Power System Operation chapter, is its perspective - Data Processing.

A major feature of the operation of modern electrical power systems is the philosophy of co-ordinated planning and control. Power system protection equipment is still installed and maintained locally at point of use, but overall management is centralised. The power system is managed from a central location by teams of engineers, each with a remit for some functional aspect or chronological section of operation. Within the National Grid Company for example, investment planning investigates system operation 7 to 2 years ahead, outage planning studies 2 years to 1 year ahead, and operational planning focuses on a few weeks to 1 day ahead.

On a functional basis the generation connections, network outages, and supply point maintenance must be planned in order to ensure continuous operation of electrical supply for the majority of customers. Outages must occur at sufficiently regular intervals so that protection equipment may be serviced to ensure that when it is required its operation may be almost guaranteed. Longer outages are necessary if, for example, plant needs to be replaced. These must be carefully timetabled so as to ensure that any major refurbishment does not interfere with any other refurbishment schemes, nor does it leave the system insecure for any other possible fault outage. Ideally this is achieved with all

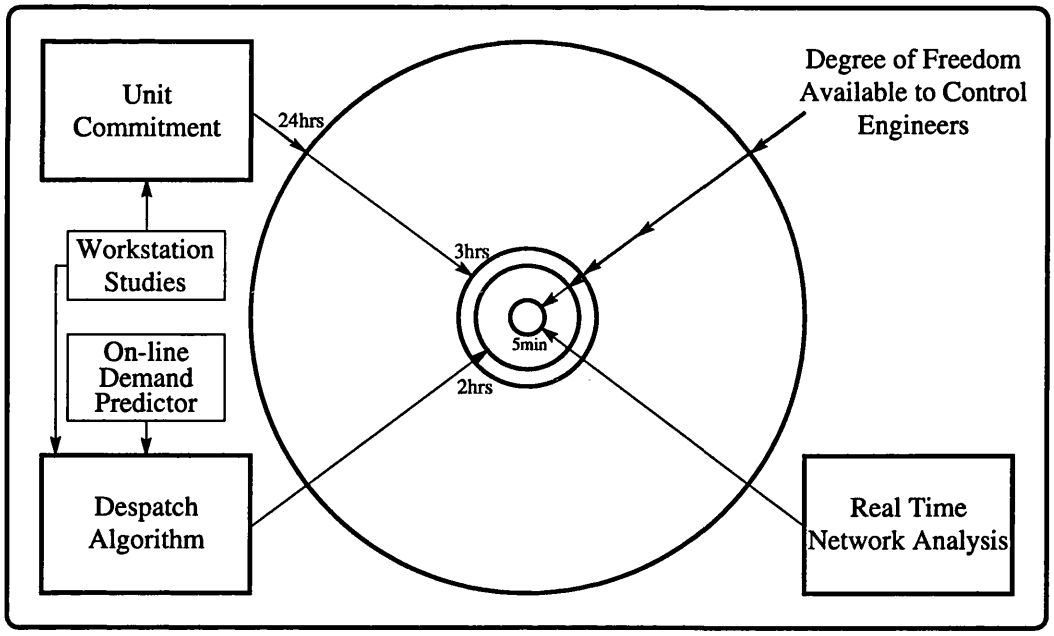


Figure 2.1: Degree of freedom available to control engineers

plant loaded in ascending order of cost - *merit order*. However, to secure the system it may be necessary to constrain plant on which should be off due to it being out of merit order.

With vast continental power systems, for example, a regional utility company has to co-ordinate its approach with other utilities with which it has inter-connections. For an islanded system the transmission utility may only have to satisfy its own requirements for outages. As may be seen planning, unit commitment and dispatch is a complex process. Once it has been completed plans laid out for the system's operation by the teams of planning engineers are then implemented by the system control engineers. The degree of freedom which remains at each stage of the scheduling and dispatch process may be seen in figure 2.1.

## 2.1 Supervisory Control And Data Acquisition

The control centre needs the ability to receive information from remote parts of the network, and the ability to effect remote changes. In order to do this

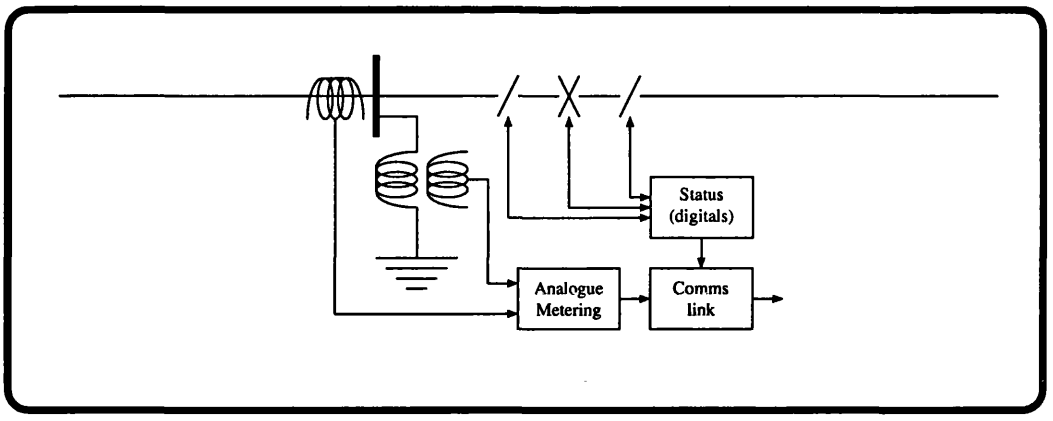


Figure 2.2: Diagram of RTU and communications

there is need for a system which allows the flow of all relevant information and control signals to the appropriate locations. Typically, circuit breakers, isolators, busbar voltages, current and power flows, transformer tap positions, *flexible alternating current transmission system* (FACTS) devices, and substation alarms must all be monitored and controlled.

The data collection points at substations are termed *Remote Terminal Units* (RTUs). This is a collective term for the transducers which convert the electrical quantities into measurements and the equipment which allows data to be transmitted along communications links.

In a power utility the above facilities are provided by a *supervisory control and data acquisition* (SCADA) system implemented using a communications network, a diagrammatic representation of which is shown in figure 2.2. This network contains channels using different media, such as telephone lines, high voltage (HV) transmission line carrier waves, optical fibre, radio and microwave links.

The SCADA network is used both for telecommand/telecontrol and for telemetry. Data at a substation is collected by the RTU and passed to the control centre. As state estimation involves processing power system data into a coherent and complete form, the remainder of section 2.1 will focus on the the collection of data via the SCADA system. In particular, the various errors

inherent in the telemetered data will be be discussed.

### 2.1.1 The Need for Information and Control

Measurement of system variables is made by various power system transducers. Voltage and current transformers provide input to metering systems. Voltage, current, and real and reactive power values are continuous and are known as *analogues*. Devices which register the status of plant installed on the power network such as switchgear return a discrete binary on or off value and are termed *digitals*.

Electrical power enters the network at generator busbars, and exits the network at locations called *grid supply points* (GSPs). Both of these two types of busbar are termed *injection busbars*. A generator bus and a GSP may be coincident. Power flows into and out of injection buses are measured by *tariff* metering. In a typical installation the specified accuracy of the tariff meters is maintained up to a specified power factor for billing purposes. This power factor is typically in the region of 0.86. Meters which measure the power flow on transmission circuits tend to be less accurate because they are not used for billing purposes and are therefore not subject to rigorous calibration. These line flow meters are calibrated on an *ad hoc* basis, perhaps when the power system plant is taken out for a routine outage.

With the maximum error percentage considered to be equal to three standard deviations ($3\sigma$) the typical analogue transducer variances are as found in table 2.1.

The status of circuit breakers and isolators on the power system are also monitored via the SCADA network. This enables the correct topology of the power network to be established. This is important information conventionally used to transform the switch status level data to a bus/branch model.

There are two methods of obtaining data of metered variables from the meters on the power system. These methods are:

| Measurement | | Error | Variance |
|---|---|---|---|
| Wound Voltage Transformers (WVT) | | +/- 0.1% | 0.0011 |
| Capacitive Voltage Transformers (CVT) | | +/- 2.0% | 0.4444 |
| Tariff Injections | Real Power | +/- 1.0% at 0.866 pf | 0.1111 |
| | Reactive Power | +/- 4.0% at 0.866 pf | 1.7778 |
| Circuit Flow | Real Power | +/- 3.0-5.0% | 1-2.7778 |
| | Reactive Power | +/- 5.0-8.0% | 2.7778-7.1111 |

Table 2.1: Typical SCADA analogue transducer variances

1. the snapshot scan
2. the sequential scan

They form a snapshot scan data set and a sequential scan data set respectively. In a snapshot data set all meters are read simultaneously. This implies some kind of co-ordination in the request of a data set, and system wide time synchronisation. With a snapshot scan the metered data set $z(t_i)$ consists of all measurements from the system at the time instant $t_i$. With a sequential scan the measurement data set is a set of measurements which are known to be made in the time interval $t_{i-1}$ to $t_i$, where this length of time, $t_i - t_{i-1}$ is the *scan rate*. No guarantee can be made as to the exact instant of any measurement reading, suffice to say that it is from the data scan period preceding the present time.

### 2.1.2 Data Errors within SCADA system

Generally the SCADA communication network is digital. Analogues are converted to digital signals by analogue to digital (A/D) converters. Readings may be inaccurate and noisy, with additional errors introduced by the quantisation in the A/D process. Switch positions are already inherently digital.

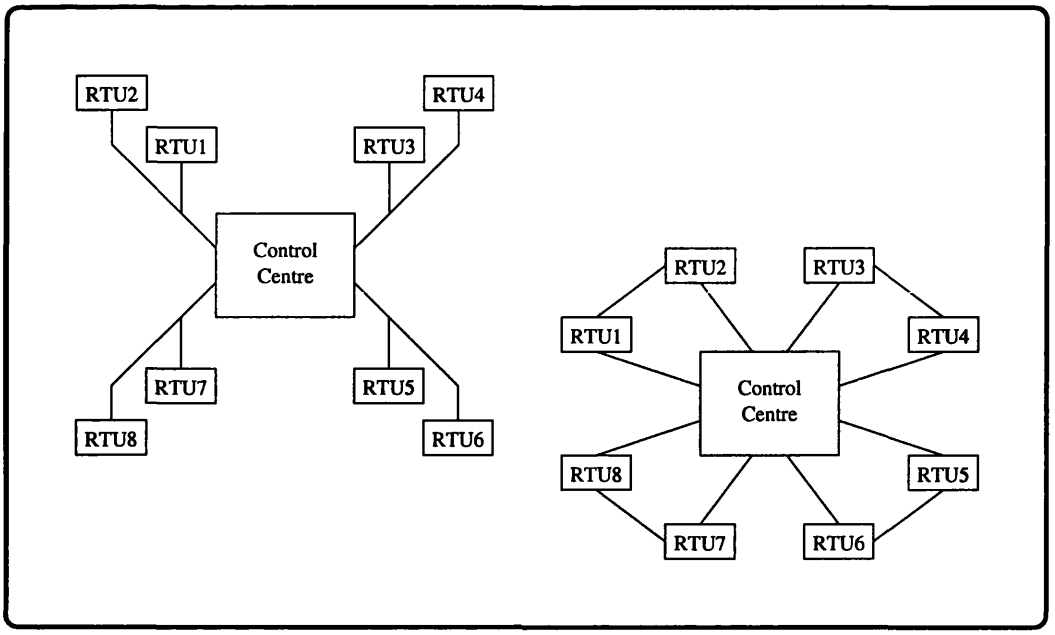


Figure 2.3: Possible SCADA RTU configurations

Older power flow metering, such as that found monitoring lower voltage HV circuit flows, typically has a resolution of seven data bits. If full scale deflection (FSD) were 2000 MW this would give a quanta resolution of 16 MW. Injection points and GSPs with more accurate tariff metering tend to have a higher resolution. This could typically be 10 bits.

Voltage measurements are typically 7 bit, with A/D converters upgraded to provide a resolution of 10 bits for *wound* voltage transformers. It is also usual to index voltage values to a range rather than sending absolute values on the communication path to the control centre. For example, in a 400kV system the range would tend to be 340 to 440kV. This would give a quanta resolution of 0.8kV in the case of 7 bit, and 0.1 kV in the case of 10 bit A/D systems.

Signals on the communication channel may also be subjected to noise and interference. The noise may be white, i.e. the amplitude of the interference being equal over the frequency spectrum, or more usually on a power system, the interference may be of the burst noise type - due to system switching transients, for example. Generally, however, due to coding and error detection built into the digital signal processing, corruption is detectable at the receiving

| Measurement | Range | No of Data Bits | Quanta Resolution |
|---|---|---|---|
| WVTs | 340-440kV | 10 | 0.1kV |
| CVTs | 340-440kV | 7 | 0.8kV |
| Tariff Injection | 2000MW | 10 | 2MW |
| Circuit Flow | 2000MW | 7 | 16MW |

Table 2.2: Typical SCADA analogue to digital conversion quanta resolutions

end of the communications channel. Values will be classified as correct, or incorrect - whereby a NULL value will be entered into the set of system data. Occasionally, corruption could occur to such an extent that, by chance, error checking could be defeated. Such corruption is unlikely, but provision needs to be made for its occurrence.

The accuracies of metering and communications channels vary throughout the world. This may be linked to the age of the system. For example, much of the operational metering equipment on the transmission system of England and Wales was originally installed during system construction in the 1960s. This metering is generally not as accurate as say that of the United States systems where most of the metering equipment was installed in the 1970s. Through mass production the cost of metering equipment decreased and the quality of equipment had increased substantially by that time. Metering on the England and Wales grid system is being updated on a rolling basis. More accurate metering is being installed, and existing metering recalibrated. High-accuracy tariff metering was installed at all commercial interfaces following privatisation.

### 2.1.3 SCADA systems in Practice

The final attributes of a SCADA system which need to be understood are the time skewing of data, and the marshalling of analogue and digital information.

The major area of error within the SCADA system is in the accuracy of the

data, and the lags which can occur due to the marshalling process. This is particularly severe in times of transient when there is a much greater amount of data to be communicated to the control centre.

Data is sent from transducers, via A/D converters along communication channels to the control centre. Typically all the data is not measured at the same instant in time, nor does it arrive at the control centre at the same time. The process of data gathering is cyclic, with typically a 10 second period over which a complete set of system data is received at the control centre.

Marshalling of the data may be thought of as the priority given to the data on its way from a meter to the control centre. Measurements are marshalled to the RTU, where in the case of the England and Wales system they are sent via a communications link to an area SCADA database. The main EMS computer reads the area databases typically every ten seconds. In the marshalling process digitals are counted as priority and the position of switches is sent immediately to the SCADA database.

It may be seen from the above discussion that there are four main forms of error on data from the SCADA system:

1. metering calibration errors
2. small random metering-communication errors
3. bad data due to transients and meter-communication failures
4. errors in network structure due to faulty switch-circuit breaker status information

Each has different causes and affects the data received at the control centre in different ways.

There is also the remote possibility that an RTU blackout could occur. This would mean that all information from an RTU was unavailable for a period of

time. As may be seen in figure 2.3, with an appropriately configured SCADA system the likelihood of this can be minimised.

### 2.1.4 Quasi-SCADA Emulation

For DOLSE to be effective, algorithms must be formulated to deal with errors in the SCADA data and the peculiarities of data collection via the SCADA network. A SCADA emulator test bed has been constructed and used for this research to test the DOLSE methodology developed. This emulation is designed to output data with the same magnitudes of error and peculiarities as have been described in the previous section.

To test the algorithms presented within this thesis a SCADA emulator has been utilised. This uses a power system simulator to output sets of noisy time skewed data, which are then used to test the Dynamic On-Line State Estimator. On the timescales of this project it would not have been practical to test DOLSE on live system data, but in any case the use of a simulator allows the state estimated results to be compared with the *true* system conditions.

Topology changes may be carried out within this quasi-SCADA emulator, and the DOLSE model can be selectively notified or not notified of these changes. This ensures that the DOLSE process can be verified.

For the purpose of finding weaknesses in the new technique of Dynamic On-Line State Estimation it has been important to construct this quasi-SCADA emulator as appropriately as possible. The error levels have been set to be of the typical values outlined at the start of this chapter. However, state estimators are only as good as their performance in difficult scenarios. For this reason the feature of being able to individually set some meters on the system to have severe or persistent errors has been necessary. The quasi-SCADA emulator is able to produce data in a variety of formats. It can produce a flat study file, a series of flat study files, time skewed data sets, pure and noisy data sets. Data may be saved to file, or may be sent over software sockets to other programs on the same computer or via software network sockets to programs

on other computers.

## 2.2 Energy Management Systems

The Energy Management System is the collective name given to the computer database, system monitoring and analysis performed at the power company's control centre. The aim of the system is to provide information from SCADA channels to the control engineers both in a raw and a processed form. The data is presented in both a raw and a processed form to enable any unreliability of the telemetered data stream and the state estimation process to be more easily identified.

### 2.2.1 Functions of the EMS

Typically every ten seconds or so, the main power system control centre computer reads the area SCADA databases. Any changes in the topological configuration of the network are marshalled to the control centre computer immediately. In a conventional EMS all of the SCADA information is fed through a module with a function termed *model update*. This is the first function in the RTNA sequence. It collects all the relevant data necessary, analogue and digital, for the RTNA sequence functions. The model update function then validates all the circuit breaker and disconnecter status information. Using this it forms a completely connected bus/branch model from the switch status data from the power system. Ideally this topological mapping from switch/section to bus/branch has been formed correctly, as in conventional state estimation all future RTNA functions depend on this. This model allows any network analysis tools which need details of the present system bus/branch topology to operate with data which is ideally valid.

### 2.2.2 Real Time Network Analysis

Real Time Network Analysis tools are software packages which perform additional processing of the information available from the State Estimator.

| *DC cycle time*, (5 min) | | *AC cycle time*, (15 min) | |
|---|---|---|---|
| 2 min | State Estimation | 6.5 min | State Estimation |
| 2.5 min | Security Analysis | 6.5 min | Security Analysis |
| 0.5 min | Free | 2 min | Free |

Table 2.3: Typical cycle times for DC and AC processes

The execution of these programs is not absolutely necessary in order to run a safe and secure system, however they do produce information which can be of use to the control engineers to assist them in their task of system operation. Generally the system has been planned to a high level of security using off-line tools to ensure that it can withstand any potentially problematic contingencies. Indeed the system would only be in danger if there were multiple unexpected events, which is so rare that operating standards do not require them to be covered.

### 2.2.3 Conventional RTNA facilities

Figure 2.4 shows a conventional RTNA software suite. The Security Analysis (DCSA and ACSA) assesses the security of the power system network by simulating the effects of contingencies considered to be critical to the system, and examines the resultant steady state conditions of circuit flows, voltage violations and generator reactive problems.

The Bus Load Forecast function provides the capability to track forecasts of the loads and time-switched breaker status every fifteen minutes, ensuring the forecasts input to the dispatch algorithm are correct.

The Security Dispatch function is activated whenever the state estimator detects an overloaded circuit on the network. It outputs how the overload may be reduced or eliminated by suggesting which generation should be re-dispatched.

The Voltage Scheduler function determines the optimal settings for genera-

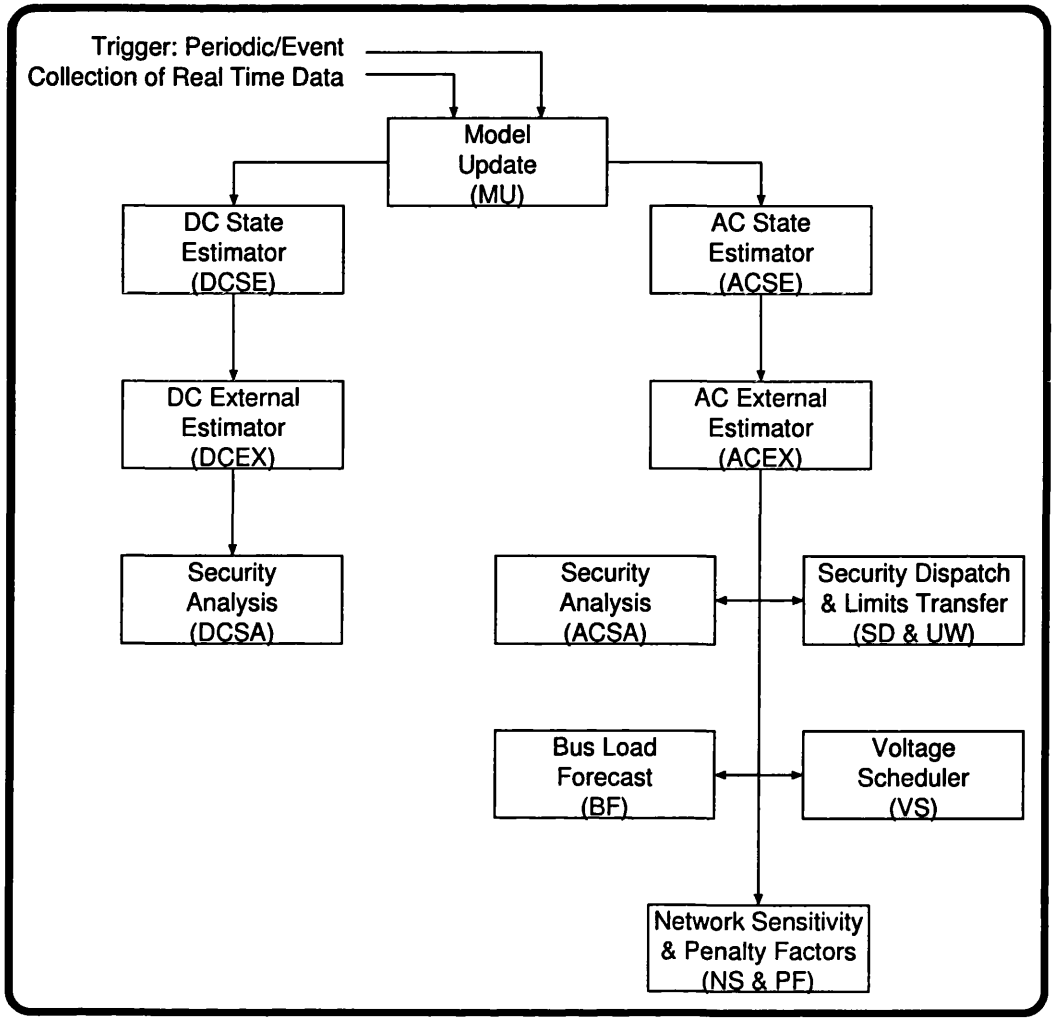


Figure 2.4: A diagrammatic representation of typical RTNA processes

tion, voltage, on-load tap change positions, quad-booster settings, Static Var Compensators, and the settings of manually switched shunt capacitance and reactance. The function is designed to minimise transmission losses and satisfy busbar voltage constraints and circuit flow limits.

The Network Sensitivity function calculates generating unit penalty factors for Automatic Generation Control, so that transmission line losses may be included in Economic Dispatch calculations.

### 2.2.4 Extended RTNA facilities

With research and development ongoing in commercial companies, new

techniques developed and proven by academia will soon become common place in future RTNA installations. This subsection explores some of these extended RTNA features.

A Dynamic Security Assessor is initialised from a set of State Estimated data. A list of credible contingencies is derived for this data set. This set of contingencies is then processed to find which contingencies cause the system to exhibit problems such as voltage, transient, and rotor angle instability. They may first be screened, for example using artificial neural networks trained on data selected by choosing the best composite indices, in order to improve the artificial neural networks' reliability.

On a power system there are various levels of protection. Automatic power system protection devices, such as those performing unit or distance protection of power system apparatus, react to faults on the power system within a few power system cycles of the time of the fault. These protection systems generally have their settings calculated and set by engineers within the utility's planning function. Once set these cannot be altered without someone going to the site of installation and physically changing the settings. The next level of protection can take several tens of seconds to operate - this is the automatic tripping of generation or *demand management* (load shedding). Settings on these longer operating protection schemes depend much more on the present operating point of the system, therefore changes in these settings may be made as the control engineer sees fit from the main control room. The automatic disconnection of generation is known as intertripping. An Intertrip Monitoring Scheme is initialised from a set of State Estimated system data and a list of intertrip settings. Contingency analysis is then performed to ensure that the settings are the most appropriate for the present system operating conditions. The output of this may then be used to advise the control engineers as to whether the intertrip settings are too severe or not comprehensive enough. A transient simulator is the most appropriate model to perform this analysis as it is able to take into account voltage, thermal and rotor angle

stability in its analysis of the situation.

## 2.3 Proposed Enhancement to EMS

In addition to using a novel technique to calculate the states of the system this work offers the capability to track the time domain response of most power system variables. Ways could be found to transform this tracking ability to utilise data found in previous Dynamic Security Assessment runs. This would further reduce the computational overhead of such schemes.

### 2.3.1 Development of Data Availability

In conventional EMS implementations several mainframe computers or a small network of workstations perform the database hosting, the State Estimation and the Real Time Network Analysis. There are, however, situations where it would be useful to have full access to data at any stage of its processing, to enable a more modular use of various manufacturers' products.

Presently Energy Management System vendors sell only the complete package - an EMS suite. A day must soon arrive when utilities will be able to select the most appropriate supplier's program for one part of the EMS data processing and another supplier's program for another. Not only will this enable the best available tool to be used for each EMS function, but will also enable different vendors' products to be directly compared on live data - something which is not presently possible. Very often a complete EMS system is installed before the utility buying it finds out whether it will perform as per their requirements. Presently it is difficult to mix and match between EMS suites.

This capability as described above would also enable the Research and Development team at a utility to more quickly identify where problems were occurring on the system, be that with the SCADA system, the EMS or the post-processing suite.

DOLSE would be able to accurately and quickly form a state estimated solution

vector which could be used as a basis for further processing within the distributed environment.

### 2.3.2 Development of RTNA capability

As was described previously, generally the information received at the Control Centre via the SCADA network is not snapshot based, it is sequentially scanned. The fundamental assumption is made at the outset that all on-line processing and RTNA is based on one snapshot of sequentially scanned data. This is one dataset, out of a possible 90 datasets available within a fifteen minute period. Decreasing the cycle time of the EMS does not solve the fundamental problem of lack of complete utilisation of the data available to the EMS. What is needed is a more holistic approach, which uses all available data, all of the time. The computer power necessary to complete this whole RTNA sequence may be too great an expense at the existing time, but in the forseeable future the expense will be minimal - making it economically viable.

EMS functions may be formulated to reduce the computational overhead of such extended RTNA functionality by maximising previous solution re-use. For example Modir [13] presents a Dynamic State Estimator specially formulated to provide previous solution re-use in Dynamic Security Assessment.

Papers such as [14] propose that the results of the previous DSA run are used to more quickly process the present DSA. They propose that the present solution may be linearly extrapolated from the past solution with a minimal amount of processing. However this could be so much better performed by applying non-linear extrapolation of the DSA run, using the information available from a matched power system simulator. Rather than knowing only the static system state at two instants in time from the previous SE run and the present one, the complete trajectory of the power system will be available. This immediately provides a better indication of the actual operation of the power system over the time period since the last DSA run. Ultimately this should enable better methods to be implemented to form a DSA solution re-

using information calculated in the previous one. It would even be possible to perform contingency analysis on a rolling basis, always using the most up to date data set, so that a contingency and its occurrence on the system bear a better resemblance to the actual system than previously.

Instead of knowing that the information is at least fifteen to thirty minutes out of date using conventional RTNA implementations, it would become possible to reduce this to a contingency evaluation lag time of only three to four minutes maximum.

Voltage collapse calculations, and predictions [15] are again based on linear models. A time domain simulator with the appropriate estimated future load variations applied in a faster than real time mode of operation is better able to determine the actual response of the system, because it models the system more completely. The state synchronised power system simulator could be used to update the model running in advance of the system, rather than the model having to be continually restarted as in a batch mode of operation.

## 2.4 Summary

This work offers the first opportunity of a continuously available consistent data stream, enabling complete parallelisation of the RTNA process. The benefits of this new approach have been detailed in this chapter.

Chapter Three

# Review of State Estimation

### 3.0.1 Concept of State

In order to state synchronise a time domain power system simulator to raw SCADA data, thus providing an enhanced state estimator, it is first necessary to understand the concept of state. This must be understood from both an engineering perspective and from an electrical power systems point of view. Once state in the field of power systems has been adequately explained, this chapter details how the state of the power system may be found.

If we examine a book concerning Control Systems, such as that by Dorf [16], it proposes that:

> The state of a system is a set of numbers such that the knowledge of these numbers and the input functions will, with the equations describing the dynamics, provide the future state and output of the system.

The state of a system represents the minimum amount of information about the system at any instant in time that is necessary so that its present behaviour can be determined without reference to the input prior to that time.

There are three main types of conventional electrical power system state estimator:

**Static State Estimation** minimises the residual error vector to form a solution.

**Tracking State Estimation** uses the previous state estimate as the basis for iteration with the present measurement set to minimise the residual error vector.

**Dynamic State Estimation** extrapolates the present solution to provide data which will be used in conjunction with the next raw data set, to minimise the residual error vector to form the next state estimated solution.

## 3.1 Conventional State Estimation Models

When modelling any system an appropriate model must be carefully selected in order to balance the level of detail needed against the computational requirements. As with any power system analysis there are two fundamental levels of model detail available for state estimation - *Direct Current* (DC) analysis, and *Alternating Current* (AC) analysis. DC equations are linear, taking into account the measurement of real power injections and real power flows. Usually in DC analysis the state variables are chosen to be the voltage angle at each busbar with one busbar being designated the *reference busbar* and assigned an angle of zero degrees. AC equations are non-linear - incorporating voltage magnitude and reactive power equations into the DC model previously described. With a reference busbar assigned, the state variables consist of the other busbar voltage angles and the voltage magnitudes at every busbar.

It should be remembered that for an over determined problem formulation, such as that applied to electrical power system state estimation, the selection of the set of states can be made from any number of sets of variables.

Schweppe [17] outlines the four important features of a State Estimation model:

1. *Measurements*: Telemetered line flows, bus injections, and bus voltage magnitudes.

2. *Pseudo Measurements*: Non-telemetered information on line flows, injections and voltage magnitudes (such as load distribution factors, or knowledge of tap changing transformer control logic).

3. *Parameter Values*: Estimates of the true parameter values at the present time. The values which describe individual transmission lines, transformers, and meter characteristics exhibit small slow variations with time which can be taken into account.

4. *Structure*: Estimates of the true structure at the present time. This represents the interconnection of transmission lines and transformers and the location of meters. They are binary variables and are mostly constant except for a few changes a day.

### 3.1.1 Direct Current Analysis

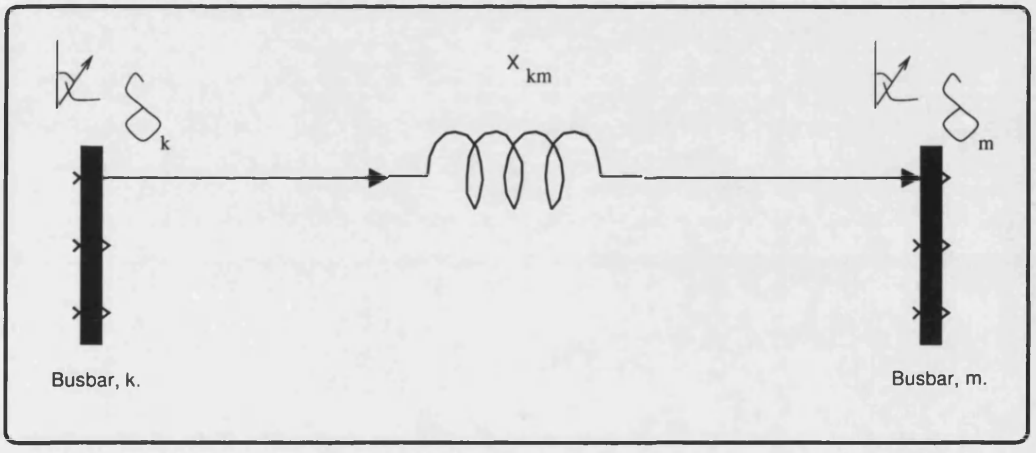


Figure 3.1: Direct current model of line

DC state estimation is based on the sum of real power at a busbar being equal to zero, and a simplified form of the standard equation for calculating the real power flow along a line. The standard equation for real power transmitted along a line from busbar $k$ to busbar $m$ is:

$$P_{km} = \frac{V_k V_m}{X_{km}} \sin \delta_{km} \tag{3.1}$$

but with $V_k$ and $V_m$ considered to be 1pu and the sine of a small angle in radians considered to be equal to that angle in radians:

$$P_{km} = X_{km}^{-1}\delta_{km} \tag{3.2}$$

Where $K$ is the set of busbars which are connected directly to busbar $k$ the sum of real powers at a busbar is equal to zero thus:

$$\sum_{m \in K} P_{km} = 0 \tag{3.3}$$

### 3.1.2 Alternating Current Analysis

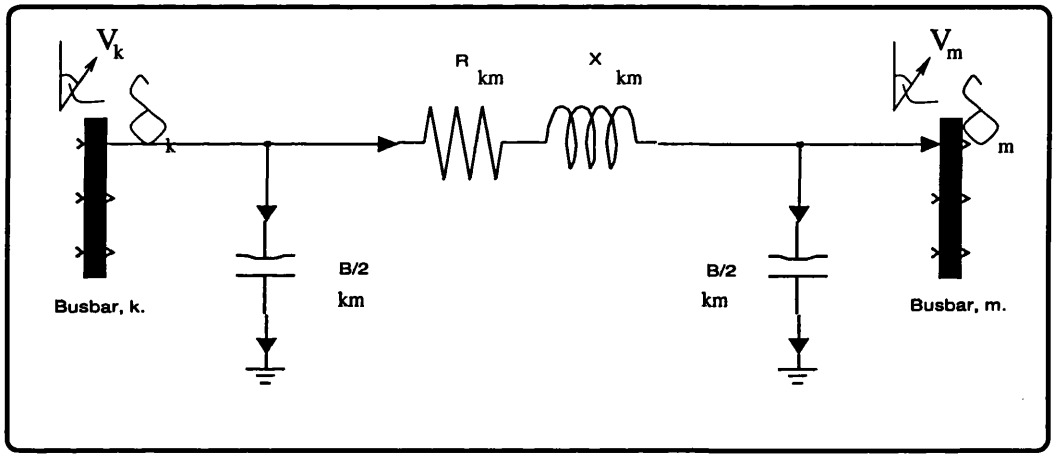


Figure 3.2: Alternating current model of line

For a transmission system the real and reactive power flows along a line are described as follows:

$$P_{km} = V_k^2 g_{km} - V_k V_m g_{km} \cos(\delta_{km}) - V_k V_m b_{km} \sin(\delta_{km}) \tag{3.4}$$

$$Q_{km} = -V_k^2 (b_{km} + b_{km}^{sh}) + V_k V_m B_{km} \cos(\delta_{km}) - V_k V_m g_{km} \sin(\delta_{km}) \tag{3.5}$$

where $g_{km}$ is the series conductance of the line, $b_{km}$ is the series susceptance of the line, and $b_{km}^{sh}$ is the shunt susceptance of the line.

In the nodal formulation of the network equations, where $K$ is the set of busbars which are connected directly to busbar $k$ the real and reactive powers summed at a busbar may be described as:

$$P_k = P_{k_{gen}} - P_{k_{demand}} + V_k \sum_{m \in K} V_m (G_{km} \cos \delta_{km} + B_{km} \sin \delta_{km}) \quad (3.6)$$

$$Q_k = Q_{k_{gen}} - Q_{k_{demand}} + V_k \sum_{m \in K} V_m (G_{km} \sin \delta_{km} - B_{km} \cos \delta_{km}) \quad (3.7)$$

where $G_{km}$ and $B_{km}$ are the appropriate real and imaginary elements of the nodal admittance matrix.

In an electrical power system the state of the network may be completely represented by a vector of complex voltages. Conventionally this state vector contains the information in *polar coordinate*, rather than in *cartesian coordinate* form. This convention means that the state is stored in a physically more meaningful way.

## 3.2 Static State Estimation

This technique was originally proposed by Schweppe et al. in 1970 [1, 2, 3] and followed up with an IEEE invited paper in 1974 [17].

This makes the DC state estimation problem linear, so it may be represented as a series of matrices thus:

$$z = Hx + e \quad (3.8)$$

With $m$ measurements and $n$ state variables:

- $x$ is a vector of $n$ states
- $z$ is a vector of $m$ measurements
- $H$ is the $m$ by $n$ Jacobian matrix
- $Hx$ is the vector of $m$ linear functions linking states to measurements

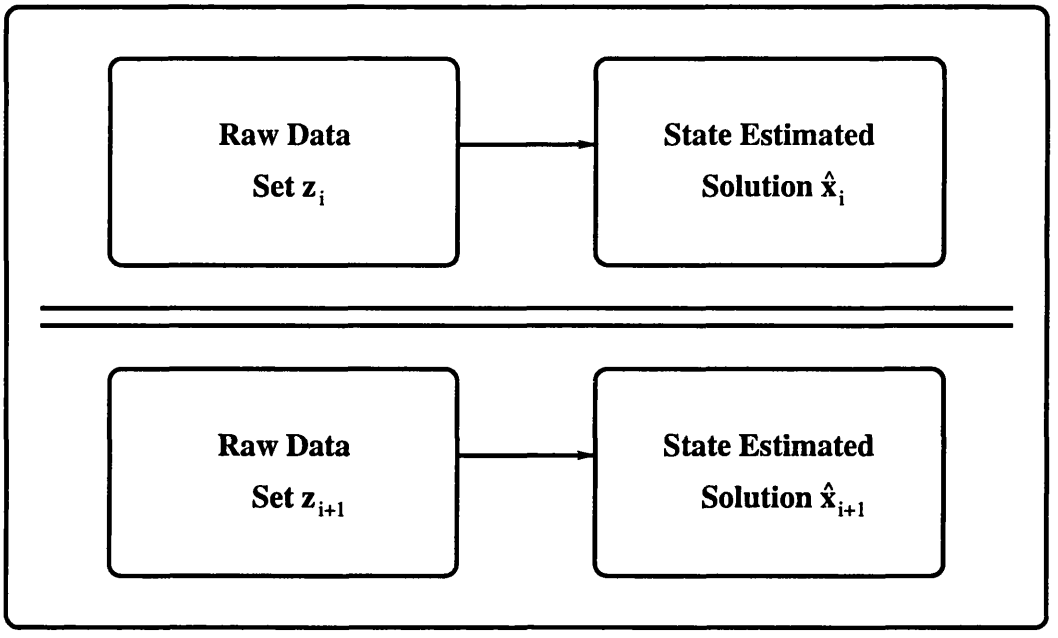


Figure 3.3: Static state estimation

- $e$ is the vector of $m$ random errors

A DC network has $n_v$ problem variables consisting of:

- bus voltage angles
- branch active power flows
- bus active power generation
- bus active power loads

connected by $n_e$ network equations.

The number of degrees of freedom of this network model is the difference between $n_v$ and $n_e$, namely $n_v - n_e$. This set of $(n_v - n_e)$ state variables is the minimum set of states needed to describe the system completely.

However when considering the state estimation of an electrical power system, access to all of the problem's variables is not necessarily available. Values are only obtained for the metered problem variables $n_{v_{metered}}$.

The set of network equations is constructed from two sets of equations. The first set expresses the direct relationship between the measured state variable and the actual state variable. The second is a sub-set of the network model equations described above, and is used to evaluate the measured variables as a function of state variables.

In this case, the number of degrees of freedom of the model becomes the difference between the number of states and the number of independent model equations.

The measurement residual error vector is:

$$r = z - H\hat{x} \tag{3.9}$$

where r is the residual error vector to be minimised by weighted least squares thus:

$$J(x) = r'Wr \tag{3.10}$$

where the weighting matrix, $W$, is formed by taking the reciprocal of the variance of the measurement:

$$W = R_z^{-1} = \begin{bmatrix} \sigma_1^{-2} & & & & \\ & \sigma_2^{-2} & & & \\ & & \ddots & & \\ & & & \ddots & \\ & & & & \sigma_m^{-2} \end{bmatrix} \tag{3.11}$$

It should be noted that the error vector $e$ of equation 3.8, is the absolute error between the measurement vector and the true state vector, $x$. Whereas the residual error vector $r$ of equation 3.9, is the error between the measurement vector and the estimate of the state vector, $\hat{x}$.

### 3.2.1 Normal Equations

From equations 3.9 and 3.10, with $\hat{x}$ being the estimate of $x$:

$$J(x) = (z - Hx)'W(z - Hx) \tag{3.12}$$

$$H'WH\hat{x} = H'Wz \tag{3.13}$$

$$\hat{x} = (H'WH)^{-1}H'Wz \tag{3.14}$$

Developing this further, if $\hat{z}$ and $\hat{r}$ are the measurement and residual vectors at the state estimate $\hat{x}$ where:

$$\hat{z} = H\hat{x} \tag{3.15}$$

$$\hat{r} = z - \hat{z} \tag{3.16}$$

Analysis of $\hat{r}$ provides the basis for bad data processing. If the element of the $\hat{r}$ corresponding to a particular metered value is larger than that variable's expected variance, it could be considered that bad data had been detected and should therefore be dealt with appropriately.

### 3.2.2 Other Approaches

Holten [18] gives a good comparison of the following methods:

- Normal equations with constraints.
- methods of Peters and Wilkinson.
- orthogonal transformation.
- hybrid method.
- Hachtel's augmented matrix method.

Another method proposed to tackle the SSE problem is to break the system into small areas, calculate a solution for each area and then recombine the results [19] [20].

The latest method proposed may be found in a paper [21] and a book by Monticelli [22]. Whereas conventional estimation checks the topology of the network when building the bus/branch model from the bus-section/switching device model, Monticelli believes in a holistic approach to find the states, parameters and model in one combined method.

Monticelli's Generalised State Estimation contains zero impedance branches to impose a zero voltage drop pseudo-measurement across each circuit breaker. If the breaker is in an open position, the pseudo measurement current is zero through that breaker. If the breaker is closed and electrical power is flowing through it, the pseudo measurement voltage drop across the device is zero. Rather than using the topology update function to build the system's topological model as a conventional state estimator would, Monticelli's generalised approach involves modelling the entire system to the switch section level of detail in the state estimation formulation. This effectively means that no assumptions whatsoever are made before the probabilistic system-wide approach is utilised.

Analysis of the analogue, switch and impedance data is carried out as if all the data were a single interacting information set. With this approach even the designated network parameters become estimated quantities. Each busbar section is modelled with its own voltage magnitude and angle effectively making it a state variable node. A zero injection pseudo measurement is added at a network busbar which has no generation or load because the fact that there are no injections at that busbar should be weighted and included within the formulation. Any series or shunt parameters are removed and replaced by state variables representing the power flows along that network element. Once a solution is reached the network parameters are calculated from the set of extended state variables.

## 3.3 Dynamic State Estimation

Static state estimators as described above are executed in a batch mode of operation. There is more data available in the Energy Management System than is actually utilised by the state estimator, to form information sets for RTNA processes. Using techniques based on more than one scan of measurements, especially utilising state estimates of previous data sets, the SE cycle time may be reduced, and therefore more data used for useful purposes

for a given amount of computing resources.

This data which is held in the EMS database is normally only used by control engineers, but not by on-line software packages because resources are unavailable to produce state estimates for every data set.

### 3.3.1 Tracking Estimators

Tracking estimators contain no model for the dynamic behaviour of the system [23], they rely on the scan interval being a short period of time.

The non-linear state estimation equations are described in terms of the present time $t_i$ thus:

$$z(t_i) = h(x(t_i)) + e(t_i) \tag{3.17}$$

For a small scan interval, $t_i - t_{i-1}$, the correction between consecutive estimates $x_i - x_{i-1}$ is considered small enough that the state estimate update can be obtained in one iteration. This update which has occurred over the time $t_{i-1}$ to time $t_i$ may then be applied to the state estimate $\widehat{x_{i-1}}$ to form the state estimate for the present scan in Schweppe's tracking approach:

$$H'(x)W[z - h(x)] = 0 \tag{3.18}$$

$$x_i = x_{i-1} + [H'(x_i)WH(x_i)]^{-1}H'(x_{i-1})W[z_i - h(x_{i-1})] \tag{3.19}$$

$$\widehat{x_i} = \widehat{x_{i-1}} + [H'(x_i)WH(x_i)]^{-1}H'(\widehat{x_{i-1}})W[z_i - h(\widehat{x_{i-1}})] \tag{3.20}$$

A linear model is assumed - no hypothesises are made concerning the time behaviour of the state vector over time.

### 3.3.2 Dynamic Estimators

There are two forms of dynamic state estimation - linear and non-linear. The the non-linear measurement model is that of equation 3.17 above, the linear measurement model is of the form:

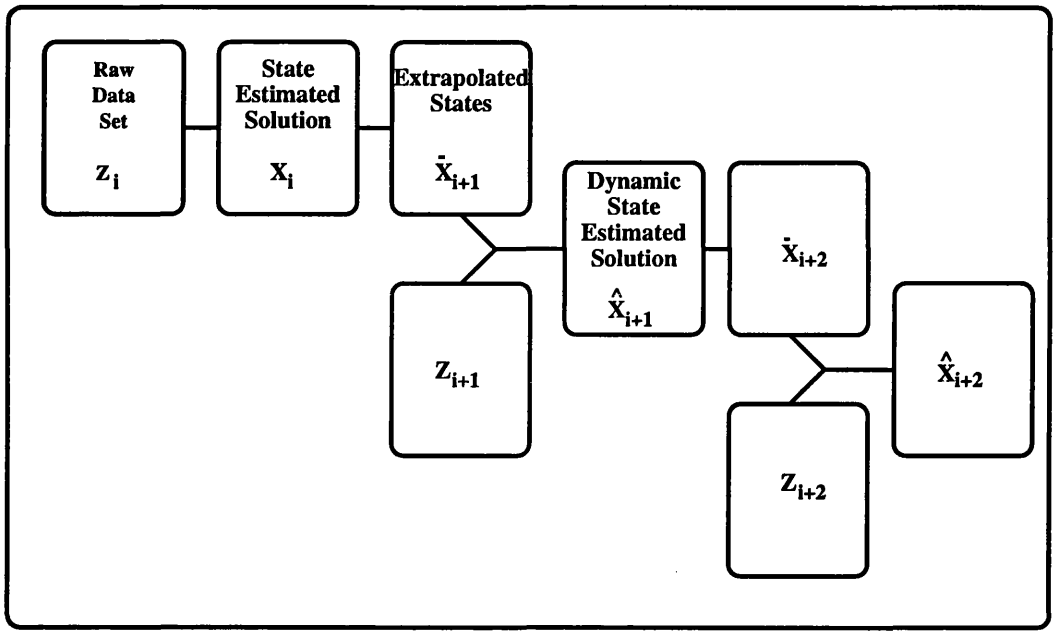


Figure 3.4: Dynamic state estimation

$$z(t_i) = H(t_i)x(t_i) + e(t_i) \tag{3.21}$$

The states from the previous scan are linearly extrapolated to form pseudo-measurements which are then used to augment the present measurement vector. Where a tilde represents the augmented vector incorporating actual and pseudo measurements, DSE formulation now states that:

$$\tilde{z}(t_i) = \begin{pmatrix} z(t_i) \\ \hat{x}(t_{i-1}) \end{pmatrix} \tag{3.22}$$

A comparison between the performance of tracking and dynamic estimators is made by Leite da Silva in [24]. Nishiya [25] presents an algorithm for Dynamic State Estimation which includes the detection of anomalies.

Mandal [26] describes a DSE based upon the Extended Kalman Filter, incorporating non-linearities such as topology changes.

### 3.3.3 Practical Experience

A typical EMS implementation incorporates two state estimators. These are a DC and an AC formulated estimator. The DC estimator is used because it converges in a shorter time than the AC estimator but only produces a DC real power flow output. This output is used for fault level calculations. The AC estimator generally takes up to three times longer to find a complete AC solution. Table 2.3 shows the relative timings of the DC and AC operations. The DC state estimator provides real power flows for each circuit and bus injection which is *observable* i.e. with enough telemetered data to find a solution. The AC state estimator outputs reactive power circuit flows, transformer tap estimates and busbar voltages in addition to real power flows, injections and voltage angles.

Both the DC and the AC limbs of the process to find the system state are split in two halves. The first half is the main state estimator. These take metered values as their inputs, perform bad data analysis to detect values which are reversed (this is caused by incorrectly installed metering) and try to find values which may also be classified as inaccurate or wrong. The SE function then attempts to solve as much of the network as is possible with the clean data values which it has filtered. The purpose of the SE function is to fill in any missing telemetered data, and to eliminate errors in the available data. Boundaries are drawn between the good and the bad regions.

The SE function only calculates values where sufficient telemetered data is available in *observable* areas. It is not able to compute a solution for areas of the system where extensive amounts of data have become unavailable. This is where the second half of the process comes into operation. These processes are termed the *external estimators*, DCEX and ACEX (see figure2.4). These programs now attempt to solve previously un-calculated parts of the power system. DCEX and ACEX use selected voltage injections and power flows calculated by the DC and AC SE functions, pre-defined quantities calculated

from all power flows and voltages on the rest of the power system (*SE boundary values*), and forecast loads or loads which are tracked. The EX functions move the boundaries out from the areas with good data, using data which has previously been declared bad. The EX function attempts to correct the bad data in order to obtain a complete set of system states.

### 3.3.4 Implementation

Results from a state estimator algorithm, with the external estimator formulated by use of Lagrange multipliers are now shown. These results were obtained when the state estimator was being tuned, specifically to illustrate the range of errors which could be encountered on an actual system. Techniques were developed to try to identify where this untuned state estimator was failing. These methods of error identification have also been useful for the testing of the DOLSE methodology. Details of the state estimator implementation are presented, the error visualisation technique is shown and then the results of this conventional static state estimator are discussed.

In the external estimator Lagrange multiplier formulation the cost function may be written thus:

$$J(x) = (z - h(x))'W(z - h(x)) - 2\lambda' g(x) \tag{3.23}$$

where $h(x)$ is a non-linear function relating the states to the measurement vector, and $g(x)$ is a non-linear function relating the states to the injection at known zero injection buses. This is incorporated into the cost function by the use of a vector of Lagrange multipliers, $\lambda$.

Partially differentiating equation 3.23 above with respect to $x$ we obtain:

$$\left.\frac{\partial J}{\partial x}\right|_{x=\widehat{x}} = -2\left[\frac{\partial h(x)}{\partial x}\right]' W\left[z - h(x)\right] - 2\left[\frac{\partial g(x)}{\partial x}\right]' \lambda = 0 \tag{3.24}$$

which must now be solved using an iterative technique. If the Newton Raphson technique is utilised, this is equivalent to linearising $h(x)$ and $g(x)$, substituting into the cost function and solving:

$$\frac{\partial J}{\partial x} = 0 \tag{3.25}$$

$$\frac{\partial J}{\partial \lambda} = 0 \tag{3.26}$$

Where $x_i$ and $x_{i+1}$ are two possible state estimates, the difference between them is $\Delta x (= x_{i+1} - x_i)$, and the observation function evaluated at the first state estimate is denoted $h(x_i)$. The Taylor series expansion of this becomes:

$$z = e + h(x_i) + \left.\frac{\partial h}{\partial x}\right|_{x=x_i} \Delta x + \ldots \tag{3.27}$$

Defining $\Delta z$ and $A$ as:

$$\Delta z = z - h(x_i) \tag{3.28}$$

$$A = \left.\frac{\partial h}{\partial x}\right|_{x=x_i} \tag{3.29}$$

and neglecting any terms higher than 1st order gives:

$$z = A\Delta x + e \tag{3.30}$$

Performing linearisation of $g(x)$:

$$0 = g(x) \tag{3.31}$$

$$0 = g(x_i) + \left.\frac{\partial g}{\partial x}\right|_{x=x_i} \Delta x + \ldots \tag{3.32}$$

$$\Delta S = 0 - g(x_i) \tag{3.33}$$

$$B = \left.\frac{\partial g}{\partial x}\right|_{x=x_i} \tag{3.34}$$

$$\Delta S = B\Delta x \tag{3.35}$$

Substituting the linearised equations into the cost function (equation 3.23) we obtain:

$$J = (\Delta z - A\Delta x)'W(\Delta z - A\Delta x) - 2\lambda'(\Delta S - B\Delta x) \tag{3.36}$$

Taking partial derivatives with respect to $\Delta x$ and rearranging gives:

$$\frac{\partial J}{\partial \Delta x} = -2A'W(\Delta Z - A\Delta x) - 2(-B)'\lambda = 0 \tag{3.37}$$

$$A'WA\Delta x + B'\lambda = A'W\Delta z \tag{3.38}$$

Taking the partial derivative of the cost function with respect to $\lambda$ and rearranging:

$$\frac{\partial J}{\partial \lambda} = -2(\Delta S - B\Delta x) = 0 \tag{3.39}$$

$$B\Delta x = \Delta S \tag{3.40}$$

Combining equations 3.38 and 3.40 in matrix form for iterative calculation to find the estimated state vector, finally at the $k$th iteration:

$$\begin{bmatrix} A_k' W A_k & B_k' \\ B_k & 0 \end{bmatrix} \begin{bmatrix} \Delta\widehat{x_k} \\ \Delta\widehat{\lambda_k} \end{bmatrix} = \begin{bmatrix} A_k' W \Delta z_k - B_k'\widehat{\lambda_k} \\ \Delta S_k \end{bmatrix} \tag{3.41}$$

where $\Delta x$ and $\Delta\lambda$ are the voltage and Lagrange multiplier corrections respectively at each iteration.

## 3.4 Error Visualisation

When investigating the operation of state estimators it has been found to be useful to look at the overall differences between the output and the input of the state estimator. Ideally one would wish to compare the true state, $x$, the measurement of that state, $z$, and the state estimate, $\hat{x}$. In practical implementations the true state is unavailable, in simulations however, we have access to all three vectors.

Bearing in mind that the AC state estimation equation is:

$$z = h(x) + e \tag{3.42}$$

at solution the minimised residual error is:

$$r = z - h(\hat{x}) \tag{3.43}$$

By plotting $h(\hat{x})$ versus $z$, the distance of the point from the line $h(\hat{x}) = z$ gives the residual. This is a useful aid to representing the solution pictorially and may be seen in figure 3.5. For example, values close to the line $h(\hat{x}) = -z$ within the horizontally shaded region are reversed metering data points.

The graph may be thought of in terms of four quadrants, (+,+), (-,+), (-,-) and (+,-) as depicted in figure 3.5.

Any values in (+,-) or (-,+) which are not in the horizontally shaded region must be due to modelling or nomenclature errors in the state estimator parameter database, or due to faulty or inaccurate reverse metering.

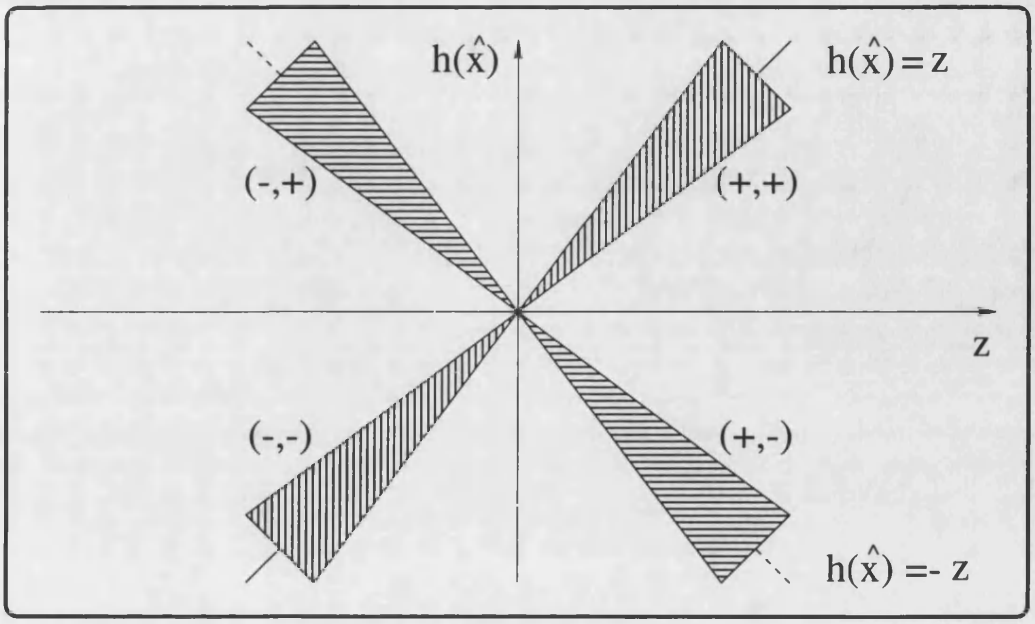


Figure 3.5: Error visualisation graph

Any points in (+,+) or (-,-) not in the vertically shaded region are outside the level of meter error expected. The solution should always lie with points in the shaded regions. If they don't, then the worst points should be discarded, and the Weighted Least Squares performed until all measurements are within the shaded regions.

### 3.4.1 Results

With error variances of the metered values within the ranges suggested in chapter 2, the following results were obtained using an AC state estimator and external estimator, as described above, on a 1000 busbar, 1500 line system.

When investigating the operation of a conventional state estimator it is more convenient to decouple the real and reactive equations in order to visualise the situation. In these terms the voltage magnitudes are variables within the set of reactive power equations and voltage angles are variables within the set of real power equations. So that the real and reactive solutions may be evaluated effectively, analysis must be performed in terms of variables which are both metered and easily calculable from the set of system states. On power systems

without Global Positioning System Universal Time Clock synchronisation voltage angles are not available from the power system metering at the busbars. This makes voltage magnitude and angles an inappropriate set of variables on which to evaluate state estimator performance.

Real and reactive line flow measurements are the most inaccurate of all the metered values available to the state estimator. Any comparison based on their real time metered values and the state estimator output would therefore be clouded because of the greater potential for errors. This leaves the variables available for direct comparison between real and state estimated values as the set of real and reactive generator outputs and real and reactive busbar loads. It is for this reason that the real and reactive metered and state estimated busbar loads have been chosen for this analysis.

The results were taken under normal operating conditions during the day. At this time one would expect the loads to be absorbing both real and reactive power. Only if embedded generation were operational would this not be the case.

As may be seen in figure 3.6 the real time metered real power load values are plotted on the x-axis against their state estimated counterparts on the y-axis. Load at a busbar is electrical power removed from the power system. It is for this reason that the loads are shown in terms of negative values. As one would expect there is a good correlation between the points and the line $y = x$.

No points lie in the lower right-hand quadrant. However several points lie in the upper left-hand quadrant. This shows that although the real time metering showed a load at these busbars the state estimator actually calculated that there was generation. This could be due to either reverse metering or to the way in which the state estimator has redistributed the errors on the estimated results when compared to the raw data.

Figure 3.7 shows the results for the reactive equations. Again reactive load is signified by a negative value because reactive power is removed from the

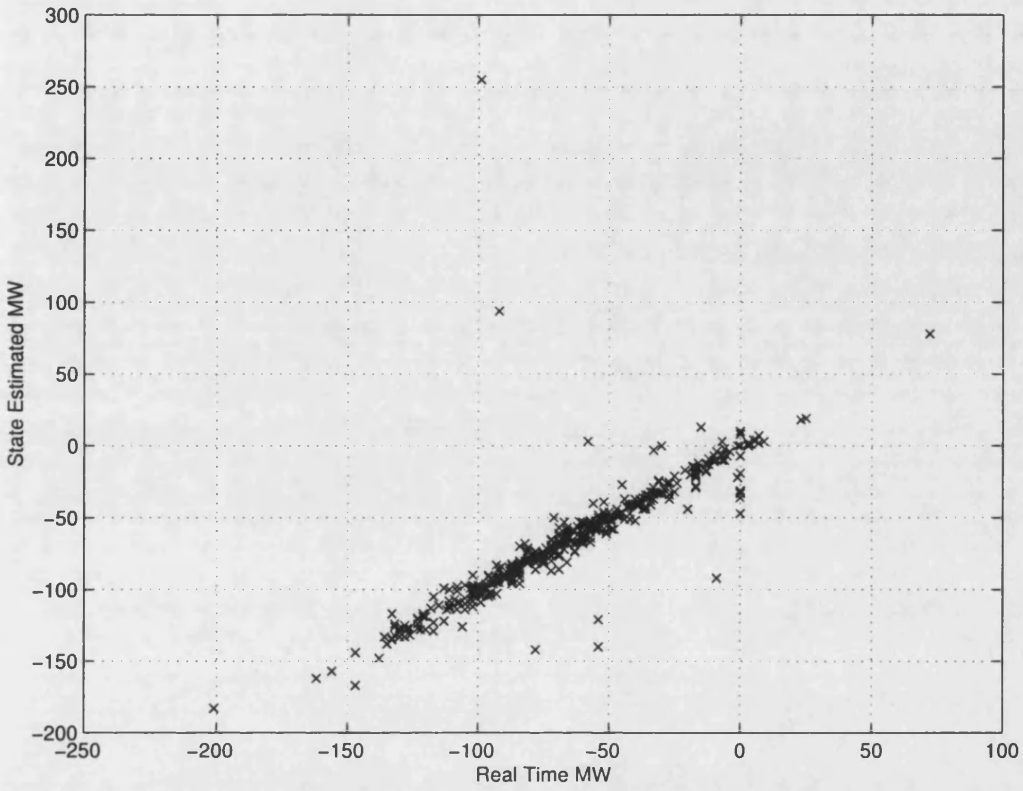


Figure 3.6: State estimated versus real time MW loads

electrical power system. This graph also shows a strong correlation between the points and the line $y = x$. However the points are more distributed than in the real power case. From the real power diagram the real time metering would suggest that five or six busbars are generating electrical power, whereas the reactive power diagram suggests that many more loads at busbars are generating reactive power. This could be because the real time metering is in fact reversed and the state estimator has not picked this up or it could be due to inaccuracies in the convergence of the reactive equations within the state estimator. It seems that the residual errors are much greater in the reactive case. Although it is possible for a GSP to be absorbing MW and generating MVAr for example, with a cable LV system or LV capacitors, it is unlikely to be the case in the system loading scenario investigated.

When thinking in terms of the set of real power equations and the set of reactive power equations it is useful to think of which variables are actually me-

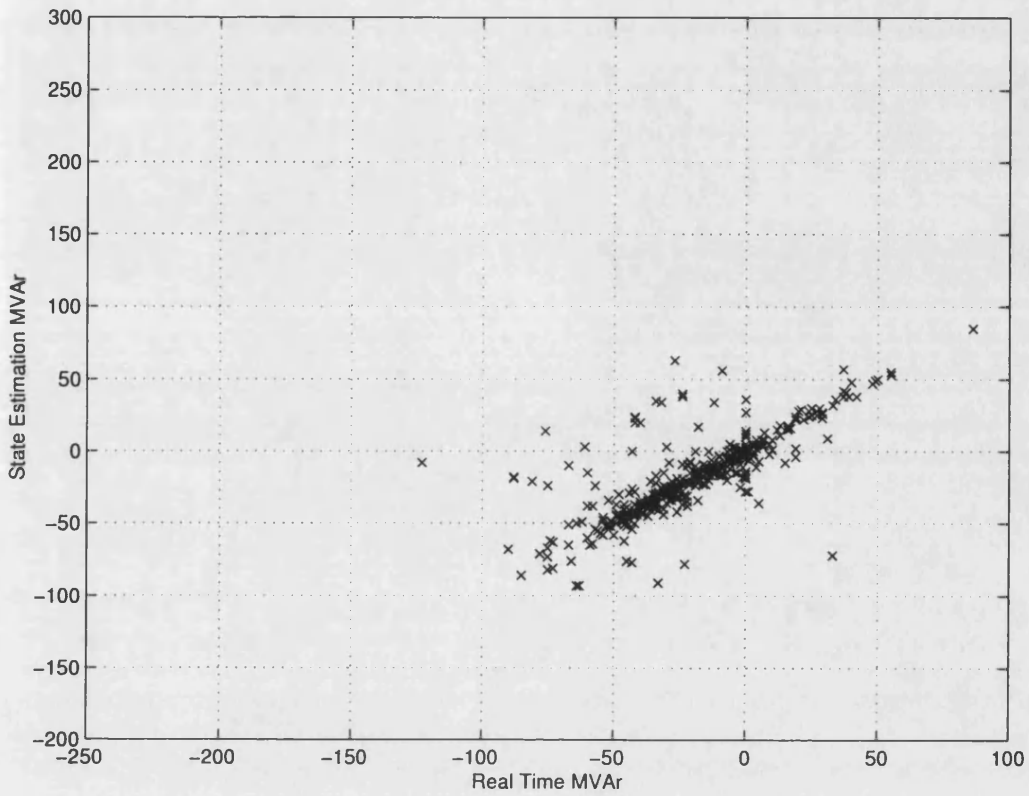


Figure 3.7: State estimated versus real time MVAr loads

tered and which are pseudo variables. As voltage angles are unavailable from non-GPS synchronised power systems these could be thought of as pseudo variables. In Tracking State Estimation these effective pseudo measurements of voltage angles from the previous solution are used in addition to the voltage magnitudes to initialise the state estimation equations. The real and reactive supply and demand are not monitored from iteration to iteration and are not used to screen incoming data, nor are they used in subsequent iterations.

The real power equations need only converge until the real power supply and demand constraint is met as voltage angle measurements are not available from the system. If the same graphs were plotted for a power system with a GPS synchronisation capability the residual errors in the real power equations would mirror the errors in the reactive equations. This is because the extra errors on the reactive load diagram are due to the state estimator converging to minimise both the supply and demand constraint of reactive power and the

voltage magnitudes at every busbar.

In effect the residual error of the voltage magnitude measurements is being redistributed onto the reactive loads. This problem does not occur in the real power equations simply because the voltage angles are effectively unavailable.

The author suspects that any attempt to integrate GPS synchronised data into static state estimation equations will result in an increase of the residual errors in the real power load estimates. Convergence problems could also result. A phenomena known as *error dumping* can be a problem in static state estimators. In order to achieve an acceptable convergence, large injections can be made on LV nodes in order to keep the solution consistent with the HV metering. In actual fact this causes more inaccurate solutions. Comparatively small metering errors can cause non-convergence.

Another area of error is in the parameters used in the network model. For example system network parameters are generally calculated as a function of the transmission line length, using the manufacturer's specifications. Slutsker [27] showed that the accuracy of the state estimator is in fact much more sensitive to errors of the model parameters than it is to errors in the metering, but in order to achieve this he assumed all metering was correct. Most state estimators trust the parameter values completely. If weights are attributed to the data to show the varying reliability of the data, this method effectively gives the parameter values a very high reliability rating, a rating which is not always justified. By using the models carefully constructed for detailed analysis, DOLSE overcomes this problem. Models which are used for off-line studies are more detailed than those normally used in on-line data processing. As the time domain simulator is computationally efficient, it is able to cope with the more detailed models usually reserved for off-line applications, but complete the required amount of data processing in on-line time frames.

### 3.4.2 Discussion

Static state estimation makes reasonable assumptions such as considering the

power system to be in steady state over some short period of time. To estimate the present flows it is reasonable first to estimate the state vector $x$ and then use the admittance matrix and Kirchoff's laws to obtain the desired estimated flows. If a line is removed bus voltages will change and therefore so will $x$. However, with the DSE formulation it is assumed that generator real powers and voltage levels, and the load real and reactive powers will not change.

In order to aid the process of state estimation it has even been proposed by Hansen and Debs [28] to use a three phase state estimator. They argue that because significant imbalances can occur in the loading of each phase they should all be modelled separately. Due to the fact that power system metering is not cheap it has generally been accepted that meters used for telemetry will all be attached to the same phase. The problem still exists that the power system is a dynamic system, therefore it needs to be modelled dynamically. No other approaches, including that proposed by Hansen and Debs, can ultimately give as good a set of results as a transient simulator system model if it is properly applied.

## 3.5 Summary

State Estimation techniques presented above have been developed by many researchers over a period of thirty years. Commercial state estimators are large complex software projects worked on by teams of software and electrical engineers. The logical extension of static state estimation is the progression towards tracking state estimators. The use of dynamic state estimators is the next step from the use of tracking estimators.

Power Companies stake their reputation on *keeping the lights on* and therefore use well-proven techniques. With the rapid development of computing power available [29] schemes such as intertrip monitoring are starting to be used [30]. The work developed in this thesis would provide data to RTNA programs which needed it on a continual basis.

### 3.5.1 Similarities and Differences

Conventional state estimation is based on probabilistic load-flow techniques. However, the state of an electrical power system is as described at the start of this chapter, namely a set of data which when combined with the inputs to the system and the model of the system completely describes the status of that system. This set of state estimated data should be available as quickly as is possible to the control engineers.

The method by which it is obtained should be robust and accurate. The next step in the modelling of a power system after load-flow analysis is transient simulation. This thesis presents work which is the next logical step from the use of load-flow techniques in state estimation. When combined with data trending techniques the incorporation of a transient simulator in the state estimation formulation is at least as robust and as accurate as conventional techniques with additional benefit besides.

Chapter Four

# Review of Power System Simulation

Power Systems must withstand disturbances. To ensure that they are capable of doing so, stability simulations are essential. Simulators in the late 1920s, called A.C. network analysers, were analogue models of the electrical power system. In the 1950s digital computers began to be applied to this simulation task. Since that time computers have become faster and their use has increased as they have become less expensive.

Due to the large amount of computing power necessary to always model the system to the highest level of detail, power system models of varying levels of detail were developed to be used as appropriate. In general for transient stability studies, system dynamics must be modelled to include effects at the 10ms time frame. For contingency analysis system states are required to be evaluated at intervals of 10ms to 100ms over a time-scale of 30 seconds.

If enough processing power is available the model equations may be solved within the simulated time-step. The full 400/275kV grid system of England and Wales contains around 1000 busbars and 1500 lines. On a Pentium II 300 MHz personal computer, the University of Bath's Power System simulator (*PowSim*) models this system accurately every 10ms at 3 times faster than real time, utilising approximately one quarter of the 128 Mb of main memory installed.

With a processor dedicated to dynamic on-line state estimation this leaves the

processor free 66% of the time to perform data processing and filtering.

Most of the material here was developed by Dale [31], Berry [32], and Chan [33] at the University of Bath.

## 4.1 Algorithms and conventional Applications

Computers available today are powerful enough to allow the simulation of an electrical power system in suffient detail for transient analysis in real time speeds or faster. Previously on-line computer applications in power utilities were confined to data management (e.g. data display) or basic data processing to ensure thermal and voltage constraints were met. However, a power system transient simulator which is capable of simulating the system in sufficient detail so as to produce rotor angle stability information, is also able to analyse the thermal and voltage behaviour of the system to ensure constraints are adhered to.

It is important that appropriate models are used for any system which is to be studied [34]. On an electrical power system simulations may be divided by the phenomena of interest, usually this directly equates to the simulation time step interval (figure 4.1). For example the EMTP package is of use to power system

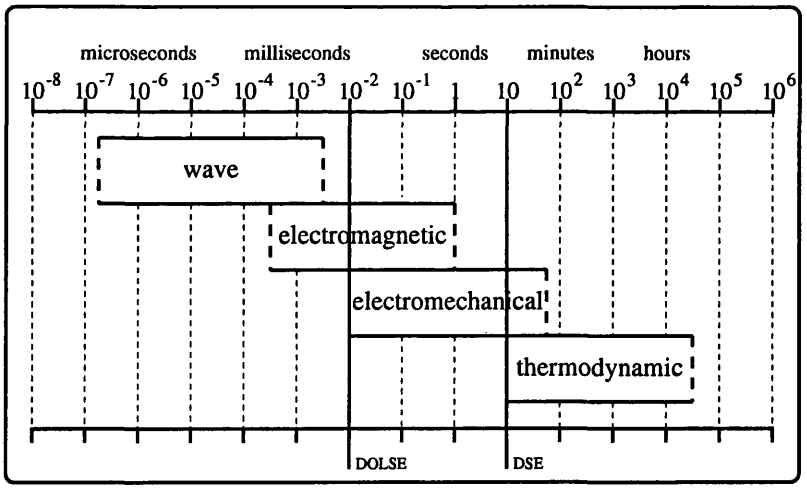


Figure 4.1: Power system dynamic phenomena time frames

protection engineers in order to study sub-cycle phenomena associated with removing a line or other item of plant should there be a fault. The fault could be man made (JCB), natural (lightning), or due to faulty/old apparatus.

The simulator which has been developed within the Power Systems Modelling and Control Group within the Power and Energy Systems Group at Bath, is concerned with the operation of the system on the time scales of electro-mechanical transient stability. It includes suitable models to accurately model the electrical generation plant, governors, automatic voltage regulators and power system stabilisers present on the power system. These systems need to be modelled in order to study the mode of operation of the system formed when the rotors of machines oscillate causing real power to oscillate between regions of the power system - inter-area oscillation.

Another type of simulator which works on a longer time step of solution, is primarily interested in thermodynamic phenomena or the phenomenon of voltage collapse. With the installation of FACTS devices these are becoming increasingly important due to the sharper voltage collapse characteristic which plant such as Static VAr Compensators can produce.

Dynamic State Estimation has relied on models which operate in the time frame as shown for them in figure 4.1. However these models are not very detailed when it is considered that they are applied to account for features in the electro-mechanical time frame. Phenomena studied on the time scales of EMTP would never be seen on SCADA data, due to the scan rate. A more detailed model which could be synchronised to the system is a transient simulator. This model is a good match for the resolution of the data available, as the data will exhibit characteristics due to the modes of operation in this time frame. Also it provides information about the power system frequency which is both useful, and necessary in DOLSE to aid the estimation of the power flow mismatch.

### 4.1.1 Electro-mechanical Transient Stability Simulation

When the electrical power system enters an oscillatory mode of operation, damage can occur. These oscillations are interactions between the rotors of the generating units attached to the system. The relative phase angle of the machines increases and decreases - in physical terms this may literally be thought of as real power washing up and down the power network. The most extreme outcome of this phenomenon applied to a single machine is an event known as a *pole slip*. This occurs when the phase of a generating unit is so far removed from the phases of the other generating units attached to the system that it is mechanically easier for the machine to lose a rotation rather than keep in step. At this instant the magnetic forces within the generator which has pole slipped are so intense that it may be thought of as the whole momentum of the rest of the system exerting a massive magnetic force and trying to pull the coils from the pole slipped rotor. If this occurs once or more it can cause the rotor to become misaligned, this would cause vibrations within the machine. This in turn would lead to excessive wear to the bearings supporting the shaft and would need to be repaired as quickly as possible in an operation costing millions of pounds.

In the same way that this phenomenon can occur between one generator and the rest of the system, inter-area oscillations occur between regions of the power system - between groups of machines. This is a problem when two regions are weakly interconnected and the flow of the electrical power is great from one region to the other. In the UK inter-area oscillation could occur between the Scottish and the English/Welsh power systems. For a complete analysis of this subject see [35]. The original introduction of *power system stabilisers* (PSS) to the control apparatus installed at a generating station was to try to reduce the occurrence of inter-area oscillation. Power system stabilisers incorporate the additional feedback of the apparent power output of a generating set into the voltage reference input to the *automatic voltage*

*regulator* (AVR). When these power system stabilisers were initially installed insufficient studies on a system-wide basis had been completed. Instead single machine infinite busbar studies had been used [36]. The unsuitability of these studies soon became apparent when the introduction of the power system stabilisers to the actual system caused more problems than they solved. It is always important to investigate power system transient phenomena on a system-wide basis to gain a complete picture of the operation. Appropriate models must be chosen in order to obtain meaningful results. The same is true of DOLSE.

## 4.2 Detail of Component Models

A power system transient stability simulator may be formulated in a variety of ways. Originally implementation consisted of incorporating both the network and machine equations within the same matrices. However, to partition the problem to maintain sparsity where appropriate, it was found at the University of Bath to be advantageous to formulate the network and each set of machine equations into separate matrices. This also had the advantage of being a suitable approach to enable parallel processing of the model. Presently it is no longer necessary to employ special parallel processing hardware for real time or faster operation, yet the original partitioned approach has been maintained.

If the network and machine equations were incorporated in the same matrix this would effectively break the mainly diagonal sparse structure of the network matrix. Indeed the machine matrices are not sparse and it is therefore important to handle the network matrix using sparse techniques, with the machine matrices using conventional techniques. This yields results faster than could be achieved by combining both network and machine equations in a single matrix.

The separation of the network and machine equations within the transient simulator conveniently allows manipulation of appropriate primary variables to enable correct operation of the synchronised simulator within the DOLSE

methodology.

### 4.2.1 Network Elements

The power system network elements are modelled as loads, lines and generators. The three phase network is represented by a single phase representation using the positive phase sequence quantities.

Power system *busbars* and tee-points are represented as nodes in the model. Transmission equipment such as lines, cables, transformers, and reactors are represented as branches of the model.

Lines are modelled using a Pi-network, with series resistance and inductance, and a shunt admittance at either end - an AC model as that in figure 3.2.

Shunt reactors and static capacitors are represented by an equivalent shunt admittance between the appropriate node and neutral.

### 4.2.2 Synchronous Machine Model

The model of the synchronous generator is based on a five-winding idealised machine which is symmetrical about the direct and quadrature axes. The original three phase quantities are resolved into components along the two axes using Parks' transformation. Balanced three-phase operation is assumed, so zero phase sequence components are not considered. Damper winding and lumped eddy current effects are represented by a single short circuit winding on each axis.

The resulting Parks' two-axis primitive machine is then described by a set of flux linkage and voltage equations. To obtain a fast calculation, this full five-winding Parks' equation set is transformed into a seventh order voltage behind sub-transient reactance representation.

### 4.2.3 Machine Saturation

As the power system simulator needs to model transients, the saturation of

machine leakage reactance under high current conditions is also simulated. This could be achieved by modifying the machine reactances with the saturation factor obtained by an open-circuit test to determine the saturation characteristic. However in practice it is more computationally economic to fix the reactances and adjust the voltage instead.

### 4.2.4 Control System Models

For the detailed evaluation of on-line system response, the effects of the exciter and governor systems are an important factor to be considered. PowSim uses the models for excitation and mechanical power control as published in IEEE Committee Reports [37, 38, 39].

In addition detailed models of the *automatic voltage regulators* (AVRs) and of *power system stabilisers* (PSSs) appropriate to specific installations worldwide may be called upon where necessary to be used by PowSim.

### 4.2.5 Solution Method

The power system equations consist of two sets of equations which have to be solved simultaneously as a function of time. This may be seen in figure 4.2. The first set is a system of differential equations which represent the dynamic behaviour of the machines and their associated control systems. The other set is a system of algebraic equations which describe the steady state behaviour of the network. These sets include steady state models of loads and algebraic equations of synchronous machines.

The simulation algorithm uses a partitioned implicit method. Non-integrable variables are extrapolated, and integrable variables are determined using the implicit trapezoidal integration method.

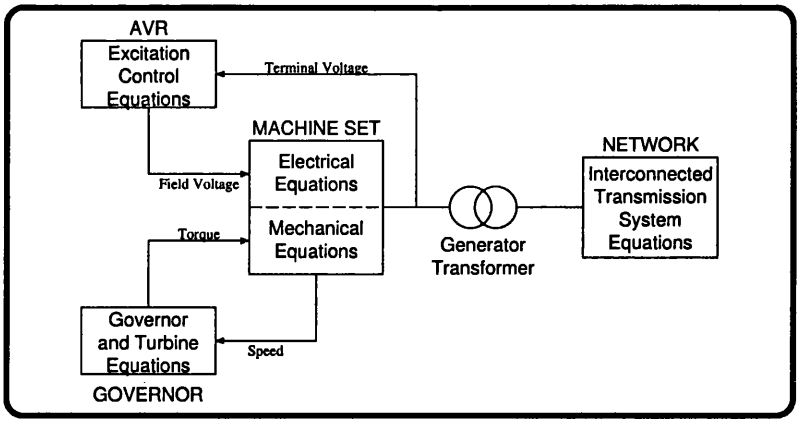


Figure 4.2: A diagrammatic representation of PowSim solution method

## 4.3 Requirements for DOLSE and Enhancements Implemented

The transient simulator models the transient mode of operation of the power network very effectively. If the internal states of the model were interfered with it would impinge on the simulator's accuracy. This must be avoided at all costs because if the accuracy of the simulation were reduced it would ultimately make synchronisation between the model and the actual system much more difficult.

Primary simulation variables are those which may be explicitly set within the formulation of a problem. Secondary variables are related to primary variables and are characterised by their total dependence upon them. In order to manipulate a secondary variable, primary variables must first be manipulated in order to effect a change. Direct modification of secondary variables is impossible.

In conventional state estimation algorithms the primary variables of interest are the voltage magnitudes and angles - the system states. The residual error is minimised by iterating the equations to calculate the correction to be applied to the states in order to find a solution. The secondary variables of real and

reactive loads and power flows are a result of the voltage states and may be related to the states via the non-linear transformation matrix $h(x)$.

Within the simulator these voltage magnitudes are available, however they are secondary variables. The primary variables which may be directly manipulated are the mechanical output torque of the generator, the armature current of the generator, the generator output tap ratio, the line tap ratio and the real and reactive busbar loads. Although the voltage magnitudes and angles are still considered to be the state variables which will be output upon solution, there is no direct mapping from the actual system values to those within the simulator. It is for this reason that the power system real and reactive stiffness characteristics must be calculated off-line in order to calculate the relationship from these secondary variables to the primary variables within the simulator - so that a state synchronised model may be achieved.

### 4.3.1 Controller Model Synchronisation

When aligning the simulator to the power system the real power generated at a machine is transformed to find the mechanical output torque of the generating set required to provide that real power output. Ideally the governor equations would be back-worked in order to find the mechanical output torque. However, because this is not possible without breaking the integrity of the simulation, the mechanical output torque change found by an incremental search is iterated until an acceptable value of real power output is achieved.

In order to alter the voltage output of the generating set the excitation current is altered using an incremental search and the equations iterated until an acceptable output value is obtained. Account must also be taken of the generation's output transformer setting as this has a direct effect on both the output voltage and current, therefore altering the generator power output.

### 4.3.2 Extended Convergence Information

In order to determine whether the simulator is modelling the system accu-

rately, it was necessary to adapt internal functions of the simulator to be able to examine the internal states which were not previously available.

The convergence of the network equations gives information as to where there could be a difference between the power system and the model's topology. The simulator iterates the machine and network equations separately in order to obtain a sufficiently accurate solution as shown in figure 4.2. Careful note must be made if the simulator begins to require more iterations in any of the sets of equations. If this is observed it is a sign that there are major errors or differences between parts of the simulation equations. If it was suspected that the extra iterations were due to a topological error then the topology determinator was used to ascertain the exact nature of the problem.

The topology determination analysis was performed only when a topology inconsistency between the DOLSE model and the power network was expected or suspected. When notified via SCADA of a switch state change, a topology inconsistency was expected; however, some provision was made for when no notification was received via SCADA.

## 4.4 Summary

Having investigated models of the power system which provide more detail than the conventional models used for Dynamic State Estimation, it has been shown that the most appropriate model to be applied to the problem of State Estimation is that which is used for transient stability assessment. The existence of a transient simulator which has the capability to model the complete power system in real time speeds or faster with the level of detail suitable for the electro-mechanical time-frame, has led to the development of several useful applications harnessing this technology. In subsequent chapters its application to State Estimation will be presented.

A description of the simulator model used in this research has been presented. It should be noted that although the University of Bath's PowSim has been

used in this research, the aim is for the work to be generic. That is in the sense that any other appropriately configured simulation engine could be utilised to perform DOLSE analysis in the future.

An important feature of the simulator used within this work is its ability to run faster than real time so that it may be used in a predictive and analytical capacity, and also its ability to *mark time* providing a model of the system which may be state synchronised to the real system. For the state synchronised simulator the ability to increase or decrease the speed is important because the model must match real time as closely as possible. This gives the state synchronised simulator the ability to *fast-forward* or *rewind* its operation. In order to perform sufficient executions of contingency analysis either for stiffness calculations or topology determination, as fast an execution as is possible is necessary.

Chapter Five

# Topology Determination

As was detailed within chapter 2, conventional state estimation relies on the topology processor. It is only in the Generalised State Estimation technique [21] where this is dispensed with. Incorporation of topology information leads to a complicated SSE implementation within which it could be difficult to trace convergence problems. A technique using contingency processing within an Electro-mechanical Transient Stability Power System Simulator is now presented, and the added advantages which this brings are shown.

With conventional State Estimation where the topology is determined by the *Network Topology Processor*, the state estimator uses the output assuming that this topology is correct and continues its task. If it is incorrect, major convergence problems can result.

## 5.0.1 Concept of Topology

The topology of the power system is the connectivity of that system. Under normal conditions the power system is operated as a single interconnected system. If outages occur, however, it is possible that the system will become several isolated power systems. These isolated power systems within what would normally be a completely connected system are termed *islands*. To check whether the system has become islanded in any way, use of a flood fill algorithm may be employed [33]. To test the validity of the switch states compared to the analogue system values a more complicated procedure is

required.

The system actually exists at a *bus-section/switching* device level. To reduce the order of the state estimation problem this level of detail is generally reduced to form a *bus/branch* detail model for the EMS State Estimator. Another important function of the model update within a conventional EMS is to keep a record of the location of the measuring devices relative to the circuit elements.

Power systems contain switches of two major types: circuit breakers and circuit isolators. The main difference between these is the circuit breakers' ability to break both operational and fault currents. Isolators are designed to operate in situations only where there is no current flowing, in order to physically electrically isolate plant.

## 5.1 Present Approaches

Singh and Glavitsch [40] present a technique based on a rule-based algorithm which validates the switch position using the information from the EMS database. The analogue measurements and switch positions are checked for consistency.

The basic formulation for an expert system could approach the problem in the following manner:

*for* (each switch)
*if* (SCADA-digital reports switch is closed
*and* SCADA-analogues report zero voltage difference across switch)
*then* flag switch status *OK*
*else* flag switch status *ERROR*
*endif*

*if* (SCADA-digital reports switch is open
*and* SCADA-analogues report zero flow)

*then* flag switch status *OK*
*else* flag switch status *ERROR*
*endif*
*endfor*

There are a variety of ways to approach the topology determination problem. That presented above is to pre-process the data with a rule based method, and then filter out any errors which this detects.

A good example of an integrated topology determination device is the advanced topology tracking method proposed by Prais and Bose [41]. This processor reduces the computational overhead required for the formation of the state estimation matrices by calculating the best ordering and factoring of the network solution matrix. It tracks the topology changes on the system. For small topology changes the topology processor instructs the SE not to rebuild the matrices. For large changes the topology tracker works like a conventional network topology processor. By knowing the magnitude of changes from one cycle to the next the computational overhead is reduced by allowing the matrices within the state estimator to be retained from one cycle to the next if the network has not significantly changed.

### 5.1.1 Artificial Intelligence Approaches

Vinod Kumar [11] proposes a topology processor and static state estimator combined, implemented using Artificial Neural Networks. The work simply treats a breaker open at one end of a line as a complete line outage, and does not utilise composite indices to ensure the best combination of features in the data are used for training. Selecting the best composite indices could perhaps have aided the arrival at a correct determination.

Another formulation of topology determination using Artificial Neural Networks (ANN) is proposed by Souza [42]. This paper proposes training ANNs

to identify specific topological configurations. Several ANNs are trained per busbar in order to ensure that a solution is always found. However, there is a significant overhead in training such a large number of ANNs and storing their configurations so as to be easily utilised. In addition, the correct ANN must be chosen to evaluate a particular topological change. The authors do not appear to consider the implications of the ANNs being trained for a particular system operating point - for example trained for a lightly loaded system but then applied to evaluate the topology of a heavily loaded system. As may be seen there is a great amount of processing and training so that all possible eventualities may be correctly identified. It is possible that a linear programming approach as suggested by Sterling and Irving [43] may be more effective.

## 5.2 Dynamic Topology Determination

For a fully deterministically specified problem such as topology determination a rule-based approach can provide a good solution method. A rule-based approach with a time domain electro-mechanical simulator at its heart is now presented. Complete modelling in the time domain has benefits in deciding which incoming SCADA data should be screened, in addition to the method's ability to identify the correct topology.

### 5.2.1 Time Domain Simulation Approach and Benefits

Conventionally load-flows with expert systems attached, or in Generalised State Estimation, extra state variables relating to pseudo measurements may be used to determine the system topology. For a technique involving a state synchronised model the aim is that most data received from the SCADA network is utilised. Incoming data from the SCADA system may not be time-stamped. Due to the marshalling process of the data network it is normally impossible to tell which values in the EMS database are from within the period of a system transient. By the time a conventional state estimator calculates that there is a problem in its initialisation data set, time has moved on and the

transitory data is removed from the database. However, as data is used as soon as possible in the DOLSE method, this could cause problems in the state synchronised model if it were corrupted.

### 5.2.2 Details of Implementation

The input for the topology determinator is a study file output from the DOLSE simulator. This study file is parsed so as to ascertain the correct set of contingencies which should be tested using time domain simulation with the methodology described below.

If a pole slip occurs during time domain simulation, the results obtained are only certain up to the point of the loss of synchronism. An algorithm was constructed which traversed the study file appropriately in order to build a suitable contingency list. The method used for this process may be more easily seen from figure 5.1. In cases (a), (b) and (c) the busbars of interest are marked with a large cross. For a suspected or expected topology change at these busbars contingency analysis must be performed for each line marked by a small cross.

However in cases (a) and (b) this would cause the islanding of part of the power system in the case of the small cross which has been circled, unless the generating plant is tripped at the same instant as the line. If the generation were not tripped, the simulation would be terminated early. In contingency analysis this would be the desired mode of operation as unstable contingencies are unacceptable and may be easily found by this feature - but in DOLSE early termination is not the desired mode of operation because the transitory and the post-fault steady state data need to be available.

In case (c) the islanding of a significant part of the system would need to be identified and dealt with in a suitable manner. In this instance the generation need not be tripped.

In the case of system islanding, the transmission line most likely to trip due to

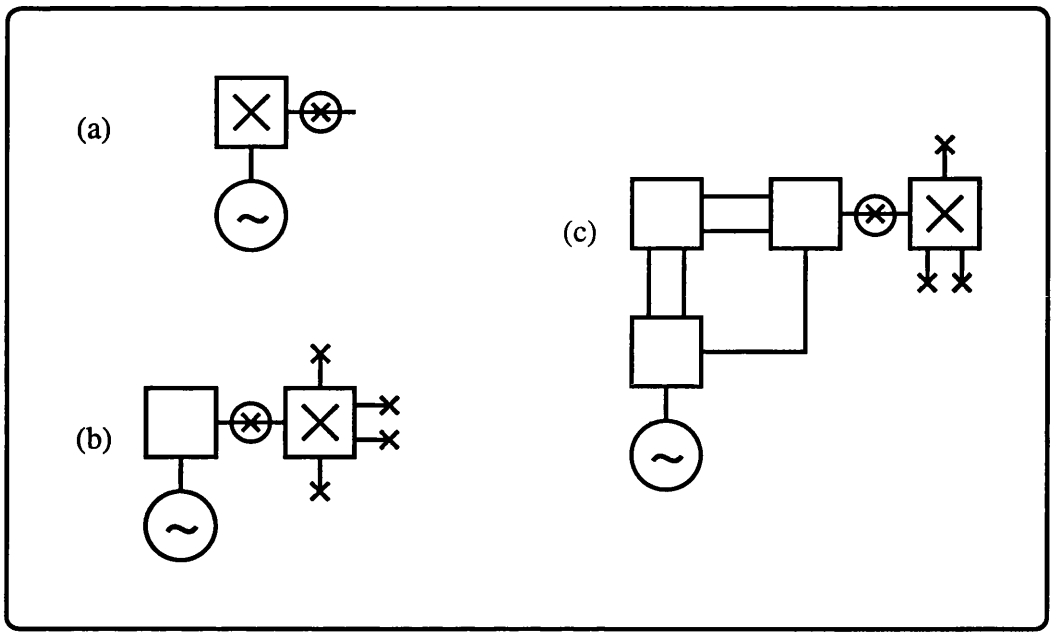


Figure 5.1: Occurrence of power system islands during topology determination

intra-area power oscillations would be the most heavily loaded transmission line on the system. Heavy loading indicates a large power flow, and a large power flow on the line interconnecting the system which is then tripped would mean that each island would suffer frequency excursions. One island would contain more generation than demand, in this section of the system the frequency would rise. The other island would contain more demand than generation, in this section the power system frequency would fall. Any calculations performed prior to the system split regarding both the real and the reactive power system stiffness would be rendered invalid. Processing after a system split is identified as a topic considered for investigation in the Suggestions For Further Work chapter 10.

Conventional power system topology processing takes its input as a switch/bus section data set. This is processed to form the bus/branch model, with careful note made of the configuration and location of the metering. Dynamic On-Line State Estimation is designed and operates around a bus/branch model. Switch section modelling within the simulator would require an appropriately

detailed study file to be used. This could be possible in the future, enabling the majority of the system to be studied in bus/branch detail with a specific part of the system modelled in switch section detail. It has been considered important to test DOLSE on a large bus/branch model as this data was easily available rather than an even larger switch section model. Using a switch section model would be possible, however the computational processing power available at the present time is insufficient to allow real time operation. A switch section model would contain in the region of 6000 nodes and 9000 connections for the England and Wales transmission system.

The major advantage of using a transient simulator as the model to determine the system topology is that a complete time history of the phenomena occurring at a topology change is available. In this work it has been found to be sufficient to record the envelope surrounding oscillations of relevant variables. Time stamping the maximum and minimum values allows easy corroboration of incoming SCADA data.

In state estimation a conventional topology processor using load-flow analysis takes no consideration of the system's dynamic response. Due to the large number of data sets available for the initialisation of the EMS data processing cycle, if a topology change has occurred, the next set of data available which is definitely post-transient may be selected in order to re-initialise the cycle. In synchronising the transient stability model to the actual power system this is not possible. Indeed the electrical power system is never in a true steady state. Using the transient simulator, better predictions may be made of the system's mode of behaviour post-transient. Therefore better utilisation of data available from the power system may be made because it can be predicted with a high degree of confidence that the data is not from within an oscillatory period.

If DOLSE were installed directly attached to a SCADA database within a conventional energy management system it would rely in the first instance on a simple mapping function to convert the switch section data from the database into bus/branch information. Generally the switch section model

has had the nomenclature carefully selected so as to be meaningful both to inspection by a control engineer and for automatic processing to form the bus/branch model. The feature of standard nomenclature could be harnessed in the future by DOLSE to allow easier integration of a switch section model to the methodology.

Complete analysis of a topology change is available using DOLSE rather than simply using Kirchoff's voltage and current laws on the pre and post fault steady state system. This DOLSE analysis can be completed within a time-frame in order to make its use beneficial.

There are two possible types of topology change, those changes which are expected and those which are unexpected. These unexpected changes may or may not be suspect. Notification of expected topology change is received at the Power System Control Centre via the SCADA communications network. If a breaker or isolator changes its configuration this information is immediately transmitted. The data is marshalled within the SCADA network to arrive at the Control Centre as quickly as is possible.

Unexpected changes are not notified to the Control Centre via SCADA. If they remain undetected it can cause problems later when the simulator is trying to maintain synchronism to the system. The most important errors which must be removed are these ordinarily undetected topological changes. Errors should be normally suspected rather than being allowed to remain unnoticed.

This is achieved by carefully processing incoming analogue data. Any analogue data which is seen to be significantly different from the previous SCADA value from that metering is flagged if the change is unexpectedly large and there has been no digital switch status change notification. Incoming analogue data which lies beyond its expected error variances when the greater part of the model is adequately synchronised is also noted. Another indication of topological change is a large change in frequency which cannot be found to be immediately attributable to a system event or occurrence that is known of within the SCADA database.

In order to ensure that the topological model within the synchronised simulator is consistent with the actual topological configuration of the power network the ordering of contingency processing is very important. The contingencies are processed in order of the expected or suspected topological change followed by any other possible system changes. If the degree of confidence in the predicted states of the system is sufficiently high after processing the expected or suspected topology change, the topology change is applied within the synchronised simulator. This value is flagged as potentially suspect until all the other contingency evaluations have been performed and it is certain that this is the change which actually occurred. If it is subsequently found not to be the case, the synchronised model is rewound and the most likely topological change as found by the topology determinator is applied.

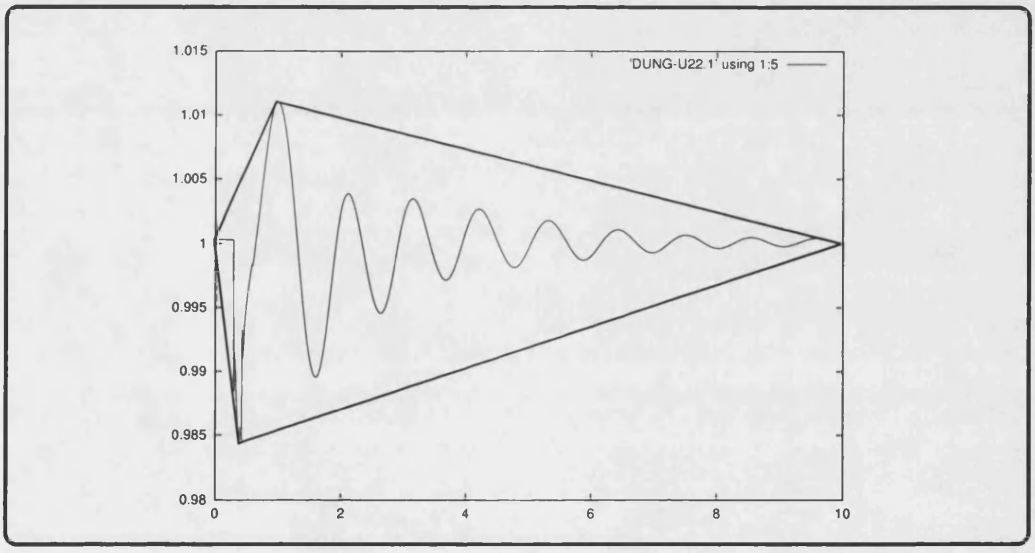


Figure 5.2: Diamond envelope around busbar voltage oscillation

The advantage of this technique is that the information provided from the simulation is not solely the final load-flow solution. Envelopes of system variables may be found by parsing the time history of that system variable. To minimise the amount of redundant data produced these envelopes may be either of a diamond or a horizontally aligned rectangular shape (see figures 5.2 and 5.3).

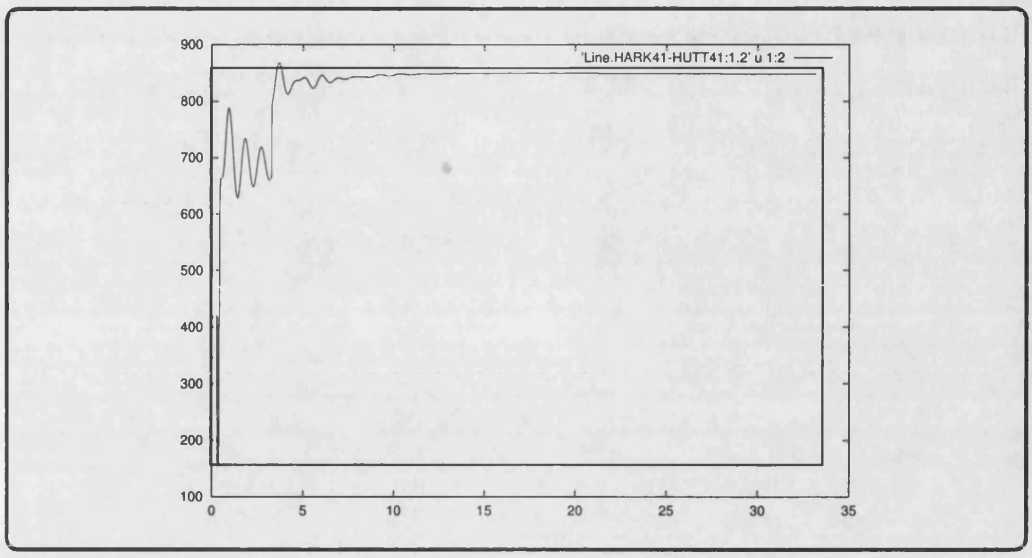


Figure 5.3: Box envelope around power flow oscillation

With variables where the transient deviation is much larger than the equilibrium pre to post-fault change, such as voltage magnitude, it has been found that the most appropriate envelope to describe the time history is a diamond. If a line is removed, the power flows on nearby lines could change value significantly between pre and post fault. These situations are best represented using a rectangular box envelope. As data arrives at the power system control centre from the SCADA network it would be expected that the data value will be within the envelope. Because data is not time stamped when it is metered there is no way of telling where on the variable's time history the metered value has occurred. It may be accepted as being consistent with the time domain simulation output and lie within the envelope or it may be rejected if it does not lie in the envelope. If this is the case then it is safe to assume that a significant system change has occurred - one which it is not possible to ascertain by simply evaluating single contingencies. Either the synchronised model must wait for a new set of time-skew minimised auto regressive filtered data or double outage contingency analysis could be performed. Due to the much larger number of possible contingencies when evaluating to a security of $n-2$ the sub-set of these contingencies involving double circuits should first be considered. This

is termed a security of $n-d$. These $n-d$ outages are more likely to occur than the larger set of the $n-2$ outages of which they are a part.

Using this technique it is possible to more selectively reject data which is out of bounds following a topology change. Previously this had been impossible to achieve. Blanket data exclusions for the period following a topology change would previously have had to be applied. This does not lead to the SCADA data stream being continually available as soon as its values lie within acceptable bounds. In the future it will be possible to utilise the entire variable envelope rather than just the box or diamond approximation. However, at the present time there is no need for a more accurate technique, and in any event it would not be practical as time stamping of data on receipt is of limited accuracy and subject to the vagaries of the SCADA network and its marshalling characteristics. With this method the expected or suspected switch/topology change is more immediately and accurately known and as such can be safely applied in the synchronised simulator. Conventional state estimation would rely on information from a multiple interacting bad data detector. With the DOLSE approach - the system model oriented approach - it is more immediately apparent where inaccuracies lie. DOLSE aims to competently take a bus/branch model and detect any anomalies within this. The same methodology can be applied to the switch section models which will be used in the future.

In summary the method is as follows:

- give the topology determination software the busbar of interest, where a topology change is either expected or suspected
- construct a contingency list of all lines connected to that busbar - include the intertrip of generation where appropriate to negate the possibility of single busbar power islands
- process the contingencies on a distributed set of heterogeneous workstations

- process the data from the time domain simulation - extract the expected envelope of operation for metered parameters at the relevant busbars local to the topology change
- compare the topology determination contingency output to the SCADA information and rank the contingencies in order of their likelihood
- determine which switch change is most likely to have occurred
- apply this topology change at the appropriate instant in the DOLSE model
- ensure that incoming SCADA data is rejected from any period of time on any busbar where oscillations are forecast to occur.

## 5.3 Topology Determination Results

Examples of the data files generated by the topology determinator may be found in appendix C. The Dynamic Security Assessor was used to determine the line most likely to cause transient instability of the power system model used. The model represented the complete grid system of England and Wales; however, it had been artificially stressed in order that the system would exhibit transient and oscillitary instability for some contingencies. This provided an extreme scenario under which DOLSE performance could be evaluated. The line outage which caused the greatest level of transient instability was found to be the double circuit outage of Lackenby 275kV to Greystones 275kV lines 1 and 2. This outage is used as the example in chapter 8, so in this example another line has been arbitarily selected. The topology determinator was instructed that Greystones 275kV was the busbar of interest, so output is given for all lines connected to Greystones 275kV substation. The SCADA emulator data set is formed with the first circuit from GRST2B to WILT6 out of service in the system emulator.

By using a minimum least squares error formulation utilising data from all the power system metered values adjacent to this substation, it is possible to find the most likely topology change.

With the detailed analysis provided using this method it is necessary to exclude gross measurement errors. Providing sufficient data is available from the system around the substation, success has been achieved by excluding the measurements of the power flows from the suspected line, and the line removed during the contingency as applied by the topology determinator. If this operation were not carried out the gross errors would override all others, rendering the calculations useless.

The additional benefit of this technique is the full time domain output which it provides. This enables analogue SCADA data values to be accepted by the on-line state synchronised simulator when the software is sure that no oscillations are occurring on the system due to known topology changes.

The results presented within appendix C show that the topology determinator has been able to correctly identify that the first circuit joining GRST2B and WILT6 is the outage which was applied within the SCADA emulator. The Mean Square Error (MSE) is lowest for contingency four, which is the contingency including the application of that particular outage to the system. However, when examining the MSE for all six contingencies applied in turn, it may be seen that the MSE is small for both contingency three and contingency four. As the topology determinator operates at the level of a bus/branch model, and as both lines have the same parameters, it is unable to conclusively prove which of the two lines is out of service.

In terms of constructing a model for Real Time Network Analysis tools, this is an acceptable approximation. In this instance the state synchronised model would apply the topology outage for which the digital switch status data corroborated the analogue real and reactive power data, namely the outage of the first circuit. In the future, when switch section level models are implemented within DOLSE, the dynamic topology determination approach

would be expanded to identify the correct solution more robustly.

## 5.4 Summary

Topology determination using the transient simulator approach described within this chapter is the best method to apply to effectively screen incoming SCADA data to ensure that a state synchronised transient simulator is not corrupted in any way. In addition to this it provides a useful function as not only a topology determinator but also as a contingency evaluator. If instability of a thermal, voltage or rotor angle nature occurs, this may be immediately notified to the control engineers as a potential future problem. The topology change which causes the instability may not have actually occurred in this instance, but the information gained by testing this contingency may be used to reconfigure the system so that it is more secure in the future.

Chapter Six

# Power System Stiffness

The model of the power system which is used within the time domain simulator is constructed from the same set of data used to form the model for the off-line simulation tools. The off-line tools use detailed models of the system for the purposes of planning. This model is detailed to the extent necessary to model the power system's transient stability, including dynamic as well as static phenomena.

A static load-flow study file is normally used to construct the contingency database as utilised for Dynamic Security Analysis. In this implementation the same file is used to generate a set of contingencies. However unlike DSA the tripping of lines is not considered, only busbar loads. In this implementation the system frequency is more carefully monitored. A contingency list is constructed by the software which contains contingencies for tripping all loads on an individual basis.

The system frequency and mean system voltage are monitored in order to help quantify the imbalance in real power and the imbalance in reactive power on the electrical power system. This information is used in the data screening process employed before data is injected into the state synchronised power system simulator.

## 6.0.1 Concept of Stiffness

The change in real power for a change in the frequency of an electrical power

system is known as the *stiffness* of the system. The smaller the change in frequency for a given real load change, the stiffer the system.

Power system frequency is generally regarded as being common to all parts of the system. For this reason it was the first quantity which was applied as an input to system control devices. These were the governors of the generating sets, originally consisting of a rotating fly-ball used as the actuator to a hydraulic system which opened or closed the throttle of the prime mover. This increased or decreased the amount of energy input to the plant, thus maintaining the speed of the plant at the desired value. Nowadays electronic governors sample the electric waveforms, obtain the frequency and perform the speed control.

Stability of a large interconnected power system is of prime importance. It is for this reason that governors have a *droop* characteristic. This is in regard to the relationship between speed and load. For stability it is ensured that as load increases, speed decreases, as in figure 6.1. The nominal operating frequency of the UK system is 50Hz, in the USA the nominal frequency is 60Hz.

As frequency deviations of the system under fault conditions vary depending on the size of the system, the loading of the system, and the magnitude of the load change or generation change, studies need to be performed using an accurate system model in order to quickly determine the stiffness at the present operating point.

Modern Power Systems typically contain a function within the EMS termed Automatic Generation Control (AGC). This function has a target to maintain power system frequency and interconnecting power flows within specified limits. It operates on a time-frame of a few seconds to a minute. Digital control signals are sent to generators which are controlled by the AGC to instruct them of their required settings in order to maintain system-wide targets.

The system which this model is applied to - the England and Wales National Grid System - is not a vertically integrated supplier of electricity. The

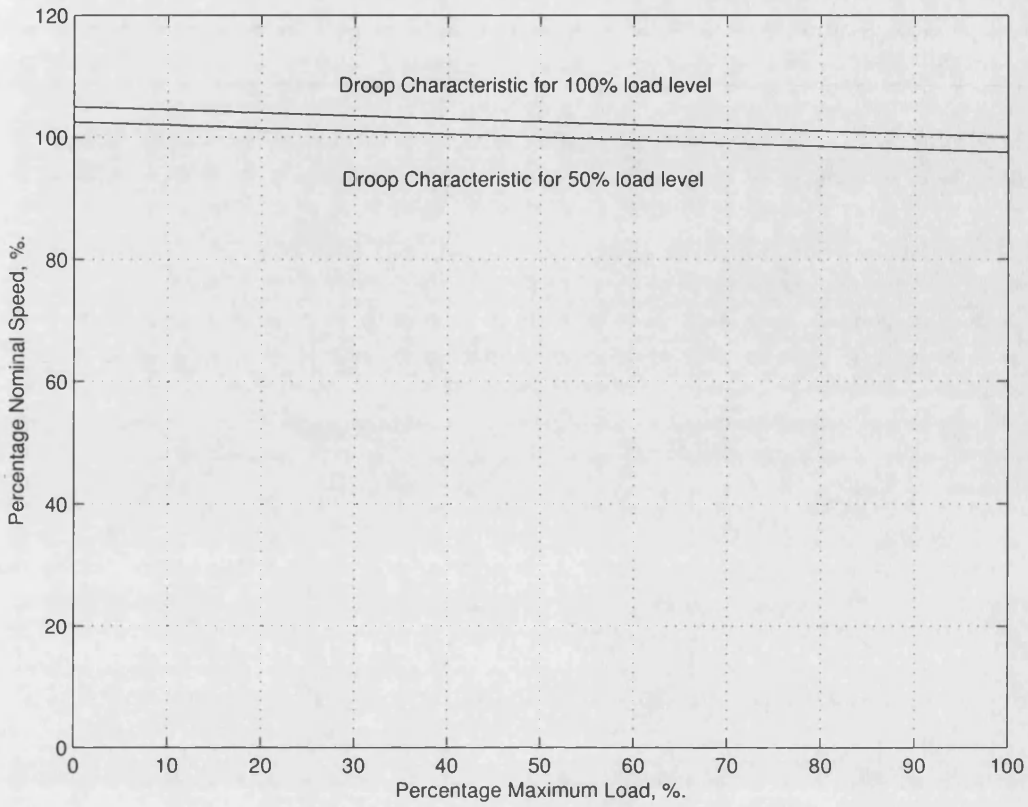


Figure 6.1: Governor speed/load characteristic exhibiting droop

generators available are ranked in order of the cost of their bids and the cheapest plant is utilised first. This *unit commitment* takes place twenty four hours in advance of the system operation. Closer to the point of system operation, dispatch is performed using the Dispatch Algorithm of the EMS. AGC does not feature in this methodology of operation for historic reasons. Individual plants are contracted to provide ancillary services decided in the time-frame of the unit commitment; they then provide a droop characteristic or rapid response capability depending on the contract type.

If Dynamic On-Line State Estimation were applied to a system which contained AGC, the model would have to incorporate the dynamic response of the AGC in addition to the dynamic response of the system. This would have to be analysed carefully and taken into account in the model synchronisation process.

It is envisaged that using the work developed here, the existing capability of AGC software could be increased. Conventional AGC simply uses linear models, but if it were to use DOLSE output rather than raw system data the system frequency sensitivity would be more easily available and even tighter frequency tolerances could ultimately be maintained.

## 6.1 Real Power Relationship ($\Delta$P/$\Delta$f)

The ratio of the change in real power, $\Delta P$, to a given change of frequency, $\Delta f$, of an interconnected power system is termed the system *stiffness*, $K$:

$$K = \frac{\Delta P}{\Delta f} \tag{6.1}$$

Figure 6.2 shows the steady state post fault system frequency for loss of loads at all substations in arbitrary areas *I* and *II* of a time domain electro-mechanical model of the England and Wales transmission system (PowSim). The two lines

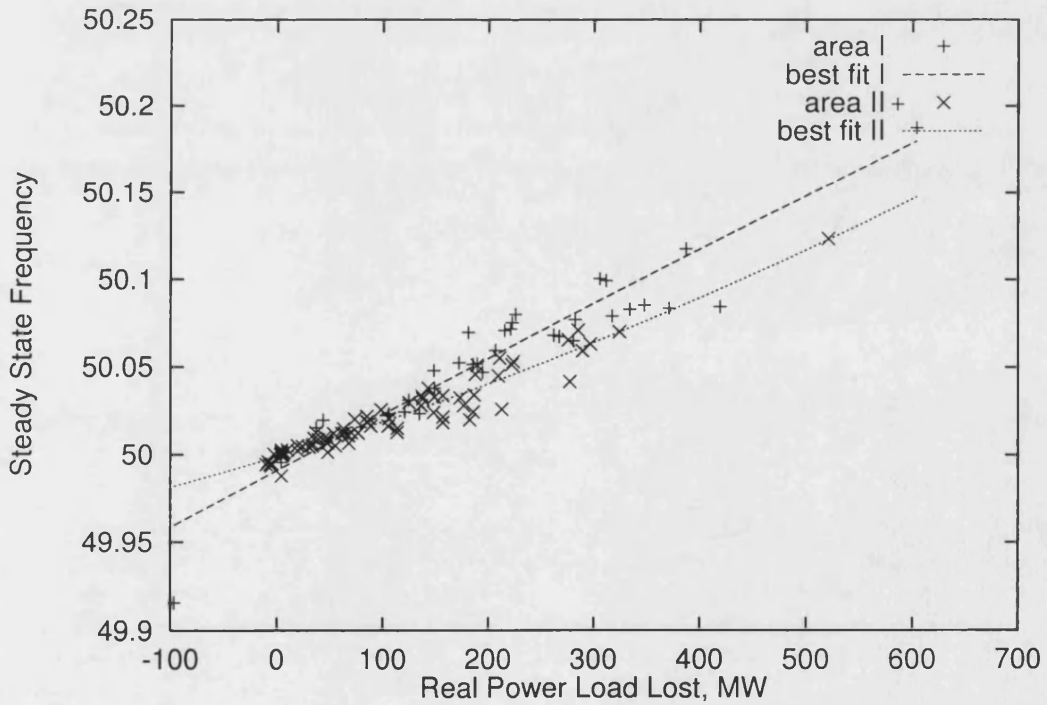


Figure 6.2: Change in frequency for a change in real power post-transient

of best-fit show that the stiffness is not uniform for loss of busbar loads of the same magnitude in different areas of the system. To ensure that steady state was achieved the simulations were run for a duration of 30 seconds post-transient before the measurement of frequency was taken.

### 6.1.1 Power System Transitory Real Stiffness

Figure 6.3 shows a plot of the peak system frequency against the loss of real power load at busbars in the same two areas of the power system. This peak in frequency occurs on average 11 seconds after the loss of the load. The similarity of the two plots shows that there is a strong relationship between the system peak frequency and the steady state frequency after 30 seconds.

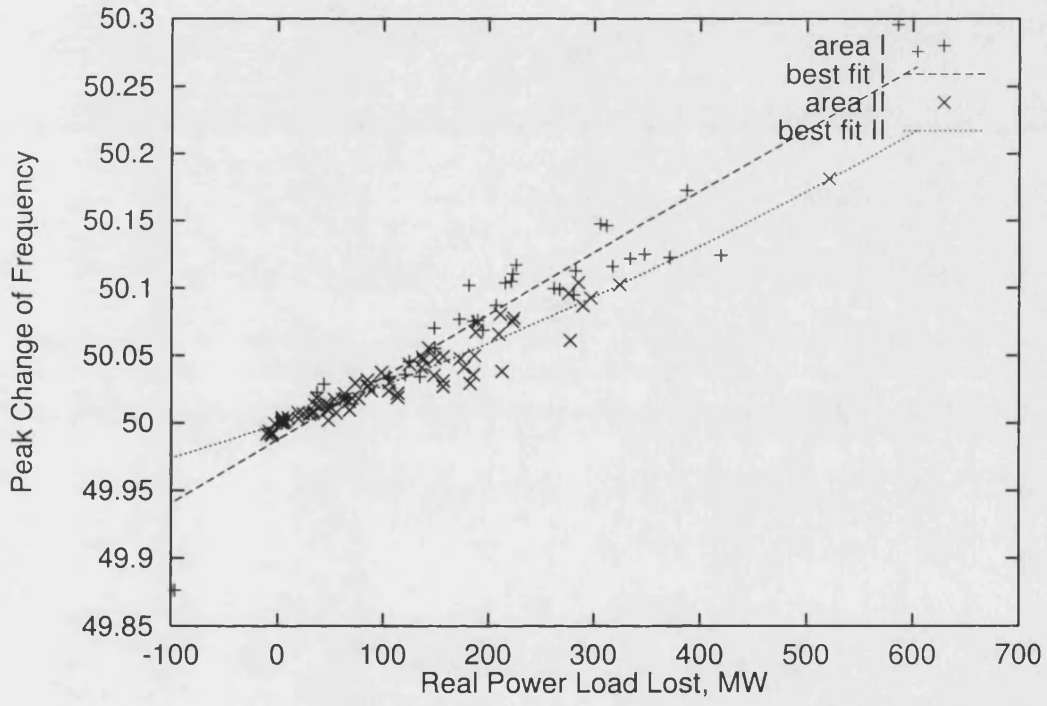


Figure 6.3: Peak of change in frequency for a change in real power

The gradient of the the lines of best fit in figure 6.3 may now be termed $K_{transient}$, and may be calculated by the ratio of $\Delta P$ to $\Delta f_{max}$:

$$K_{transient} = \frac{\Delta P}{\Delta f_{max}} \tag{6.2}$$

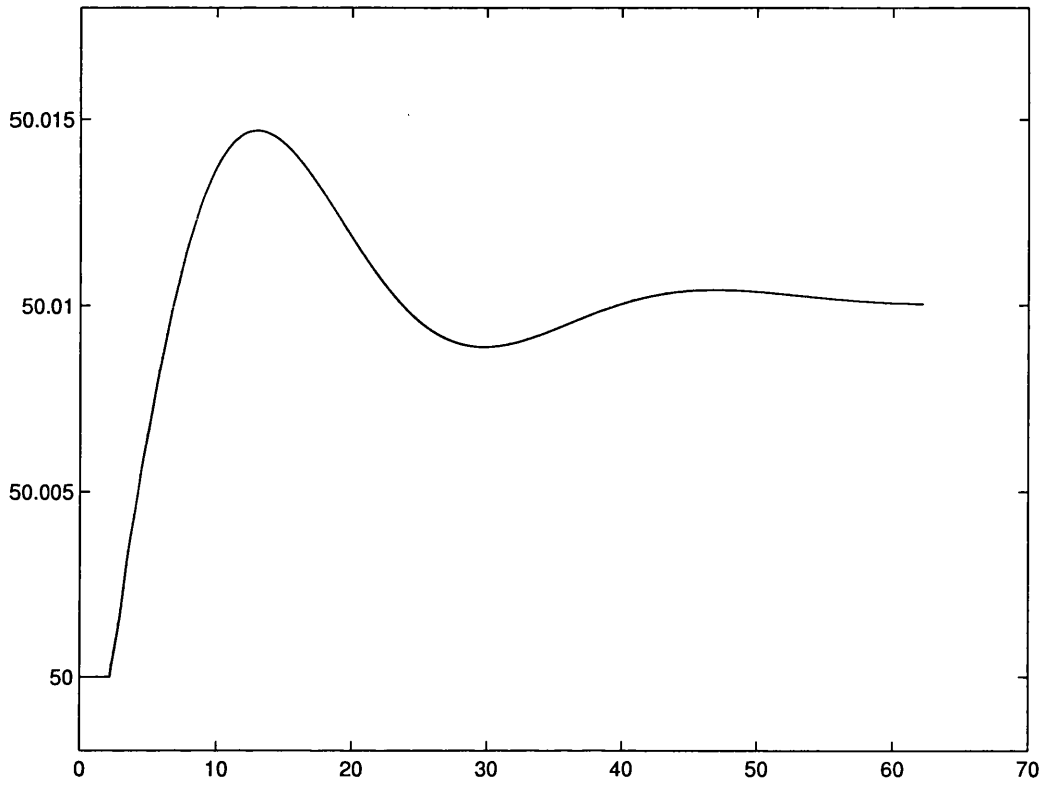


Figure 6.4: System frequency following loss of load at SIZE81

If system stiffness is calculated off-line by running power system studies, this may be used on-line with frequency information to estimate the rate of change of real power imbalance. Use of the frequency data in this manner aids the estimator to track the power system.

The calculation of the $K_{transient}$ characteristic off-line may be achieved three times more quickly than the calculation of the original $K$ stiffness characteristic. It should be noted that once an increase in frequency has been detected from the frequency trace, with pre-calculated estimation of $K_{transient}$ it is possible to ascertain the changes in the real load imbalance of the system within approximately 12 seconds (dependent on governor characteristic), rather than having to wait for the system to settle into steady state (minimum of 30 seconds). This makes $K_{transient}$ immediately more useful than $K$ (see figure 6.4).

### 6.1.2 Real Stiffness in event of System Split

If the power system becomes unstable and is split into more than one system, any method which relies on knowing the system wide frequency value and system wide stiffness will run into difficulties. It is most likely that in the event of a system split the lines which trip will be the most heavily loaded on the system. Therefore with at least two distinct islands one island frequency will rise because generation is greater than demand, and in the other island frequency will fall as the demand would be greater than generation. Methods to incorporate the modelling of the power network when it is in an islanded state are discussed in the Suggestions For Further Work chapter (10).

Location of the frequency measurement equipment which provides the data to plot the frequency trace must be known, and the effect of load/generation changes must be known relative to those locations, in order to correctly determine the stiffness response.

## 6.2 Reactive Power Relationship ($\Delta Q/\Delta V$)

When considering the equations describing the power system it is appropriate for some applications to work in terms of a decoupled formulation, namely the separation of the real and reactive power equations. The variables within either set of equations have a minimal impact on the solution of the other set of equations. In these terms frequency is strongly linked to real power imbalance, and voltage magnitude is strongly linked to reactive power imbalance.

Although it is convenient to decouple the equations, the interactions should be carefully borne in mind. As may be seen from figure 3.2 the AC line model includes the shunt capacitance. The natural loading of the line occurs when the reactive power absorbed by the series reactance is equal to the reactive power generated by the shunt capacitance. It should therefore be noted that large real power flows through a region without reactive compensation can cause a

significant voltage drop. The reason for this is the absorption of reactive power by system equipment which is run above its natural loading. The cause of this phenomena is large Mega-Watt flows but the results are seen in the reactive equations.

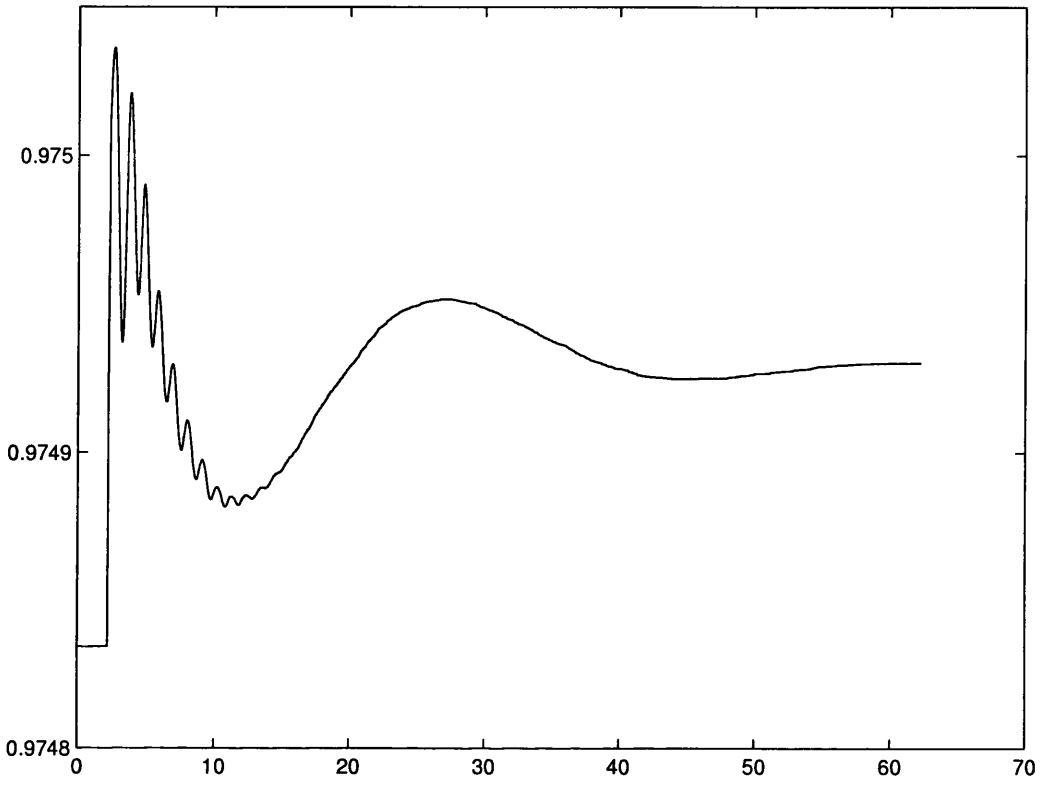


Figure 6.5: Mean system voltage following loss of load at SIZE81

Reactive power may be thought of as that part of the apparent power which achieves no useful work, but is necessary due to the electro-static and electro-magnetic storage requirements of the system. Due to the $I^2X$ losses of an overhead transmission system being typically ten times greater than the $I^2R$ losses, reactive power balance is more of a local phenomena rather than a system wide one.

Reactive power balance is indicated by the voltage magnitude. Reactive power is needed to support the network voltage. A deficit of reactive power causes the voltage to fall, whereas too much reactive power causes the voltage to rise. At each time-step of the load loss simulations the mean of the voltage at all

busbars was calculated. In this work this has been termed the Mean System Voltage (MSV). Figure 6.5 shows the mean system voltage for the loss of the load at Sizewell unit 1's generation busbar. This is quite a small load of 26 MW and 13.32 MVAr. This rise in system voltage is not measurable on a per meter basis, however when using all voltage meters available on the system by taking the mean of their readings we can obtain some insight into the reactive power balance on the system as a whole.

As may be seen from figure 6.5 the change in the mean system voltage is non-linear. The best method to calculate the Mean System Voltage off-line so that it may be used on-line, is full time domain electro-mechanical time-frame simulation. This is best able to fully take into account all the phenomena which the incoming SCADA data is liable to be affected by.

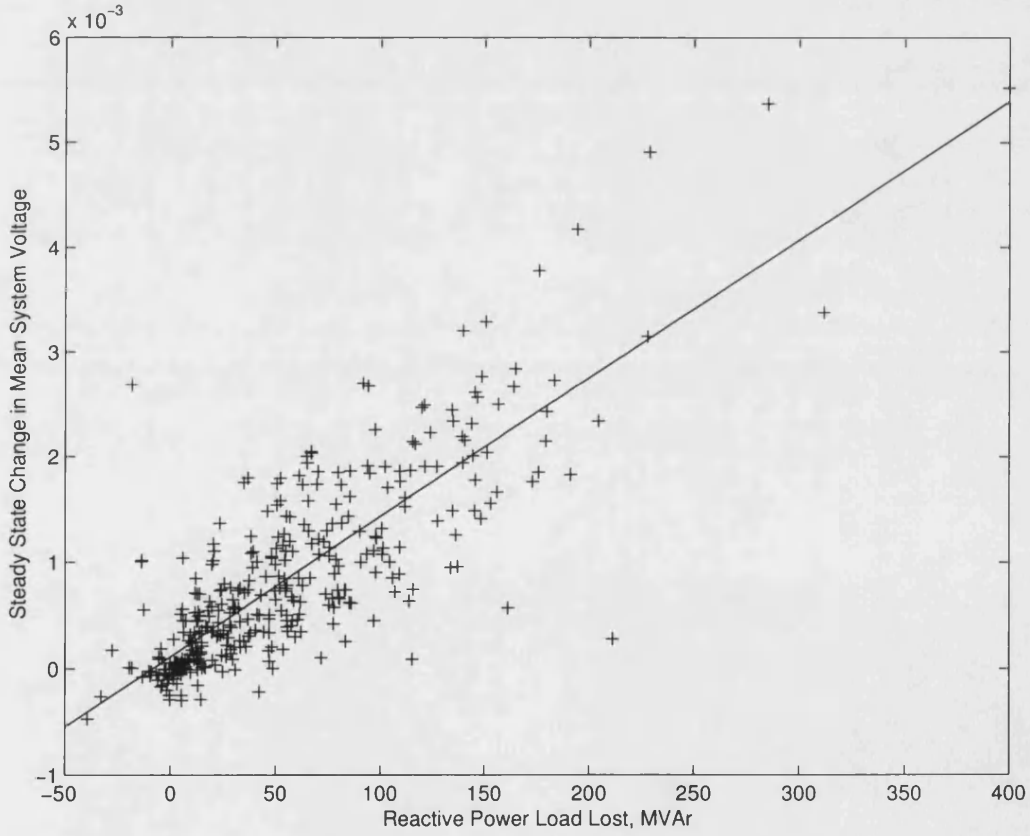


Figure 6.6: Change in mean system voltage for a change in reactive power post-transient

As for the real power example previously in this chapter, we will consider the steady state mean system voltage, and the peak mean system voltage seen after the loss of a load. Figure 6.6 shows a plot of the mean system voltage versus the magnitude of reactive power lost after the system has reached a steady state mode of operation following the loss of the load. The line of best fit of these points has also been plotted on the same axes. As may be seen this line of best fit has a gradient similar to that which we would expect. As the magnitude of the reactive load lost increases, so the mean system voltage also increases.

### 6.2.1 Power System Transient Reactive Stiffness

When running the DOLSE state synchronised power system model it is important that it tracks the behaviour of the real system as soon as information may be processed from system data. The time until the system reaches steady state in terms of the mean system voltage oscillation is approximately the same as the length of time that it takes the system to reach a mode of steady state operation in terms of the system operating frequency. The power system is always changing, and could be considered never to be in a steady state mode of operation. This means that the voltage rise seen over the 40 second period could not necessarily be attributed to the loss of a specific magnitude of reactive load over that period on an actual power system. For this reason it would be more advantageous if there was information regarding the reactive stiffness in terms of a peak value of the rise seen in the Mean System Voltage.

Figure 6.7 shows the relationship between the peak of mean system voltage versus the magnitude of the reactive power lost. From this figure it may be seen that there is again a trend in the data as would be expected - the peak mean system voltage increases as the size of the reactive load lost increases. In using the simulator it is possible to take the mean of the system voltage for every busbar in the system once per time-step. On the actual system this degree of synchronisation is impossible to achieve. For this reason use of the peak mean system voltage could not be implemented in a practical way

- unless some form of measurement synchronisation were performed to a high time resolution, such as by using the Global Positioning System Universal Time Clock as described in appendix F. If the system were in steady state use could be made of the steady state mean system voltage information obtained from the off-line calculations.

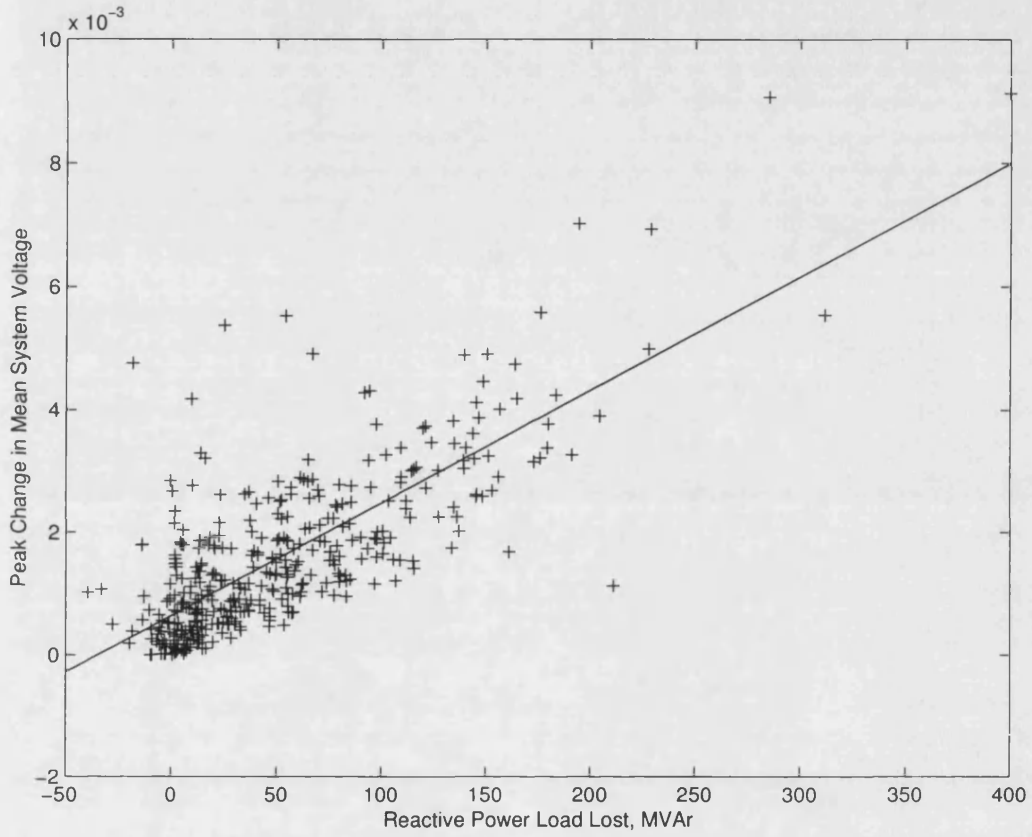


Figure 6.7: Peak change in mean system voltage for a change in reactive power

## 6.3 Software to Calculate Real and Reactive Stiffness

During the course of this research a version of the power system simulator has been modified to allow the output of variables pertinent to the evaluation of the power system's real and reactive stiffness characteristics. Full numerical results from this implementation may be found in appendix D for the loss of

any real or reactive load connected to the system. The model used for this is a full representation of the UK National Grid System. To enable a complete evaluation of the phenomena the simulation was run for a duration of sixty seconds for the application of each of the 406 contingencies in turn.

### 6.3.1 Details of Implementation

A version of the power system simulation engine has been created which is able to directly output information regarding the stiffness characteristic of the electrical power system being modelled. It is supplied with a network study file and machine parameter database. The network study file is parsed to extract information regarding the possible contingencies which may be applied to the network in order to obtain the desired information. A contingency file is generated which simulates the whole system in the time domain for twenty second periods for contingencies which will have a direct impact on the power system's real or reactive stiffness. Each twenty second period has a contingency applied to the initial network state. This contingency list is the sub-set of all possible contingencies containing system changes where any real or reactive load is lost.

The results are collated within the power system simulation engine to avoid the huge quantity of storage space needed to keep all of the time domain transient response plots. The line of best-fit is calculated for each region of the power system and this information is passed to the database wrapping the state synchronised power system simulator. This ensures that it might better control the incremental search to match the model voltages and reactances to that of the system.

### 6.3.2 Results

The graphs of the stiffness characteristic presented in this chapter are the results of the system stiffness calculation engine. Full numerical results may be found in appendix D.

## 6.4 Stiffness Calculations within DOLSE

The methods outlined above have been found to be useful in the running of DOLSE. Rather than assuming that the generation and load are in balance, monitoring the frequency trace allows the software to determine the direction and approximate magnitude of any imbalance.

The database is updated from the real and reactive stiffness calculation contingency runs with information of the stiffness characteristic. When given the power system frequency and voltage magnitude data from the EMS, the database calculates the real power imbalance and the mean system steady state voltage. These are then used by the database to find the revised acceptable variance for each data type.

### 6.4.1 Interpretation

As has been discussed previously it is always necessary to model the system in an appropriate amount of detail in order to investigate phenomena of interest. A generator response to a change in loading may be found to fall into several categories. These may be discriminated between by considering the time-frame over which information is sought. For example Moore [44] investigates the response of a generator to momentary disturbances. Such disturbances are caused by short circuits in the transmission network which are cleared by power system protection devices. This chapter investigates the frequency response of the system over a longer time-frame. By studying what happens to voltage and frequency when a large load is disconnected from the system, it is possible to gain a better understanding of the longer term frequency excursions of the network.

The instantaneous generation characteristic of an electrical power system is highly non-linear. For example, machine maximum output limitations, excitation controllers, and governor limits all interact in a complex manner.

Due to the system's non-linear nature, the stiffness characteristic must be determined completely for a given point of operation. In this work that given point is the present operating point of the power system. From this point, for small power and frequency disturbances, it is appropriate to approximate the stiffness characteristic to be a linear relationship.

When considering the real power stiffness characteristic it is important to remember that it is made up of two components. Take for example an increase in the loading of the system - power system frequency falls, generation units increase their real power output and frequency dependent system loads reduce their real power demand. To ensure that a complete analysis of the transitory frequency response had been properly completed a series of simulations were run for a duration of sixty seconds. These simulations were completed entirely in the time domain. This ensured that no unexpected phenomena occurred.

It was expected that a transitory system stiffness could be identified. This is the increase or decrease of the power system frequency before the governor action of the generation plant comes into effect. In the loss of a system load the generators decrease their output to retain the nominal frequency. Transitory system stiffness for the system used in the example, was found to occur after approximately 12 seconds.

### 6.4.2 Limitations

In the models utilised to formulate this analysis only one load has been altered at any instant. The results have been formed on a system-wide basis. In a real power system it could be much more difficult to determine the demand imbalance of the system from frequency or voltage data. This analysis is performed as a rough guide to aid the DOLSE model to synchronise to the actual system. Events are examined in isolation within this research and then an attempt is made to apply them to the larger picture. It may be found that on a real system this was inappropriate.

As the power system frequency is the same system wide, if more transducers

are added to the system to measure its magnitude, the accuracy of the result will be improved. Power system voltage varies widely over the system, however the mean system wide steady state voltage does yield useful information regarding the reactive power balance. If part of the system has a low voltage the MSV will lower accordingly, however the MSV will not give any indication as to *where* the reactive imbalance is occurring - an imbalance which needs to be met on a local basis.

## 6.5 Summary

This chapter has presented the work undertaken to investigate the real and reactive stiffness characteristic of an electrical power system. The stiffness characteristic results both for steady state and transient stiffness have been presented and discussed. The application of the information gained from this analysis within DOLSE has been discussed.

Chapter Seven

# Total Dynamic On-Line State Estimation Implementation

Data is required by the Real Time Network Analysis Tools and information is needed by the control engineers as quickly as is possible. The incoming SCADA data is received frequently enough that differences between data from one measurement reading to the next can be considered to be due to phenomena within the electro-mechanical time-frame. The method used to process the incoming data needs to take account of this.

By using a time domain transient simulator in a variety of different novel ways the incoming data may be processed with consideration of electro-mechanical effects. In addition to this when notification of a topology change is received at the control centre the full effect can be modelled and the resultant state known before incoming analogue SCADA data can be utilised. Once incoming SCADA data is known to be free from any electro-mechanical transient oscillations, the incoming analogue data can then be used as soon as it is valid to do so in order to re-state synchronise the simulations to the real system.

## 7.1 Overview

Data is received from the SCADA network at the control centre where it is decoded and sent to the Dynamic On-Line State Estimator. Bad data or data from a period of system transient is identified as such and is rejected. Data

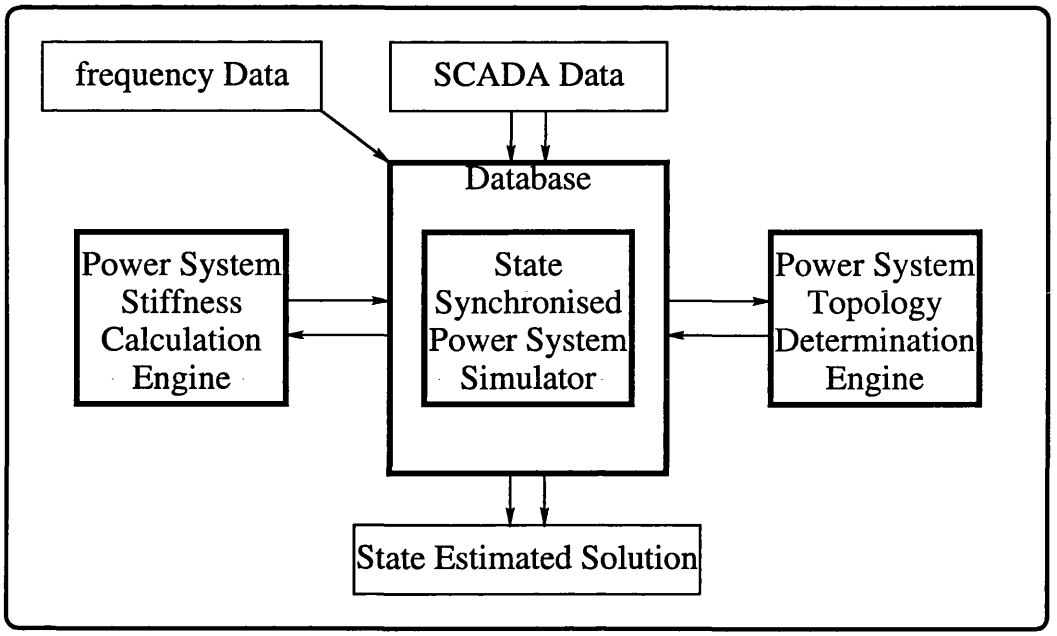


Figure 7.1: Diagram of Dynamic On-Line State Estimation implementation

which is deemed within tolerance of its expected value is accepted and used to state synchronise an electro-mechanical time domain transient simulator to the power network. The tolerance varies depending upon how close the system is to a steady state. This is estimated from data regarding the system's real power balance.

In addition to the state synchronised model there are two main tools in the suite of software which aid in the state estimation and time domain state synchronisation process. These are a time domain topology determinator as described in chapter 5, and a time domain power system stiffness characteristic calculation engine as described in chapter 6. The functional interactions may be seen in figure 7.1.

## 7.2 Hardware

The hardware used comprises a suite of PC based Linux workstations. These are a dual processor Pentium-Pro running at 200MHz, and two Pentium-II 300MHz machines. They are linked by two networks, the first is used for

control of the machines and runs at 10 Mega-bits per second via a hub, the second is a switched 100 Mega-bits per second network used for data transfer.

This configuration ensures that 100 Mbit/s is always available for large data transfers, with the control function and status monitoring managing quite comfortably within the bandwidth provided by the 10 Mbit/s network. Also the control function is effectively fenced off from the data flows. This means that even when the data network is heavily stressed, process and job control can still occur. The same functionality could have been provided by facilities within the TCP/IP stack, by assigning a higher priory to control packets, and maximum bandwidth utilisation for data packets. However the method implemented is not operating system dependent and is therefore more versatile.

For running studies with the 100 bus and 150 line network model initially used for testing, the dual Pentium-Pro machine was used to run both the SCADA emulator and the Dynamic On-Line State Estimator. The two Pentium-IIs were used to perform the contingency analysis for calculating the stiffness characteristic of the system, and for the topology determination.

For running larger studies, one Pentium-II was used to host the SCADA emulator, whilst the other ran DOLSE. The dual processor machine was then used to perform more selective stiffness calculations, and topology determination.

With the implementation of the two networks, it was possible to stop the stiffness calculations if it happened that the processing power was required to perform topology determination. This is a useful methodology to adopt since if it is scaled up to use more computing resources, a main scheduler can be used to decide which function each machine within the network of workstations is best used for at any particular time. High Availability (HA) could also be more robustly implemented with this approach.

## 7.3 Software Techniques

When constructing modelling software which is designed to be executed at real time speeds or faster, careful consideration needs to be made of the methods employed.

### 7.3.1 Network Sockets

The software developed has the ability to either send data to flat files to be loaded by subsequent programs which need to use the data, or transfer data between programs which require it in a fast dynamic manner by employing software sockets.

On a UNIX system virtual software sockets may be created bound to either a memory address, the network stack or the file system. Two programs (or more if necessary) are able to communicate along these software sockets.

When the programs in the DOLSE suite are running on separate computers they communicate using network sockets.

### 7.3.2 POSIX Threads

When writing programs it is important to use the best facilities of the standard programming libraries which are available. Communication can take place between programs on remote computers using network protocols, namely sockets bound to ports within the TCP/IP network stack. This is available within all implementations of TCP/IP on all platforms.

On UNIX systems which are inherently multi-user, multi-tasking machines, inter process communication is possible. Software *pipes* may be utilised to transfer data from one program to another. Data may alternatively be shared between programs running on the same host by enabling shared memory routines.

Another method of programming available is that of software threads [45]. This is especially useful on multi-processor workstations, but also within programs wishing to maximise data throughput on interfaces which may perhaps be slow, threading programs can have advantages on uni-processor systems. The standard implementation is POSIX threads, implemented on UNIX. The function calls and methodology would be substantially different in the Microsoft Windows programming interface. However this may be ignored as critical programs would never be deployed on Microsoft servers. Threads have been employed within software constructed for this research.

## 7.4 Methods Proposed

The initial basis for the software utilised within this work is the power system simulator constructed at the University of Bath as described in chapter 4. This program was written in the C programming language in order to correctly simulate the power system efficiently by using the most appropriate algorithms and implemented with software memory address pointers wherever possible. It is also modular in structure, thus enabling function reuse in external programs. There are three main approaches which were considered for implementation of DOLSE. These are as follows:

- the reverse power system simulator approach
- the back-worked synchronisation approach
- the wrap around convergence reporting approach

The first possible approach above to effectively reverse a power system simulator completely would have needed a fresh start from scratch and would have made the solution non-generic. For any advancements in the simulator technology DOLSE would have had to be completely re-crafted.

Whilst investigating the incorporation of a time domain power system simulator into its new role as a power system state estimator it was realised that within the simulator there are effectively two types of variables which may be manipulated. Primary variables have a direct mapping with their real world counterparts. Secondary variables have a more complicated mapping between the simulated variables and the real world variables from which they are derived.

Due to the existence of secondary variables the approach used needed to be able to adequately incorporate these variables within the formulation. For this reason the second approach above, that of back-worked synchronisation had to be employed. Primary variables such as mechanical output torque of the generator, and the excitation of the field windings were gradually altered until the appropriate change in the secondary variable of interest had been achieved.

These primary and secondary variables may be likened to different elements of the non-linear state to measurement conversion matrix $H$. As the states are constructed from the voltage magnitudes and angles, the only measured quantities to have a one to one mapping are the voltage magnitudes. In a decoupled formulation the reactive powers are considered to have a non-linear impact on the voltage magnitudes, and the real power measurements a non-linear impact on the voltage angles at each busbar. In a non-decoupled formulation the mapping is more complex.

Primary variables with a direct mapping between measured values and variables within the simulator are real and reactive loads. These may be set within the simulator directly from system measurements. Real and reactive generation output is set by altering the mechanical output torque of the generator and the excitation respectively. Variables such as these may be considered to be secondary.

For example, the interaction between the real power generated, `Pg`, and the mechanical output torque of the generator set, `Tmo`, will now be demonstrated:

```
check (SCADA Pg is within generator's capabilities)
calculate (inital estimate of final value of Tmo)
calculate (the maximum permissible change in Tmo per timestep)
[the rate limit]
while (magnitude of error between present simulator Pg and incoming
       SCADA Pg is greater than the maximum permissable error)
alter Tmo appropriately by the rate limited amount
do a simulation timestep
endwhile
```

As may be seen from the above, to avoid upsetting the convergence of the simulator manipulation of the secondary variables was performed as an iterative process. If the changes in simulated generator's mechanical output torque were too large it was found that this could cause instability in the simulation. In conventional state estimation iterations are performed to find the correction to be applied to the states so that the error is smaller - eventually minimised - at each solution step. If this approach had been applied to DOLSE the simulator may have failed to converge adequately. In DOLSE the model is effectively *pushed* to the new solution.

This may be likened to fitting an $n$th order polynomial curve through a set of points, with the objective that the curve remains a straight line. In this case the curve is the simulator, with a converged solution represented as a straight line. The points may be considered to be the incoming SCADA data. If the line had the ability to bend, as the simulator could because it is a dynamic model, the line could be forced to converge more closely to several sub-sets of points, rather than the complete set of points. The best approach is to guide the line between the points ensuring that it remains a straight line and minimising the errors at the same time.

By monitoring the inputs and outputs of the simulator, whilst maintaining control over the speed at which it simulates, a modular structure was maintained. This enabled the third technique above, that of convergence reporting, to be implemented. If the state synchronised simulator began to take more iterations to converge to a solution at each time step this was monitored. Either the

topology determinator was dispatched to investigate the topology configuration in the region of a particular busbar in order to ascertain the configuration or the simulator was re-initialised.

The modular approach adopted will aid the methodologies implemented to migrate well in the future when more powerful computers are available. If the simulator were restructured or redesigned to take advantage of new techniques developed, or new hardware advances, DOLSE will not be left behind. The methodology of this work is to ensure that the clearly defined interfaces may still be used to incorporate the latest Power System Simulation techniques within this work.

### 7.4.1 Database

An important aspect of state synchronising the time domain model is the rejection of bad data. The state-synchronised model is encapsulated by a database which provides this functionality. This employs a variety of methods to monitor the incoming data.

**Trending Function** monitors the rate of change of the incoming data for each metered value.

**System Limits** ensures that no dynamic system equipment such as generators receive any instructions to try and synchronise their output to a value which is outside of their operational limits.

**SCADA Data Source** for any software programs which require the data as an input to their analysis, presently used to supply just programs within the DOLSE suite of packages, but could be extended in the future to supply further raw and state-synchronised data sets as needed.

If the topology of the power system remains the same it is possible to check that the incoming SCADA data is within specified tolerances of the previous SCADA value for that data item. If it is outside the permitted range of values

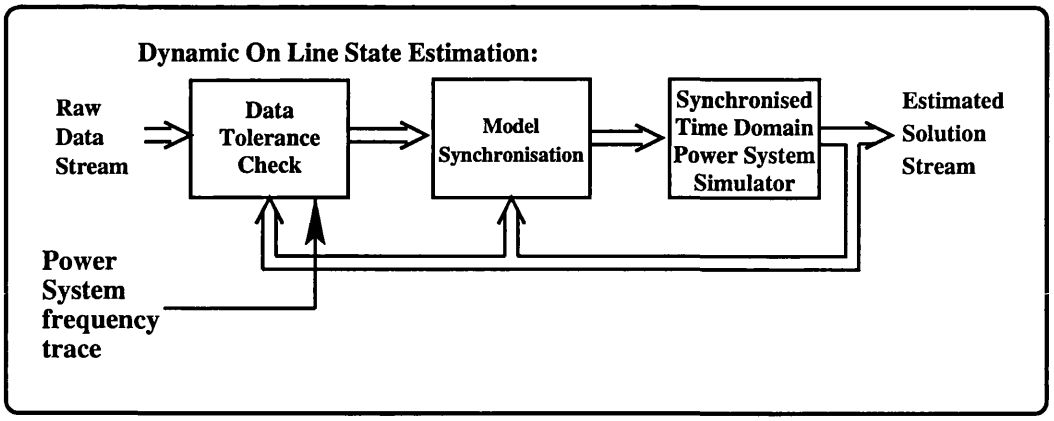


Figure 7.2: Diagram of state synchronised power system simulator implementation

it is flagged as such and is not injected into the state synchronised simulator. If no topology change is notified to the control centre and subsequent incoming SCADA values for that data item corroborate the larger than expected change, the topology determination engine is dispatched to investigate the possibility of a topological inconsistency. If one is found it is applied within the state sychronised simulator.

In addition to monitoring the rate of change of the magnitudes of incoming SCADA data items, the database also ensures that inappropriate requests are not sent to the state synchronised power system simulator. For example if the metered power generated exceeds the maximum genereration possible from the synchronous generators attached to a particular busbar, it is important that the simulator is not instructed to attempt to achieve the excessive real power output from those generation sets.

## 7.5 Software Implementation

This section details the interactions between the pieces of software depicted in the preceding chapters. It is the combination of these programs and databases which combine to form Dynamic On-Line State Estimation.

At the time of initialisation of the software, care must be taken to ensure that

the data set is correct and is not interfered with by any changes of the system topology. All data is time stamped upon arrival. A SCADA system which is not synchronised with GPS does not time stamp meter readings when they are taken, so the best information regarding time which can be attached to a metered value is therefore the time at which it reaches the power system control centre. Account must be taken of the level of change on the power system. During periods of high numbers of changes the information may be marshalled and the analogue metered values will likely reach the control room later than under steady state operating conditions. Due to the limited bandwidth of the SCADA network it is at the time when most information is needed that it becomes more difficult to be certain that it can be obtained quickly and accurately.

At time of initialisation there are two methods which could be used to form a data set which is more representative of the system than one data set. These are:

- form minimum skew data snapshot
- form an *auto-regressive* [46] data set from several sets of time skewed data

Not all of the data will be relevant to the input of the state estimator, so there is a sub-set of the SCADA data which needs to be time skew minimised to provide an input to the Dynamic On-Line State Estimator.

With all of the incoming data time stamped when it arrives at the Control Centre if SCADA data is collected over a period of time, it is then possible to search the data sets from that period to find a smaller period of time which contains a percentage of all relevant metered values off the system. This percentage can be selected depending on the reliability of the SCADA system.

As has been discussed previously the data flow from the RTUs is bandwidth limited by the communications channel. Each RTU sends data on a cyclical basis as frequently as it is able. If the largest substation takes for example

ten seconds to send a complete data set, smaller substations could take in the region of two to three seconds. If an arbitrary time is selected the data may be searched to find which is the oldest piece of necessary data available at that arbitrary time. If this is repeated for a selection of arbitrary times the data set containing the least time skewed relevant data may be easily selected.

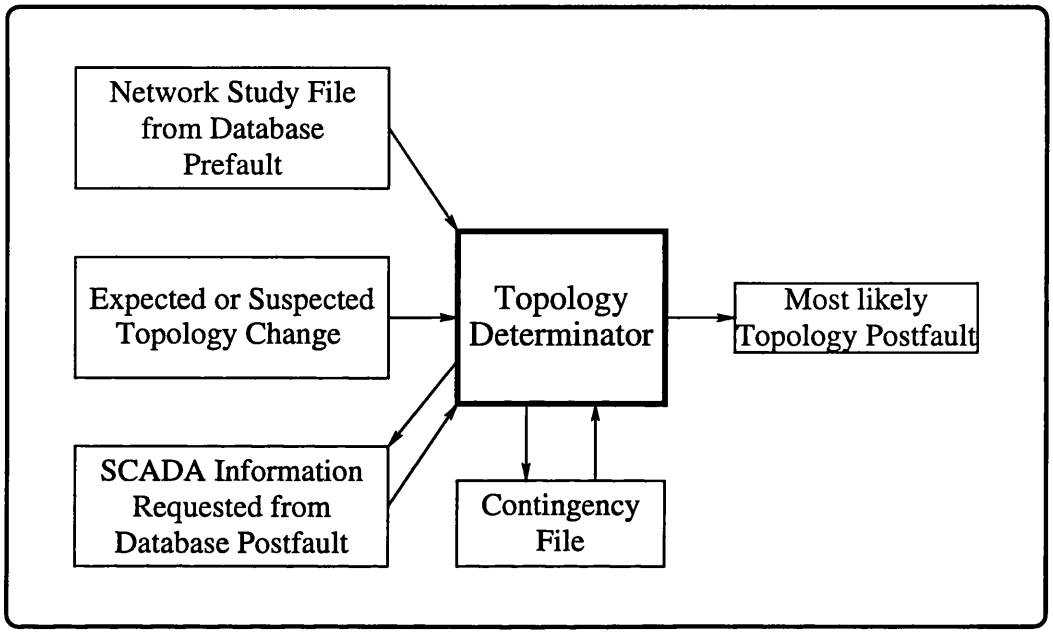


Figure 7.3: Diagram of topology determinator implementation

The occurrence of topology changes also needs to be taken into consideration. Any set of SCADA data which is or may be subject to a topology change should be marked as such, and be excluded from selection in the above process. It is also important to take into account the possibility of oscillations in the SCADA data after a transient has occurred. This is not studied in the initialisation of DOLSE, but is taken into account when DOLSE is operating in an on-line mode. A functional diagram of the operation of the topology determinator may be seen in figure 7.3.

An auto-regressive filter effectively weights the data in the favour of the most recently occurring data. For a system in steady state with a frequency equal to its nominal value, it is appropriate to take several time skew minimised data sets and take the mean average of the data sets in order to calculate a set of

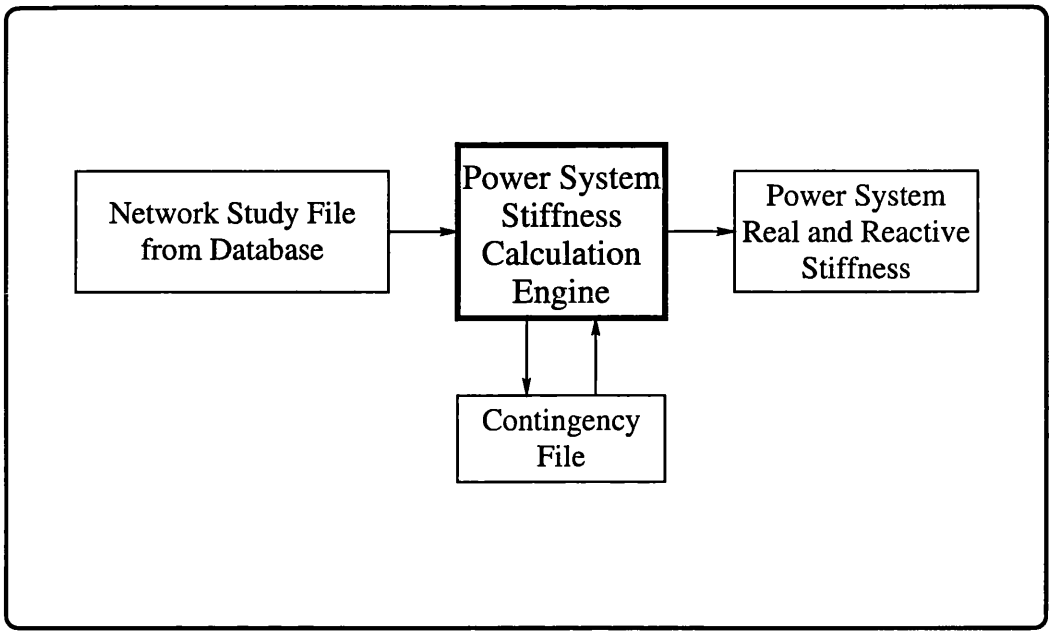


Figure 7.4: Diagram of power system stiffness calculation engine implementation

data with which to initialise DOLSE. However, the power system frequency is seldom at its nominal value. There is virtually always some degree of demand or generation imbalance. For this reason an auto-regressive filter has been chosen in order to calculate the initial data set. The weight attributed to each set of data decreases with the input data set's age. The weighting has been linked to the power system frequency information. This alleviates errors in the initial data set, yet takes account of the fact that the system is not stationary.

Ideally DOLSE operates in a completely on-line manner, with data from the SCADA network being available to the state estimator as soon as it arrives at the control centre.

The stiffness characteristic calculated off-line (figure 7.4) is used in DOLSE's on-line mode of operation. Let us first consider a situation in which the DOLSE topological model is the same as the system, and no topological changes occur.

The following secondary variables are of interest:

The system frequency was monitored by taking a frequency reading once

| Secondary variable | Information yielded |
|---|---|
| frequency | real power balance |
| mean system voltage magnitude | reactive power balance |

Table 7.1: Secondary variables and the information they yield

every second. This information was used within DOLSE in order to tighten or slacken the tolerances on the input trending analysis performed within the state estimator.

If a step change is seen to occur which is unexpected and has not been accompanied by notification of a topology reconfiguration the topology determination software is dispatched with details of the busbar closest to the unexpected metered data change. It then constructs a contingency list containing all possible line outages around that busbar, and performs contingency analysis noting the time duration of expected periods of system oscillation from those topology changes to notify the database of the length of time within which it could receive more suspect data.

If a topology change is notified to the control centre by the SCADA communications network, the state synchronised simulator outputs a snapshot of all internal information to a disk file so that it may re-initialise itself at this point if it is subsequently found that it needs to do so. The state synchronised simulator applies the change and then runs faster than real time to evaluate the time period of the system oscillations and to form the new state of the system as quickly as possible. Input from the SCADA network is stored but not applied to the time domain model until after the time period of oscillation which was predicted has elapsed.

If it is subsequently ascertained that the notification of the topology change was erroneous, the state synchronised simulator then reloads with the set of internal data which was saved to disk before the topology change occurred in order to restore itself to the previous state pre-transient. If a Delayed Auto

Re-closure has operated on a thirty second timeout for the breaker which originally opened, DOLSE continues to run - re-closing the line within the simulation model, running faster than real time to monitor the time duration of oscillations of the system, and not injecting incoming SCADA data into the state synchronised simulator until the predicted oscillation duration time has passed.

## 7.6 Summary

The software suite used to form Dynamic On-Line State Estimation has been presented. The SCADA data is subject to phenomena on the power system which occur within electro-mechanical time scales. Therefore an electro-mechanical time domain power system simulator has been incorporated within the methodologies as appropriate. Results of the software discussed within this chapter are now presented and discussed in the next.

Chapter Eight

# Dynamic On-Line State Estimation Results

## 8.1 Dynamic On-Line State Estimation Test Bed

In order to test the Dynamic On-Line State Estimator a test bed was constructed to model the behaviour of the actual power system. Data from the National Grid System of England and Wales system was only available in the form of a state estimated results file. It was combined with the appropriate machine, governor, automatic voltage regulator, power system stabiliser and load model data-bank to form a complete representation of the network. This real time system emulator is a version of the PowSim engine slowed to run at actual system speed contained within an X-windows Motif widget interface. This emulator was then used to provide the input to the SCADA emulator.

The SCADA emulator produces time-skewed data sets over a ten second period. All data values have appropriate levels of random error applied. To model extreme metering errors a separate accuracy file is used to advise the emulator to add greater levels of error to specific metered values. Care has been taken to ensure that the random number generator at the heart of this process of adding errors is sufficiently random. An algorithm for random numbers was used from a reputable source [47].

The system emulator may be altered on a manual or pre-programmed basis. It is possible to alter the system emulator by increasing or decreasing genera-

tion or loading level or by altering the system topology. Lines may be disconnected at either the sending or receiving end or may be completely switched out. Faults may be thrown for specified periods at any busbar to simulate real system events. Several pre-programmed event files (*"take"* files) were generated so that the operation of DOLSE could be seen in a variety of scenarios.

To aid in the replication of results using this software, the results contained within this thesis have been obtained using files to save the data at each stage, rather than the advanced network and file socket interfaces which could be used to operate the software.

The exact model used by the transmission company of England and Wales of the full UK system has been utilised with the orders of models as shown in the Power System Simulation chapter (6). However, full details of this model cannot be published for reasons of confidentiality.

The orders of magnitude of the errors applied to the data are as outlined in the Power System Operation and Data Processing chapter (2) for a typical system.

For purposes of testing, a variety of contingencies were applied to the power system model. These included a selection of line outages, loss of busbar loads (both real and reactive) and loss of generation. Outages were presented to DOLSE in both an expected and an unexpected manner. The unexpected changes were applied in the system emulator - thus altering voltages and power flows of the system - without the SCADA digital information being communicated to DOLSE. It was then left to DOLSE to flag a suspected problem and to perform topology determination contingency analysis in order to find the error.

A selection of faults were thrown on the system emulator to test DOLSE's ability to form a solution quickly post-transient. These were selected by performing exhaustive contingency analysis on the test system, and selecting a set of network outages which caused a range of responses for the given system. This analysis was performed using The University of Bath's time

domain dynamic security assessor - OASIS.

## 8.2 Results from Dynamic On-Line State Estimator

Within the SCADA emulation and Dynamic On-Line State Estimation test bed, it is possible to study not only the data regarding the metered variables of the power system, but also data of the true values which the metered data represents. As has been previously described, at the heart of the SCADA emulator is a time domain simulator which acts as the real system before data corruption. Data is available from this real system simultaneously with the quasi-SCADA data. As an example to show the differences between the actual system/DOLSE error distribution and the quasi-SCADA data/DOLSE error distribution the initialisation of DOLSE will first be considered.

The actual system model saved an uncorrupted state vector to disk when asked to produce a time skewed noisy data set to act as the initialisation data for the DOLSE simulator. The state synchronised model was then started from this time skewed noisy data set with no filtering or construction of minimum skew time data sets as would be implemented within DOLSE normally. When considering the analysis of the state vector, only the voltage magnitudes at each busbar are obtainable directly from the metered values. Voltage angles are unobtainable. So in the consideration of the difference between DOLSE and the actual system and DOLSE and the metered values, only the voltage magnitudes at each busbar will be considered.

Figure 8.1 is a histogram of the errors between the DOLSE state vector and the state vector of the system underlying the quasi-SCADA emulator. Figure 8.2 is a histogram of the errors between the DOLSE state vector and the SCADA metered busbar voltage magnitudes.

Figure 8.3 shows the difference between the actual system voltage magnitudes and the quasi-SCADA voltage magnitudes. The errors are seen to lie in a rectangular distribution between the maximum error of plus and minus 2

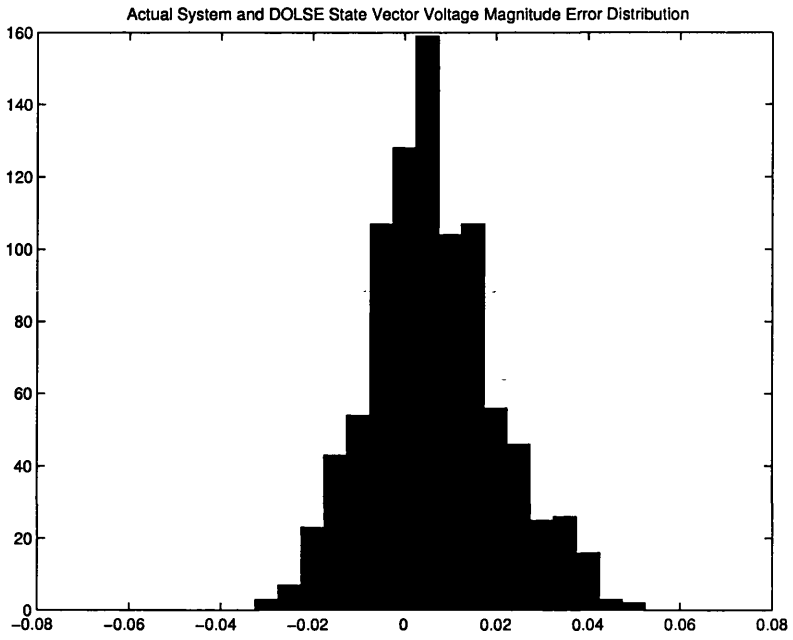


Figure 8.1: Actual system/DOLSE voltage magnitude error distribution, frequency versus per unit error

percent. Despite DOLSE being initialised with a noisy time skewed data set, the error distributions clearly show that DOLSE is closer to the underlying true system state than it is to the quasi-SCADA data.

### 8.2.1 Line Outage and Delayed Auto Re-closure

The University of Bath's Dynamic Security Assessor was tasked with complete analysis of the transient stability of the system used to test DOLSE in this section. The ranked list of the 500 worst contingencies may be found in appendix B. In order to fully test the power system for transient stability problems the DSA applies a solid busbar fault for a period of 80ms before then tripping the line. Analysis is performed for each line twice, alternately with the busbar fault applied at either end of each line. This analysis was completed for all single and double circuit contingencies.

The most problematic outage in terms of transient stability as determined by the DSA was that of the double circuit (lines one and two) joining a busbar at

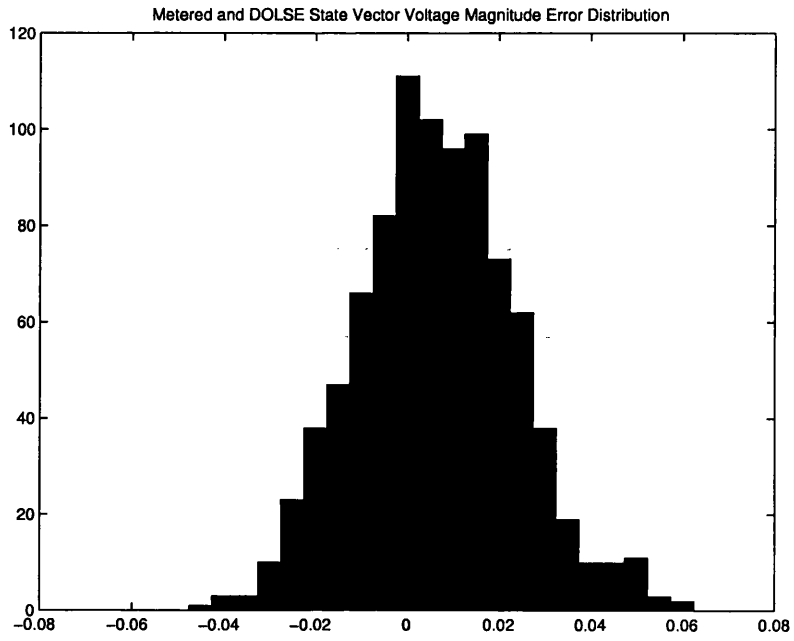


Figure 8.2: Metered data/DOLSE voltage magnitude error distribution, frequency versus per unit error

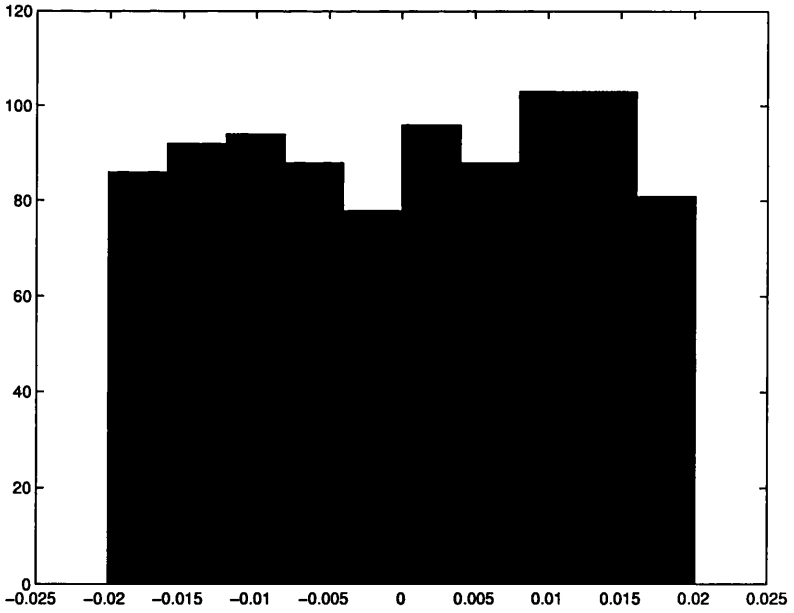


Figure 8.3: Voltage magnitude error distribution, frequency versus per unit error

Lackenby substation (LACK2) to a busbar at Greystones substation (GRST2B). Greystones generating unit three pole slips within 0.75 seconds of the 80ms busbar fault and the line outage of the double circuit described. In order to make the analysis even more difficult for DOLSE the parallel transformers from Hunterston (HUER) 400kV to Hunterston 132kV substation was also removed prior to the outage of the Greystones to Lackenby circuits. The majority of faults which cause the outage of a line are resolved by removing the line from service. In order to maintain the stability of the power system, most major transmission network circuits' protection incorporates a delayed automatic re-closure facility, whereby the line is returned to service after a period of typically approximately 30 seconds. To simulate this facility the Lackenby/Greystones double circuit is reconnected to the system on a simulated delayed automatic re-closure scheme.

| Data Set Number | Textual Description |
|---|---|
| 1 | Outage of parallel transformers from HUER4 to HUER1 |
| 2 | Outage of double circuit from LACK2 to GRST2B |
| 3 | Complete set of analogue data used to state synchronise DOLSE model |
| 4 | LACK2 to GRST2B reinstated on Delayed Auto Reclose (DAR) |
| 5 | Final on-line data set accepted by DOLSE |

Table 8.1: On-line data sets and the operations which they represent

Five on-line data sets were constructed in all, the details of which are given in table 8.1.

All of the figures used in this section contain the error distribution for both the voltage magnitudes and voltage angles. The errors are between the DOLSE model state vector and the actual system state vector. Each figure contains error distributions for the voltage magnitudes and angles separately. The

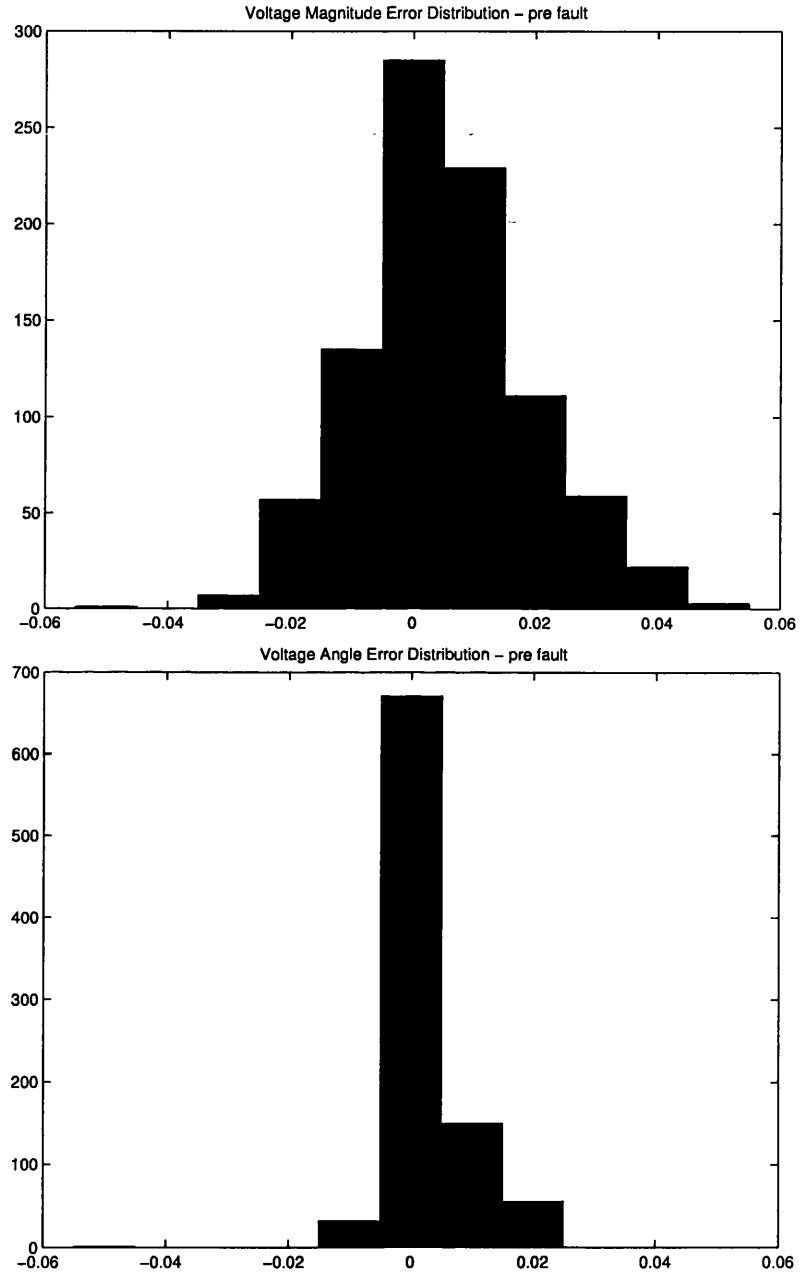


Figure 8.4: Voltage magnitude and angle error distributions - pre LACK2-GRST2B:1:2 fault, frequency versus per unit error

voltage magnitude error distribution always appears at the top of the figure, with the voltage angle error distribution appearing below. Each figure depicts the error distributions after the on-line data has been passed to DOLSE.

For the following results presented, the histogram was chosen as the most appropriate method to display the measurements obtained from the DOLSE test bed. An odd number of equally sized bins were chosen with one bin centred on zero error between estimated and actual states. Five bins in a positive error direction and five bins in a negative error direction were then added over the range of the error data collected. These bins were then used to contain the states' errors, and the results then plotted. If too few bins had been used the histograms would not show the frequency distribution of error to a sufficient level of detail, if too many bins had been used no meaningful groupings of the sizes of error observed in the data would have been seen. The choice of size and number of bins was found to be the best compromise between these two extremes. The histograms show groupings of the actual error rather than groupings of the error magnitudes, so that if any offset in the errors were found this would be clearly seen on the graphs.

Figure 8.4 shows the error distributions after the HUER4-HUER1 parallel transformers has been removed. DOLSE was notified of the topology reconfiguration via SCADA and applied the switch status change in its internal model. It *fast forwarded* to find the duration of the system transient oscillation caused by this outage.

Figure 8.5 shows the error distributions after the LACK2-GRST2B double circuit outage. DOLSE was again notified of topology change via SCADA, and applied the topology change within its model. Since the beginning of the previous topology change DOLSE has been able to correctly ascertain that it would not be safe to attempt to inject any SCADA analogue metered values into the simulator, because the system has not been free from transient oscillations for a sufficient period of time to make this a viable proposition.

A conventional state estimator may well have accepted these data sets which

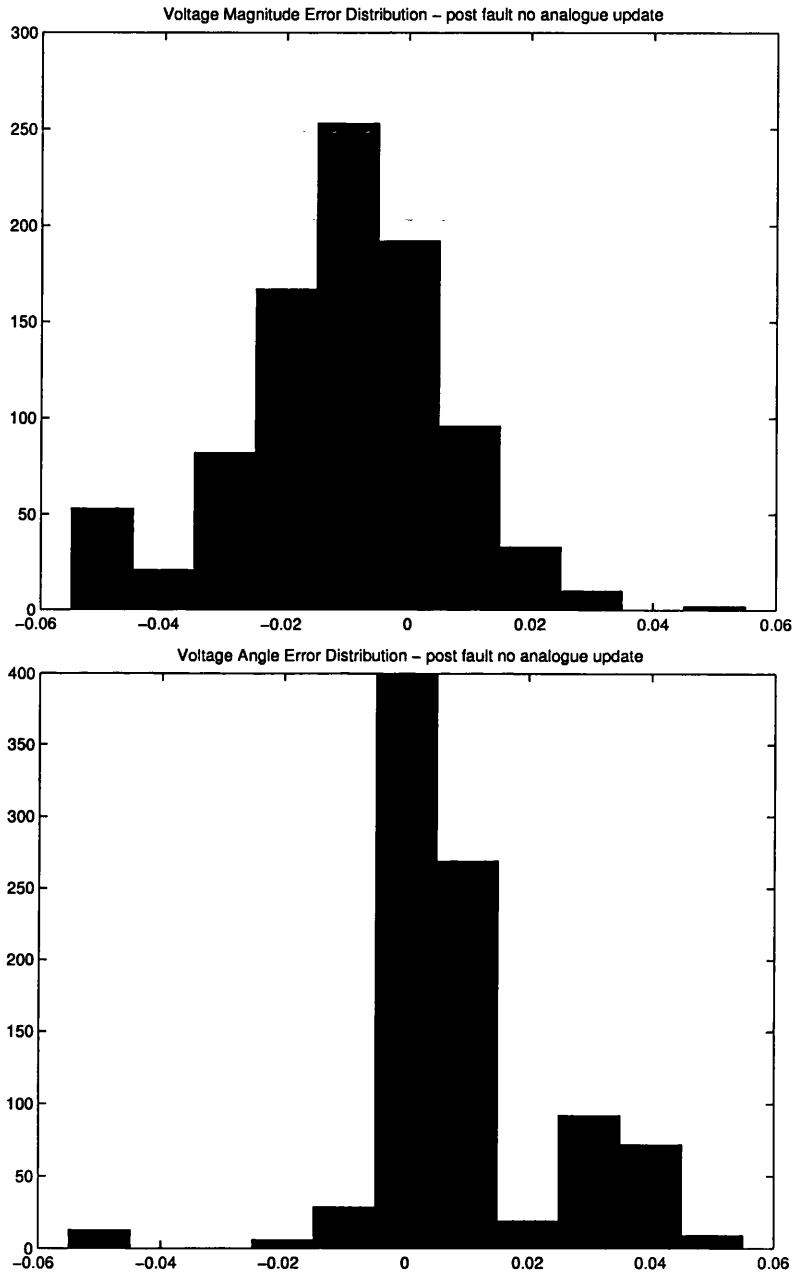


Figure 8.5: Voltage magnitude and angle error distributions - post fault no analogue update, frequency versus per unit error

are subject to electro-mechanical oscillations and incorrectly attempted to calculate a state estimated solution from them. DOLSE is able to continue providing a state vector to any analysis programs which require it, without using the incoming oscillatory SCADA data.

Figure 8.6 presents the results after DOLSE is able to take a clean scan of analogue measurements from the system which are deemed to be clear from the oscillations caused by the two double circuit outages which have occurred so far. The graphs show that the voltage magnitude errors were still within acceptable bounds, however the voltage angles display evidence of a 0.045 radian offset. This was due to the fact that both the system emulator and state synchronised simulator within DOLSE began to exhibit oscillitary instability with the topology configuration they contained. The state vectors were output at differing times within the period of the oscillation, and so show the difference in voltage angles at each busbar.

The double circuit outage has just been returned to service on a delayed auto re-closure scheme. Figure 8.7 shows the error distributions of the system states. The topology change has been notified to DOLSE, and has been applied in the state synchronised system model. Analogue data is not injected into the state synchronised model for the duration which the transient is calculated to last.

The final error distribution figure, figure 8.8, is taken after the state synchronised model has been injected with SCADA analogue data immediately following the end of the expected period of system transient oscillations. The error distribution of the voltage angles shows less error than the previous figure.

Although DOLSE is able to effectively predict the system state by only applying the topology change within the time domain model of the state synchronised power system simulator, better results are achieved once analogue data has been accepted again to help synchronise the model. This data is however available much more quickly to DOLSE than a conventional estimator, because DOLSE can completely evaluate the length of time for which the ana-

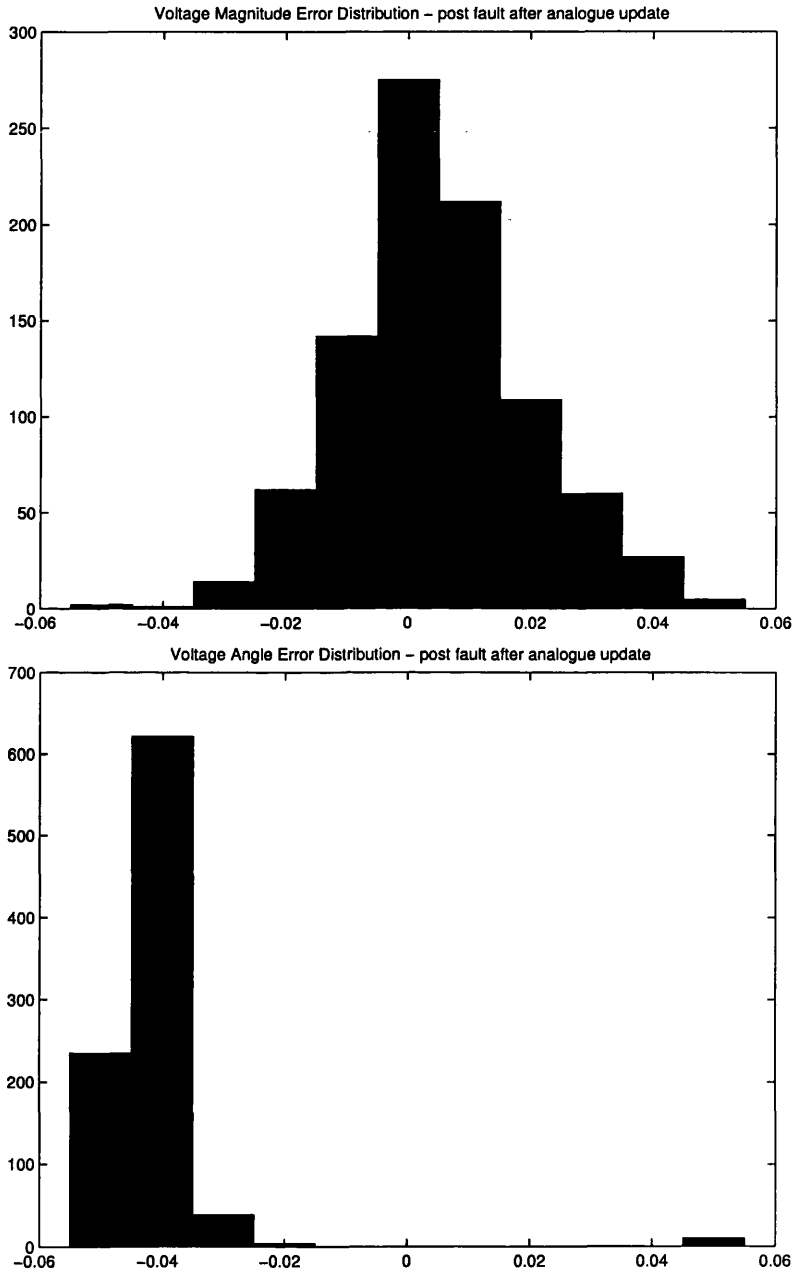


Figure 8.6: Voltage magnitude and angle error distributions - post fault after analogue update, frequency versus per unit error

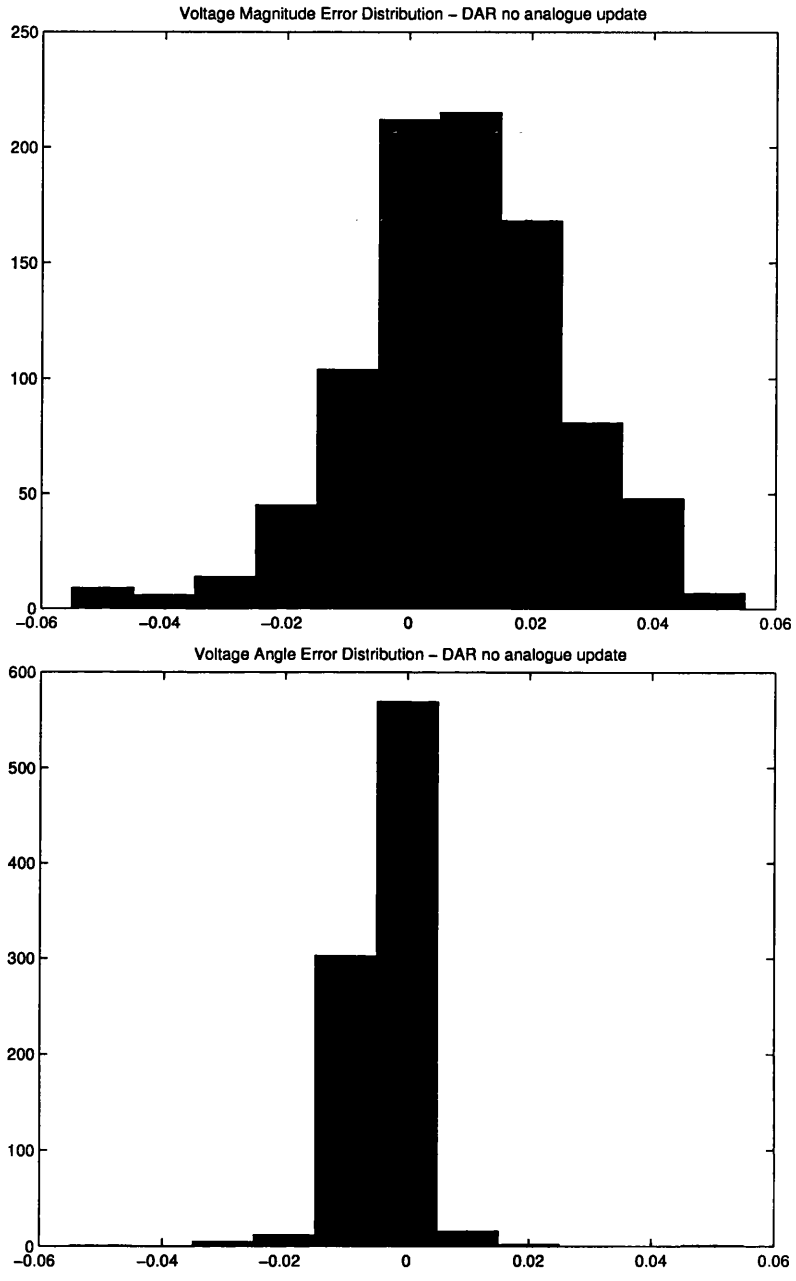


Figure 8.7: Voltage magnitude and angle error distributions - DAR no analogue update, frequency versus per unit error

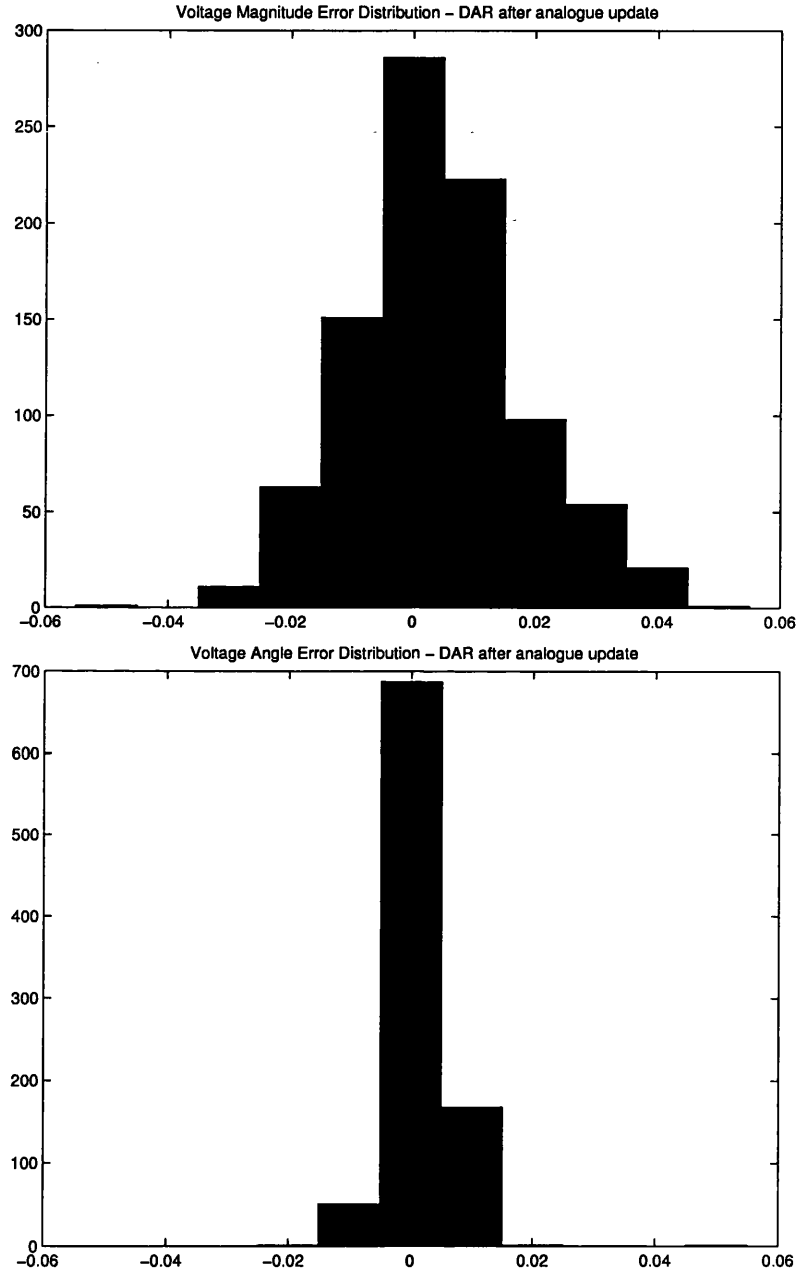


Figure 8.8: Voltage magnitude and angle error distributions - DAR after analogue update, frequency versus per unit error

logue SCADA data will be in transient oscillation. As soon as it calculates these are over it will accept incoming analogue data once again.

## 8.3 Discussion of Results

The test case depicted in the discussions above shows the operation of the Dynamic On-Line State Estimator in very adverse conditions. The actual model of the simulation used to initialise the system and SCADA emulator was artificially stressed to make it more liable to exhibit transient and oscillatory phenomena than would otherwise normally be encountered in a real operational power system network. The third set of results presented in this chapter in figure 8.6 show the offset error in estimated voltage angles when compared to the voltage angles of the system emulator. If the DOLSE software in its present form were to experience problems when implemented on a real power system, it would be in just such a scenario where it would exhibit gross errors.

Chapter Nine

# Conclusions

Data is available from an electric power system continually. It is sent via communication channels from the substations to control centres as frequently as the available bandwidth will allow.

Static State Estimation does not utilise all data available from the Supervisory Control and Data Acquisition network. Tracking State Estimation and Dynamic State Estimation use more data but only incorporate basic load-flow models. The data sample rate from the SCADA network falls within the bounds of the period of interest normally associated with electro-mechanical models. TSE uses no model of the time evolution of the system, DSE uses linear extrapolation or thermodynamic models at best.

To completely utilise all SCADA data full account needs to be taken of phenomena occurring within the electro-mechanical time-frame. The best form of model available is fast time domain transient simulation. However, the SCADA sampling rate is insufficient and data collection time too great to provide complete synchronisation of the model to the power system as would be acheived in applications such as predictive control. Therefore the aim has been to construct a state synchronised time domain transient simulator.

Detailed models contain primary and secondary variables. Primary variables may be explicitly set with secondary variables completely dependent on primary and secondary variables via the model. Metered variables are fed to a database which monitors and trends the data. This alters primary variables

within the simulation to achieve an acceptable representation of the system. Appropriate primary variables are also manipulated by incremental search in order to effect change of secondary variables.

The advantages of this approach include the ability to completely store the time domain response of the system and use it as a guide to Control Engineers of the system state as well as an input to Real Time Network Analysis functions built to make use of the data. The most upto date state estimate is continuously available.

When a topology change occurs the simulator is able to complete this switching action within the time domain model. The simulator is then executed faster than real time so that it may be immediately ascertained which incoming analogue data is susceptible to system oscillations. Any data value which is deemed to be from affected by a period of oscillation is initially rejected from the incoming SCADA data. When the incoming data is deemed free of transient errors it may immediately be used to continue to state synchronise the model.

To ensure topology changes are correct contingency analysis is performed around a busbar of expected change with the results compared to the incoming data from the SCADA network. The stiffness characteristic of the system is calculated off-line and used to aid the trending and incremental search performed by the database encapsulated power system simulator in an on-line mode.

The time domain topology determination engine was capable of identifying which topology change had occurred on the system in the region of a specified busbar, while working with a bus/branch model rather than a switch/section model. In the case of the outage of one circuit of a double circuit connection between two busbars, it was able to correctly identify that one of the two circuits had been removed from service. Although not an ideal mode of operation this is an acceptable solution to build a network representation and calculate a state estimate for use by the RTNA suite of programs.

The power system stiffness calculation engine output was found to be most useful in providing an estimate of the real power balance of the power system. Its use to change the tolerances of the trending function within the database was essential for correct state synchronisation of the time domain model to the actual power system. As information regarding the system voltage magnitudes cannot be metered at the same instant system wide, the Mean System Voltage calculations to obtain the reactive power system stiffness characteristic were found to be less useful. In the future, time synchronisation of meter readings will make this a more useful index of system operation.

The results of the software developed have been presented at each stage of data processing using a SCADA emulator to provide the raw data. The power system study file used to initialise the SCADA emulator model was exhaustively searched to provide information regarding the system's stability for the outage of any single or double circuit line using a Dynamic Security Assessor. The software was then tested using the most severe contingencies possible. As the network model had been artificially stressed so that the system exhibited transient and oscillatory instability for some contingencies, this testing utilised scenarios which were actually much more severe than any which are normally encountered during operation of an actual electric power system.

The results in chapter 8 show that the techniques perform well in extreme conditions. The estimated voltage magnitudes and voltage angles at each busbar are within acceptable tolerance of the system emulator state vector. Even during oscillatory instability the accuracy of DOLSE ouput of estimated voltage magnitudes was not impacted.

Over the course of the development of this project the software has been run on a variety of power systems of different sizes. As such it is not specific to the full England and Wales National Grid System model - the techniques developed in this work could be transferred to any other power system - as long as an accurate model of the system is known.

The results from this work show that it is an encouraging development in the field of electrical power system state estimation. Never before have such detailed system models been incorporated into the state estimation formulation. Indeed it has been shown that the phenomena witnessed on incoming SCADA data necessitate the use of such detailed models for accurate state estimation analysis.

As with any investigation into a new approach areas have been identified which need to be studied further. These further considerations for future research are presented in the next chapter - Suggestions for Further Work.

Chapter Ten

# Suggestions for Further Work

As is the case with most research, there is a significant amount of further work which is possible to extend and enhance the research presented in this thesis. Some of the most important areas are outlined in this chapter. C.S. Lewis once said:

> The more one learns about a subject area, the more one realises there is even more to learn and yet more to discover.

The next few years herald an exciting time for the further development of DOLSE. At the present time the data overhead requirements would be difficult to acommodate with EMS systems in service today. The capability which will be added to the EMS of the future, however, is the availability of all power system data via a computer hosting a database server - exporting information on another network to systems which need it.

This data could be incorporated into an object oriented database such as GOLD [48]. From here it would be available for data processing programs such as DOLSE to make use of. The output format of a program such as GOLD would be designed from the outset to be highly configurable and would be well documented, so it would be a simple task to link the DOLSE software inputs and outputs to such a data repository.

As has been discussed in chapter 2, programs such as Dynamic Security Assessment [49] and General Intertrip Monitoring Schemes [30] must wait

until a data set is available to them from the batch run state estimation facility. Within a few years this software will be able to run in parallel with commercially purchased EMS and provide data much more rapidly to the new applications developed by power system software engineers, therefore allowing control engineers to reap the benefits of a faster information stream in order to more tightly control the power system.

## 10.1 Continuation of System Stiffness Analysis

The calculation of power system stiffness within this thesis has been confined to analysis of the response of the power system for the loss of busbar loads. As such this provides the system response for only half the possible contingencies which would cause either a real or reactive power imbalance. The power system real and reactive stiffness charcteristics have been assumed to be the same linear relationship for a positive or negative imbalance of either quantity. The other set of contingencies which should be studied are the tripping of each and every generating set and the subsequent frequency and mean system voltage responses.

It would be expected that for the loss of a generator the system frequncy would fall, and the mean system voltage would also fall. However, the exact response of these phenomena would need to be carefully examined as the loss of a generator also removes some of the governing and automatic voltage regulation capability from that region of the power system.

## 10.2 Oscillatory Mode Identification

As has been illustrated by the offset of voltage angle error in the third set of results in chapter 8, DOLSE operation is presently limited to state estimation of the system when it is not subject to oscillatory instability. Fortunately instances of this occurance are very rare, however the electro-mechanical model of the system within DOLSE is sufficiently detailed to enable periods of dynamic

instability to be identified as such. This functionality needs to be added to DOLSE and stategies constructed for the best way of dealing with such instability.

## 10.3 Operation in Event of System Split

Although under normal operating conditions the power system is operated as one synchronised entity, in extreme conditions the system could become partitioned into two or more islands. Possible strategies include the formation of study files to simulate each island and employing these to find the effect of the system split on each part of the system. An island is likely to contain an imbalance of generation - the effect of islanding needs to be carefully studied and stategies within DOLSE implemented.

## 10.4 Global Positioning System

The availability of signals on a world-wide basis from the Navstar constellation of satellites yields many new potential applications in a variety of fields. Various researchers have noted the impact which the Global Positioning System (GPS) could have on electrical power systems [50]. If the geographical location is exactly known the equations may be back-worked to provide a very accurate source of time - the Universal Time Clock (UTC). Fortunately, being stationary installations, the position of each substation may be measured once using a very accurate GPS device which need not then be left at the substation. This position may then be used as the basis of UTC calculations employing a less expensive GPS receiver installed at the substation. Within state estimation calculations at the present time, the set of metered values contains voltage magnitudes at every busbar but no voltage angle indication. This is impossible to achieve without some form of time synchronisation - which with GPS is now available.

The installation of GPS UTC at every substation would be expensive if carried out in one go. As with any installation on an electrical power system the devices could only be installed on a rolling basis to coincide with planned outages. For this reason it would be advantageous to calculate which substations would be the most appropriate places for an initial installation of GPS equipment. The quasi-SCADA emulator test bed and Dynamic On-Line State Estimator which have been constructed for the work completed in this thesis would be an ideal apparatus to perform such an investigation. A series of tests could be performed with voltage angles available from specified substations on each run. The DOLSE software could then be modified to accept this information and incorporate it into its solution. If an index could be formed to represent the usefulness of the angle information, the order in which the substations should be made GPS capable could be ranked.

Another application of GPS within state estimation would be to provide a non time-skewed data set. Substations could then be instructed to take readings of all meters at a specified instant in time and then transmit this instantaneous system snapshot back to the Control Centre as quickly as was feasible (determined by the bandwidth of the SCADA network).

Further detail of GPS may be found in appendix F.

## 10.5 Small Substation Synchronisation

The SCADA system always operates to maximise the bandwidth utilisation along the communications channel from the substation to the control centre. This feature can be exploited.

Smaller substation have the same bandwidth available to them as to a large substation. However there are fewer analogue metering devices or switch statuses to report. This means that the data which is sent from a small substation to the control centre can be sent more frequently.

Utilisation of this feature of the SCADA network would provide a means of synchronising the simulator more closely to the small substations - thus providing a closer state estimate to the state of the actual power system.

If the SCADA configuration is as that of figure 2.3 (b), if the direct connection from the substation to the control centre were to fail the substations selected to be the main synchronised substations could be dynamically updated to use those sending the data with the highest update rate.

## 10.6 Parameter Estimation

Monticelli [22] suggests benefits from State Estimation based on multiple scans of measurements, including:

- faster, more accurate results
- enough information to perform parameter estimation

With the more suitable model available within the transient simulator using the redundancy in multiple measurement sets it should be possible to synchronise the simulator not only to the system states but also the system's parameters. Sufficient information, however, is not available from the generators' responses because of the low sampling rate of the SCADA system. In order to calculate the parameters of the generators a much higher sampling frequency would be necessary. A method would then have to be developed to match the time history of the actual generators to those modelled within the simulator.

The parameter estimation which would be possible would be that of the network parameters. The series resistance and reactance and the shunt susceptance within the simulator are presently calculated from the data available regarding these variables on a line length basis. The length of the line and per unit length parameters are known and the resistance, reactance and susceptance values for the whole line are calculated from these.

An important aspect which has not been covered in this work is that of parameter estimation. All the models contained are those which are believed to be in existence on the real system. For example, all network parameters are calculated on the basis of the length of the power lines rather than actual metered values. It may be that the balanced representation is inappropriate, for example due to the non existence of phase swapping on the transmission towers of the network. The governors, Automatic Voltage Regulators and Power System Stabilisers are modelled from the design specifications. These were the control mechanisms as they would have been manufactured. Settings could well have changed since that time. Indeed as the systems are tuned, or parts age, the models' behaviour may well have diverged from the actual installed control equipment.

The models within the simulator have been validated against other simulators, but validation against the behaviour of the complete power system is historically a difficult task. An interesting example of the mismatch between theory and practice may be taken from the study of inter-area oscillations. The predicted frequency of the inter-area oscillation as found from power system simulators tends to differ significantly from that which is observed. Differences such as this need to be resolved in order for complete confidence in a technique such as the one presented.

## 10.7 Comprehensive Validation

Comprehensive evaluation of complex software and methodologies such as those employed in this work is a large undertaking. An analysis of all of the software's modes of operation is as complex as the simulation of the electrical power system, for it is a model of this system which the software contains.

Care has been taken in the construction of the software so that it should be able to detect if the errors between its internal values and those received from power system metering are getting too large. In the worst case the package

will re-initailise itself from a time-skew minimised data set.

Comprehensive evaluation needs to be performed using live system data. The technology and bandwidth necessary to achieve this should be available soon, perhaps within two or three years.

## 10.8 Voltage Collapse Prediction

Similar techniques could be used to calculate the likelihood of voltage collapse as were used in chapter 6. The simulator could be used off-line to test the proximity of the system to voltage collapse. Additional functionality would need to be incorporated into the simulator such as the logic used to alter the turns ratio of automatic tapping transformers.

## 10.9 Deployed Models

State synchronised models could also be deployed within controllers throughout the power system. The benefits of this may be illustrated by the following example: the human brain is constructed of cells called neurons. Due to the chemical make up of these cells, they are able to fire only once every 10ms. This gives them an effective sampling frequency of 100Hz. Using conventional techniques and a digital controller it would be impossible to even achieve the function of, for example, a hand catching a ball. The brain must be modelling the scenario in a great amount of detail in order for such an event to occur. The formulation of a state synchronised simulator is the first step to such a methodology for power system control.

Synchronised models of the power system could be deployed throughout that system and updated using predictive model error correction techniques as are commonplace within the video encoding arena. These models could provide the facility to plant such as Static Var Compensators to move from target or local follow modes of operation to achieving settings which are more

acceptable for system wide harmonious operation.

With the increasing introduction of ancillary services market places, reactive power trading is becoming common place. No longer does the utility own generating plant which would have previously provided these facilities with no reference to their cost.

Indeed the author believes that in the same way that Power System Stabilisers had to be deployed to enhance the real power operation of the system, the next important deployment will be needed to minimise reactive interactions. System wide models are important for monitoring power system stabiliser performance on a system wide basis. At the least, regional models should be used on-line to study operation in a region rather than just local operation of SVCs. The harmonic, voltage stability and dynamic implications of many FACTS devices have yet to be fully realised. This software will help to improve the recording of the reactive measurements of the power system.

## 10.10 Limitations

The methods as outlined in this thesis cope acceptably well when modelling the power system in a steady state. Good results are also obtained when either one or more topology changes are expected. The topology change may be applied in the dynamic model yielding an almost immediate state estimated solution. The time domain model immediately models the change of system variables due to the topological reconfiguration, change in generation or load. This work presents the most detailed model ever used to construct such a methodology.

However if a topology change is unexpected the simulator can accurately model the system to try and establish which reconfiguration has occurred, but this takes time. If multiple unexpected contingencies have occurred the least computationally intensive approach is to take auto-regressed time-skew minimised independent data sets and re-initialise the system model.

In the future when EMSs become a network of heterogeneous workstations each capable of completing any of the EMS functions, it will become possible to easily incorporate new hardware as it becomes available on a rolling basis. To enable the tracking of the dynamic system completely using the time domain transient model it will only be necessary to purchase a few extra processing nodes in order to provide the requisite computational resource.

Effectively this work has used a perfect model within DOLSE - the same as the model behind the dynamics of the SCADA emulator which has had noise applied to its outputs. Further work should focus on attaching the DOLSE software to a live Energy Management Data-feed which can provide it with the requisite amount of data or to a SCADA emulator which has changed the parameters and even the model structures in a significant way when compared to the DOLSE model.

## 10.11 Summary

Although the DOLSE methodology presented within this thesis functions adequately, additional features both to make the operation of DOLSE even more robust, and to expand the functionality of DOLSE have been proposed within this chapter.

The next work to be undertaken to ensure robust operation of DOLSE is the continuation of the investigation into the power system stiffness characteristic to include analysis of the system after the loss of generation. Functionality needs to be incorporated within the power system simulator so that oscillatory modes of operation can be identified in the state synchronised model and incoming SCADA data dealt with appropriately. Stategies also need to be implemented for the operation of DOLSE in the event of a system split.

Incorporation of global positioning system universal time clock and close synchronisation of the DOLSE model to small-substation SCADA data needs to be carefully considered and functionality implemented.

Methods of including parameter estimation into DOLSE need to be explored, and comprehensive validation of the simulator model stucture must be undertaken.

The use of DOLSE for voltage collapse prediction and deployed models for control, are all possibilities of research which would expand the functionality of DOLSE for the future.

Appendix A

# Schematic Diagram of the Electrical Power System of England and Wales

This appendix contains a map of the system used for the analysis presented within this thesis.

It is reproduced here by kind permission of the National Grid Company Ltd., UK.

**S** Figure A.4.1 Existing and Planned System - 1998/99

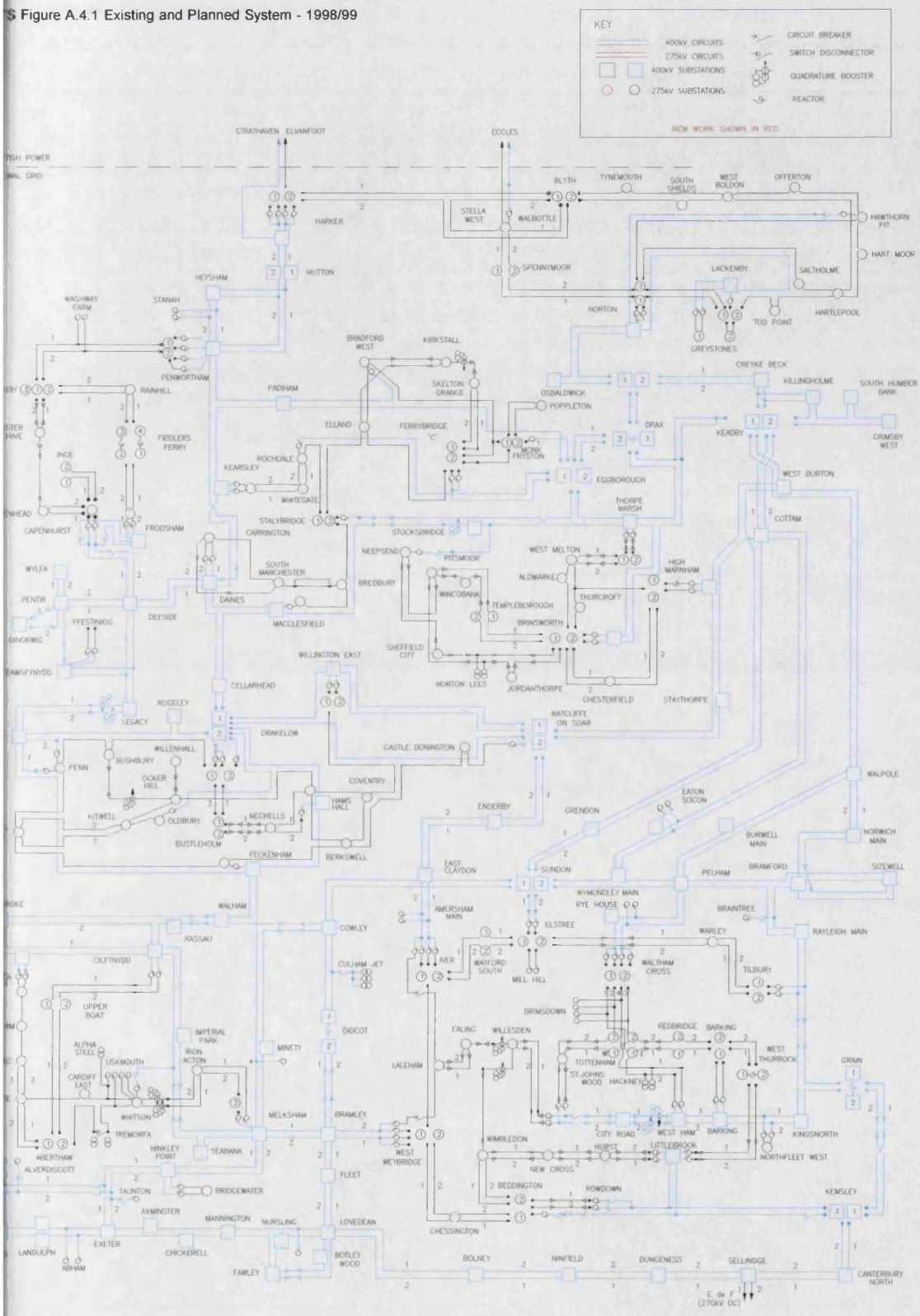

Appendix B

# Dynamic Security Assessment Ranking for Test System

To evaluate the performance of DOLSE, the most critical parts of the system were chosen. In order to ascertain where there were potential problems on the system, a total contingency run using the University of Bath's Dynamic Security Assessor was undertaken. This evaluated the transient reponse of the power system study model used for the majority of results within this thesis. This file had been originally artificially destabilised. The Grid System of England in Wales would never be run in such an insecure configuration.

The list below is the first 500 least stable contingencies which were evaluated by the DSA. The entire list included all 1927 single and double line outages evaluated twice: the first time with a destabilising 80ms busbar to earth fault applied at the first end of the line and the second time with the same duration and type of fault at the other end of the line. In total, to evaluate the system completely, these 3854 single and double line outages were completed on three Linux workstations using full time domain simulation.

The severity index was calculated using an algorithmic approach based on the decay time of the oscillations seen on the waveforms. This approach has limitations to be aware of. The main limitation is that although it output the identification *Diverging* for some contingencies seen below, if the time histories of the transients were reviewed it was possible to see that some change has occurred on the system which the algorithm could not evaluate appropriately.

The term diverging does not mean that the system has entered into a limit cycle mode of operation, which is another meaning for the term.

```
Contingency Evaluation Results @ Wed Sep 22 14:19:16 1999
   Number of contingencies     3854
   Evaluation Cycle            0
   Evaluation Time             191:19.95
   Study Time                  1:30

Pole Slipped
Ranking  1  No: 3712 Type: LINE  Name: LACK2-GRST2B:2 LACK2-GRST2B:1
Ranking  2  No: 3711 Type: LINE  Name: GRST2B-LACK2:2 GRST2B-LACK2:1
Ranking  3  No:  781 Type: LINE  Name: EASO4-LITB4:1
Ranking  4  No:  782 Type: LINE  Name: LITB4-EASO4:1
Ranking  5  No: 3548 Type: LINE  Name: WYLF4-PENT4:2 WYLF4-PENT4:1
Ranking  6  No: 3547 Type: LINE  Name: PENT4-WYLF4:2 PENT4-WYLF4:1
Diverging:
Ranking  7  No: 3119 Type: LINE  Name: PEHE2-PEHE81:1
Ranking  8  No: 3120 Type: LINE  Name: PEHE81-PEHE2:1
Ranking  9  No: 3108 Type: LINE  Name: TORN81-TORN4:1
Ranking 10  No: 3107 Type: LINE  Name: TORN4-TORN81:1
Ranking 11  No: 3076 Type: LINE  Name: DRAX81-DRAX4J:1
Ranking 12  No: 3075 Type: LINE  Name: DRAX4J-DRAX81:1
Ranking 13  No: 3104 Type: LINE  Name: LITB81-LITB4:1
Ranking 14  No: 3066 Type: LINE  Name: SIZE81-SIZE4:1
Ranking 15  No: 3096 Type: LINE  Name: RYEH81-RYEH4:1
Ranking 16  No: 3106 Type: LINE  Name: LITB82-LITB4:1
Ranking 17  No: 3090 Type: LINE  Name: KEAD82-KEAD4J:1
Ranking 18  No: 3084 Type: LINE  Name: KILL83-KILL4:1
Ranking 19  No: 3054 Type: LINE  Name: HINP83-HINP4:1
Ranking 20  No: 3053 Type: LINE  Name: HINP4-HINP83:1
Ranking 21  No: 3080 Type: LINE  Name: KILL81-KILL4:1
Ranking 22  No: 3697 Type: LINE  Name: BRIG1-KEAD1:2 BRIG1-KEAD1:1
Ranking 23  No: 3088 Type: LINE  Name: KEAD81-KEAD4J:1
Ranking 24  No: 3279 Type: LINE  Name: SELL1J-SELL4:2 SELL1J-SELL4:1
Ranking 25  No: 3082 Type: LINE  Name: KILL82-KILL4:1
Ranking 26  No: 3116 Type: LINE  Name: CHAP81-CHAP1:1
Ranking 27  No: 3092 Type: LINE  Name: SHBA81-SHBA4:1
Ranking 28  No: 3094 Type: LINE  Name: SHBA82-SHBA4:1
Ranking 29  No: 3062 Type: LINE  Name: DUNG81-DUNG2:1
Ranking 30  No: 3078 Type: LINE  Name: DRAX82-DRAX4K:1
Ranking 31  No: 3109 Type: LINE  Name: HUER4-HUER81:1
Ranking 32  No: 3086 Type: LINE  Name: KILL84-KILL4:1
Ranking 33  No: 3048 Type: LINE  Name: HEYS81-HEYS4:1
Ranking 34  No:  427 Type: LINE  Name: CANT1J-CANT4:1
Ranking 35  No: 3072 Type: LINE  Name: GRST83-GRST2B:1
Ranking 36  No:  429 Type: LINE  Name: CANT1K-CANT4:1
Ranking 37  No:  384 Type: LINE  Name: RAYL1K-BRWE1J:1
Ranking 38  No: 3115 Type: LINE  Name: CHAP1-CHAP81:1
Ranking 39  No: 3058 Type: LINE  Name: HATL81-HATL2J:1
Ranking 40  No: 3056 Type: LINE  Name: WYLF81-WYLF4:1
Ranking 41  No: 3060 Type: LINE  Name: HATL82-HATL2K:1
Ranking 42  No: 3098 Type: LINE  Name: RYEH82-RYEH4:1
Ranking 43  No: 3055 Type: LINE  Name: WYLF4-WYLF81:1
Ranking 44  No: 3193 Type: LINE  Name: WARL1-WARL2:2 WARL1-WARL2:1
```

```
Ranking 45  No: 3698 Type: LINE  Name: KEAD1-BRIG1:2 KEAD1-BRIG1:1
Ranking 46  No: 3213 Type: LINE  Name: CITR1K-CITR4:2 CITR1K-CITR4:1
Ranking 47  No: 3074 Type: LINE  Name: GRST84-GRST2B:1
Ranking 48  No: 3068 Type: LINE  Name: GRST81-GRST2A:1
Ranking 49  No: 3047 Type: LINE  Name: HEYS4-HEYS81:1
Ranking 50  No: 3110 Type: LINE  Name: HUER81-HUER4:1
Ranking 51  No: 3113 Type: LINE  Name: LOAN2-LOAN82:1
Ranking 52  No: 3176 Type: LINE  Name: SJOW6K-SJOW2:2 SJOW6K-SJOW2:1
Ranking 53  No: 3111 Type: LINE  Name: LOAN2-LOAN81:1
Ranking 54  No: 3112 Type: LINE  Name: LOAN81-LOAN2:1
Ranking 55  No: 3063 Type: LINE  Name: DUNG4-DUNG82:1
Ranking 56  No: 3114 Type: LINE  Name: LOAN82-LOAN2:1
Ranking 57  No: 3079 Type: LINE  Name: KILL4-KILL81:1
Ranking 58  No: 3095 Type: LINE  Name: RYEH4-RYEH81:1
Ranking 59  No:  383 Type: LINE  Name: BRWE1J-RAYL1K:1
Ranking 60  No: 3064 Type: LINE  Name: DUNG82-DUNG4:1
Ranking 61  No: 3103 Type: LINE  Name: LITB4-LITB81:1
Ranking 62  No:  231 Type: LINE  Name: BOLN1M-BOLN4:1
Ranking 63  No: 3102 Type: LINE  Name: DEES82-DEES4:1
Ranking 64  No: 3100 Type: LINE  Name: DEES81-DEES4:1
Ranking 65  No: 3285 Type: LINE  Name: COWL1K-COWL4:2 COWL1K-COWL4:1
Ranking 66  No: 3269 Type: LINE  Name: KINO1-KINO4:2 KINO1-KINO4:1
Ranking 67  No: 3091 Type: LINE  Name: SHBA4-SHBA81:1
Ranking 68  No: 3070 Type: LINE  Name: GRST82-GRST2A:1
Ranking 69  No: 3057 Type: LINE  Name: HATL2J-HATL81:1
Ranking 70  No: 3059 Type: LINE  Name: HATL2K-HATL82:1
Ranking 71  No: 3178 Type: LINE  Name: SJOW6J-SJOW2:2 SJOW6J-SJOW2:1
Ranking 72  No: 3387 Type: LINE  Name: BURW1-BURW4:2 BURW1-BURW4:1
Ranking 73  No: 3134 Type: LINE  Name: LEVE81-LEVE3:1
Ranking 74  No: 3265 Type: LINE  Name: SIZE1J-SIZE4:2 SIZE1J-SIZE4:1
Ranking 75  No: 3267 Type: LINE  Name: SIZE1K-SIZE4:2 SIZE1K-SIZE4:1
Ranking 76  No: 3303 Type: LINE  Name: SUND1J-SUND4:2 SUND1J-SUND4:1
Badly Damped:
Ranking 77  No: 3067 Type: LINE  Name: GRST2A-GRST81:1
Ranking 78  No: 3273 Type: LINE  Name: DUNG2-DUNG4:2 DUNG2-DUNG4:1
Diverging:
Ranking 79  No: 3186 Type: LINE  Name: NEWX6J-NEWX2:2 NEWX6J-NEWX2:1
Badly Damped:
Ranking 80  No: 3061 Type: LINE  Name: DUNG2-DUNG81:1
Ranking 81  No: 1225 Type: LINE  Name: HURS1L-HURS2:1
Ranking 82  No: 3065 Type: LINE  Name: SIZE4-SIZE81:1
Ranking 83  No:   89 Type: LINE  Name: BARK1K-BARK2K:1
Ranking 84  No: 3118 Type: LINE  Name: GLLE81-GLLE1:1
Ranking 85  No: 3231 Type: LINE  Name: LOVE1K-LOVE4:2 LOVE1K-LOVE4:1
Ranking 86  No:  137 Type: LINE  Name: BEDD1M-BEDD2J:1
Ranking 87  No: 3083 Type: LINE  Name: KILL4-KILL83:1
Ranking 88  No: 2427 Type: LINE  Name: WIMB1M-WIMB2:1
Ranking 89  No:  535 Type: LINE  Name: CHSI1K-CHSI2:1
Ranking 90  No:  533 Type: LINE  Name: CHSI1J-CHSI2:1
Ranking 91  No:  219 Type: LINE  Name: BOLN1J-BOLN4:1
Ranking 92  No: 3133 Type: LINE  Name: LEVE3-LEVE81:1
Ranking 93  No: 3705 Type: LINE  Name: CREB1K-CREB4:2 CREB1K-CREB4:1
Ranking 94  No: 3069 Type: LINE  Name: GRST2A-GRST82:1
Ranking 95  No: 2425 Type: LINE  Name: WIMB1L-WIMB2:1
Ranking 96  No: 3211 Type: LINE  Name: CITR1J-CITR4:2 CITR1J-CITR4:1
Ranking 97  No: 3567 Type: LINE  Name: RAIN1K-RAIN2:2 RAIN1K-RAIN2:1
```

```
Ranking 98  No: 3599 Type: LINE  Name: WHGA1-WHGA2:2 WHGA1-WHGA2:1
Ranking 99  No: 3419 Type: LINE  Name: WALP1J-WALP4:2 WALP1J-WALP4:1
Ranking100  No: 3637 Type: LINE  Name: SKLG1J-SKLG2:2 SKLG1J-SKLG2:1
Severity Indexed:
Ranking101  No: 3087 Type: LINE  Name: KEAD4J-KEAD81:1                 SI:   -92.96  DI:  -0.0829
Ranking102  No: 3077 Type: LINE  Name: DRAX4K-DRAX82:1                 SI:  -113.75  DI:  -0.0988
Ranking103  No: 3071 Type: LINE  Name: GRST2B-GRST83:1                 SI:  -122.86  DI:  -0.1094
Ranking104  No: 3639 Type: LINE  Name: SKLG1K-SKLG2:2 SKLG1K-SKLG2:1   SI:  -123.18  DI:  -0.0801
Ranking105  No: 3593 Type: LINE  Name: SMAN1-SMAN2:2 SMAN1-SMAN2:1     SI:  -141.72  DI:  -0.0895
Ranking106  No: 3105 Type: LINE  Name: LITB4-LITB82:1                  SI:  -144.28  DI:  -0.0986
Ranking107  No: 3229 Type: LINE  Name: LOVE1J-LOVE4:2 LOVE1J-LOVE4:1   SI:  -147.85  DI:  -0.0922
Ranking108  No: 3081 Type: LINE  Name: KILL4-KILL82:1                  SI:  -159.45  DI:  -0.1126
Ranking109  No: 3699 Type: LINE  Name: GRIW1-GRIW4:2 GRIW1-GRIW4:1     SI:  -164.84  DI:  -0.1004
Ranking110  No:  351 Type: LINE  Name: BRLE1K-BRLE4:1                  SI:  -173.15  DI:  -0.1038
Ranking111  No:  349 Type: LINE  Name: BRLE1J-BRLE4:1                  SI:  -173.85  DI:  -0.1042
Ranking112  No: 3305 Type: LINE  Name: SUND1K-SUND4:2 SUND1K-SUND4:1   SI:  -180.08  DI:  -0.1080
Ranking113  No: 3223 Type: LINE  Name: BOTW1-BOTW4:2 BOTW1-BOTW4:1     SI:  -190.49  DI:  -0.1132
Ranking114  No: 3584 Type: LINE  Name: KEAR3-KEAR2:2 KEAR3-KEAR2:1     SI:  -196.74  DI:  -0.1154
Ranking115  No: 3217 Type: LINE  Name: WHAM1-WHAM4:2 WHAM1-WHAM4:1     SI:  -202.90  DI:  -0.1193
Ranking116  No: 3431 Type: LINE  Name: STAY1-STAY4:2 STAY1-STAY4:1     SI:  -207.93  DI:  -0.1220
Ranking117  No: 3531 Type: LINE  Name: IRON1-IRON4:2 IRON1-IRON4:1     SI:  -208.62  DI:  -0.1225
Ranking118  No: 3138 Type: LINE  Name: SLOY81-SLOY1:1                  SI:  -211.62  DI:  -0.1246
Ranking119  No: 3613 Type: LINE  Name: CAPE1J-CAPE2J:2 CAPE1J-CAPE2J:1 SI:  -214.35  DI:  -0.1257
Ranking120  No: 3184 Type: LINE  Name: NEWX6K-NEWX2:2 NEWX6K-NEWX2:1   SI:  -219.70  DI:  -0.1274
Ranking121  No: 3455 Type: LINE  Name: RUGE1-RUGE4:2 RUGE1-RUGE4:1     SI:  -226.36  DI:  -0.1313
Ranking122  No: 3695 Type: LINE  Name: OSBA1-OSBA4:2 OSBA1-OSBA4:1     SI:  -230.02  DI:  -0.1342
Ranking123  No: 3274 Type: LINE  Name: DUNG4-DUNG2:2 DUNG4-DUNG2:1     SI:  -237.93  DI:  -0.1466
Ranking124  No: 3136 Type: LINE  Name: KIIN81-KIIN1:1                  SI:  -241.12  DI:  -0.1377
Ranking125  No:  225 Type: LINE  Name: BOLN1K-BOLN4:1                  SI:  -245.19  DI:  -0.1396
Ranking126  No: 3266 Type: LINE  Name: SIZE4-SIZE1J:2 SIZE4-SIZE1J:1   SI:  -248.47  DI:  -0.1536
Ranking127  No: 3268 Type: LINE  Name: SIZE4-SIZE1K:2 SIZE4-SIZE1K:1   SI:  -248.47  DI:  -0.1536
Ranking128  No: 3073 Type: LINE  Name: GRST2B-GRST84:1                 SI:  -251.31  DI:  -0.1646
Ranking129  No: 3126 Type: LINE  Name: FASN81-FASN1:1                  SI:  -252.48  DI:  -0.1442
Ranking130  No: 1389 Type: LINE  Name: KEMS1L-KEMS4K:1                 SI:  -262.99  DI:  -0.1484
Ranking131  No: 3219 Type: LINE  Name: CHSI1-CHSI2:2 CHSI1-CHSI2:1     SI:  -262.99  DI:  -0.1494
Ranking132  No: 3132 Type: LINE  Name: ERRO82-ERRO1K:1                 SI:  -263.09  DI:  -0.1489
Ranking133  No: 3099 Type: LINE  Name: DEES4-DEES81:1                  SI:  -266.34  DI:  -0.1632
Ranking134  No: 3124 Type: LINE  Name: BEAU82-BEAU1Y:1                 SI:  -271.54  DI:  -0.1537
Ranking135  No: 3122 Type: LINE  Name: BEAU81-BEAU1X:1                 SI:  -271.71  DI:  -0.1538
Ranking136  No: 3051 Type: LINE  Name: HINP2K-HINP82:1                 SI:  -272.05  DI:  -0.1586
Ranking137  No: 3052 Type: LINE  Name: HINP82-HINP2K:1                 SI:  -272.39  DI:  -0.1534
Ranking138  No: 3421 Type: LINE  Name: WALP1K-WALP4:2 WALP1K-WALP4:1   SI:  -273.79  DI:  -0.1552
Ranking139  No: 3050 Type: LINE  Name: HINP81-HINP2J:1                 SI:  -278.65  DI:  -0.1565
Ranking140  No: 3151 Type: LINE  Name: LALE1J-LALE2:2 LALE1J-LALE2:1   SI:  -281.71  DI:  -0.1587
Ranking141  No: 3153 Type: LINE  Name: LALE1K-LALE2:2 LALE1K-LALE2:1   SI:  -283.31  DI:  -0.1595
Ranking142  No: 3049 Type: LINE  Name: HINP2J-HINP81:1                 SI:  -283.74  DI:  -0.1644
Ranking143  No: 3128 Type: LINE  Name: FAUG81-FAUG1:1                  SI:  -293.13  DI:  -0.1647
Ranking144  No: 3130 Type: LINE  Name: ERRO81-ERRO1J:1                 SI:  -294.55  DI:  -0.1646
Ranking145  No: 3453 Type: LINE  Name: PENN1K-PENN2:2 PENN1K-PENN2:1   SI:  -304.35  DI:  -0.1701
Ranking146  No: 3796 Type: LINE  Name: HUER1-HUER4:2 HUER1-HUER4:1     SI:  -305.16  DI:  -0.1778
Ranking147  No: 3451 Type: LINE  Name: PENN1J-PENN2:2 PENN1J-PENN2:1   SI:  -305.30  DI:  -0.1706
Ranking148  No: 3509 Type: LINE  Name: HAMH1K-HAMH4:2 HAMH1K-HAMH4:1   SI:  -327.57  DI:  -0.1818
Ranking149  No: 3283 Type: LINE  Name: COWL1J-COWL4:2 COWL1J-COWL4:1   SI:  -330.30  DI:  -0.1832
Ranking150  No: 3443 Type: LINE  Name: CASD1-CASD2:2 CASD1-CASD2:1     SI:  -333.71  DI:  -0.1845
Ranking151  No: 3433 Type: LINE  Name: WBUR1-WBUR4:2 WBUR1-WBUR4:1     SI:  -334.77  DI:  -0.1855
Ranking152  No: 3235 Type: LINE  Name: NURS1-NURS4:2 NURS1-NURS4:1     SI:  -345.03  DI:  -0.1908
```

```
Ranking153  No: 3281 Type: LINE  Name: SELL1K-SELL4:2 SELL1K-SELL4:1   SI:  -349.76  DI:  -0.1934
Ranking154  No: 3311 Type: LINE  Name: AXMI1-AXMI4:2 AXMI1-AXMI4:1     SI:  -359.39  DI:  -0.1994
Ranking155  No: 3773 Type: LINE  Name: CURR1-CURR2:2 CURR1-CURR2:1     SI:  -366.63  DI:  -0.2097
Ranking156  No: 3676 Type: LINE  Name: THUR6-THUR2:2 THUR6-THUR2:1     SI:  -381.51  DI:  -0.2088
Ranking157  No: 3093 Type: LINE  Name: SHBA4-SHBA82:1                  SI:  -396.12  DI:  -0.2266
Ranking158  No: 3751 Type: LINE  Name: STES1-STEW2:2 STES1-STEW2:1     SI:  -399.96  DI:  -0.2210
Ranking159  No: 3703 Type: LINE  Name: CREB1J-CREB4:2 CREB1J-CREB4:1   SI:  -401.98  DI:  -0.2195
Ranking160  No: 3233 Type: LINE  Name: NINF1J-NINF4:2 NINF1J-NINF4:1   SI:  -404.05  DI:  -0.2204
Ranking161  No: 3627 Type: LINE  Name: ELLA1K-ELLA2:2 ELLA1K-ELLA2:1   SI:  -405.54  DI:  -0.2213
Ranking162  No: 3737 Type: LINE  Name: TYNE1-TYNE2:2 TYNE1-TYNE2:1     SI:  -407.37  DI:  -0.2243
Ranking163  No: 3791 Type: LINE  Name: COYL1-COYL3:2 COYL1-COYL3:1     SI:  -408.52  DI:  -0.2283
Ranking164  No: 3728 Type: LINE  Name: HAWP6-HAWP2:2 HAWP6-HAWP2:1     SI:  -413.62  DI:  -0.2262
Ranking165  No: 3765 Type: LINE  Name: HEYS1-HEYS4:2 HEYS1-HEYS4:1     SI:  -421.25  DI:  -0.2304
Ranking166  No: 3475 Type: LINE  Name: OLDB1-OLDB2:2 OLDB1-OLDB2:1     SI:  -425.01  DI:  -0.2303
Ranking167  No:  297 Type: LINE  Name: BRIG1-KEAD1:1                   SI:  -426.72  DI:  -0.2307
Ranking168  No: 3792 Type: LINE  Name: COYL3-COYL1:2 COYL3-COYL1:1     SI:  -428.16  DI:  -0.2355
Ranking169  No: 3761 Type: LINE  Name: PENE1K-PEWO2:2 PENE1K-PEWO2:1   SI:  -428.64  DI:  -0.2334
Ranking170  No: 3629 Type: LINE  Name: KIRK1-KIRK2:2 KIRK1-KIRK2:1     SI:  -437.23  DI:  -0.2370
Ranking171  No:  353 Type: LINE  Name: BRLE1L-BRLE4:1                  SI:  -440.11  DI:  -0.2372
Ranking172  No:  355 Type: LINE  Name: BRLE1M-BRLE4:1                  SI:  -440.11  DI:  -0.2372
Ranking173  No: 3473 Type: LINE  Name: OCKH1-OCKH2:2 OCKH1-OCKH2:1     SI:  -440.54  DI:  -0.2382
Ranking174  No: 3640 Type: LINE  Name: SKLG2-SKLG1K:2 SKLG2-SKLG1K:1   SI:  -441.49  DI:  -0.2426
Ranking175  No: 3638 Type: LINE  Name: SKLG2-SKLG1J:2 SKLG2-SKLG1J:1   SI:  -441.54  DI:  -0.2426
Ranking176  No: 3378 Type: LINE  Name: UPPB3-UPPB2N:2 UPPB3-UPPB2N:1   SI:  -443.11  DI:  -0.2389
Ranking177  No: 3719 Type: LINE  Name: SALH1-SALH2:2 SALH1-SALH2:1     SI:  -443.91  DI:  -0.2437
Ranking178  No: 3785 Type: LINE  Name: TORN1-TORN4:2 TORN1-TORN4:1     SI:  -444.88  DI:  -0.2467
Ranking179  No:  299 Type: LINE  Name: BRIG1-KEAD1:2                   SI:  -451.06  DI:  -0.2429
Ranking180  No: 3658 Type: LINE  Name: NEEP3-NEEP2:2 NEEP3-NEEP2:1     SI:  -452.55  DI:  -0.2433
Ranking181  No: 3625 Type: LINE  Name: ELLA1J-ELLA2:2 ELLA1J-ELLA2:1   SI:  -462.32  DI:  -0.2496
Ranking182  No: 1837 Type: LINE  Name: PENE1J-PEWO2:1                  SI:  -462.89  DI:  -0.2492
Ranking183  No: 3726 Type: LINE  Name: HARM6-HARM2:2 HARM6-HARM2:1     SI:  -463.76  DI:  -0.2509
Ranking184  No: 3577 Type: LINE  Name: KEAR1K-KEAR2:2 KEAR1K-KEAR2:1   SI:  -464.56  DI:  -0.2509
Ranking185  No: 3575 Type: LINE  Name: KEAR1J-KEAR2:2 KEAR1J-KEAR2:1   SI:  -464.58  DI:  -0.2510
Ranking186  No: 3800 Type: LINE  Name: STLE3S-STLE1:2 STLE3S-STLE1:1   SI:  -467.01  DI:  -0.2544
Ranking187  No: 3631 Type: LINE  Name: KNAR1-KNAR2:2 KNAR1-KNAR2:1     SI:  -467.72  DI:  -0.2518
Ranking188  No: 3837 Type: LINE  Name: PEHE1-PEHE2:2 PEHE1-PEHE2:1     SI:  -468.24  DI:  -0.2628
Ranking189  No: 3692 Type: LINE  Name: FERR6-FERR2K:2 FERR6-FERR2K:1   SI:  -472.77  DI:  -0.2544
Ranking190  No: 3854 Type: LINE  Name: PEHE2-KINT2:2 PEHE2-KINT2:1     SI:  -476.33  DI:  -0.3395
Ranking191  No: 3636 Type: LINE  Name: POPP3-POPP2:2 POPP3-POPP2:1     SI:  -478.22  DI:  -0.2561
Ranking192  No: 3586 Type: LINE  Name: MACC3-MACC2:2 MACC3-MACC2:1     SI:  -481.77  DI:  -0.2578
Ranking193  No: 3672 Type: LINE  Name: SHEC3-SHEC2:2 SHEC3-SHEC2:1     SI:  -486.08  DI:  -0.2602
Ranking194  No: 3367 Type: LINE  Name: RASS1-RASS4:2 RASS1-RASS4:1     SI:  -490.98  DI:  -0.2637
Ranking195  No: 3693 Type: LINE  Name: DRAX1-DRAX4K:2 DRAX1-DRAX4K:1   SI:  -491.16  DI:  -0.2642
Ranking196  No: 3799 Type: LINE  Name: STLE1-STLE3S:2 STLE1-STLE3S:1   SI:  -493.54  DI:  -0.2691
Ranking197  No: 3180 Type: LINE  Name: NEWX2-HURS2:2 NEWX2-HURS2:1     SI:  -512.70  DI:  -0.2831
Ranking198  No: 3137 Type: LINE  Name: SLOY1-SLOY81:1                  SI:  -513.08  DI:  -0.2824
Ranking199  No: 3125 Type: LINE  Name: FASN1-FASN81:1                  SI:  -514.76  DI:  -0.2838
Ranking200  No: 1993 Type: LINE  Name: ROOS1-SEFI1:1                   SI:  -520.09  DI:  -0.2778
Ranking201  No: 3127 Type: LINE  Name: FAUG1-FAUG81:1                  SI:  -525.44  DI:  -0.2886
Ranking202  No: 3632 Type: LINE  Name: KNAR2-KNAR1:2 KNAR2-KNAR1:1     SI:  -533.04  DI:  -0.2862
Ranking203  No: 3117 Type: LINE  Name: GLLE1-GLLE81:1                  SI:  -538.16  DI:  -0.2881
Ranking204  No: 1240 Type: LINE  Name: ROOS1-HUTT1:1                   SI:  -539.04  DI:  -0.2876
Ranking205  No: 3179 Type: LINE  Name: HURS2-NEWX2:2 HURS2-NEWX2:1     SI:  -539.26  DI:  -0.2969
Ranking206  No: 3246 Type: LINE  Name: NINF4-DUNG4:2 NINF4-DUNG4:1     SI:  -549.01  DI:  -0.3097
Ranking207  No: 3245 Type: LINE  Name: DUNG4-NINF4:2 DUNG4-NINF4:1     SI:  -551.71  DI:  -0.3113
Ranking208  No: 3736 Type: LINE  Name: SSHI3-SSHI2:2 SSHI3-SSHI2:1     SI:  -554.88  DI:  -0.2958
```

```
Ranking209  No: 1994 Type: LINE  Name: SEFI1-ROOS1:1                    SI:  -554.89  DI:  -0.2948
Ranking210  No: 3674 Type: LINE  Name: THOM6-THOM2J:2 THOM6-THOM2J:1    SI:  -556.48  DI:  -0.2959
Ranking211  No: 3144 Type: LINE  Name: LALE2-EALI2:2 LALE2-EALI2:1      SI:  -569.43  DI:  -0.3100
Ranking212  No:  487 Type: LINE  Name: CARR1L-CARR2K:1                   SI:  -573.20  DI:  -0.3038
Ranking213  No: 3143 Type: LINE  Name: EALI2-LALE2:2 EALI2-LALE2:1      SI:  -575.02  DI:  -0.3128
Ranking214  No: 2005 Type: LINE  Name: RYEH1-RYEH4T:1                   SI:  -576.37  DI:  -0.3058
Ranking215  No: 2776 Type: LINE  Name: DOUN2-BEAU2:1                    SI:  -577.08  DI:  -0.3134
Ranking216  No: 3375 Type: LINE  Name: UPPB1-UPPB2M:2 UPPB1-UPPB2M:1    SI:  -577.52  DI:  -0.3069
Ranking217  No:  425 Type: LINE  Name: CALD1-HARK1J:1                   SI:  -580.28  DI:  -0.3082
Ranking218  No: 3734 Type: LINE  Name: OFFE3-OFFE2:2 OFFE3-OFFE2:1      SI:  -588.41  DI:  -0.3124
Ranking219  No: 2993 Type: LINE  Name: DOUN1-DOUN2:1                    SI:  -589.66  DI:  -0.3176
Ranking220  No: 3738 Type: LINE  Name: TYNE2-TYNE1:2 TYNE2-TYNE1:1      SI:  -595.12  DI:  -0.3246
Ranking221  No: 3651 Type: LINE  Name: CHTE1J-CHTE2:2 CHTE1J-CHTE2:1    SI:  -595.69  DI:  -0.3164
Ranking222  No: 3600 Type: LINE  Name: WHGA2-WHGA1:2 WHGA2-WHGA1:1      SI:  -596.99  DI:  -0.3238
Ranking223  No: 3129 Type: LINE  Name: ERRO1J-ERRO81:1                   SI:  -601.26  DI:  -0.3235
Ranking224  No: 3653 Type: LINE  Name: CHTE1K-CHTE2:2 CHTE1K-CHTE2:1    SI:  -608.84  DI:  -0.3230
Ranking225  No: 1835 Type: LINE  Name: PEMB4-WALH4:1                    SI:  -613.80  DI:  -0.3303
Ranking226  No: 3388 Type: LINE  Name: BURW4-BURW1:2 BURW4-BURW1:1      SI:  -615.92  DI:  -0.3338
Ranking227  No: 3131 Type: LINE  Name: ERRO1K-ERRO82:1                   SI:  -619.40  DI:  -0.3318
Ranking228  No: 3774 Type: LINE  Name: CURR2-CURR1:2 CURR2-CURR1:1      SI:  -622.90  DI:  -0.3439
Ranking229  No: 3675 Type: LINE  Name: THUR2-THUR6:2 THUR2-THUR6:1      SI:  -624.21  DI:  -0.3354
Ranking230  No: 3630 Type: LINE  Name: KIRK2-KIRK1:2 KIRK2-KIRK1:1      SI:  -627.61  DI:  -0.3361
Ranking231  No: 3386 Type: LINE  Name: PEMB4-CILF4:2 PEMB4-CILF4:1      SI:  -628.16  DI:  -0.3387
Ranking232  No: 3568 Type: LINE  Name: RAIN2-RAIN1K:2 RAIN2-RAIN1K:1    SI:  -633.93  DI:  -0.3405
Ranking233  No: 3194 Type: LINE  Name: WARL2-WARL1:2 WARL2-WARL1:1      SI:  -634.08  DI:  -0.3407
Ranking234  No: 3000 Type: LINE  Name: BEAU1X-BEAU1J:1                   SI:  -640.15  DI:  -0.3504
Ranking235  No: 3002 Type: LINE  Name: BEAU1Y-BEAU1K:1                   SI:  -642.59  DI:  -0.3515
Ranking236  No: 3313 Type: LINE  Name: CHIC1-CHIC4:2 CHIC1-CHIC4:1      SI:  -645.85  DI:  -0.3419
Ranking237  No: 3135 Type: LINE  Name: KIIN1-KIIN81:1                   SI:  -647.35  DI:  -0.3455
Ranking238  No: 3795 Type: LINE  Name: HUER4-HUER1:2 HUER4-HUER1:1      SI:  -659.89  DI:  -0.3614
Ranking239  No: 3174 Type: LINE  Name: SJOW1K-MILH1:2 SJOW1K-MILH1:1    SI:  -661.48  DI:  -0.3497
Ranking240  No: 2994 Type: LINE  Name: DOUN2-DOUN1:1                    SI:  -662.92  DI:  -0.3537
Ranking241  No: 3614 Type: LINE  Name: CAPE2J-CAPE1J:2 CAPE2J-CAPE1J:1  SI:  -671.66  DI:  -0.3580
Ranking242  No: 3312 Type: LINE  Name: AXMI4-AXMI1:2 AXMI4-AXMI1:1      SI:  -678.34  DI:  -0.3656
Ranking243  No: 3121 Type: LINE  Name: BEAU1X-BEAU81:1                   SI:  -678.89  DI:  -0.3643
Ranking244  No: 2999 Type: LINE  Name: BEAU1J-BEAU1X:1                   SI:  -678.96  DI:  -0.3644
Ranking245  No:  300 Type: LINE  Name: KEAD1-BRIG1:2                     SI:  -681.23  DI:  -0.3588
Ranking246  No: 3788 Type: LINE  Name: DUMF1-CHAP1:2 DUMF1-CHAP1:1      SI:  -683.55  DI:  -0.3717
Ranking247  No: 1085 Type: LINE  Name: HAKB1-HARK1M:1                   SI:  -685.62  DI:  -0.3734
Ranking248  No: 1095 Type: LINE  Name: CHAP1-HAKB1:1                    SI:  -687.35  DI:  -0.3795
Ranking249  No: 3182 Type: LINE  Name: WIMB2-NEWX2:2 WIMB2-NEWX2:1      SI:  -688.97  DI:  -0.3714
Ranking250  No: 3678 Type: LINE  Name: WIBA3-WIBA2:2 WIBA3-WIBA2:1      SI:  -689.22  DI:  -0.3615
Ranking251  No: 3595 Type: LINE  Name: STAL1J-STAL2:2 STAL1J-STAL2:1    SI:  -690.29  DI:  -0.3638
Ranking252  No: 3720 Type: LINE  Name: SALH2-SALH1:2 SALH2-SALH1:1      SI:  -692.35  DI:  -0.3782
Ranking253  No: 3237 Type: LINE  Name: BOLN4-NINF4:2 BOLN4-NINF4:1      SI:  -693.48  DI:  -0.3795
Ranking254  No: 3238 Type: LINE  Name: NINF4-BOLN4:2 NINF4-BOLN4:1      SI:  -694.09  DI:  -0.3799
Ranking255  No: 1096 Type: LINE  Name: HAKB1-CHAP1:1                    SI:  -694.94  DI:  -0.3808
Ranking256  No: 3594 Type: LINE  Name: SMAN2-SMAN1:2 SMAN2-SMAN1:1      SI:  -695.43  DI:  -0.3727
Ranking257  No: 3232 Type: LINE  Name: LOVE4-LOVE1K:2 LOVE4-LOVE1K:1    SI:  -697.34  DI:  -0.3764
Ranking258  No: 3787 Type: LINE  Name: CHAP1-DUMF1:2 CHAP1-DUMF1:1      SI:  -699.09  DI:  -0.3808
Ranking259  No: 3621 Type: LINE  Name: BRAW1J-BRAW2:2 BRAW1J-BRAW2:1    SI:  -701.23  DI:  -0.3694
Ranking260  No: 1239 Type: LINE  Name: HUTT1-ROOS1:1                    SI:  -701.69  DI:  -0.3707
Ranking261  No:  182 Type: LINE  Name: LISD2Q-BIRK2:1                   SI:  -702.79  DI:  -0.3752
Ranking262  No:  181 Type: LINE  Name: BIRK2-LISD2Q:1                   SI:  -702.85  DI:  -0.3752
Ranking263  No: 1145 Type: LINE  Name: HARK1M-HARK2K:1                  SI:  -704.93  DI:  -0.3821
Ranking264  No: 3173 Type: LINE  Name: MILH1-SJOW1K:2 MILH1-SJOW1K:1    SI:  -707.02  DI:  -0.3726
```

```
Ranking265  No: 2775 Type: LINE  Name: BEAU2-DOUN2:1                        SI:  -708.76  DI:  -0.3810
Ranking266  No: 2319 Type: LINE  Name: WALP1J-WALP4:1                       SI:  -708.90  DI:  -0.3725
Ranking267  No: 1086 Type: LINE  Name: HARK1M-HAKB1:1                       SI:  -710.19  DI:  -0.3865
Ranking268  No: 3001 Type: LINE  Name: BEAU1K-BEAU1Y:1                      SI:  -715.32  DI:  -0.3825
Ranking269  No: 3123 Type: LINE  Name: BEAU1Y-BEAU82:1                      SI:  -715.38  DI:  -0.3825
Ranking270  No: 3597 Type: LINE  Name: STAL1K-STAL2:2 STAL1K-STAL2:1        SI:  -715.99  DI:  -0.3766
Ranking271  No: 3493 Type: LINE  Name: COVE1-COVE2:3 COVE1-COVE2:1          SI:  -716.84  DI:  -0.3769
Ranking272  No: 3549 Type: LINE  Name: TRAW1-TRAW2:2 TRAW1-TRAW2:1          SI:  -719.54  DI:  -0.3781
Ranking273  No: 3544 Type: LINE  Name: PENT4-DINO4:2 PENT4-DINO4:1          SI:  -720.55  DI:  -0.3863
Ranking274  No: 3838 Type: LINE  Name: PEHE2-PEHE1:2 PEHE2-PEHE1:1          SI:  -723.51  DI:  -0.4051
Ranking275  No: 3101 Type: LINE  Name: DEES4-DEES82:1                       SI:  -724.50  DI:  -0.3906
Ranking276  No: 3495 Type: LINE  Name: COVE1-COVE2:2 COVE1-COVE2:1          SI:  -724.74  DI:  -0.3808
Ranking277  No: 3299 Type: LINE  Name: ECLA1-ECLA4:2 ECLA1-ECLA4:1          SI:  -726.69  DI:  -0.3818
Ranking278  No: 3491 Type: LINE  Name: COVE1-COVE2:3 COVE1-COVE2:2          SI:  -728.25  DI:  -0.3826
Ranking279  No: 3628 Type: LINE  Name: ELLA2-ELLA1K:2 ELLA2-ELLA1K:1        SI:  -730.09  DI:  -0.3885
Ranking280  No:  227 Type: LINE  Name: BOLN1L-BOLN4:1                       SI:  -731.39  DI:  -0.3831
Ranking281  No:  387 Type: LINE  Name: BURW1-BURW4:1                        SI:  -737.03  DI:  -0.3862
Ranking282  No:  389 Type: LINE  Name: BURW1-BURW4:2                        SI:  -738.63  DI:  -0.3870
Ranking283  No: 2007 Type: LINE  Name: RYEH1-RYEH4U:1                       SI:  -745.73  DI:  -0.3905
Ranking284  No: 3696 Type: LINE  Name: OSBA4-OSBA1:2 OSBA4-OSBA1:1          SI:  -746.91  DI:  -0.4021
Ranking285  No:  775 Type: LINE  Name: EASO1-EASO4Q:1                       SI:  -748.35  DI:  -0.3919
Ranking286  No: 3181 Type: LINE  Name: NEWX2-WIMB2:2 NEWX2-WIMB2:1          SI:  -750.23  DI:  -0.4032
Ranking287  No: 3626 Type: LINE  Name: ELLA2-ELLA1J:2 ELLA2-ELLA1J:1        SI:  -750.64  DI:  -0.3988
Ranking288  No: 3731 Type: LINE  Name: NORT1K-NORT2:2 NORT1K-NORT2:1        SI:  -751.48  DI:  -0.3966
Ranking289  No: 2321 Type: LINE  Name: WALP1J-WALP4:2                       SI:  -755.98  DI:  -0.3961
Ranking290  No: 3827 Type: LINE  Name: KEIT1-BLHI2:2 KEIT1-BLHI2:1          SI:  -757.99  DI:  -0.4065
Ranking291  No: 3543 Type: LINE  Name: DINO4-PENT4:2 DINO4-PENT4:1          SI:  -758.58  DI:  -0.4078
Ranking292  No: 3385 Type: LINE  Name: CILF4-PEMB4:2 CILF4-PEMB4:1          SI:  -759.50  DI:  -0.4062
Ranking293  No:  232 Type: LINE  Name: BOLN4-BOLN1M:1                       SI:  -762.14  DI:  -0.4067
Ranking294  No: 3835 Type: LINE  Name: CRAI1-KINT1:2 CRAI1-KINT1:1          SI:  -762.95  DI:  -0.4095
Ranking295  No: 3355 Type: LINE  Name: WALH1K-WALH4:2 WALH1K-WALH4:1        SI:  -763.63  DI:  -0.4002
Ranking296  No: 3444 Type: LINE  Name: CASD2-CASD1:2 CASD2-CASD1:1          SI:  -765.37  DI:  -0.4034
Ranking297  No: 3376 Type: LINE  Name: UPPB2M-UPPB1:2 UPPB2M-UPPB1:1        SI:  -766.61  DI:  -0.4045
Ranking298  No: 3826 Type: LINE  Name: SLOY1-KIIN1:2 SLOY1-KIIN1:1          SI:  -769.41  DI:  -0.4148
Ranking299  No: 3215 Type: LINE  Name: CITR4-WHAM4:2 CITR4-WHAM4:1          SI:  -771.17  DI:  -0.4161
Ranking300  No: 3280 Type: LINE  Name: SELL4-SELL1J:2 SELL4-SELL1J:1        SI:  -772.22  DI:  -0.4125
Ranking301  No: 3295 Type: LINE  Name: ECLA1-ECLA4:3 ECLA1-ECLA4:2          SI:  -776.20  DI:  -0.4065
Ranking302  No: 3775 Type: LINE  Name: ECCL1-ECCL4:2 ECCL1-ECCL4:1          SI:  -777.71  DI:  -0.4132
Ranking303  No:  199 Type: LINE  Name: BLYT1-BLYT2K:1                       SI:  -778.11  DI:  -0.4093
Ranking304  No: 3353 Type: LINE  Name: WALH1J-WALH4:2 WALH1J-WALH4:1        SI:  -779.94  DI:  -0.4084
Ranking305  No: 2029 Type: LINE  Name: SELL1J-SELL4:1                       SI:  -780.73  DI:  -0.4078
Ranking306  No: 1941 Type: LINE  Name: RAYL1J-RAYL1L:1                      SI:  -781.41  DI:  -0.4084
Ranking307  No: 3262 Type: LINE  Name: RAYL1J-RAYL1L:2 RAYL1J-RAYL1L:1     SI:  -781.50  DI:  -0.4085
Ranking308  No:  197 Type: LINE  Name: BLYT1-BLYT2J:1                       SI:  -782.90  DI:  -0.4117
Ranking309  No: 2432 Type: LINE  Name: WISD2Q-WIMB2:1                       SI:  -786.10  DI:  -0.4196
Ranking310  No: 3752 Type: LINE  Name: STEW2-STES1:2 STEW2-STES1:1          SI:  -789.20  DI:  -0.4223
Ranking311  No: 3297 Type: LINE  Name: ECLA1-ECLA4:3 ECLA1-ECLA4:1          SI:  -789.75  DI:  -0.4133
Ranking312  No: 3716 Type: LINE  Name: LACK6-LACK2:3 LACK6-LACK2:1          SI:  -791.50  DI:  -0.4166
Ranking313  No: 2826 Type: LINE  Name: ERRO1J-FAUG1:1                       SI:  -791.70  DI:  -0.4242
Ranking314  No: 3718 Type: LINE  Name: LACK6-LACK2:2 LACK6-LACK2:1          SI:  -793.74  DI:  -0.4177
Ranking315  No:  298 Type: LINE  Name: KEAD1-BRIG1:1                        SI:  -794.38  DI:  -0.4154
Ranking316  No: 1146 Type: LINE  Name: HARK2K-HARK1M:1                      SI:  -795.57  DI:  -0.4325
Ranking317  No: 3777 Type: LINE  Name: ECCL1-GALA1:2 ECCL1-GALA1:1          SI:  -796.08  DI:  -0.4204
Ranking318  No: 3758 Type: LINE  Name: BLYT6-BLYT2K:2 BLYT6-BLYT2K:1        SI:  -797.83  DI:  -0.4189
Ranking319  No: 1231 Type: LINE  Name: HURS2-NEWX2:1                        SI:  -797.97  DI:  -0.4254
Ranking320  No: 2031 Type: LINE  Name: SELL1J-SELL4:2                       SI:  -798.51  DI:  -0.4167
```

```
Ranking321  No: 3714 Type: LINE  Name: LACK6-LACK2:3 LACK6-LACK2:2      SI:  -798.74  DI:  -0.4202
Ranking322  No: 3257 Type: LINE  Name: BRFO1-BRFO4:2 BRFO1-BRFO4:1      SI:  -798.95  DI:  -0.4198
Ranking323  No: 2825 Type: LINE  Name: FAUG1-ERRO1J:1                    SI:  -800.02  DI:  -0.4304
Ranking324  No:  153 Type: LINE  Name: BEDD4Q-LITT4U:1                   SI:  -801.13  DI:  -0.4259
Ranking325  No: 3247 Type: LINE  Name: BRFO1-BRFO4:4 BRFO1-BRFO4:3      SI:  -802.44  DI:  -0.4216
Ranking326  No: 3216 Type: LINE  Name: WHAM4-CITR4:2 WHAM4-CITR4:1      SI:  -806.32  DI:  -0.4328
Ranking327  No: 1836 Type: LINE  Name: WALH4-PEMB4:1                     SI:  -806.76  DI:  -0.4296
Ranking328  No: 3249 Type: LINE  Name: BRFO1-BRFO4:4 BRFO1-BRFO4:2      SI:  -808.31  DI:  -0.4245
Ranking329  No: 3840 Type: LINE  Name: FAUG1-FASN1:2 FAUG1-FASN1:1      SI:  -811.21  DI:  -0.4379
Ranking330  No: 3175 Type: LINE  Name: SJOW2-SJOW6K:2 SJOW2-SJOW6K:1    SI:  -812.07  DI:  -0.4310
Ranking331  No: 1232 Type: LINE  Name: NEWX2-HURS2:1                     SI:  -812.51  DI:  -0.4331
Ranking332  No:  566 Type: LINE  Name: PEMB4-CILF4:1                     SI:  -815.48  DI:  -0.4316
Ranking333  No: 3214 Type: LINE  Name: CITR4-CITR1K:2 CITR4-CITR1K:1    SI:  -819.46  DI:  -0.4364
Ranking334  No: 1942 Type: LINE  Name: RAYL1L-RAYL1J:1                   SI:  -819.67  DI:  -0.4275
Ranking335  No: 2852 Type: LINE  Name: ERRO1J-KIIN1:1                    SI:  -820.00  DI:  -0.4384
Ranking336  No: 3255 Type: LINE  Name: BRFO1-BRFO4:3 BRFO1-BRFO4:1      SI:  -823.01  DI:  -0.4319
Ranking337  No: 3261 Type: LINE  Name: RAYL1L-RAYL1J:2 RAYL1L-RAYL1J:1 SI:  -825.12  DI:  -0.4303
Ranking338  No: 3823 Type: LINE  Name: TEAL1-TEAL2:2 TEAL1-TEAL2:1      SI:  -825.65  DI:  -0.4427
Ranking339  No: 3821 Type: LINE  Name: TEAL1-TEAL2:3 TEAL1-TEAL2:1      SI:  -825.65  DI:  -0.4427
Ranking340  No: 3251 Type: LINE  Name: BRFO1-BRFO4:4 BRFO1-BRFO4:1      SI:  -826.77  DI:  -0.4337
Ranking341  No: 3819 Type: LINE  Name: TEAL1-TEAL2:3 TEAL1-TEAL2:2      SI:  -826.90  DI:  -0.4433
Ranking342  No: 1233 Type: LINE  Name: HURS2-NEWX2:2                     SI:  -827.76  DI:  -0.4403
Ranking343  No:  426 Type: LINE  Name: HARK1J-CALD1:1                    SI:  -827.76  DI:  -0.4348
Ranking344  No: 3230 Type: LINE  Name: LOVE4-LOVE1J:2 LOVE4-LOVE1J:1    SI:  -828.18  DI:  -0.4416
Ranking345  No: 3253 Type: LINE  Name: BRFO1-BRFO4:3 BRFO1-BRFO4:2      SI:  -829.30  DI:  -0.4350
Ranking346  No: 3839 Type: LINE  Name: FASN1-FAUG1:2 FASN1-FAUG1:1      SI:  -830.17  DI:  -0.4486
Ranking347  No: 2431 Type: LINE  Name: WIMB2-WISD2Q:1                    SI:  -831.48  DI:  -0.4426
Ranking348  No:  568 Type: LINE  Name: PEMB4-CILF4:2                     SI:  -833.61  DI:  -0.4407
Ranking349  No: 2827 Type: LINE  Name: FAUG1-ERRO1K:1                    SI:  -835.51  DI:  -0.4481
Ranking350  No:  771 Type: LINE  Name: EALI2-LALE2:2                     SI:  -835.66  DI:  -0.4434
Ranking351  No:  769 Type: LINE  Name: EALI2-LALE2:1                     SI:  -835.66  DI:  -0.4434
Ranking352  No: 2047 Type: LINE  Name: SIZE1K-SIZE4:2                    SI:  -839.21  DI:  -0.4382
Ranking353  No: 2043 Type: LINE  Name: SIZE1J-SIZE4:2                    SI:  -839.21  DI:  -0.4382
Ranking354  No: 3097 Type: LINE  Name: RYEH4-RYEH82:1                    SI:  -839.51  DI:  -0.4481
Ranking355  No: 2779 Type: LINE  Name: FOYE2-BLHI2:1                     SI:  -840.30  DI:  -0.4495
Ranking356  No: 1234 Type: LINE  Name: NEWX2-HURS2:2                     SI:  -840.83  DI:  -0.4473
Ranking357  No: 3725 Type: LINE  Name: HARM2-HARM6:2 HARM2-HARM6:1      SI:  -846.57  DI:  -0.4541
Ranking358  No: 2041 Type: LINE  Name: SIZE1J-SIZE4:1                    SI:  -847.54  DI:  -0.4423
Ranking359  No: 2045 Type: LINE  Name: SIZE1K-SIZE4:1                    SI:  -847.54  DI:  -0.4423
Ranking360  No: 3635 Type: LINE  Name: POPP2-POPP3:2 POPP2-POPP3:1      SI:  -847.87  DI:  -0.4436
Ranking361  No: 3644 Type: LINE  Name: ALDW3G-ALDW2:2 ALDW3G-ALDW2:1    SI:  -850.08  DI:  -0.4419
Ranking362  No: 1385 Type: LINE  Name: KEMS1J-KEMS4J:1                   SI:  -859.00  DI:  -0.4471
Ranking363  No: 1387 Type: LINE  Name: KEMS1J-KEMS4K:1                   SI:  -859.26  DI:  -0.4472
Ranking364  No: 2858 Type: LINE  Name: ERRO1J-BONB1Q:1                   SI:  -865.42  DI:  -0.4612
Ranking365  No: 3417 Type: LINE  Name: NORW1-NORM4:2 NORW1-NORM4:1      SI:  -867.64  DI:  -0.4535
Ranking366  No: 3389 Type: LINE  Name: ENDE1-ENDE4:3 ENDE1-ENDE4:2      SI:  -870.19  DI:  -0.4536
Ranking367  No: 3393 Type: LINE  Name: ENDE1-ENDE4:2 ENDE1-ENDE4:1      SI:  -870.58  DI:  -0.4538
Ranking368  No: 3502 Type: LINE  Name: FECK6-FECK2:2 FECK6-FECK2:1      SI:  -870.88  DI:  -0.4529
Ranking369  No:  154 Type: LINE  Name: LITT4U-BEDD4Q:1                   SI:  -871.46  DI:  -0.4627
Ranking370  No: 3742 Type: LINE  Name: WBOL6-WBOL2:3 WBOL6-WBOL2:1      SI:  -871.80  DI:  -0.4556
Ranking371  No: 3744 Type: LINE  Name: WBOL6-WBOL2:2 WBOL6-WBOL2:1      SI:  -871.80  DI:  -0.4556
Ranking372  No: 3778 Type: LINE  Name: GALA1-ECCL1:2 GALA1-ECCL1:1      SI:  -872.47  DI:  -0.4584
Ranking373  No: 3740 Type: LINE  Name: WBOL6-WBOL2:3 WBOL6-WBOL2:2      SI:  -872.98  DI:  -0.4562
Ranking374  No:  770 Type: LINE  Name: LALE2-EALI2:1                     SI:  -878.21  DI:  -0.4648
Ranking375  No:  772 Type: LINE  Name: LALE2-EALI2:2                     SI:  -878.21  DI:  -0.4648
Ranking376  No: 3391 Type: LINE  Name: ENDE1-ENDE4:3 ENDE1-ENDE4:1      SI:  -880.68  DI:  -0.4588
```

```
Ranking377  No: 2526 Type: LINE  Name: ERSK1Q-BRAE1:1                  SI:  -880.92  DI:  -0.4666
Ranking378  No: 3727 Type: LINE  Name: HAWP2-HAWP6:2 HAWP2-HAWP6:1     SI:  -881.35  DI:  -0.4703
Ranking379  No: 2771 Type: LINE  Name: BEAU2-BLHI2:1                   SI:  -886.28  DI:  -0.4735
Ranking380  No: 2964 Type: LINE  Name: STIR3-STIR1S:1                  SI:  -891.56  DI:  -0.4666
Ranking381  No: 3286 Type: LINE  Name: COWL4-COWL1K:2 COWL4-COWL1K:1   SI:  -892.44  DI:  -0.4764
Ranking382  No: 2966 Type: LINE  Name: STIR3-STIR1T:1                  SI:  -893.39  DI:  -0.4675
Ranking383  No: 3407 Type: LINE  Name: NORW1-NORM4:4 NORW1-NORM4:3     SI:  -900.38  DI:  -0.4698
Ranking384  No: 3532 Type: LINE  Name: IRON4-IRON1:2 IRON4-IRON1:1     SI:  -900.89  DI:  -0.4776
Ranking385  No: 2027 Type: LINE  Name: SEFI1-HARK1K:1                  SI:  -901.57  DI:  -0.4683
Ranking386  No: 3831 Type: LINE  Name: KINT1-KINT2:3 KINT1-KINT2:1     SI:  -904.04  DI:  -0.4832
Ranking387  No: 2607 Type: LINE  Name: DEVO1Q-KINC1:1                  SI:  -905.04  DI:  -0.4802
Ranking388  No: 2821 Type: LINE  Name: FASN1-FAUG1:1                   SI:  -907.06  DI:  -0.4865
Ranking389  No: 2823 Type: LINE  Name: FASN1-FAUG1:2                   SI:  -907.06  DI:  -0.4865
Ranking390  No: 3500 Type: LINE  Name: FECK6-FECK2:3 FECK6-FECK2:1     SI:  -910.48  DI:  -0.4727
Ranking391  No: 3833 Type: LINE  Name: KINT1-KINT2:2 KINT1-KINT2:1     SI:  -910.79  DI:  -0.4866
Ranking392  No: 3691 Type: LINE  Name: FERR2K-FERR6:2 FERR2K-FERR6:1   SI:  -913.15  DI:  -0.4800
Ranking393  No: 3829 Type: LINE  Name: KINT1-KINT2:3 KINT1-KINT2:2     SI:  -915.59  DI:  -0.4890
Ranking394  No: 2914 Type: LINE  Name: DEVO3-DEVO1R:1                  SI:  -916.98  DI:  -0.4790
Ranking395  No: 2912 Type: LINE  Name: DEVO3-DEVO1Q:1                  SI:  -917.28  DI:  -0.4792
Ranking396  No: 3409 Type: LINE  Name: NORW1-NORM4:4 NORW1-NORM4:2     SI:  -917.67  DI:  -0.4785
Ranking397  No: 3413 Type: LINE  Name: NORW1-NORM4:3 NORW1-NORM4:2     SI:  -917.82  DI:  -0.4785
Ranking398  No: 3813 Type: LINE  Name: DALL2-WIYH2:2 DALL2-WIYH2:1     SI:  -918.06  DI:  -0.4904
Ranking399  No: 3415 Type: LINE  Name: NORW1-NORM4:3 NORW1-NORM4:1     SI:  -918.76  DI:  -0.4790
Ranking400  No: 2611 Type: LINE  Name: DEVO1R-KINC1:1                  SI:  -919.53  DI:  -0.4875
Ranking401  No: 3700 Type: LINE  Name: GRIW4-GRIW1:2 GRIW4-GRIW1:1     SI:  -923.25  DI:  -0.4872
Ranking402  No: 3411 Type: LINE  Name: NORW1-NORM4:4 NORW1-NORM4:1     SI:  -924.77  DI:  -0.4820
Ranking403  No: 2507 Type: LINE  Name: BALL2-COYL2:1                   SI:  -925.33  DI:  -0.4889
Ranking404  No: 3498 Type: LINE  Name: FECK6-FECK2:3 FECK6-FECK2:2     SI:  -925.56  DI:  -0.4802
Ranking405  No: 3377 Type: LINE  Name: UPPB2N-UPPB3:2 UPPB2N-UPPB3:1   SI:  -926.12  DI:  -0.4845
Ranking406  No: 2958 Type: LINE  Name: SHRU3-SHRU2R:1                  SI:  -927.44  DI:  -0.4851
Ranking407  No: 2956 Type: LINE  Name: SHRU3-SHRU2Q:1                  SI:  -932.26  DI:  -0.4875
Ranking408  No: 3762 Type: LINE  Name: PEWO2-PENE1K:2 PEWO2-PENE1K:1   SI:  -938.54  DI:  -0.4945
Ranking409  No: 1091 Type: LINE  Name: HAKB4-STHA4:1                   SI:  -938.89  DI:  -0.4992
Ranking410  No: 3177 Type: LINE  Name: SJOW2-SJOW6J:2 SJOW2-SJOW6J:1   SI:  -938.99  DI:  -0.4945
Ranking411  No: 2325 Type: LINE  Name: WALP1K-WALP4:2                   SI:  -940.06  DI:  -0.4881
Ranking412  No: 2616 Type: LINE  Name: TONG1-DUMF1:1                   SI:  -940.23  DI:  -0.4976
Ranking413  No: 2615 Type: LINE  Name: DUMF1-TONG1:1                   SI:  -943.37  DI:  -0.4980
Ranking414  No: 2731 Type: LINE  Name: MOTH1-WISH1:1                   SI:  -946.13  DI:  -0.4970
Ranking415  No: 3763 Type: LINE  Name: PEWO2-PEWO4:2 PEWO2-PEWO4:1     SI:  -946.82  DI:  -0.5018
Ranking416  No: 2658 Type: LINE  Name: KEOO1-GLLE1:1                   SI:  -949.33  DI:  -0.5141
Ranking417  No:  563 Type: LINE  Name: CILF4-MELK4:1                   SI:  -950.84  DI:  -0.5026
Ranking418  No: 3706 Type: LINE  Name: CREB4-CREB1K:2 CREB4-CREB1K:1   SI:  -952.62  DI:  -0.5078
Ranking419  No: 3517 Type: LINE  Name: CELL1-CELL4:4 CELL1-CELL4:3     SI:  -954.11  DI:  -0.4969
Ranking420  No:  910 Type: LINE  Name: FERR1K-FERR1J:1                 SI:  -954.36  DI:  -0.4952
Ranking421  No:  127 Type: LINE  Name: BEDD1J-BEDD2J:1                 SI:  -956.74  DI:  -0.4961
Ranking422  No: 2028 Type: LINE  Name: HARK1K-SEFI1:1                  SI:  -959.14  DI:  -0.5005
Ranking423  No: 2163 Type: LINE  Name: SUND1J-SUND4:1                  SI:  -959.44  DI:  -0.4974
Ranking424  No: 3185 Type: LINE  Name: NEWX2-NEWX6J:2 NEWX2-NEWX6J:1   SI:  -964.03  DI:  -0.5067
Ranking425  No: 3525 Type: LINE  Name: CELL1-CELL4:3 CELL1-CELL4:1     SI:  -964.68  DI:  -0.5022
Ranking426  No: 3523 Type: LINE  Name: CELL1-CELL4:3 CELL1-CELL4:2     SI:  -964.69  DI:  -0.5022
Ranking427  No: 3521 Type: LINE  Name: CELL1-CELL4:4 CELL1-CELL4:1     SI:  -964.80  DI:  -0.5023
Ranking428  No: 3519 Type: LINE  Name: CELL1-CELL4:4 CELL1-CELL4:2     SI:  -964.83  DI:  -0.5023
Ranking429  No: 2716 Type: LINE  Name: LEVT1R-LEVE1R:1                 SI:  -965.62  DI:  -0.5110
Ranking430  No: 2714 Type: LINE  Name: LEVT1Q-LEVE1Q:1                 SI:  -966.20  DI:  -0.5112
Ranking431  No: 2981 Type: LINE  Name: WISH1-WISH2:1                   SI:  -966.22  DI:  -0.5069
Ranking432  No: 2165 Type: LINE  Name: SUND1J-SUND4:2                  SI:  -967.27  DI:  -0.5013
```

```
Ranking433  No: 1463 Type: LINE  Name: LACK2-LACK4:1                    SI:  -971.55  DI:  -0.5308
Ranking434  No:  653 Type: LINE  Name: CREB1K-CREB4:1                   SI:  -973.45  DI:  -0.5049
Ranking435  No: 3745 Type: LINE  Name: STEN1-STEW2:3 STEN1-STEW2:2      SI:  -975.20  DI:  -0.5090
Ranking436  No: 2968 Type: LINE  Name: STLE3S-STLE1:1                   SI:  -978.61  DI:  -0.5097
Ranking437  No: 2970 Type: LINE  Name: STLE3S-STLE1:2                   SI:  -980.13  DI:  -0.5105
Ranking438  No:  226 Type: LINE  Name: BOLN4-BOLN1K:1                   SI:  -980.65  DI:  -0.5159
Ranking439  No: 3701 Type: LINE  Name: KEAD1-KEAD4K:2 KEAD1-KEAD4K:1    SI:  -983.36  DI:  -0.5103
Ranking440  No: 1703 Type: LINE  Name: NINF1K-NINF4:1                   SI:  -984.18  DI:  -0.5101
Ranking441  No: 2934 Type: LINE  Name: LEVE3-LEVE1R:1                   SI:  -987.91  DI:  -0.5216
Ranking442  No: 2932 Type: LINE  Name: LEVE3-LEVE1Q:1                   SI:  -988.26  DI:  -0.5218
Ranking443  No: 2323 Type: LINE  Name: WALP1K-WALP4:1                   SI:  -988.59  DI:  -0.5124
Ranking444  No: 3152 Type: LINE  Name: LALE2-LALE1J:2 LALE2-LALE1J:1    SI:  -991.28  DI:  -0.5193
Ranking445  No: 3851 Type: LINE  Name: KINT2-TEAL2:2 KINT2-TEAL2:1      SI:  -992.31  DI:  -0.5649
Ranking446  No: 3759 Type: LINE  Name: SPEN1-SPEN2M:2 SPEN1-SPEN2M:1    SI:  -992.79  DI:  -0.5175
Ranking447  No: 1699 Type: LINE  Name: NINF1J-NINF4:1                   SI:  -994.29  DI:  -0.5153
Ranking448  No: 2898 Type: LINE  Name: CUPA3-CUPA1R:1                   SI:  -995.09  DI:  -0.5197
Ranking449  No: 2896 Type: LINE  Name: CUPA3-CUPA1Q:1                   SI:  -995.12  DI:  -0.5197
Ranking450  No: 3154 Type: LINE  Name: LALE2-LALE1K:2 LALE2-LALE1K:1    SI:  -995.30  DI:  -0.5213
Ranking451  No: 3853 Type: LINE  Name: KINT2-PEHE2:2 KINT2-PEHE2:1      SI:  -995.58  DI:  -0.5785
Ranking452  No:  909 Type: LINE  Name: FERR1J-FERR1K:1                   SI:  -995.85  DI:  -0.5163
Ranking453  No: 3089 Type: LINE  Name: KEAD4J-KEAD82:1                   SI:  -996.33  DI:  -0.5303
Ranking454  No: 2967 Type: LINE  Name: STLE1-STLE3S:1                   SI:  -997.29  DI:  -0.5215
Ranking455  No: 3847 Type: LINE  Name: KINT2-TEAL2:3 KINT2-TEAL2:2      SI:  -997.45  DI:  -0.5698
Ranking456  No: 3849 Type: LINE  Name: KINT2-TEAL2:3 KINT2-TEAL2:1      SI:  -997.45  DI:  -0.5698
Ranking457  No: 2969 Type: LINE  Name: STLE1-STLE3S:2                   SI:  -997.48  DI:  -0.5216
Ranking458  No: 3615 Type: LINE  Name: CAPE1K-CAPE2J:2 CAPE1K-CAPE2J:1 SI:  -997.75  DI:  -0.5174
Ranking459  No: 1943 Type: LINE  Name: RAYL1J-RAYL4:1                   SI:  -999.11  DI:  -0.5175
Ranking460  No: 2149 Type: LINE  Name: STEW4Q-STWB4Q:1                  SI: -1000.38  DI:  -0.5302
Ranking461  No: 2151 Type: LINE  Name: STEW4R-STWB4R:1                  SI: -1000.38  DI:  -0.5302
Ranking462  No: 1701 Type: LINE  Name: NINF1J-NINF4:2                   SI: -1002.16  DI:  -0.5193
Ranking463  No: 3749 Type: LINE  Name: STEN1-STEW2:2 STEN1-STEW2:1      SI: -1002.47  DI:  -0.5225
Ranking464  No: 3368 Type: LINE  Name: RASS4-RASS1:2 RASS4-RASS1:1      SI: -1004.40  DI:  -0.5266
Ranking465  No: 3432 Type: LINE  Name: STAY4-STAY1:2 STAY4-STAY1:1      SI: -1005.84  DI:  -0.5304
Ranking466  No: 2657 Type: LINE  Name: GLLE1-KEOO1:1                    SI: -1009.19  DI:  -0.5374
Ranking467  No:  655 Type: LINE  Name: CREB1K-CREB4:2                   SI: -1010.96  DI:  -0.5236
Ranking468  No: 3260 Type: LINE  Name: SIZE4-BRFO4:2 SIZE4-BRFO4:1      SI: -1013.85  DI:  -0.5395
Ranking469  No: 2691 Type: LINE  Name: KEOO1-MAYT1T:1                   SI: -1015.03  DI:  -0.5383
Ranking470  No:  994 Type: LINE  Name: DUBR4Q-FORD4Q:1                  SI: -1015.30  DI:  -0.5325
Ranking471  No: 2537 Type: LINE  Name: CHAP1-HAWI1:1                    SI: -1015.41  DI:  -0.5395
Ranking472  No: 3459 Type: LINE  Name: BISW1-BISW2:3 BISW1-BISW2:2      SI: -1016.68  DI:  -0.5269
Ranking473  No: 3187 Type: LINE  Name: WIMB1J-WIMB2:3 WIMB1J-WIMB2:2    SI: -1017.13  DI:  -0.5274
Ranking474  No: 3463 Type: LINE  Name: BISW1-BISW2:2 BISW1-BISW2:1      SI: -1021.59  DI:  -0.5294
Ranking475  No: 3489 Type: LINE  Name: BUST2-NECH2:2 BUST2-NECH2:1      SI: -1022.06  DI:  -0.5380
Ranking476  No: 3747 Type: LINE  Name: STEN1-STEW2:3 STEN1-STEW2:1      SI: -1024.45  DI:  -0.5335
Ranking477  No: 3766 Type: LINE  Name: HEYS4-HEYS1:2 HEYS4-HEYS1:1      SI: -1025.75  DI:  -0.5438
Ranking478  No: 2137 Type: LINE  Name: STES1-STEW2:1                    SI: -1025.95  DI:  -0.5328
Ranking479  No: 2139 Type: LINE  Name: STES1-STEW2:2                    SI: -1026.53  DI:  -0.5331
Ranking480  No: 3259 Type: LINE  Name: BRFO4-SIZE4:2 BRFO4-SIZE4:1      SI: -1027.13  DI:  -0.5462
Ranking481  No: 1503 Type: LINE  Name: LEGA1K-LEGA4J:1                   SI: -1028.27  DI:  -0.5322
Ranking482  No: 3189 Type: LINE  Name: WIMB1J-WIMB2:3 WIMB1J-WIMB2:1    SI: -1030.43  DI:  -0.5340
Ranking483  No: 2933 Type: LINE  Name: LEVE1R-LEVE3:1                   SI: -1031.08  DI:  -0.5434
Ranking484  No: 3191 Type: LINE  Name: WIMB1J-WIMB2:2 WIMB1J-WIMB2:1    SI: -1032.05  DI:  -0.5348
Ranking485  No:  997 Type: LINE  Name: FORD4R-DUBR4R:1                   SI: -1032.43  DI:  -0.5426
Ranking486  No: 2931 Type: LINE  Name: LEVE1Q-LEVE3:1                   SI: -1033.00  DI:  -0.5443
Ranking487  No:  998 Type: LINE  Name: DUBR4R-FORD4R:1                  SI: -1033.62  DI:  -0.5433
Ranking488  No: 3490 Type: LINE  Name: NECH2-BUST2:2 NECH2-BUST2:1      SI: -1033.62  DI:  -0.5432
```

```
Ranking489  No: 1167 Type: LINE  Name: HATL2J-SALH2:1                 SI: -1033.95  DI:  -0.5554
Ranking490  No: 1158 Type: LINE  Name: HUTT4N-HARK4:1                 SI: -1034.13  DI:  -0.5450
Ranking491  No: 3527 Type: LINE  Name: CELL1-CELL4:2 CELL1-CELL4:1    SI: -1035.18  DI:  -0.5375
Ranking492  No: 2692 Type: LINE  Name: MAYT1T-KEOO1:1                 SI: -1035.35  DI:  -0.5477
Ranking493  No:  732 Type: LINE  Name: EGGB4J-DRAX4J:1                SI: -1035.67  DI:  -0.5509
Ranking494  No:  993 Type: LINE  Name: FORD4Q-DUBR4Q:1                SI: -1036.49  DI:  -0.5440
Ranking495  No: 3461 Type: LINE  Name: BISW1-BISW2:3 BISW1-BISW2:1    SI: -1037.29  DI:  -0.5372
Ranking496  No: 1156 Type: LINE  Name: HUTT4M-HARK4:1                 SI: -1037.57  DI:  -0.5468
Ranking497  No: 2774 Type: LINE  Name: FOYE2-BEAU2:1                  SI: -1038.70  DI:  -0.5497
Ranking498  No: 2790 Type: LINE  Name: PEHE2-KINT2:2                  SI: -1038.73  DI:  -0.5819
Ranking499  No:  697 Type: LINE  Name: DINO4-PENT4:1                  SI: -1039.19  DI:  -0.5471
Ranking500  No: 3327 Type: LINE  Name: EXET1-EXET4:2 EXET1-EXET4:1    SI: -1039.75  DI:  -0.5421
```

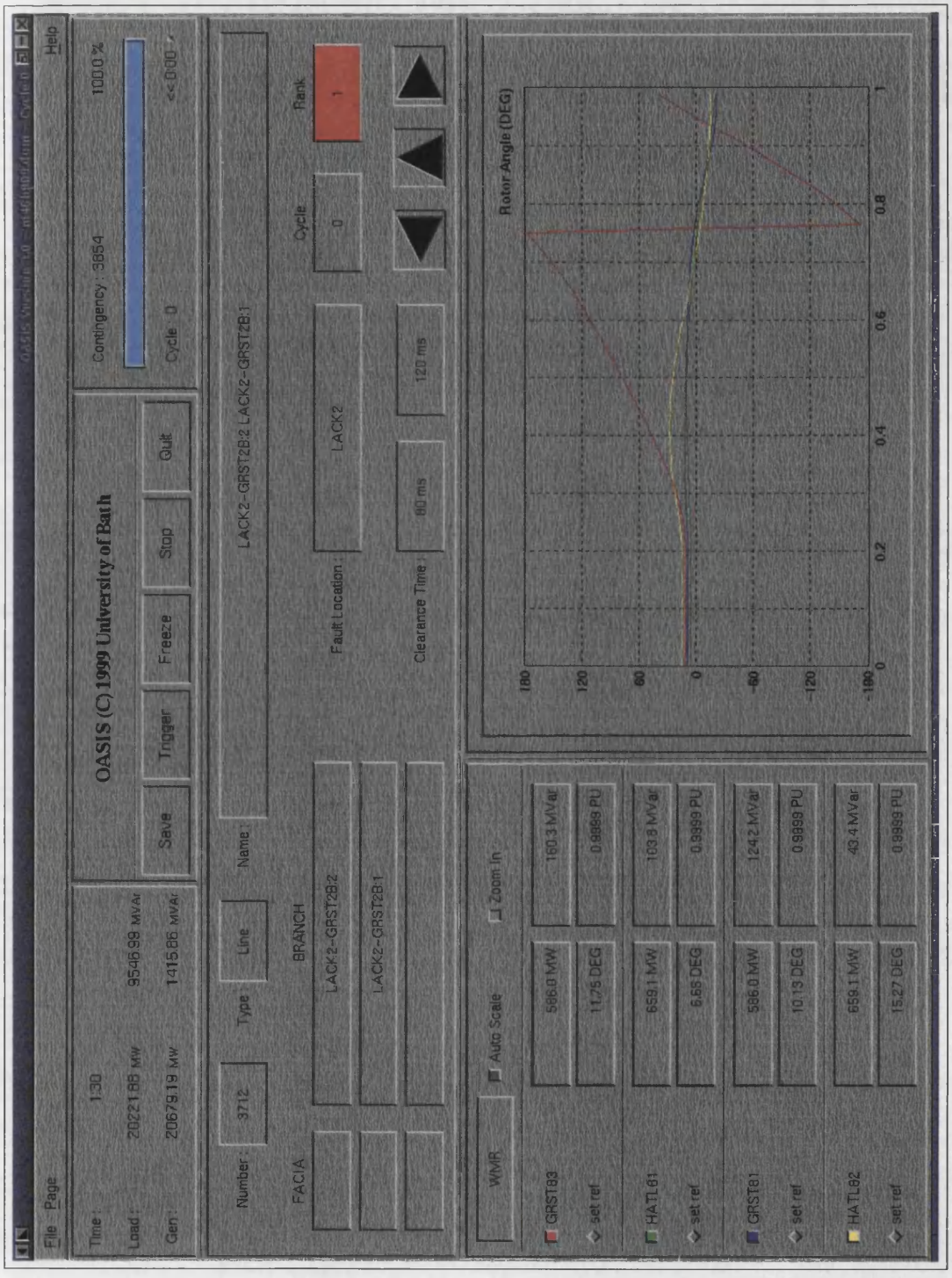


Figure B.1: DSA output screen for worst contingency

Appendix C

# Topology Determination Data Output Example

## C.1 Contingency File

Contingency file generated for topology determination study run by DOLSE topology determinator, with GRST2B 275kV as the busbar of interest.

```
DOLSE Topology Determination: Busbar of interest: GRST2B
6,,5,6,20
# This line trip would have left generators islanded
DOLSEtd GRST2B ctgno 1 : GRST2B-GRST84:1
1,2,,,,
6,100,GRST84
2,100,,,,GRST2B,GRST84,1
#
#
# This line trip would have left generators islanded
DOLSEtd GRST2B ctgno 2 : GRST2B-GRST83:1
2,2,,,,
6,100,GRST83
2,100,,,,GRST2B,GRST83,1
#
#
DOLSEtd GRST2B ctgno 3 : GRST2B-WILT6:2
3,1,,,,
2,100,,,,GRST2B,WILT6,2
#
#
DOLSEtd GRST2B ctgno 4 : GRST2B-WILT6:1
4,1,,,,
```

```
2,100,,,,GRST2B,WILT6,1
#
#
DOLSEtd GRST2B ctgno 5 : GRST2B-LACK2:2
5,1,,,,
2,100,,,,GRST2B,LACK2,2
#
#
DOLSEtd GRST2B ctgno 6 : GRST2B-LACK2:1
6,1,,,,
2,100,,,,GRST2B,LACK2,1
#
#
,GRST2B
,GRST84
,GRST83
,WILT6
,LACK2
,,,GRST2B,GRST84,1
,,,GRST2B,GRST83,1
,,,GRST2B,WILT6,2
,,,GRST2B,WILT6,1
,,,GRST2B,LACK2,2
,,,GRST2B,LACK2,1
```

## C.2 Information Request

SCADA Information Request file generated by the topology determinator, ready to be filled in by the DOLSE SCADA database handler.

```
DOLSE generated Information Required List
5,6
,GRST2B,,,,,,
,GRST84,,,,,,
,GRST83,,,,,,
,WILT6,,,,,,
,LACK2,,,,,,
,,,GRST2B,GRST84,1,,,,
,,,GRST2B,GRST83,1,,,,
,,,GRST2B,WILT6,2,,,,
,,,GRST2B,WILT6,1,,,,
,,,GRST2B,LACK2,2,,,,
```

```
,,,GRST2B,LACK2,1,,,,
```

## C.3 Completed Information Request

The DOLSE SCADA database handler provides the information requested.

```
DOLSE generated Information Required List - DONE
5,6
#zone,name, Pg, Qg, Vm, Va, Pl, Ql
Q2,GRST2B, 0, 0, 0.996319, , 0.120422, 0.0392445
Q2,GRST84, 3.08684, 0.823647, 0.985963, , 0, 0
Q2,GRST83, 5.82604, 1.54389, 0.999274, , 0, 0
Q2,WILT6, 0, 0, 0.994624, , 0.507998, 0.253749
Q2,LACK2, 0, 0, 0.994956, , 0, 0
#type,zone1,zone2,bus1,bus2,cctno, P1, Q1, P2, Q2
,Q2,Q2,GRST2B,GRST84,1, -3.09258, -0.343576, 3.0972, 0.809963
,Q2,Q2,GRST2B,GRST83,1, -5.848, -0.624888, 5.85722, 1.60019
,Q2,Q2,GRST2B,WILT6,2, 0.551938, 0.0854792, -0.550999, -0.0433212
,Q2,Q2,GRST2B,WILT6,1, 0, 0, 0, 0
,Q2,Q2,GRST2B,LACK2,2, 4.1357, 0.420926, -4.13512, -0.43343
,Q2,Q2,GRST2B,LACK2,1, 4.1343, 0.421668, -4.13371, -0.434174
```

## C.4 Output Information

Topology Determination output file showing the relevant output for the contingencies from the contingencies of interest in the contingency list above.

```
DOLSEtd GRST2B ctgno 1 : GRST2B-GRST84:1
5,6
#zone,name, Pg, Qg, Vm, Va, Pl, Ql
Q2,GRST2B, 0, 0, 1.0022, 0, 0.119974, 0.0395913
Q2,LACK2, 0, 0, 1.00201, 0, 0, 0
Q2,WILT6, 0, 0, 1.00375, 0, 0.51188, 0.262338
Q2,GRST83, 6.07126, 1.77377, 1.0057, 0, 0, 0
Q2,GRST84, 3.09912, 0.811873, 0, 0, 0, 0
#type,zone1,zone2,bus1,bus2,cctno, P1, Q1, P2, Q2
,Q2,Q2,GRST2B,LACK2,1, 2.68578, 0.296574, -2.68553, -0.312313
,Q2,Q2,GRST2B,LACK2,2, 2.68578, 0.296574, -2.68553, -0.312313
,Q2,Q2,GRST2B,WILT6,1, 0.300777, 0.0495081, -0.300498, -0.0354219
```

```
,Q2,Q2,GRST2B,WILT6,2, 0.268537, 0.0452348, -0.268315, -0.0322275
,Q2,Q2,GRST2B,GRST83,1, -6.0614, -0.727666, 6.07129, 1.77391
,Q2,Q2,GRST2B,GRST84,1, 0, 0, 0, 0
#
#
DOLSEtd GRST2B ctgno 2 : GRST2B-GRST83:1
5,6
#zone,name, Pg, Qg, Vm, Va, Pl, Ql
Q2,GRST2B, 0, 0, 1.0031, 0, 0.119974, 0.0395913
Q2,LACK2, 0, 0, 1.00299, 0, 0, 0
Q2,WILT6, 0, 0, 1.00617, 0, 0.51188, 0.262338
Q2,GRST83, 5.8604, 1.60335, 0, 0, 0, 0
Q2,GRST84, 3.31477, 1.04311, 1.01191, 0, 0, 0
#type,zone1,zone2,bus1,bus2,cctno, P1, Q1, P2, Q2
,Q2,Q2,GRST2B,LACK2,1, 1.42561, 0.198983, -1.42554, -0.216396
,Q2,Q2,GRST2B,LACK2,2, 1.42561, 0.198983, -1.42554, -0.216396
,Q2,Q2,GRST2B,WILT6,1, 0.178329, 0.0359987, -0.17823, -0.028424
,Q2,Q2,GRST2B,WILT6,2, 0.159198, 0.0328421, -0.15912, -0.0256503
,Q2,Q2,GRST2B,GRST83,1, 0, 0, 0, 0
,Q2,Q2,GRST2B,GRST84,1, -3.3095, -0.506652, 3.3148, 1.04327
#
#
DOLSEtd GRST2B ctgno 3 : GRST2B-WILT6:2
5,6
#zone,name, Pg, Qg, Vm, Va, Pl, Ql
Q2,GRST2B, 0, 0, 0.999952, 0, 0.119974, 0.0395913
Q2,LACK2, 0, 0, 0.999678, 0, 0, 0
Q2,WILT6, 0, 0, 0.997702, 0, 0.51188, 0.262338
Q2,GRST83, 5.85984, 1.60035, 0.999883, 0, 0, 0
Q2,GRST84, 3.09887, 0.810071, 0.999881, 0, 0, 0
#type,zone1,zone2,bus1,bus2,cctno, P1, Q1, P2, Q2
,Q2,Q2,GRST2B,LACK2,1, 4.11724, 0.418906, -4.11666, -0.431455
,Q2,Q2,GRST2B,LACK2,2, 4.11724, 0.418906, -4.11666, -0.431455
,Q2,Q2,GRST2B,WILT6,1, 0.590393, 0.0899078, -0.589318, -0.046934
,Q2,Q2,GRST2B,WILT6,2, 0, 0, 0, 0
,Q2,Q2,GRST2B,GRST83,1, -5.85061, -0.62415, 5.85984, 1.60035
,Q2,Q2,GRST2B,GRST84,1, -3.09426, -0.343165, 3.09887, 0.810071
#
#
DOLSEtd GRST2B ctgno 4 : GRST2B-WILT6:1
5,6
#zone,name, Pg, Qg, Vm, Va, Pl, Ql
Q2,GRST2B, 0, 0, 0.999953, 0, 0.119974, 0.0395913
Q2,LACK2, 0, 0, 0.999677, 0, 0, 0
Q2,WILT6, 0, 0, 0.997413, 0, 0.51188, 0.262338
```

```
Q2,GRST83, 5.85977, 1.60023, 0.999881, 0, 0, 0
Q2,GRST84, 3.09884, 0.810001, 0.999879, 0, 0, 0
#type,zone1,zone2,bus1,bus2,cctno, P1, Q1, P2, Q2
,Q2,Q2,GRST2B,LACK2,1, 4.13636, 0.421045, -4.13578, -0.433544
,Q2,Q2,GRST2B,LACK2,2, 4.13636, 0.421045, -4.13578, -0.433544
,Q2,Q2,GRST2B,WILT6,1, 0, 0, 0, 0
,Q2,Q2,GRST2B,WILT6,2, 0.552038, 0.0854844, -0.551099, -0.0433106
,Q2,Q2,GRST2B,GRST83,1, -5.85054, -0.624061, 5.85977, 1.60023
,Q2,Q2,GRST2B,GRST84,1, -3.09422, -0.343109, 3.09884, 0.810001
#
#
DOLSEtd GRST2B ctgno 5 : GRST2B-LACK2:2
5,6
#zone,name, Pg, Qg, Vm, Va, Pl, Ql
Q2,GRST2B, 0, 0, 0.999825, 0, 0.119974, 0.0395913
Q2,LACK2, 0, 0, 0.999298, 0, 0, 0
Q2,WILT6, 0, 0, 0.999787, 0, 0.51188, 0.262338
Q2,GRST83, 5.85993, 1.60466, 0.999873, 0, 0, 0
Q2,GRST84, 3.09892, 0.812597, 0.999871, 0, 0, 0
#type,zone1,zone2,bus1,bus2,cctno, P1, Q1, P2, Q2
,Q2,Q2,GRST2B,LACK2,1, 8.00372, 0.808906, -8.00151, -0.806447
,Q2,Q2,GRST2B,LACK2,2, 0, 0, 0, 0
,Q2,Q2,GRST2B,WILT6,1, 0.433911, 0.0653224, -0.433331, -0.0403026
,Q2,Q2,GRST2B,WILT6,2, 0.387415, 0.059714, -0.386953, -0.0369424
,Q2,Q2,GRST2B,GRST83,1, -5.8507, -0.628047, 5.85993, 1.60466
,Q2,Q2,GRST2B,GRST84,1, -3.0943, -0.345481, 3.09892, 0.812597
#
#
DOLSEtd GRST2B ctgno 6 : GRST2B-LACK2:1
5,6
#zone,name, Pg, Qg, Vm, Va, Pl, Ql
Q2,GRST2B, 0, 0, 0.999825, 0, 0.119974, 0.0395913
Q2,LACK2, 0, 0, 0.999298, 0, 0, 0
Q2,WILT6, 0, 0, 0.999787, 0, 0.51188, 0.262338
Q2,GRST83, 5.85993, 1.60466, 0.999873, 0, 0, 0
Q2,GRST84, 3.09892, 0.812597, 0.999871, 0, 0, 0
#type,zone1,zone2,bus1,bus2,cctno, P1, Q1, P2, Q2
,Q2,Q2,GRST2B,LACK2,1, 0, 0, 0, 0
,Q2,Q2,GRST2B,LACK2,2, 8.00372, 0.808906, -8.00151, -0.806447
,Q2,Q2,GRST2B,WILT6,1, 0.433911, 0.0653224, -0.433331, -0.0403026
,Q2,Q2,GRST2B,WILT6,2, 0.387415, 0.059714, -0.386953, -0.0369424
,Q2,Q2,GRST2B,GRST83,1, -5.8507, -0.628047, 5.85993, 1.60466
,Q2,Q2,GRST2B,GRST84,1, -3.0943, -0.345481, 3.09892, 0.812597
```

## C.5 Output Information Analysed

In order to form a square matrix the line data was padded with the requisite number of preceding zeros. The mean of the square error is appended after each matrix.

```
error1 =

         0         0   -0.0059         0    0.0004   -0.0003
         0         0   -0.0071         0         0         0
         0         0   -0.0091         0   -0.0039   -0.0086
   -0.2452   -0.2299   -0.0064         0         0         0
   -0.0123    0.0118    0.9860         0         0         0
         0         0    1.4485    0.1251   -1.4482   -0.1219
         0         0    1.4499    0.1244   -1.4496   -0.1211
         0         0         0         0         0         0
         0         0    0.2834    0.0402   -0.2827   -0.0111
         0         0    0.2134    0.1028   -0.2141   -0.1737
         0         0         0         0         0         0


ans =

    0.3393


error2 =

         0         0   -0.0068         0    0.0004   -0.0003
         0         0   -0.0080         0         0         0
         0         0   -0.0115         0   -0.0039   -0.0086
   -0.0344   -0.0595    0.9993         0         0         0
   -0.2279   -0.2195   -0.0259         0         0         0
         0         0    2.7087    0.2227   -2.7082   -0.2178
         0         0    2.7101    0.2219   -2.7096   -0.2170
         0         0         0         0         0         0
         0         0    0.3927    0.0526   -0.3919   -0.0177
         0         0         0         0         0         0
         0         0    0.2169    0.1631   -0.2176   -0.2333
```

```
ans =

    1.0739


error3 =

         0         0   -0.0036         0    0.0004   -0.0003
         0         0   -0.0047         0         0         0
         0         0   -0.0031         0   -0.0039   -0.0086
   -0.0338   -0.0565   -0.0006         0         0         0
   -0.0120    0.0136   -0.0139         0         0         0
         0         0    0.0171    0.0028   -0.0170   -0.0027
         0         0    0.0185    0.0020   -0.0185   -0.0020
         0         0         0         0         0         0
         0         0         0         0         0         0
         0         0    0.0026   -0.0007   -0.0026   -0.0002
         0         0    0.0017   -0.0004   -0.0017   -0.0001


ans =

   2.1703e-04


error4 =

         0         0   -0.0036         0    0.0004   -0.0003
         0         0   -0.0047         0         0         0
         0         0   -0.0028         0   -0.0039   -0.0086
   -0.0337   -0.0563   -0.0006         0         0         0
   -0.0120    0.0136   -0.0139         0         0         0
         0         0   -0.0021    0.0006    0.0021   -0.0006
         0         0   -0.0007   -0.0001    0.0007    0.0001
         0         0         0         0         0         0
         0         0   -0.0001   -0.0000    0.0001   -0.0000
         0         0    0.0025   -0.0008   -0.0026   -0.0000
         0         0    0.0016   -0.0005   -0.0016   -0.0000


ans =

   1.5146e-04
```

```
error5 =

         0         0   -0.0035         0    0.0004   -0.0003
         0         0   -0.0043         0         0         0
         0         0   -0.0052         0   -0.0039   -0.0086
   -0.0339   -0.0608   -0.0006         0         0         0
   -0.0121    0.0111   -0.0139         0         0         0
         0         0   -3.8694   -0.3872    3.8678    0.3723
         0         0         0         0         0         0
         0         0         0         0         0         0
         0         0    0.1645    0.0258   -0.1640   -0.0064
         0         0    0.0027    0.0032   -0.0027   -0.0045
         0         0    0.0017    0.0019   -0.0017   -0.0026


ans =

    1.0442


error6 =

         0         0   -0.0035         0    0.0004   -0.0003
         0         0   -0.0043         0         0         0
         0         0   -0.0052         0   -0.0039   -0.0086
   -0.0339   -0.0608   -0.0006         0         0         0
   -0.0121    0.0111   -0.0139         0         0         0
         0         0         0         0         0         0
         0         0   -3.8680   -0.3880    3.8664    0.3730
         0         0         0         0         0         0
         0         0    0.1645    0.0258   -0.1640   -0.0064
         0         0    0.0027    0.0032   -0.0027   -0.0045
         0         0    0.0017    0.0019   -0.0017   -0.0026


ans =

    1.0435
```

# Appendix D

# Power System Stiffness Characteristic Output Data

This appendix contains details of the time domain simulation results used for the examples within chapter 6.

| Busbar Load Magnitudes | | | Frequency | | | Mean System Voltage | | | | |
|---|---|---|---|---|---|---|---|---|---|---|
| Busbar | Real | Reactive | Time | Max | Final | Time | Min | Time | Max | Final |
| ABHA11 | 47.68 | 22.57 | 13.09 | 50.0138 | 50.0094 | 2.2 | 0.974884 | 0.2 | 0.976825 | 0.975316 |
| ABHA12 | 61.22 | 29.75 | 13.22 | 50.0175 | 50.012 | 2.2 | 0.974884 | 2.62 | 0.975752 | 0.975444 |
| ABTH11 | 67.93 | 54.74 | 13.91 | 50.0096 | 50.0065 | 2.2 | 0.974884 | 2.42 | 0.975974 | 0.975614 |
| ABTH12 | 113.37 | 100.64 | 13.93 | 50.0189 | 50.0128 | 2.2 | 0.974884 | 2.43 | 0.976904 | 0.976202 |
| ALDW31 | 89.94 | 46.89 | 12.9 | 50.0418 | 50.0286 | 2.2 | 0.974884 | 2.22 | 0.975648 | 0.975354 |
| ALVE11 | 47.8 | 46.97 | 13.52 | 50.0096 | 50.0066 | 2.2 | 0.974884 | 0.2 | 0.976202 | 0.97539 |
| AMEM11 | 89.11 | 31.98 | 13.14 | 50.0313 | 50.0214 | 2.2 | 0.974884 | 2.57 | 0.976036 | 0.975619 |
| ANDO11 | 4.39 | 1.75 | 13 | 50.0014 | 50.001 | 2.2 | 0.974884 | 0.2 | 0.97539 | 0.974924 |
| AXMI11 | 137.07 | 54.89 | 13.11 | 50.0489 | 50.0334 | 2.2 | 0.974884 | 2.65 | 0.976755 | 0.975988 |
| BARK11 | 290.64 | 150.56 | 13.27 | 50.0894 | 50.061 | 2.2 | 0.974884 | 2.54 | 0.979786 | 0.978178 |
| BARK31 | 56.88 | 13.77 | 13.06 | 50.0219 | 50.015 | 2.2 | 0.974884 | 0.2 | 0.978178 | 0.975387 |
| BARK32 | 60.05 | 19.46 | 13.09 | 50.0215 | 50.0147 | 2.2 | 0.974884 | 2.58 | 0.975774 | 0.975466 |
| BEAU21 | -130.48 | 22.71 | 0 | 50 | 49.9451 | 3.16 | 0.974378 | 0.2 | 0.977041 | 0.975429 |
| BEDD11 | 177.36 | 34.87 | 13.25 | 50.0492 | 50.0336 | 2.2 | 0.974884 | 2.56 | 0.977505 | 0.976638 |
| BEDD12 | 176.17 | 36.72 | 13.24 | 50.0463 | 50.0316 | 2.2 | 0.974884 | 2.55 | 0.97754 | 0.97668 |
| BEDD13 | 54.84 | 4.85 | 13.17 | 50.0163 | 50.0111 | 2.2 | 0.974884 | 0.2 | 0.97668 | 0.975396 |
| BEDD14 | 58.6 | 5.5 | 13.25 | 50.0167 | 50.0114 | 2.2 | 0.974884 | 2.58 | 0.975721 | 0.975443 |
| BELV11 | 13.61 | -4.21 | 0 | 50 | 50.0041 | 2.2 | 0.974884 | 0.2 | 0.975443 | 0.974978 |
| BESW11 | 347.82 | 143.8 | 13.06 | 50.1253 | 50.0854 | 2.2 | 0.974884 | 2.53 | 0.978502 | 0.977199 |
| BIRK11 | 206.82 | 90.68 | 12.88 | 50.1121 | 50.0765 | 2.2 | 0.974884 | 3.56 | 0.97645 | 0.975883 |
| BISW11 | 419.27 | 227.76 | 13.14 | 50.1242 | 50.0845 | 2.2 | 0.974884 | 2.41 | 0.979876 | 0.978034 |
| BLHI21 | 129.46 | 42.2 | 12.63 | 50.0943 | 50.0644 | 2.55 | 0.974123 | 3.19 | 0.975777 | 0.974667 |
| BLYT61 | 163.21 | 21.19 | 12.69 | 50.1109 | 50.0757 | 2.6 | 0.974434 | 3.21 | 0.976184 | 0.974918 |
| BOLN11 | 597.44 | 284.99 | 13.16 | 50.204 | 50.1389 | 2.2 | 0.974884 | 2.6 | 0.983954 | 0.980256 |
| BONN21 | 123.3 | 71.71 | 12.68 | 50.091 | 50.0622 | 0.2 | 0.974667 | 3.25 | 0.975912 | 0.974987 |
| BOTW11 | 84.87 | 18.6 | 13.1 | 50.0318 | 50.0218 | 2.2 | 0.974884 | 0.2 | 0.975988 | 0.975515 |
| BRAI11 | 35.96 | 24.95 | 13.24 | 50.0094 | 50.0064 | 2.2 | 0.974884 | 0.2 | 0.980256 | 0.975244 |

*continued on next page*

*continued from previous page*

| Busbar Load Magnitudes | | | Frequency | | | Mean System Voltage | | | | |
|---|---|---|---|---|---|---|---|---|---|---|
| Busbar | Real | Reactive | Time | Max | Final | Time | Min | Time | Max | Final |
| BRAW11 | 208.16 | 136.3 | 12.96 | 50.083 | 50.0566 | 2.2 | 0.974884 | 2.31 | 0.977134 | 0.976142 |
| BRAW12 | 214.32 | 80.07 | 12.87 | 50.1029 | 50.0702 | 2.2 | 0.974884 | 2.22 | 0.976486 | 0.975847 |
| BRBO11 | 4.22 | 1.69 | 12.84 | 50.0001 | 50.0001 | 2.2 | 0.974884 | 0.2 | 0.975847 | 0.974892 |
| BRBO12 | 4.22 | 1.69 | 12.7 | 50.003 | 50.0021 | 2.2 | 0.974884 | 3.22 | 0.974914 | 0.974898 |
| BRED11 | 253.62 | 134.7 | 12.92 | 50.1071 | 50.0731 | 2.2 | 0.974884 | 2.33 | 0.977294 | 0.97637 |
| BRFO11 | 606.5 | 399.86 | 13.07 | 50.2077 | 50.1419 | 2.2 | 0.974884 | 2.46 | 0.984013 | 0.980406 |
| BRGG11 | 6.03 | 2.41 | 12.75 | 50.0041 | 50.0028 | 2.2 | 0.974884 | 0.2 | 0.97637 | 0.974911 |
| BRGG81 | 10 | 5.12 | 12.64 | 50.0034 | 50.0023 | 2.2 | 0.974884 | 3.7 | 0.974963 | 0.974942 |
| BRGG86 | 10 | 5.12 | 12.71 | 50.0041 | 50.0028 | 2.2 | 0.974884 | 3.78 | 0.974961 | 0.974936 |
| BRIM11 | 131.43 | 54.15 | 13.18 | 50.0423 | 50.0289 | 2.2 | 0.974884 | 0.2 | 0.980406 | 0.976149 |
| BRIM12 | 131.31 | 51.28 | 13.14 | 50.0444 | 50.0304 | 2.2 | 0.974884 | 2.56 | 0.976781 | 0.976121 |
| BRLE11 | 148.96 | 38.19 | 13.18 | 50.0482 | 50.0329 | 2.2 | 0.974884 | 2.6 | 0.976892 | 0.976126 |
| BRLE12 | 143.05 | 5.82 | 13.07 | 50.0557 | 50.038 | 2.2 | 0.974884 | 2.63 | 0.976679 | 0.975922 |
| BRLE13 | 45.38 | 17.21 | 13.08 | 50.0147 | 50.01 | 2.2 | 0.974884 | 0.2 | 0.975922 | 0.975272 |
| BRLE14 | 55.24 | 57.8 | 13.96 | 50.0074 | 50.005 | 2.2 | 0.974884 | 2.45 | 0.975875 | 0.975558 |
| BROD61 | 15.68 | 1.72 | 12.82 | 50.0079 | 50.0054 | 2.2 | 0.974884 | 3.57 | 0.974986 | 0.974944 |
| BROM31 | 60.12 | 19.57 | 15.37 | 50.0028 | 50.0018 | 2.2 | 0.974884 | 2.38 | 0.97618 | 0.975863 |
| BROM32 | 60.12 | 19.57 | 15.37 | 50.0028 | 50.0018 | 2.2 | 0.974884 | 2.38 | 0.97618 | 0.975863 |
| BROM33 | 60.41 | 20.15 | 15.18 | 50.0029 | 50.0019 | 2.2 | 0.974884 | 2.38 | 0.976213 | 0.975896 |
| BROM34 | 60.41 | 20.15 | 15.18 | 50.0029 | 50.0019 | 2.2 | 0.974884 | 2.38 | 0.976213 | 0.975896 |
| BRWA11 | 222.44 | 102.05 | 13.16 | 50.0754 | 50.0514 | 2.2 | 0.974884 | 2.64 | 0.978155 | 0.976788 |
| BRWE11 | -19.99 | -39.42 | 14.59 | 49.9979 | 49.9986 | 2.22 | 0.974157 | 0.2 | 0.975896 | 0.97441 |
| BURW11 | 214.25 | 127.18 | 13.13 | 50.0771 | 50.0527 | 0.2 | 0.97441 | 2.48 | 0.977895 | 0.976789 |
| BUSB21 | 57.71 | -0.64 | 0 | 50 | 50.0275 | 2.57 | 0.974605 | 3.21 | 0.975255 | 0.974808 |
| BUSH11 | 267.13 | 173.03 | 13.07 | 50.0991 | 50.0675 | 2.2 | 0.974884 | 0.2 | 0.978034 | 0.976648 |
| BUST11 | 334.01 | 179.75 | 13.06 | 50.1219 | 50.083 | 2.2 | 0.974884 | 2.5 | 0.978654 | 0.977313 |
| CANT11 | 70.68 | 43 | 13.14 | 50.0257 | 50.0176 | 2.2 | 0.974884 | 0.2 | 0.976789 | 0.975574 |
| CANT12 | 70.68 | 43 | 13.12 | 50.0257 | 50.0176 | 2.2 | 0.974884 | 2.59 | 0.976006 | 0.975576 |
| CAPEA11 | 159.03 | 83.43 | 12.93 | 50.0809 | 50.0552 | 2.2 | 0.974884 | 2.34 | 0.976089 | 0.975625 |
| CARE11 | 187.64 | 46.08 | 13.13 | 50.0674 | 50.046 | 2.2 | 0.974884 | 2.63 | 0.977443 | 0.976365 |
| CARM11 | 4.39 | 1.75 | 13.22 | 50.0008 | 50.0006 | 2.2 | 0.974884 | 0.2 | 0.976365 | 0.974924 |
| CARR11 | 111.08 | 42.16 | 12.94 | 50.0519 | 50.0354 | 2.2 | 0.974884 | 2.22 | 0.975698 | 0.975385 |
| CARR12 | 227.02 | 75.61 | 12.94 | 50.108 | 50.0737 | 2.2 | 0.974884 | 3.58 | 0.976565 | 0.975941 |
| CELL11 | 603.8 | 311.5 | 12.92 | 50.276 | 50.1875 | 2.2 | 0.974884 | 2.47 | 0.980419 | 0.978264 |
| CHIC11 | 62.92 | 28.25 | 13.09 | 50.0217 | 50.0148 | 2.2 | 0.974884 | 2.63 | 0.975761 | 0.975412 |
| CHSI11 | 149.84 | 52.22 | 13.56 | 50.028 | 50.0191 | 2.2 | 0.974884 | 2.49 | 0.977409 | 0.976676 |
| CHSI12 | 50.74 | 17.71 | 13.24 | 50.0116 | 50.0079 | 2.2 | 0.974884 | 0.2 | 0.976676 | 0.975431 |
| CHSI13 | 69.47 | 54.62 | 0 | 50 | 49.9985 | 2.2 | 0.974884 | 2.35 | 0.976308 | 0.975901 |
| CHSI14 | 69.46 | 54.43 | 0 | 50 | 49.9986 | 2.2 | 0.974884 | 2.35 | 0.976306 | 0.9759 |
| CHTE11 | 221.16 | 109.41 | 12.95 | 50.1051 | 50.0717 | 2.2 | 0.974884 | 0.2 | 0.978264 | 0.976026 |
| CHTE12 | 215.42 | 101.25 | 12.91 | 50.1038 | 50.0708 | 2.2 | 0.974884 | 2.22 | 0.976714 | 0.976017 |
| CITR11 | 217.58 | 121.1 | 13.4 | 50.0555 | 50.0379 | 2.2 | 0.974884 | 2.51 | 0.978616 | 0.977376 |
| CITR12 | 217.46 | 119.91 | 13.38 | 50.0558 | 50.0381 | 2.2 | 0.974884 | 2.51 | 0.978586 | 0.977352 |
| CLYM21 | 200.89 | 5.3 | 12.63 | 50.1341 | 50.0916 | 2.56 | 0.973873 | 3.2 | 0.976124 | 0.974585 |
| COCK21 | -23.42 | -0.2 | 12.62 | 49.9884 | 49.9921 | 0.2 | 0.974585 | 2.51 | 0.975023 | 0.97494 |
| CONQ11 | 107.06 | 106.96 | 13.04 | 50.0322 | 50.022 | 2.2 | 0.974884 | 2.33 | 0.976091 | 0.975606 |
| CORB11 | 206.82 | 78.77 | 13.01 | 50.0873 | 50.0596 | 2.2 | 0.974884 | 2.59 | 0.977298 | 0.976434 |
| CORN11 | 104.91 | 90.12 | 13.18 | 50.0329 | 50.0225 | 2.2 | 0.974884 | 2.43 | 0.976804 | 0.976175 |
| CORN81 | 5 | 2.56 | 12.95 | 50.0025 | 50.0017 | 2.2 | 0.974884 | 0.2 | 0.976175 | 0.974947 |

*continued on next page*

*continued from previous page*

| Busbar Load Magnitudes | | | Frequency | | | Mean System Voltage | | | | |
|---|---|---|---|---|---|---|---|---|---|---|
| Busbar | Real | Reactive | Time | Max | Final | Time | Min | Time | Max | Final |
| CORN82 | 5 | 2.56 | 12.82 | 50.0027 | 50.0018 | 2.2 | 0.974884 | 2.55 | 0.974973 | 0.974943 |
| CORR61 | -20.67 | 28.67 | 0 | 50 | 49.988 | 3.12 | 0.974715 | 0.2 | 0.975606 | 0.975026 |
| COTT41 | 43.72 | -19.75 | 0 | 50 | 50.0197 | 2.26 | 0.974738 | 3.83 | 0.975074 | 0.974895 |
| COVE11 | 371.18 | 183.41 | 13.12 | 50.1227 | 50.0836 | 2.2 | 0.974884 | 2.47 | 0.979122 | 0.977614 |
| COWE11 | 7.02 | 3.51 | 13.03 | 50.0018 | 50.0012 | 2.2 | 0.974884 | 0.2 | 0.975412 | 0.974941 |
| COWL11 | 285.39 | 97.35 | 13.13 | 50.1041 | 50.071 | 2.2 | 0.974884 | 2.6 | 0.978647 | 0.977139 |
| COWL12 | 209.41 | 114.52 | 13.24 | 50.0659 | 50.045 | 2.2 | 0.974884 | 2.56 | 0.977889 | 0.976751 |
| CREB11 | 150 | 73.88 | 12.88 | 50.0816 | 50.0557 | 2.2 | 0.974884 | 3.59 | 0.976056 | 0.975587 |
| CREB12 | 299.96 | 104.37 | 12.84 | 50.1719 | 50.1172 | 2.2 | 0.974884 | 3.6 | 0.976795 | 0.975887 |
| CURR21 | 67.96 | 2.98 | 12.67 | 50.0473 | 50.0323 | 2.53 | 0.974463 | 3.19 | 0.975302 | 0.974742 |
| DALK21 | 11.81 | 6.58 | 12.63 | 50.0067 | 50.0046 | 0.2 | 0.974742 | 3.23 | 0.97496 | 0.97489 |
| DALK22 | 11.81 | 6.58 | 12.62 | 50.007 | 50.0048 | 11.27 | 0.974881 | 3.26 | 0.974974 | 0.974904 |
| DEES84 | 20 | 9.11 | 12.77 | 50.0137 | 50.0094 | 2.2 | 0.974884 | 0.2 | 0.975887 | 0.97495 |
| DEES85 | 20 | 9.11 | 12.79 | 50.0134 | 50.0091 | 2.2 | 0.974884 | 3.2 | 0.975012 | 0.974948 |
| DEES86 | 20 | 9.11 | 12.81 | 50.0124 | 50.0084 | 2.2 | 0.974884 | 3.14 | 0.975003 | 0.974944 |
| DEES87 | 20 | 9.11 | 12.75 | 50.0129 | 50.0088 | 2.2 | 0.974884 | 3.23 | 0.975008 | 0.974946 |
| DERW11 | 172.13 | 56.8 | 13.01 | 50.0769 | 50.0524 | 2.2 | 0.974884 | 0.2 | 0.977614 | 0.976078 |
| DEVM41 | 143.44 | -1.87 | 0 | 50 | 50.0648 | 2.58 | 0.974181 | 3.21 | 0.975754 | 0.97468 |
| DIDC85 | 10 | 13.33 | 13.25 | 50.0041 | 50.0028 | 2.2 | 0.974884 | 0.2 | 0.976751 | 0.975013 |
| DIDC87 | 36.62 | -4.66 | 0 | 50 | 50.0126 | 2.2 | 0.974884 | 2.66 | 0.975269 | 0.975072 |
| DIDC88 | 36.62 | -4.66 | 0 | 50 | 50.0126 | 2.2 | 0.974884 | 2.66 | 0.975269 | 0.975072 |
| DINO81 | 12 | 6.15 | 12.72 | 50.0077 | 50.0052 | 11.28 | 0.974874 | 0.2 | 0.974946 | 0.9749 |
| DINO82 | 12 | 6.15 | 12.64 | 50.0078 | 50.0053 | 11.2 | 0.974874 | 3.19 | 0.974943 | 0.9749 |
| DINO83 | 12 | 6.15 | 12.64 | 50.0077 | 50.0053 | 11.22 | 0.974876 | 3.28 | 0.974945 | 0.974901 |
| DINO84 | 2.48 | 6.15 | 12.47 | 50.0016 | 50.0011 | 2.2 | 0.974884 | 2.22 | 0.974905 | 0.974889 |
| DINO85 | 12 | 6.15 | 12.67 | 50.0076 | 50.0052 | 11.22 | 0.974876 | 3.2 | 0.974944 | 0.974901 |
| DINO86 | 2.48 | -3.16 | 0 | 50 | 50.0013 | 2.28 | 0.974863 | 0.2 | 0.974901 | 0.974878 |
| DONR61 | 119.42 | 32.24 | 12.94 | 50.059 | 50.0403 | 0.2 | 0.974878 | 3.57 | 0.975786 | 0.975455 |
| DRAK11 | 148.44 | 55.03 | 12.94 | 50.0703 | 50.048 | 2.2 | 0.974884 | 2.63 | 0.976149 | 0.975637 |
| DRAX11 | 82.11 | 57.4 | 12.89 | 50.0438 | 50.0299 | 2.2 | 0.974884 | 2.22 | 0.975571 | 0.975288 |
| DRAX12 | 75.11 | 46.84 | 12.92 | 50.0398 | 50.0272 | 2.2 | 0.974884 | 3.56 | 0.975452 | 0.975223 |
| DUNG21 | 43.2 | 40.31 | 13.07 | 50.0173 | 50.0118 | 2.2 | 0.974884 | 0.2 | 0.977352 | 0.975245 |
| EALI61 | 160.03 | 115.56 | 14.35 | 50.015 | 50.0101 | 2.2 | 0.974884 | 2.39 | 0.977917 | 0.977026 |
| EASO11 | 60.02 | 1.41 | 12.97 | 50.0319 | 50.0218 | 2.2 | 0.974884 | 0.2 | 0.977026 | 0.975159 |
| EASO12 | 77.51 | -27.77 | 0 | 50 | 50.0329 | 2.2 | 0.974884 | 3.78 | 0.975388 | 0.975058 |
| ECCL11 | -14.8 | -9.72 | 12.69 | 49.9902 | 49.9933 | 0.2 | 0.97468 | 0 | 0.974884 | 0.97482 |
| ECLA11 | 280.79 | 134.31 | 13.18 | 50.0952 | 50.065 | 2.2 | 0.974884 | 2.55 | 0.978702 | 0.97733 |
| EERH21 | 79.67 | -1.63 | 0 | 50 | 50.0388 | 2.56 | 0.974438 | 3.2 | 0.975396 | 0.974746 |
| EGGB41 | -0.41 | 4.91 | 0 | 50 | 49.9956 | 3.02 | 0.974838 | 0.2 | 0.975223 | 0.974895 |
| EGGB42 | 7.78 | 46.7 | 0 | 50 | 49.9949 | 3.02 | 0.974859 | 2.32 | 0.975353 | 0.975052 |
| EKIS21 | 41.62 | -3.12 | 0 | 50 | 50.0184 | 2.55 | 0.974675 | 3.2 | 0.975124 | 0.97482 |
| ELLA11 | 324.97 | 152.9 | 12.88 | 50.1488 | 50.1015 | 2.2 | 0.974884 | 2.31 | 0.977567 | 0.976442 |
| ELST11 | 134.41 | 84.72 | 13.37 | 50.0294 | 50.0201 | 2.2 | 0.974884 | 2.45 | 0.977025 | 0.976318 |
| ELST12 | 95.17 | 67.24 | 13.72 | 50.0171 | 50.0116 | 2.2 | 0.974884 | 2.43 | 0.976589 | 0.976058 |
| ELST13 | 35.88 | 13.59 | 13.07 | 50.0119 | 50.0081 | 2.2 | 0.974884 | 0.2 | 0.976058 | 0.975211 |
| ELST14 | 29.91 | 9.48 | 13.06 | 50.0102 | 50.007 | 2.2 | 0.974884 | 2.57 | 0.97529 | 0.975148 |
| ELTH11 | 78.23 | -12.9 | 0 | 50 | 50.0216 | 2.2 | 0.974884 | 2.63 | 0.975834 | 0.975437 |
| ELVA21 | 39.26 | 6.29 | 12.69 | 50.0273 | 50.0186 | 2.59 | 0.974798 | 3.22 | 0.975165 | 0.974892 |
| ENDE11 | 120.46 | 78.08 | 13.24 | 50.0358 | 50.0244 | 2.2 | 0.974884 | 0.2 | 0.97733 | 0.975776 |

*continued on next page*

*continued from previous page*

| Busbar Load Magnitudes | | | Frequency | | | Mean System Voltage | | | | |
|---|---|---|---|---|---|---|---|---|---|---|
| Busbar | Real | Reactive | Time | Max | Final | Time | Min | Time | Max | Final |
| ERNE11 | 46.81 | 30.73 | 13.3 | 50.0103 | 50.007 | 2.2 | 0.974884 | 2.59 | 0.975666 | 0.975453 |
| EXET11 | 137.65 | 53.52 | 13.14 | 50.0467 | 50.0319 | 2.2 | 0.974884 | 2.64 | 0.976793 | 0.976041 |
| FAWL11 | 98.34 | 11.55 | 13.04 | 50.0375 | 50.0256 | 2.2 | 0.974884 | 2.64 | 0.976126 | 0.975595 |
| FAWL41 | -5.43 | 29.6 | 0 | 50 | 49.9936 | 2.2 | 0.974884 | 0.2 | 0.976041 | 0.974974 |
| FECK61 | 194.61 | 81.61 | 13.07 | 50.0689 | 50.047 | 2.2 | 0.974884 | 2.53 | 0.976976 | 0.976251 |
| FELL11 | 4.83 | 1.93 | 12.75 | 50.017 | 50.0116 | 10.35 | 0.974831 | 0.2 | 0.976442 | 0.974888 |
| FERRA61 | 64.58 | 32.8 | 12.92 | 50.032 | 50.0218 | 2.2 | 0.974884 | 2.22 | 0.975345 | 0.975149 |
| FERRB11 | 192.74 | 105.66 | 12.89 | 50.0925 | 50.0631 | 2.2 | 0.974884 | 2.3 | 0.976439 | 0.975738 |
| FERRB12 | 194.07 | 79.68 | 12.88 | 50.1015 | 50.0692 | 2.2 | 0.974884 | 3.42 | 0.976209 | 0.975622 |
| FIDF11 | 79.68 | 26.85 | 12.88 | 50.042 | 50.0287 | 0.2 | 0.974879 | 3.44 | 0.975383 | 0.975174 |
| FIDF12 | 133.41 | 52.74 | 12.88 | 50.0677 | 50.0462 | 2.2 | 0.974884 | 2.34 | 0.97579 | 0.975427 |
| FIDF21 | 3.36 | -10.38 | 0 | 50 | 50.0017 | 2.29 | 0.974816 | 0.2 | 0.975622 | 0.974861 |
| FIDF23 | -5.77 | -2.61 | 12.55 | 49.9954 | 49.9969 | 3.15 | 0.974843 | 11.09 | 0.974893 | 0.974879 |
| FLEE11 | 148.17 | 111.87 | 13.43 | 50.0353 | 50.0241 | 2.2 | 0.974884 | 2.55 | 0.977267 | 0.976494 |
| FLEE12 | 157.12 | 121.43 | 13.66 | 50.0315 | 50.0215 | 2.2 | 0.974884 | 2.52 | 0.97761 | 0.97679 |
| FLEE13 | 157.04 | 145.48 | 13.84 | 50.027 | 50.0184 | 2.2 | 0.974884 | 2.48 | 0.977508 | 0.976664 |
| FLEE14 | 156.86 | 55.08 | 13.18 | 50.0493 | 50.0337 | 2.2 | 0.974884 | 2.6 | 0.977136 | 0.976318 |
| FOYE21 | 24.13 | -4.66 | 0 | 50 | 50.0076 | 2.45 | 0.974565 | 3.12 | 0.974895 | 0.974713 |
| FROD11 | 244.47 | 109.1 | 12.84 | 50.1318 | 50.0899 | 2.2 | 0.974884 | 3.44 | 0.976427 | 0.975774 |
| GALA11 | 159.65 | -33.04 | 0 | 50 | 50.0779 | 2.53 | 0.973996 | 3.18 | 0.975952 | 0.974622 |
| GLOU11 | 210.88 | 61.19 | 13.08 | 50.0807 | 50.0551 | 2.2 | 0.974884 | 2.6 | 0.977777 | 0.976703 |
| GLOU12 | 277.43 | 164.8 | 13.41 | 50.0613 | 50.0418 | 2.2 | 0.974884 | 2.5 | 0.979067 | 0.977725 |
| GLRO21 | 28.81 | 3.53 | 12.67 | 50.0193 | 50.0132 | 0.2 | 0.974622 | 3.2 | 0.975064 | 0.974846 |
| GRAI41 | 19.78 | 28.1 | 13.87 | 50.0059 | 50.004 | 2.2 | 0.974884 | 2.22 | 0.97559 | 0.975294 |
| GREN11 | 262.14 | 123.88 | 13.07 | 50.0998 | 50.0682 | 2.2 | 0.974884 | 2.53 | 0.978349 | 0.977112 |
| GREN12 | 149.12 | 74.47 | 13.09 | 50.0553 | 50.0378 | 2.2 | 0.974884 | 0.2 | 0.977112 | 0.976181 |
| GRIW11 | 89.06 | 37.99 | 12.89 | 50.0526 | 50.0359 | 2.2 | 0.974884 | 0.2 | 0.975774 | 0.975219 |
| GRMO21 | 29 | 1.3 | 12.62 | 50.0208 | 50.0142 | 2.54 | 0.974692 | 3.19 | 0.975062 | 0.974817 |
| GRSTA21 | -6.76 | 5.07 | 12.48 | 50.0058 | 50.004 | 2.39 | 0.974738 | 0.2 | 0.975219 | 0.974833 |
| GRSTB21 | -8.99 | 7.39 | 0 | 50 | 49.9887 | 3.23 | 0.974694 | 2.61 | 0.974952 | 0.974883 |
| GRTO61 | 39.22 | 2.58 | 12.69 | 50.0267 | 50.0182 | 2.6 | 0.974762 | 3.23 | 0.975188 | 0.974879 |
| HACK61 | 162.51 | 85.48 | 13.28 | 50.0446 | 50.0304 | 2.2 | 0.974884 | 2.51 | 0.977645 | 0.976746 |
| HAMH11 | 185.52 | 58.17 | 13.04 | 50.0754 | 50.0515 | 2.2 | 0.974884 | 2.58 | 0.976614 | 0.975984 |
| HAMH12 | -96.78 | 211.17 | 0 | 50 | 49.9154 | 3.8 | 0.974406 | 2.26 | 0.976009 | 0.975164 |
| HARK11 | 135.41 | 48.18 | 12.73 | 50.0919 | 50.0628 | 10.34 | 0.97478 | 3.25 | 0.975948 | 0.97509 |
| HARK12 | 191.53 | 59.37 | 12.72 | 50.1264 | 50.0863 | 10.38 | 0.974755 | 3.25 | 0.976351 | 0.975182 |
| HARM61 | 74.05 | 26.26 | 12.72 | 50.0476 | 50.0325 | 11.33 | 0.974831 | 3.25 | 0.975499 | 0.974997 |
| HATL81 | 13 | 5.92 | 12.67 | 50.0089 | 50.0061 | 2.61 | 0.974818 | 0.2 | 0.974997 | 0.974871 |
| HATL82 | 13 | 5.92 | 12.63 | 50.0089 | 50.0061 | 2.62 | 0.974833 | 3.19 | 0.974986 | 0.974875 |
| HAWI11 | 57.2 | -9.51 | 0 | 50 | 50.0279 | 2.55 | 0.974665 | 3.2 | 0.975303 | 0.974855 |
| HAWP61 | 100.78 | 35.9 | 12.77 | 50.0632 | 50.0432 | 11.33 | 0.974873 | 3.25 | 0.975717 | 0.975092 |
| HEYS11 | 147.56 | 77.5 | 12.82 | 50.085 | 50.058 | 2.2 | 0.974884 | 3.3 | 0.975853 | 0.975307 |
| HEYS81 | 2.54 | 16.47 | 13 | 50.001 | 50.0007 | 2.99 | 0.974842 | 0.2 | 0.975307 | 0.974895 |
| HEYS82 | 19.58 | 16.47 | 12.77 | 50.0129 | 50.0088 | 11.34 | 0.974858 | 3.29 | 0.974996 | 0.974901 |
| HEYS83 | 13 | 5.92 | 12.75 | 50.0085 | 50.0058 | 11.17 | 0.974866 | 3.17 | 0.974964 | 0.974895 |
| HEYS84 | 13 | 5.92 | 12.74 | 50.0082 | 50.0056 | 11.14 | 0.974867 | 3.17 | 0.974961 | 0.974894 |
| HIGM21 | 4.14 | 53.57 | 0 | 50 | 49.9956 | 2.2 | 0.974884 | 2.32 | 0.975368 | 0.975064 |
| HINP21 | 4.19 | -0.38 | 0 | 50 | 50.0027 | 2.2 | 0.974884 | 0.2 | 0.977725 | 0.974937 |
| HINP22 | 4.18 | 6.05 | 12.82 | 50.0023 | 50.0016 | 2.2 | 0.974884 | 2.66 | 0.974972 | 0.97493 |

*continued on next page*

*continued from previous page*

| Busbar Load Magnitudes | | | Frequency | | | Mean System Voltage | | | | |
|---|---|---|---|---|---|---|---|---|---|---|
| Busbar | Real | Reactive | Time | Max | Final | Time | Min | Time | Max | Final |
| HUER41 | 181.25 | -0.47 | 0 | 50 | 50.0848 | 2.59 | 0.973904 | 3.22 | 0.976034 | 0.974593 |
| HUTT11 | 140.7 | 96.9 | 12.86 | 50.0847 | 50.0578 | 2.2 | 0.974884 | 3.33 | 0.976041 | 0.975335 |
| ICCK11 | 85.51 | 57.96 | 12.9 | 50.0478 | 50.0326 | 2.2 | 0.974884 | 3.61 | 0.975584 | 0.975331 |
| INDQ11 | 223.79 | 65 | 13.11 | 50.0778 | 50.0531 | 2.2 | 0.974884 | 2.64 | 0.978068 | 0.976822 |
| INKI41 | 24.12 | -2.13 | 0 | 50 | 50.0131 | 0.2 | 0.974593 | 3.21 | 0.975057 | 0.974842 |
| IROA11 | 275.96 | 91.77 | 13.13 | 50.096 | 50.0655 | 2.2 | 0.974884 | 2.63 | 0.979163 | 0.977584 |
| IROA12 | 296.94 | 139.62 | 13.22 | 50.0927 | 50.0632 | 2.2 | 0.974884 | 2.61 | 0.979771 | 0.978092 |
| IRON11 | 305.81 | 112.02 | 12.96 | 50.1473 | 50.1004 | 2.2 | 0.974884 | 2.61 | 0.977395 | 0.976409 |
| IVER11 | 100.33 | 50.42 | 13.43 | 50.0203 | 50.0138 | 2.2 | 0.974884 | 0.2 | 0.976746 | 0.976013 |
| IVER12 | 113.71 | 38.27 | 13.17 | 50.0332 | 50.0227 | 2.2 | 0.974884 | 2.55 | 0.976508 | 0.975968 |
| IVER61 | 130.11 | 52.26 | 13.28 | 50.0324 | 50.0221 | 2.2 | 0.974884 | 2.51 | 0.977104 | 0.976463 |
| JORD31 | 43.61 | 12.73 | 12.83 | 50.0227 | 50.0155 | 2.2 | 0.974884 | 0.2 | 0.975331 | 0.975078 |
| KAIM21 | 23.33 | 7.34 | 12.76 | 50.0144 | 50.0098 | 0.2 | 0.974842 | 3.24 | 0.97505 | 0.974904 |
| KEAD11 | 266.88 | 61.05 | 12.85 | 50.1645 | 50.1122 | 2.2 | 0.974884 | 3.78 | 0.976688 | 0.975734 |
| KEAR11 | 240.88 | 98.04 | 12.93 | 50.1057 | 50.0721 | 2.2 | 0.974884 | 2.32 | 0.976892 | 0.976112 |
| KEAR12 | 284.19 | 156 | 12.98 | 50.1104 | 50.0753 | 2.2 | 0.974884 | 2.32 | 0.977791 | 0.97655 |
| KEAR31 | 92.07 | 41.17 | 12.91 | 50.0382 | 50.0261 | 2.2 | 0.974884 | 0.2 | 0.97655 | 0.975395 |
| KEIT21 | 41.95 | -3.98 | 0 | 50 | 50.018 | 2.51 | 0.974527 | 3.17 | 0.975068 | 0.974729 |
| KEMS11 | 134.66 | 65.78 | 13.18 | 50.048 | 50.0328 | 2.2 | 0.974884 | 2.59 | 0.976956 | 0.976176 |
| KEMS12 | 63.27 | 49.59 | 13.35 | 50.0177 | 50.0121 | 2.2 | 0.974884 | 0.2 | 0.976176 | 0.975615 |
| KIBY11 | 246.51 | 97.8 | 12.86 | 50.1279 | 50.0872 | 2.2 | 0.974884 | 3.4 | 0.976483 | 0.975789 |
| KILS21 | 84.4 | -1.02 | 0 | 50 | 50.0398 | 2.58 | 0.974502 | 3.22 | 0.975424 | 0.974784 |
| KILS22 | 84.4 | -1.02 | 0 | 50 | 50.0394 | 2.58 | 0.974507 | 3.22 | 0.97542 | 0.974787 |
| KINC21 | 157.39 | 14.32 | 12.64 | 50.107 | 50.0731 | 2.54 | 0.973985 | 3.19 | 0.975852 | 0.974595 |
| KINLP11 | -0.54 | 1.63 | 0 | 50 | 49.9995 | 2.2 | 0.974884 | 0.2 | 0.975615 | 0.974893 |
| KINLP81 | 20 | 9.11 | 12.85 | 50.0152 | 50.0104 | 2.2 | 0.974884 | 3.75 | 0.975119 | 0.975018 |
| KINO11 | 212.76 | 93.82 | 13.16 | 50.0797 | 50.0544 | 2.2 | 0.974884 | 2.59 | 0.978061 | 0.976797 |
| KINT21 | 154.11 | 115.42 | 12.66 | 50.1331 | 50.0909 | 2.59 | 0.974402 | 3.23 | 0.976415 | 0.974974 |
| KIRK11 | 185.82 | 55.49 | 12.88 | 50.0926 | 50.0632 | 2.2 | 0.974884 | 3.43 | 0.976196 | 0.975664 |
| KITW11 | 585.92 | -18.52 | 0 | 50 | 50.2012 | 2.2 | 0.974884 | 2.68 | 0.979641 | 0.977569 |
| LACK61 | 181.57 | 14.2 | 12.7 | 50.1205 | 50.0822 | 2.61 | 0.974406 | 3.23 | 0.976338 | 0.97493 |
| LALE11 | 45.71 | 18.36 | 13.41 | 50.0104 | 50.0071 | 2.2 | 0.974884 | 0.2 | 0.976797 | 0.975376 |
| LALE12 | 53.84 | 29.55 | 13.58 | 50.0091 | 50.0062 | 2.2 | 0.974884 | 2.46 | 0.975796 | 0.97553 |
| LALE13 | 45.68 | 12.3 | 13.21 | 50.0128 | 50.0088 | 2.2 | 0.974884 | 2.22 | 0.975573 | 0.97533 |
| LALE14 | 36.15 | 16.66 | 13.29 | 50.0076 | 50.0052 | 2.2 | 0.974884 | 2.22 | 0.975533 | 0.975286 |
| LAMB21 | 142.53 | -0.59 | 0 | 50 | 50.0689 | 2.56 | 0.974079 | 3.21 | 0.975795 | 0.974632 |
| LAND11 | -6.6 | 15.85 | 0 | 50 | 49.9945 | 2.7 | 0.974809 | 0.2 | 0.978092 | 0.974907 |
| LAWF11 | -13.39 | 4.84 | 0 | 50 | 49.9948 | 2.68 | 0.974767 | 0.2 | 0.975286 | 0.974829 |
| LEAT11 | 13.48 | -5.53 | 0 | 50 | 50.004 | 0.2 | 0.974829 | 2.64 | 0.975044 | 0.974973 |
| LEGA11 | 419.77 | 56.83 | 12.76 | 50.2423 | 50.1652 | 2.2 | 0.974884 | 3.73 | 0.977507 | 0.976311 |
| LEIC11 | 282.65 | 109.58 | 13.05 | 50.113 | 50.0771 | 2.2 | 0.974884 | 2.57 | 0.97779 | 0.97665 |
| LINM21 | 37.08 | 1.61 | 12.71 | 50.0254 | 50.0173 | 0.2 | 0.974632 | 3.21 | 0.975124 | 0.97485 |
| LINT11 | -85.85 | 2.33 | 0 | 50 | 49.9589 | 3.19 | 0.974254 | 0.2 | 0.976311 | 0.974942 |
| LINT12 | -85.88 | 6.87 | 0 | 50 | 49.9582 | 3.18 | 0.974261 | 2.54 | 0.975279 | 0.974973 |
| LISD11 | 267.04 | 51.96 | 12.79 | 50.1508 | 50.1028 | 2.2 | 0.974884 | 3.25 | 0.976522 | 0.975642 |
| LITT11 | 96.21 | 48.11 | 13.27 | 50.0275 | 50.0188 | 2.2 | 0.974884 | 2.55 | 0.976459 | 0.975931 |
| LITT12 | 96.21 | 48.11 | 13.24 | 50.0271 | 50.0185 | 2.2 | 0.974884 | 2.55 | 0.976469 | 0.97594 |
| LITT13 | 96.21 | 48.11 | 13.22 | 50.0278 | 50.019 | 2.2 | 0.974884 | 2.55 | 0.976449 | 0.975922 |
| LOAN21 | 3.95 | 0.46 | 12.17 | 50.0007 | 50.0005 | 2.37 | 0.974776 | 0 | 0.974884 | 0.974828 |

*continued on next page*

*continued from previous page*

| Busbar Load Magnitudes | | | Frequency | | | Mean System Voltage | | | | |
|---|---|---|---|---|---|---|---|---|---|---|
| Busbar | Real | Reactive | Time | Max | Final | Time | Min | Time | Max | Final |
| LOVE11 | 289.32 | 145.33 | 13.19 | 50.0869 | 50.0593 | 2.2 | 0.974884 | 2.6 | 0.979006 | 0.977499 |
| LOVE12 | 189.41 | 23.28 | 13.06 | 50.075 | 50.0512 | 2.2 | 0.974884 | 0.2 | 0.977499 | 0.97625 |
| MACC31 | 61.74 | 23.63 | 12.97 | 50.0289 | 50.0197 | 2.2 | 0.974884 | 0.2 | 0.975642 | 0.9752 |
| MAGA61 | 47.88 | 58.6 | 15.95 | 50.0021 | 50.0013 | 2.2 | 0.974884 | 0.2 | 0.97625 | 0.975524 |
| MANN11 | 520.99 | 194.36 | 13.12 | 50.1813 | 50.1236 | 2.2 | 0.974884 | 2.63 | 0.981908 | 0.97906 |
| MAWO11 | -8.25 | 9.44 | 0 | 50 | 49.996 | 2.68 | 0.974787 | 0.2 | 0.97906 | 0.97485 |
| MELK11 | 176.62 | 94.95 | 13.39 | 50.0412 | 50.0281 | 0.2 | 0.97485 | 2.56 | 0.977621 | 0.976727 |
| MELK12 | 185.69 | 116.78 | 13.63 | 50.0358 | 50.0244 | 2.2 | 0.974884 | 2.51 | 0.977949 | 0.977003 |
| MILE11 | 35.23 | 6.16 | 13.03 | 50.0134 | 50.0091 | 2.2 | 0.974884 | 0.2 | 0.975886 | 0.975224 |
| MILH11 | 97.45 | 38.99 | 13.19 | 50.0307 | 50.021 | 2.2 | 0.974884 | 2.55 | 0.976308 | 0.975834 |
| MILH12 | 124.24 | 39.29 | 13.11 | 50.042 | 50.0287 | 2.2 | 0.974884 | 2.56 | 0.976577 | 0.975983 |
| MITY11 | 136.47 | 70.53 | 13.19 | 50.0412 | 50.0281 | 2.2 | 0.974884 | 0.2 | 0.977003 | 0.9761 |
| MITY12 | 124.43 | 41.04 | 13.11 | 50.0435 | 50.0297 | 2.2 | 0.974884 | 2.61 | 0.976511 | 0.975886 |
| MOSM21 | 60.56 | 1.46 | 12.67 | 50.038 | 50.0259 | 2.55 | 0.974574 | 3.2 | 0.975224 | 0.974786 |
| NECH11 | 189.34 | 73.01 | 13 | 50.076 | 50.0519 | 2.2 | 0.974884 | 2.57 | 0.976731 | 0.976075 |
| NECH12 | 124.26 | 66.42 | 13.05 | 50.0456 | 50.0312 | 2.2 | 0.974884 | 2.54 | 0.976183 | 0.975736 |
| NEEP31 | 81.81 | 36.79 | 12.91 | 50.0384 | 50.0262 | 2.2 | 0.974884 | 2.22 | 0.975614 | 0.97535 |
| NEIL21 | 143.74 | 48.71 | 12.66 | 50.0989 | 50.0676 | 2.62 | 0.974506 | 3.24 | 0.975915 | 0.974886 |
| NEIL41 | 79.98 | 24.71 | 12.71 | 50.0541 | 50.0369 | 2.62 | 0.974637 | 3.25 | 0.97542 | 0.974857 |
| NEWA11 | 63.77 | 29.96 | 13.12 | 50.0179 | 50.0122 | 2.2 | 0.974884 | 2.62 | 0.975784 | 0.975467 |
| NEWX61 | 167.46 | 64.82 | 13.7 | 50.0287 | 50.0196 | 2.2 | 0.974884 | 2.48 | 0.977712 | 0.976886 |
| NEWX62 | 167.43 | 67 | 13.75 | 50.0272 | 50.0185 | 2.2 | 0.974884 | 2.47 | 0.97775 | 0.976917 |
| NFLE11 | 7.48 | 5.57 | 13.15 | 50.0017 | 50.0012 | 2.2 | 0.974884 | 0.2 | 0.976917 | 0.974977 |
| NFLW11 | 75.14 | 36.88 | 13.19 | 50.0243 | 50.0166 | 2.2 | 0.974884 | 2.57 | 0.976046 | 0.975623 |
| NFLW12 | 26.74 | 11.71 | 13.12 | 50.0092 | 50.0063 | 2.2 | 0.974884 | 0.2 | 0.975623 | 0.975137 |
| NFLW13 | 27.06 | 10.47 | 13.12 | 50.0093 | 50.0064 | 2.2 | 0.974884 | 2.59 | 0.975282 | 0.975133 |
| NHYD61 | 156.31 | 50.62 | 13.2 | 50.0444 | 50.0303 | 2.2 | 0.974884 | 2.53 | 0.977182 | 0.976423 |
| NINF11 | 351.29 | 163.93 | 13.09 | 50.1426 | 50.0972 | 2.2 | 0.974884 | 2.64 | 0.979626 | 0.977552 |
| NORL31 | 29.71 | 14.31 | 12.97 | 50.0141 | 50.0096 | 2.2 | 0.974884 | 0.2 | 0.97535 | 0.975045 |
| NORM11 | -7.98 | 0.54 | 0 | 50 | 49.997 | 2.7 | 0.974811 | 0.2 | 0.977552 | 0.974843 |
| NORM13 | -7.99 | 0.54 | 0 | 50 | 49.998 | 2.58 | 0.974823 | 0 | 0.974884 | 0.974846 |
| NORT11 | 252.72 | 113.9 | 12.74 | 50.1557 | 50.1062 | 2.2 | 0.974884 | 3.31 | 0.977126 | 0.97552 |
| NORT12 | 162.04 | 77.85 | 12.77 | 50.0965 | 50.0658 | 2.2 | 0.974884 | 3.31 | 0.976355 | 0.97546 |
| NOTR11 | 318.35 | 156.48 | 13.01 | 50.1331 | 50.0909 | 0.2 | 0.974846 | 2.51 | 0.978892 | 0.977385 |
| NOTR12 | 106.08 | 51.55 | 13.04 | 50.043 | 50.0293 | 2.2 | 0.974884 | 0.2 | 0.977385 | 0.975752 |
| NURS11 | 324.24 | 148.55 | 13.19 | 50.1027 | 50.0701 | 2.2 | 0.974884 | 2.61 | 0.979346 | 0.97765 |
| OCKH11 | 134.69 | 100.84 | 13.17 | 50.0345 | 50.0235 | 2.2 | 0.974884 | 2.38 | 0.976536 | 0.975956 |
| OFFE31 | 31.25 | -13.48 | 0 | 50 | 50.0159 | 2.51 | 0.974658 | 0.2 | 0.97546 | 0.974807 |
| OLDB11 | 105.85 | 62.86 | 13.06 | 50.0343 | 50.0234 | 2.2 | 0.974884 | 2.48 | 0.976045 | 0.975664 |
| OLDS11 | -2.87 | 10.05 | 15.08 | 50.0006 | 50.0004 | 2.2 | 0.974884 | 0.2 | 0.97765 | 0.975058 |
| OLDS12 | 5.36 | 22.04 | 0 | 50 | 49.9997 | 2.2 | 0.974884 | 2.22 | 0.9754 | 0.975186 |
| OSBA11 | 188.3 | 85.23 | 12.84 | 50.1076 | 50.0735 | 0.2 | 0.974807 | 3.42 | 0.976119 | 0.975504 |
| PADI11 | 178.68 | 133.81 | 12.94 | 50.0806 | 50.055 | 2.2 | 0.974884 | 2.32 | 0.97663 | 0.975835 |
| PAIG11 | 105.71 | 49.81 | 13.15 | 50.0302 | 50.0206 | 2.2 | 0.974884 | 2.63 | 0.976389 | 0.975864 |
| PELH11 | 77.14 | 5.96 | 12.99 | 50.0378 | 50.0258 | 2.2 | 0.974884 | 0.2 | 0.975752 | 0.975336 |
| PELH12 | 77.21 | 7.24 | 13 | 50.0366 | 50.025 | 2.2 | 0.974884 | 2.64 | 0.975662 | 0.975332 |
| PEMB11 | 104.98 | 75.73 | 13.37 | 50.0239 | 50.0163 | 2.2 | 0.974884 | 2.53 | 0.976561 | 0.976023 |
| PEMB71 | 4.26 | 62.16 | 0 | 50 | 49.9879 | 2.2 | 0.974884 | 0.2 | 0.976023 | 0.975231 |
| PENE11 | 129.09 | 61.36 | 12.9 | 50.0656 | 50.0448 | 2.2 | 0.974884 | 0.2 | 0.975835 | 0.975395 |

*continued on next page*

*continued from previous page*

| Busbar Load Magnitudes | | | Frequency | | | Mean System Voltage | | | | |
|---|---|---|---|---|---|---|---|---|---|---|
| Busbar | Real | Reactive | Time | Max | Final | Time | Min | Time | Max | Final |
| PENE12 | 96.76 | 55.44 | 12.9 | 50.0466 | 50.0318 | 2.2 | 0.974884 | 2.31 | 0.975682 | 0.975337 |
| PENN11 | 317.34 | 179.39 | 13.04 | 50.1162 | 50.0792 | 2.2 | 0.974884 | 2.47 | 0.978264 | 0.977033 |
| PENT11 | 169.25 | 17.66 | 12.77 | 50.1031 | 50.0704 | 2.2 | 0.974884 | 3.15 | 0.975838 | 0.975271 |
| PENW11 | 44.98 | -18.43 | 0 | 50 | 50.0222 | 11.17 | 0.97478 | 0.2 | 0.975271 | 0.974889 |
| PENW12 | 122.34 | 8.51 | 12.83 | 50.074 | 50.0505 | 2.2 | 0.974884 | 3.2 | 0.975642 | 0.975148 |
| PERH11 | 1.14 | -9.2 | 0 | 50 | 50.0018 | 2.32 | 0.974809 | 0.2 | 0.975148 | 0.974853 |
| PERH12 | 1.14 | -9.2 | 0 | 50 | 50.0018 | 2.32 | 0.974809 | 3.08 | 0.974886 | 0.974853 |
| PERS21 | 79.27 | 5.11 | 12.67 | 50.052 | 50.0355 | 2.53 | 0.974268 | 3.18 | 0.975285 | 0.974635 |
| PETP11 | -6.53 | -5.56 | 12.78 | 49.9966 | 49.9977 | 2.55 | 0.974798 | 0.2 | 0.975332 | 0.974827 |
| PETP81 | 5 | 2.56 | 12.68 | 50.005 | 50.0034 | 0.2 | 0.974827 | 3.79 | 0.97495 | 0.974917 |
| PETP82 | 5 | 2.56 | 12.85 | 50.0019 | 50.0013 | 2.2 | 0.974884 | 2.56 | 0.974933 | 0.974916 |
| PITS31 | 59.33 | 28.83 | 12.91 | 50.0267 | 50.0183 | 0.2 | 0.974853 | 2.22 | 0.975485 | 0.975274 |
| PITS32 | 6.47 | 5.36 | 12.8 | 50.0026 | 50.0018 | 2.2 | 0.974884 | 0.2 | 0.975274 | 0.974932 |
| PLYM11 | 70.31 | 32.94 | 13.15 | 50.0185 | 50.0126 | 2.2 | 0.974884 | 2.62 | 0.975969 | 0.97564 |
| PLYT11 | 19.41 | 14.79 | 13.38 | 50.0033 | 50.0022 | 2.2 | 0.974884 | 0.2 | 0.97564 | 0.975132 |
| POIS11 | -10.23 | 12.8 | 0 | 50 | 49.9944 | 2.69 | 0.974783 | 0.2 | 0.975132 | 0.974874 |
| POIS12 | -4.61 | 19.83 | 0 | 50 | 49.9947 | 0.2 | 0.974874 | 2.22 | 0.975095 | 0.974963 |
| POPP31 | 39.91 | 10.71 | 12.87 | 50.0231 | 50.0158 | 2.2 | 0.974884 | 3.27 | 0.97514 | 0.97501 |
| POPP81 | 0.13 | -2.15 | 0 | 50 | 50.0004 | 2.32 | 0.97486 | 0.2 | 0.97501 | 0.974873 |
| PYLE11 | 85.96 | 24.09 | 13.13 | 50.0275 | 50.0187 | 2.2 | 0.974884 | 2.62 | 0.976101 | 0.975626 |
| PYLE12 | 84.9 | 23.46 | 13.13 | 50.0272 | 50.0186 | 2.2 | 0.974884 | 2.62 | 0.976085 | 0.975616 |
| PYWO11 | 30.18 | 25.15 | 13.17 | 50.0064 | 50.0044 | 2.2 | 0.974884 | 0.2 | 0.975616 | 0.975214 |
| RAIN11 | 217.38 | 50.01 | 12.81 | 50.1217 | 50.083 | 0.2 | 0.974873 | 3.27 | 0.976204 | 0.975532 |
| RAIN12 | 196.64 | 82.96 | 12.9 | 50.102 | 50.0695 | 2.2 | 0.974884 | 2.32 | 0.976184 | 0.975623 |
| RASS11 | 173.14 | 85.42 | 13.32 | 50.0476 | 50.0325 | 2.2 | 0.974884 | 2.57 | 0.97738 | 0.976504 |
| RATS11 | 387.04 | 204.44 | 13.01 | 50.1727 | 50.1177 | 2.2 | 0.974884 | 2.56 | 0.978785 | 0.977223 |
| RAYL11 | 312.82 | 94.19 | 13.08 | 50.1174 | 50.0801 | 2.2 | 0.974884 | 2.58 | 0.97919 | 0.97756 |
| RAYL12 | 216.02 | 62.89 | 13.1 | 50.0866 | 50.0591 | 2.2 | 0.974884 | 2.6 | 0.977749 | 0.976618 |
| RAYL13 | 98.98 | 28.51 | 13.07 | 50.0421 | 50.0287 | 2.2 | 0.974884 | 0.2 | 0.976618 | 0.975646 |
| READ11 | 4.39 | 1.75 | 13.12 | 50.001 | 50.0007 | 2.2 | 0.974884 | 0.2 | 0.976504 | 0.974922 |
| REBR31 | 82.7 | 25.45 | 13.13 | 50.029 | 50.0198 | 2.2 | 0.974884 | 2.58 | 0.976101 | 0.975682 |
| REDD61 | 4.61 | 1.84 | 12.84 | 50.0015 | 50.001 | 2.2 | 0.974884 | 0.2 | 0.977223 | 0.974915 |
| ROCH11 | 314.77 | 191.25 | 12.96 | 50.1223 | 50.0834 | 2.2 | 0.974884 | 2.32 | 0.978155 | 0.976713 |
| ROCK81 | 1.36 | 4.27 | 12.96 | 50.0002 | 50.0001 | 2.2 | 0.974884 | 0.2 | 0.976713 | 0.974903 |
| ROOS11 | 4.83 | 1.93 | 12.48 | 50.003 | 50.0021 | 10.46 | 0.974881 | 3.27 | 0.974919 | 0.974891 |
| RUGE11 | 222.75 | 78.91 | 12.94 | 50.1105 | 50.0754 | 2.2 | 0.974884 | 2.66 | 0.976664 | 0.975909 |
| RYEH11 | 172.7 | -13.92 | 0 | 50 | 50.0564 | 2.2 | 0.974884 | 2.65 | 0.976671 | 0.975889 |
| RYEH12 | 172.81 | -13.75 | 0 | 50 | 50.0559 | 2.2 | 0.974884 | 2.64 | 0.976683 | 0.975901 |
| SALH11 | 41.01 | 24.24 | 12.77 | 50.0246 | 50.0168 | 2.2 | 0.974884 | 3.3 | 0.975239 | 0.975011 |
| SALH12 | 41.11 | 12.51 | 12.77 | 50.0264 | 50.018 | 11.31 | 0.974855 | 3.23 | 0.975215 | 0.974946 |
| SASA11 | 30.2 | 28.49 | 12.88 | 50.0137 | 50.0094 | 2.2 | 0.974884 | 2.37 | 0.975158 | 0.975063 |
| SAUS11 | 39.01 | 11.22 | 13.04 | 50.0127 | 50.0087 | 2.2 | 0.974884 | 2.64 | 0.975436 | 0.975228 |
| SELL11 | 112.19 | 12.64 | 13.02 | 50.0533 | 50.0364 | 2.2 | 0.974884 | 2.66 | 0.97624 | 0.975586 |
| SELL12 | 1.13 | 12.64 | 0 | 50 | 49.999 | 2.2 | 0.974884 | 0.2 | 0.975586 | 0.974965 |
| SELL13 | 1.13 | 12.64 | 0 | 50 | 49.9991 | 2.2 | 0.974884 | 2.22 | 0.975062 | 0.974964 |
| SELL14 | 112.02 | 13.65 | 13.03 | 50.0533 | 50.0364 | 2.2 | 0.974884 | 2.66 | 0.976241 | 0.975587 |
| SELL41 | 40.72 | 54.3 | 13.07 | 50.0504 | 50.0344 | 2.2 | 0.974884 | 2.64 | 0.976428 | 0.975731 |
| SGER11 | 24.13 | 9.97 | 13.08 | 50.0068 | 50.0046 | 2.2 | 0.974884 | 2.64 | 0.975242 | 0.975123 |
| SGER12 | 5.85 | 7.89 | 13.63 | 50.0005 | 50.0003 | 2.2 | 0.974884 | 0.2 | 0.975123 | 0.974978 |

*continued on next page*

*continued from previous page*

| Busbar Load Magnitudes | | | Frequency | | | Mean System Voltage | | | | |
|---|---|---|---|---|---|---|---|---|---|---|
| Busbar | Real | Reactive | Time | Max | Final | Time | Min | Time | Max | Final |
| SHEC31 | 66.1 | 22.5 | 12.88 | 50.0333 | 50.0228 | 2.2 | 0.974884 | 3.61 | 0.975389 | 0.975204 |
| SITT11 | 4.44 | 3.07 | 12.96 | 50.001 | 50.0007 | 2.2 | 0.974884 | 0.2 | 0.975587 | 0.974929 |
| SIZE11 | 21.35 | 27.38 | 13.02 | 50.0206 | 50.0141 | 2.2 | 0.974884 | 2.56 | 0.975381 | 0.975176 |
| SIZE41 | 33.17 | 55.82 | 13.57 | 50.0053 | 50.0036 | 2.2 | 0.974884 | 2.22 | 0.975581 | 0.975236 |
| SIZE81 | 26 | 13.32 | 12.82 | 50.0147 | 50.01 | 2.2 | 0.974884 | 0.2 | 0.975176 | 0.97498 |
| SIZE82 | 26 | 13.32 | 12.89 | 50.0149 | 50.0102 | 2.2 | 0.974884 | 2.61 | 0.975089 | 0.974982 |
| SJOW11 | 178 | 79.72 | 13.25 | 50.0503 | 50.0344 | 2.2 | 0.974884 | 2.52 | 0.977663 | 0.976734 |
| SJOW12 | 177.75 | 77.04 | 13.04 | 50.0723 | 50.0494 | 2.2 | 0.974884 | 2.61 | 0.97711 | 0.976247 |
| SJOW61 | 127.23 | 103.35 | 13.94 | 50.0189 | 50.0128 | 2.2 | 0.974884 | 2.41 | 0.9774 | 0.976591 |
| SJOW62 | 296.13 | 176.02 | 13.79 | 50.0583 | 50.0397 | 2.2 | 0.974884 | 2.44 | 0.980464 | 0.978664 |
| SKLGB11 | 263.75 | 148.25 | 12.93 | 50.1125 | 50.0768 | 2.2 | 0.974884 | 2.3 | 0.977473 | 0.976295 |
| SKLGB12 | 256.27 | 96.9 | 12.87 | 50.1236 | 50.0843 | 2.2 | 0.974884 | 2.22 | 0.976789 | 0.975993 |
| SMAN11 | 89.01 | 9.3 | 12.88 | 50.0476 | 50.0325 | 2.2 | 0.974884 | 0.2 | 0.975993 | 0.975202 |
| SMAN12 | 90.01 | 33.05 | 12.93 | 50.0413 | 50.0282 | 2.2 | 0.974884 | 2.22 | 0.97559 | 0.975327 |
| SMEA21 | -19.41 | 3.02 | 0 | 50 | 49.994 | 0.2 | 0.974635 | 2.54 | 0.974959 | 0.974909 |
| SPEN11 | 102.13 | 55.57 | 12.79 | 50.0615 | 50.042 | 2.2 | 0.974884 | 3.32 | 0.975877 | 0.975275 |
| SPEN12 | 78.69 | 34.85 | 12.78 | 50.0482 | 50.0329 | 2.2 | 0.974884 | 3.27 | 0.975597 | 0.975142 |
| SPEN13 | 72.75 | 37.02 | 12.75 | 50.0439 | 50.03 | 2.2 | 0.974884 | 3.3 | 0.975599 | 0.97519 |
| SSHI31 | 55.96 | 30.25 | 12.76 | 50.0333 | 50.0227 | 2.2 | 0.974884 | 3.3 | 0.975395 | 0.97509 |
| STAH11 | 164.95 | 115.73 | 12.95 | 50.0779 | 50.0531 | 2.2 | 0.974884 | 2.31 | 0.976294 | 0.975631 |
| STAL11 | 352.13 | 175.86 | 12.9 | 50.1506 | 50.1027 | 2.2 | 0.974884 | 2.31 | 0.9781 | 0.976736 |
| STAYC11 | 225.85 | 70.65 | 12.97 | 50.1173 | 50.08 | 2.2 | 0.974884 | 2.64 | 0.976743 | 0.975957 |
| STEN11 | 98.77 | 55.34 | 12.8 | 50.0565 | 50.0386 | 2.2 | 0.974884 | 0.2 | 0.976736 | 0.975386 |
| STEN12 | 156.63 | 75.41 | 12.74 | 50.0982 | 50.067 | 2.2 | 0.974884 | 3.29 | 0.976423 | 0.975483 |
| STES11 | 163.72 | 77.03 | 12.76 | 50.0931 | 50.0635 | 2.2 | 0.974884 | 3.31 | 0.976429 | 0.975547 |
| STHA21 | 45.95 | -6.08 | 0 | 50 | 50.0263 | 2.54 | 0.974559 | 3.19 | 0.975219 | 0.974776 |
| STSB61 | 15.46 | 11.04 | 12.88 | 50.0075 | 50.0051 | 2.2 | 0.974884 | 0.2 | 0.975547 | 0.974964 |
| STUD11 | 34.11 | 19.57 | 13.1 | 50.0086 | 50.0059 | 2.2 | 0.974884 | 2.61 | 0.975389 | 0.975225 |
| SUND11 | 242.35 | 146.48 | 13.19 | 50.0741 | 50.0506 | 2.2 | 0.974884 | 2.47 | 0.978757 | 0.97745 |
| SUND12 | 178.81 | 109.27 | 13.27 | 50.054 | 50.0369 | 2.2 | 0.974884 | 2.49 | 0.9777 | 0.976746 |
| SWAN11 | 212.77 | 134.96 | 13.74 | 50.0382 | 50.026 | 2.2 | 0.974884 | 2.48 | 0.978337 | 0.977223 |
| SWAN12 | 186.43 | 69.71 | 13.28 | 50.05 | 50.0341 | 2.2 | 0.974884 | 2.58 | 0.977576 | 0.97662 |
| TAUN11 | 73.43 | 13.07 | 13.07 | 50.0297 | 50.0203 | 2.2 | 0.974884 | 0.2 | 0.97662 | 0.975417 |
| TEAL21 | 127.52 | 161.3 | 12.71 | 50.1162 | 50.0794 | 0.2 | 0.974776 | 3.29 | 0.976563 | 0.975455 |
| TEMP31 | 33.31 | 14.93 | 12.91 | 50.0155 | 50.0106 | 2.2 | 0.974884 | 2.22 | 0.975203 | 0.975097 |
| THOM61 | 4.13 | 33.06 | 0 | 50 | 49.994 | 2.2 | 0.974884 | 2.32 | 0.97529 | 0.975087 |
| THUR61 | 129.31 | 61.79 | 12.93 | 50.0631 | 50.0431 | 2.2 | 0.974884 | 2.22 | 0.975905 | 0.975513 |
| TILB13 | 40.45 | 13.5 | 13.04 | 50.0156 | 50.0107 | 2.2 | 0.974884 | 0.2 | 0.976746 | 0.975216 |
| TILB14 | 40.65 | 14.83 | 13.04 | 50.0147 | 50.01 | 2.2 | 0.974884 | 2.59 | 0.975455 | 0.975241 |
| TINP31 | 32.41 | 26.67 | 12.9 | 50.0134 | 50.0092 | 2.2 | 0.974884 | 0.2 | 0.975513 | 0.975103 |
| TINP32 | -0.2 | -6.89 | 0 | 50 | 50.0009 | 2.34 | 0.974807 | 0.2 | 0.975103 | 0.974847 |
| TORN41 | -44.4 | 44.31 | 0 | 50 | 49.9848 | 3.12 | 0.974833 | 2.42 | 0.975574 | 0.975231 |
| TOTN11 | 19.39 | 12.09 | 12.97 | 50.0077 | 50.0053 | 2.2 | 0.974884 | 0.2 | 0.975417 | 0.975038 |
| TOTT11 | 68.85 | 11.54 | 13.06 | 50.0275 | 50.0188 | 2.2 | 0.974884 | 2.61 | 0.975742 | 0.975412 |
| TOTT12 | 119.22 | 11.89 | 13.01 | 50.0512 | 50.035 | 2.2 | 0.974884 | 2.63 | 0.97631 | 0.975732 |
| TRAW11 | -26.28 | 14.9 | 0 | 50 | 49.9874 | 3.08 | 0.974766 | 2.27 | 0.974986 | 0.974895 |
| TREM31 | 53.44 | 12.95 | 13.12 | 50.0177 | 50.0121 | 2.2 | 0.974884 | 2.62 | 0.975632 | 0.975339 |
| TYNE11 | 170.55 | 60.38 | 12.73 | 50.1074 | 50.0733 | 2.2 | 0.974884 | 3.26 | 0.976402 | 0.975345 |
| TYNE51 | -2.87 | 8.74 | 0 | 50 | 49.9978 | 2.2 | 0.974884 | 0.2 | 0.975345 | 0.974953 |

*continued on next page*

*continued from previous page*

| Busbar Load Magnitudes | | | Frequency | | | Mean System Voltage | | | | |
|---|---|---|---|---|---|---|---|---|---|---|
| Busbar | Real | Reactive | Time | Max | Final | Time | Min | Time | Max | Final |
| UPPB11 | 113.59 | 97.72 | 13.68 | 50.0221 | 50.015 | 2.2 | 0.974884 | 2.49 | 0.976771 | 0.976129 |
| UPPB31 | 88.57 | 45.39 | 13.32 | 50.0239 | 50.0163 | 2.2 | 0.974884 | 2.57 | 0.97623 | 0.975749 |
| USKM11 | 182.48 | 139.2 | 13.86 | 50.0293 | 50.0199 | 2.2 | 0.974884 | 2.46 | 0.978058 | 0.977076 |
| USKM12 | 76.59 | 37.35 | 13.31 | 50.0181 | 50.0124 | 2.2 | 0.974884 | 0.2 | 0.977076 | 0.975711 |
| USKM31 | 3.47 | 4.93 | 0 | 50 | 50 | 2.2 | 0.974884 | 0.2 | 0.975711 | 0.974937 |
| WALP11 | 297.35 | 144.43 | 12.91 | 50.1632 | 50.1114 | 2.2 | 0.974884 | 2.63 | 0.97809 | 0.976892 |
| WALP12 | 297.36 | 151.23 | 12.93 | 50.159 | 50.1085 | 2.2 | 0.974884 | 2.6 | 0.978135 | 0.976923 |
| WARL11 | 184.24 | 65.53 | 13.18 | 50.066 | 50.045 | 2.2 | 0.974884 | 2.58 | 0.977437 | 0.976463 |
| WASF11 | 161.36 | 80.05 | 12.9 | 50.0806 | 50.055 | 2.2 | 0.974884 | 2.31 | 0.976072 | 0.975555 |
| WATFS11 | 138.57 | 63.65 | 13.26 | 50.0405 | 50.0277 | 2.2 | 0.974884 | 2.52 | 0.976934 | 0.97624 |
| WATFS12 | 52.83 | 13.07 | 13.08 | 50.0173 | 50.0118 | 2.2 | 0.974884 | 0.2 | 0.97624 | 0.975376 |
| WBOL61 | 212.69 | 86.13 | 12.74 | 50.1306 | 50.0891 | 2.2 | 0.974884 | 3.28 | 0.976755 | 0.975501 |
| WBUR11 | 181.02 | 80.5 | 12.88 | 50.102 | 50.0696 | 2.2 | 0.974884 | 3.74 | 0.976165 | 0.975542 |
| WFIE21 | 63 | 30.63 | 12.66 | 50.0525 | 50.0359 | 2.59 | 0.974649 | 3.22 | 0.975435 | 0.974875 |
| WHAM11 | 206.07 | 50.63 | 13.11 | 50.076 | 50.0519 | 2.2 | 0.974884 | 2.59 | 0.977713 | 0.976628 |
| WHGA11 | 232.19 | 145.3 | 13 | 50.0856 | 50.0584 | 2.2 | 0.974884 | 2.32 | 0.977474 | 0.976371 |
| WHSO31 | 67.63 | 34.99 | 13.37 | 50.016 | 50.0109 | 2.2 | 0.974884 | 2.56 | 0.975939 | 0.975598 |
| WHSO32 | 33.06 | 20.2 | 13.4 | 50.0072 | 50.0049 | 2.2 | 0.974884 | 0.2 | 0.975598 | 0.975243 |
| WIBA31 | 20.04 | 14.35 | 12.91 | 50.0083 | 50.0057 | 2.2 | 0.974884 | 0.2 | 0.976371 | 0.975025 |
| WIEN11 | 37.12 | -5.75 | 0 | 50 | 50.0154 | 2.2 | 0.974884 | 0.2 | 0.975542 | 0.974993 |
| WILL11 | 311.9 | 139.46 | 12.97 | 50.1459 | 50.0994 | 2.2 | 0.974884 | 2.62 | 0.97793 | 0.976825 |
| WILT61 | 102.76 | 83.32 | 12.78 | 50.0621 | 50.0424 | 2.2 | 0.974884 | 3.35 | 0.975834 | 0.975139 |
| WIMB11 | 48.68 | 24.21 | 14.02 | 50.0059 | 50.004 | 2.2 | 0.974884 | 0.2 | 0.976628 | 0.975489 |
| WIMB12 | 147.25 | 70.2 | 14.18 | 50.0161 | 50.0109 | 2.2 | 0.974884 | 2.41 | 0.977475 | 0.976742 |
| WIMB13 | 339.55 | 228.68 | 15.67 | 50.018 | 50.0117 | 2.2 | 0.974884 | 2.38 | 0.981818 | 0.979793 |
| WISD11 | 194.86 | 66.88 | 13.3 | 50.0486 | 50.0332 | 2.2 | 0.974884 | 0.2 | 0.979793 | 0.976931 |
| WISD61 | 133.74 | 81.25 | 14.08 | 50.0155 | 50.0105 | 2.2 | 0.974884 | 2.43 | 0.977349 | 0.976617 |
| WISH21 | 138.24 | 12.87 | 12.69 | 50.0945 | 50.0646 | 2.56 | 0.97426 | 3.21 | 0.975785 | 0.974727 |
| WIYH21 | 80.82 | 46.96 | 12.69 | 50.0567 | 50.0387 | 0.2 | 0.974727 | 3.27 | 0.975514 | 0.974955 |
| WMEL11 | 199 | 93.52 | 12.91 | 50.0917 | 50.0626 | 2.2 | 0.974884 | 2.22 | 0.976614 | 0.975961 |
| WMEL12 | 289.96 | 127.53 | 12.93 | 50.1407 | 50.0959 | 2.2 | 0.974884 | 2.32 | 0.977139 | 0.976275 |
| WWEY11 | 126.26 | 20.63 | 13.14 | 50.0415 | 50.0283 | 2.2 | 0.974884 | 0.2 | 0.976617 | 0.975988 |
| WWEY12 | 125.61 | 20.36 | 13.15 | 50.0379 | 50.0259 | 2.2 | 0.974884 | 2.58 | 0.976662 | 0.976055 |
| WYLF11 | 332.88 | 137.19 | 12.74 | 50.1972 | 50.1344 | 2.2 | 0.974884 | 3.22 | 0.976899 | 0.975845 |
| WYMO11 | 232.26 | 140.36 | 13.17 | 50.076 | 50.0519 | 2.2 | 0.974884 | 2.48 | 0.978267 | 0.977041 |

Appendix E

# DOLSE State Vector Output Example

This appendix contains data concerning the power system state vector. The column entitled DOLSE contains the state vector obtained using the Dynamic On-Line State Estimator. These results are taken just after the tripping and dynamic auto-reclosure of the double circuit deemed to be the worst possible outage in terms of dynamic stability as calculated by the University of Bath's Dynamic Security Assessor. This network had been artificially destabilsed to give a worst-case condition for the DOLSE test.

| | Real System | | Metered | DOLSE | | Error | |
|---|---|---|---|---|---|---|---|
| Busbar | Vm | Va | Vm | Vm | Va | Vm | Va |
| ABHA1 | 0.998466 | -0.3462 | 1.001920 | 0.992992 | -0.3418 | -0.0055 | 0.0044 |
| ABHA4T | 1.002451 | -0.2984 | 0.992648 | 1.007073 | -0.2941 | 0.0046 | 0.0043 |
| ABHA4U | 1.000893 | -0.3015 | 0.983960 | 0.993486 | -0.2973 | -0.0074 | 0.0042 |
| ABTH1J | 0.998296 | -0.3770 | 1.007227 | 1.021614 | -0.3771 | 0.0233 | -0.0001 |
| ABTH1K | 0.998296 | -0.3771 | 1.015804 | 1.030422 | -0.3772 | 0.0321 | -0.0001 |
| ABTH2J | 1.004622 | -0.3433 | 0.985090 | 1.021645 | -0.3429 | 0.0170 | 0.0004 |
| ABTH2K | 1.003815 | -0.3413 | 1.022528 | 1.003184 | -0.3408 | -0.0006 | 0.0005 |
| ALDW2 | 0.995866 | -0.0017 | 0.989900 | 0.977463 | 0.0007 | -0.0184 | 0.0024 |
| ALDW3F | 0.998955 | -0.0017 | 0.982281 | 0.977500 | 0.0007 | -0.0215 | 0.0024 |
| ALDW3G | 0.998954 | -0.0075 | 1.009070 | 0.982635 | -0.0054 | -0.0163 | 0.0021 |
| ALVE1 | 0.998528 | -0.3233 | 0.982729 | 0.985762 | -0.3200 | -0.0128 | 0.0033 |
| ALVE4T | 1.003559 | -0.2893 | 1.010046 | 0.995519 | -0.2855 | -0.0080 | 0.0038 |
| ALVE4U | 1.003942 | -0.2888 | 1.007247 | 0.985461 | -0.2849 | -0.0185 | 0.0039 |
| AMEM1 | 0.997927 | -0.2520 | 1.006337 | 0.987091 | -0.2494 | -0.0108 | 0.0026 |
| AMEM4T | 1.002491 | -0.2268 | 0.986313 | 0.993189 | -0.2248 | -0.0093 | 0.0020 |
| AMEM4U | 1.003775 | -0.2329 | 0.986495 | 0.991075 | -0.2309 | -0.0127 | 0.0020 |
| AXMI1 | 0.998420 | -0.3262 | 0.988327 | 0.994172 | -0.3205 | -0.0042 | 0.0057 |
| AXMI4 | 1.001783 | -0.2963 | 0.983239 | 1.005842 | -0.2923 | 0.0041 | 0.0040 |
| AYRR2Q | 1.015290 | 0.4243 | 1.026541 | 0.981835 | 0.4152 | -0.0335 | -0.0091 |
| AYRR2R | 1.015288 | 0.4243 | 1.011686 | 0.991404 | 0.4152 | -0.0239 | -0.0091 |

*continued on next page*

*continued from previous page*

| | Real System | | Metered | DOLSE | | Error | |
|---|---|---|---|---|---|---|---|
| Busbar | Vm | Va | Vm | Vm | Va | Vm | Va |
| AYRR3 | 0.999154 | 0.4044 | 1.004758 | 0.988203 | 0.3960 | -0.0110 | -0.0084 |
| BALL2 | 1.016990 | 0.4242 | 1.031390 | 0.976363 | 0.4151 | -0.0406 | -0.0091 |
| BARK1J | 0.997900 | -0.2683 | 1.001299 | 0.994895 | -0.2660 | -0.0030 | 0.0023 |
| BARK1K | 0.997901 | -0.2683 | 0.978754 | 0.979711 | -0.2652 | -0.0182 | 0.0031 |
| BARK2J | 1.004910 | -0.2370 | 1.009429 | 1.008953 | -0.2340 | 0.0040 | 0.0030 |
| BARK2K | 1.004462 | -0.2369 | 0.985058 | 1.001485 | -0.2342 | -0.0030 | 0.0027 |
| BARK2Q | 1.004914 | -0.2370 | 1.020308 | 1.026467 | -0.2340 | 0.0216 | 0.0030 |
| BARK2R | 1.004466 | -0.2369 | 0.990646 | 0.993876 | -0.2342 | -0.0106 | 0.0027 |
| BARK3J | 0.997900 | -0.3014 | 1.008459 | 1.005612 | -0.2987 | 0.0077 | 0.0027 |
| BARK3K | 0.997900 | -0.2965 | 0.981238 | 0.992900 | -0.2927 | -0.0050 | 0.0038 |
| BARK3L | 0.997900 | -0.2936 | 1.003910 | 1.016080 | -0.2911 | 0.0182 | 0.0025 |
| BARK4 | 0.999225 | -0.2372 | 0.987571 | 0.986105 | -0.2346 | -0.0131 | 0.0026 |
| BEAU1J | 1.000137 | 0.5859 | 0.998770 | 0.996930 | 0.5911 | -0.0032 | 0.0052 |
| BEAU1K | 1.000134 | 0.5855 | 0.985715 | 0.996169 | 0.5899 | -0.0040 | 0.0044 |
| BEAU1X | 1.000136 | 0.5859 | 0.996520 | 1.001095 | 0.5911 | 0.0010 | 0.0052 |
| BEAU1Y | 1.000134 | 0.5855 | 1.001959 | 0.993704 | 0.5899 | -0.0064 | 0.0044 |
| BEAU2 | 0.998096 | 0.6399 | 1.011689 | 0.991689 | 0.6456 | -0.0064 | 0.0057 |
| BEAU81 | 0.999998 | 0.6588 | 1.007202 | 0.993498 | 0.6656 | -0.0065 | 0.0068 |
| BEAU82 | 0.999997 | 0.6584 | 0.985058 | 0.982272 | 0.6659 | -0.0177 | 0.0075 |
| BEDD1J | 0.998096 | -0.3362 | 0.996518 | 0.980009 | -0.3339 | -0.0181 | 0.0023 |
| BEDD1K | 0.998096 | -0.3299 | 1.007358 | 0.997622 | -0.3287 | -0.0005 | 0.0012 |
| BEDD1L | 0.998099 | -0.3271 | 1.016834 | 0.969143 | -0.3251 | -0.0290 | 0.0020 |
| BEDD1M | 0.998101 | -0.3259 | 0.994463 | 0.974475 | -0.3238 | -0.0236 | 0.0021 |
| BEDD2J | 0.999209 | -0.2889 | 1.018166 | 0.981575 | -0.2869 | -0.0176 | 0.0020 |
| BEDD2K | 1.003599 | -0.2917 | 1.018162 | 1.001342 | -0.2895 | -0.0023 | 0.0022 |
| BEDD4Q | 1.008052 | -0.2457 | 1.013630 | 0.987681 | -0.2422 | -0.0204 | 0.0035 |
| BESW1 | 0.998327 | -0.2772 | 1.005139 | 1.004130 | -0.2770 | 0.0058 | 0.0002 |
| BESW2 | 1.000739 | -0.2352 | 1.010214 | 1.011084 | -0.2336 | 0.0103 | 0.0016 |
| BIRK1J | 0.998180 | -0.1190 | 1.000242 | 0.968704 | -0.1176 | -0.0295 | 0.0014 |
| BIRK2 | 1.014895 | -0.0978 | 1.028820 | 0.980190 | -0.0967 | -0.0347 | 0.0011 |
| BISW1 | 0.998349 | -0.2902 | 0.988508 | 0.996105 | -0.2900 | -0.0022 | 0.0002 |
| BISW2 | 0.998825 | -0.2401 | 0.984979 | 1.001663 | -0.2381 | 0.0028 | 0.0020 |
| BLHI2 | 0.999810 | 0.6758 | 1.006414 | 0.996705 | 0.6820 | -0.0031 | 0.0062 |
| BLYT1 | 1.001427 | 0.3497 | 0.993983 | 0.996569 | 0.3408 | -0.0049 | -0.0089 |
| BLYT2J | 1.001496 | 0.3109 | 0.979528 | 1.008904 | 0.3047 | 0.0074 | -0.0062 |
| BLYT2K | 1.001003 | 0.3064 | 0.978086 | 1.014361 | 0.3003 | 0.0134 | -0.0061 |
| BLYT6 | 1.001436 | 0.2736 | 0.996557 | 1.026383 | 0.2686 | 0.0249 | -0.0050 |
| BOLN1J | 0.998443 | -0.3117 | 0.984188 | 1.004928 | -0.3098 | 0.0065 | 0.0019 |
| BOLN1K | 0.998437 | -0.3184 | 0.993789 | 0.981751 | -0.3142 | -0.0167 | 0.0042 |
| BOLN1L | 0.998460 | -0.2995 | 0.989326 | 0.996602 | -0.2974 | -0.0019 | 0.0021 |
| BOLN1M | 0.998436 | -0.3185 | 0.989120 | 0.978403 | -0.3152 | -0.0200 | 0.0033 |
| BOLN4 | 0.993095 | -0.2429 | 0.984785 | 0.985027 | -0.2401 | -0.0081 | 0.0028 |
| BONB1Q | 0.999743 | 0.4671 | 1.008723 | 0.994409 | 0.4600 | -0.0053 | -0.0071 |
| BONB1R | 0.999354 | 0.4704 | 0.996249 | 0.987598 | 0.4639 | -0.0118 | -0.0065 |
| BONN1 | 0.999410 | 0.4617 | 0.982308 | 0.992740 | 0.4536 | -0.0067 | -0.0081 |
| BONN2 | 1.002199 | 0.5020 | 0.984945 | 1.004046 | 0.4954 | 0.0018 | -0.0066 |
| BOTW1 | 0.998327 | -0.3183 | 0.997303 | 1.000350 | -0.3165 | 0.0020 | 0.0018 |
| BOTW4 | 1.001754 | -0.2899 | 1.008736 | 0.998690 | -0.2874 | -0.0031 | 0.0025 |
| BRAE1 | 1.001860 | 0.4047 | 1.007135 | 1.011166 | 0.3932 | 0.0093 | -0.0115 |

*continued on next page*

*continued from previous page*

| | Real System | | Metered | DOLSE | | Error | |
|---|---|---|---|---|---|---|---|
| Busbar | Vm | Va | Vm | Vm | Va | Vm | Va |
| BRAI1 | 0.998112 | -0.2223 | 0.999998 | 0.997057 | -0.2200 | -0.0011 | 0.0023 |
| BRAI4T | 0.996221 | -0.1530 | 0.992059 | 0.995745 | -0.1496 | -0.0005 | 0.0034 |
| BRAW1J | 0.999000 | -0.0887 | 0.985963 | 0.952481 | -0.0833 | -0.0465 | 0.0054 |
| BRAW1K | 0.999000 | -0.0899 | 1.006040 | 0.970703 | -0.0859 | -0.0283 | 0.0040 |
| BRAW2 | 0.991283 | -0.0500 | 0.989661 | 0.960263 | -0.0468 | -0.0310 | 0.0032 |
| BRAW4Q | 0.994872 | -0.0190 | 1.008682 | 0.982916 | -0.0168 | -0.0120 | 0.0022 |
| BRED1 | 0.998713 | -0.0907 | 0.983942 | 0.980097 | -0.0908 | -0.0186 | -0.0001 |
| BRED2 | 1.000477 | -0.0607 | 0.988432 | 0.976525 | -0.0597 | -0.0240 | 0.0010 |
| BRFO1 | 0.998292 | -0.1620 | 0.983726 | 0.994883 | -0.1580 | -0.0034 | 0.0040 |
| BRFO4 | 0.994353 | -0.0984 | 1.009825 | 0.985738 | -0.0947 | -0.0086 | 0.0037 |
| BRIG1 | 1.026435 | 0.1458 | 1.029077 | 1.022388 | 0.1563 | -0.0040 | 0.0105 |
| BRIM1 | 0.997779 | -0.2779 | 1.005439 | 0.994504 | -0.2763 | -0.0033 | 0.0016 |
| BRIM1Y | 0.997811 | -0.2198 | 0.980689 | 1.009422 | -0.2163 | 0.0116 | 0.0035 |
| BRIM1Z | 0.997811 | -0.2198 | 1.010875 | 0.996640 | -0.2170 | -0.0012 | 0.0028 |
| BRIM2S | 1.003278 | -0.2198 | 1.014474 | 0.999140 | -0.2163 | -0.0041 | 0.0035 |
| BRIM2T | 1.003856 | -0.2209 | 1.004194 | 1.007311 | -0.2181 | 0.0035 | 0.0028 |
| BRIM2U | 1.003416 | -0.2198 | 0.994053 | 1.005259 | -0.2170 | 0.0018 | 0.0028 |
| BRIM2V | 1.003589 | -0.2210 | 1.008401 | 1.001160 | -0.2178 | -0.0024 | 0.0032 |
| BRIN2J | 1.001788 | -0.0125 | 0.992601 | 0.989185 | -0.0097 | -0.0126 | 0.0028 |
| BRIN2K | 0.996163 | -0.0072 | 1.007368 | 0.982828 | -0.0048 | -0.0133 | 0.0024 |
| BRIN4T | 0.998443 | 0.0379 | 1.005758 | 0.969163 | 0.0411 | -0.0293 | 0.0032 |
| BRLE1J | 0.998196 | -0.3439 | 0.995321 | 1.004247 | -0.3449 | 0.0061 | -0.0010 |
| BRLE1K | 0.998198 | -0.3439 | 0.982589 | 0.988960 | -0.3444 | -0.0092 | -0.0005 |
| BRLE1L | 0.998195 | -0.3172 | 1.006073 | 1.001901 | -0.3171 | 0.0037 | 0.0001 |
| BRLE1M | 0.998195 | -0.3172 | 1.002296 | 0.980994 | -0.3146 | -0.0172 | 0.0026 |
| BRLE4 | 1.004394 | -0.2817 | 1.003078 | 0.997754 | -0.2798 | -0.0066 | 0.0019 |
| BRWA1 | 0.998689 | -0.2903 | 0.992760 | 0.982188 | -0.2872 | -0.0165 | 0.0031 |
| BRWA2Q | 0.997925 | -0.2478 | 1.010186 | 0.981961 | -0.2445 | -0.0160 | 0.0033 |
| BRWA2R | 0.997902 | -0.2477 | 0.983429 | 0.988663 | -0.2440 | -0.0092 | 0.0037 |
| BRWE1J | 1.032932 | -0.1099 | 1.051399 | 1.028634 | -0.0980 | -0.0043 | 0.0119 |
| BRWE1K | 0.998070 | -0.1936 | 0.989229 | 0.958563 | -0.1887 | -0.0395 | 0.0049 |
| BURW1 | 0.997629 | -0.1919 | 0.984851 | 1.004517 | -0.1905 | 0.0069 | 0.0014 |
| BURW4 | 0.991138 | -0.1318 | 1.003245 | 1.004748 | -0.1294 | 0.0136 | 0.0024 |
| BUSB2 | 1.008557 | 0.4440 | 1.027986 | 0.998095 | 0.4352 | -0.0105 | -0.0088 |
| BUSH1 | 0.998313 | -0.2551 | 0.999134 | 0.988270 | -0.2529 | -0.0100 | 0.0022 |
| BUSH2 | 1.003550 | -0.2286 | 1.007449 | 0.990514 | -0.2265 | -0.0130 | 0.0021 |
| BUST1 | 0.998303 | -0.2753 | 0.979207 | 0.982573 | -0.2741 | -0.0157 | 0.0012 |
| BUST1Z | 0.998312 | -0.2272 | 1.009818 | 0.977371 | -0.2252 | -0.0209 | 0.0020 |
| BUST2 | 1.010001 | -0.2272 | 0.995545 | 1.007982 | -0.2252 | -0.0020 | 0.0020 |
| CALD1 | 1.028051 | 0.3106 | 1.006854 | 1.009037 | 0.3058 | -0.0190 | -0.0048 |
| CANT1J | 1.028279 | -0.2041 | 1.026814 | 1.021743 | -0.2014 | -0.0065 | 0.0027 |
| CANT1K | 1.028282 | -0.2024 | 1.039372 | 1.010969 | -0.1971 | -0.0173 | 0.0053 |
| CANT4 | 0.996833 | -0.1700 | 0.980586 | 0.984162 | -0.1663 | -0.0127 | 0.0037 |
| CAPE1J | 0.998190 | -0.1349 | 0.980243 | 0.971532 | -0.1352 | -0.0267 | -0.0003 |
| CAPE1K | 0.998190 | -0.1042 | 1.004130 | 0.962093 | -0.1029 | -0.0361 | 0.0013 |
| CAPE2J | 1.009406 | -0.1013 | 1.009205 | 0.979217 | -0.1001 | -0.0302 | 0.0012 |
| CAPE2K | 1.005385 | -0.0814 | 0.996353 | 0.998824 | -0.0809 | -0.0066 | 0.0005 |
| CAPE2Q | 1.012552 | -0.0929 | 1.014399 | 1.001091 | -0.0923 | -0.0115 | 0.0006 |
| CAPE2R | 1.004959 | -0.0942 | 1.012124 | 0.982216 | -0.0928 | -0.0227 | 0.0014 |

*continued on next page*

*continued from previous page*

| | Real System | | Metered | DOLSE | | Error | |
|---|---|---|---|---|---|---|---|
| Busbar | Vm | Va | Vm | Vm | Va | Vm | Va |
| CAPE2Z | 1.004871 | -0.0813 | 0.993360 | 0.986741 | -0.0807 | -0.0181 | 0.0006 |
| CAPE4T | 1.004907 | -0.0813 | 1.004792 | 0.993589 | -0.0807 | -0.0113 | 0.0006 |
| CAPE4U | 1.004248 | -0.0814 | 1.011230 | 0.993635 | -0.0809 | -0.0106 | 0.0005 |
| CARE1 | 0.998296 | -0.3766 | 0.995147 | 1.022947 | -0.3766 | 0.0247 | 0.0000 |
| CARE2 | 1.008837 | -0.3446 | 1.007256 | 1.026420 | -0.3442 | 0.0176 | 0.0004 |
| CARR1J | 0.998416 | -0.1107 | 0.979814 | 0.975316 | -0.1088 | -0.0231 | 0.0019 |
| CARR1K | 0.998541 | -0.0910 | 1.003821 | 0.964986 | -0.0894 | -0.0336 | 0.0016 |
| CARR1L | 0.998475 | -0.0850 | 0.988456 | 0.971776 | -0.0846 | -0.0267 | 0.0004 |
| CARR2J | 0.999921 | -0.0651 | 1.017820 | 0.980798 | -0.0644 | -0.0191 | 0.0007 |
| CARR2K | 0.996072 | -0.0702 | 0.990140 | 0.967702 | -0.0693 | -0.0284 | 0.0009 |
| CARR4Q | 0.998564 | -0.0581 | 0.982593 | 0.986866 | -0.0575 | -0.0117 | 0.0006 |
| CARR4R | 0.998457 | -0.0582 | 1.010124 | 0.976043 | -0.0576 | -0.0224 | 0.0006 |
| CASD1 | 0.998208 | -0.2159 | 0.988652 | 0.999764 | -0.2139 | 0.0016 | 0.0020 |
| CASD2 | 0.998910 | -0.1938 | 1.011927 | 1.000264 | -0.1913 | 0.0014 | 0.0025 |
| CELL1 | 0.998544 | -0.1939 | 1.001635 | 0.998676 | -0.1933 | 0.0001 | 0.0006 |
| CELL4 | 0.996667 | -0.1239 | 1.007379 | 0.992925 | -0.1220 | -0.0037 | 0.0019 |
| CHAP1 | 1.004496 | 0.4225 | 1.008444 | 0.994650 | 0.4287 | -0.0098 | 0.0062 |
| CHAP81 | 0.999688 | 0.5209 | 1.000978 | 0.985265 | 0.5299 | -0.0144 | 0.0090 |
| CHIC1 | 0.998381 | -0.3151 | 0.984696 | 1.020797 | -0.3121 | 0.0224 | 0.0030 |
| CHIC4 | 0.998862 | -0.2983 | 0.994835 | 1.012113 | -0.2948 | 0.0133 | 0.0035 |
| CHSI1 | 0.998100 | -0.3253 | 1.007012 | 0.984934 | -0.3225 | -0.0132 | 0.0028 |
| CHSI1J | 0.998101 | -0.3304 | 0.989191 | 0.999846 | -0.3276 | 0.0017 | 0.0028 |
| CHSI1K | 0.998101 | -0.3306 | 1.018660 | 1.006080 | -0.3307 | 0.0080 | -0.0001 |
| CHSI2 | 1.001485 | -0.2924 | 0.985298 | 0.996377 | -0.2903 | -0.0051 | 0.0021 |
| CHTE1J | 0.998701 | -0.0687 | 0.978804 | 0.975111 | -0.0680 | -0.0236 | 0.0007 |
| CHTE1K | 0.998702 | -0.0677 | 1.004139 | 0.980363 | -0.0654 | -0.0183 | 0.0023 |
| CHTE2 | 0.996171 | -0.0219 | 1.011293 | 0.968529 | -0.0197 | -0.0276 | 0.0022 |
| CILF2Q | 1.000502 | -0.3320 | 0.989770 | 1.007110 | -0.3311 | 0.0066 | 0.0009 |
| CILF2R | 1.001490 | -0.3322 | 0.998372 | 0.996262 | -0.3318 | -0.0052 | 0.0004 |
| CILF4 | 1.008116 | -0.3152 | 1.005480 | 1.007176 | -0.3137 | -0.0009 | 0.0015 |
| CITR1J | 0.998016 | -0.2726 | 1.013187 | 0.996696 | -0.2709 | -0.0013 | 0.0017 |
| CITR1K | 0.998014 | -0.2946 | 1.004286 | 0.995228 | -0.2931 | -0.0028 | 0.0015 |
| CITR4 | 0.999790 | -0.2429 | 0.982484 | 1.001088 | -0.2402 | 0.0013 | 0.0027 |
| CLYM1 | 0.999145 | 0.4287 | 1.011764 | 1.001606 | 0.4222 | 0.0025 | -0.0065 |
| CLYM2 | 1.006438 | 0.4551 | 1.024215 | 1.004193 | 0.4475 | -0.0022 | -0.0076 |
| COAL2Q | 1.004439 | 0.4172 | 1.004032 | 1.009434 | 0.4098 | 0.0050 | -0.0074 |
| COAL2R | 1.002370 | 0.3958 | 0.994240 | 1.018030 | 0.3890 | 0.0157 | -0.0068 |
| COCK2 | 1.005996 | 0.4607 | 0.996483 | 1.012144 | 0.4518 | 0.0061 | -0.0089 |
| COCK4Q | 1.006401 | 0.4564 | 1.014919 | 1.015144 | 0.4465 | 0.0087 | -0.0099 |
| COCK4R | 1.006401 | 0.4564 | 1.017567 | 1.024670 | 0.4477 | 0.0183 | -0.0087 |
| CONQ1 | 0.998059 | -0.1077 | 0.985892 | 1.015522 | -0.1076 | 0.0175 | 0.0001 |
| COTT4 | 0.996226 | -0.0337 | 0.983420 | 1.002951 | -0.0293 | 0.0067 | 0.0044 |
| COVE1 | 0.998314 | -0.2894 | 1.002009 | 1.004928 | -0.2870 | 0.0066 | 0.0024 |
| COVE1Z | 0.998316 | -0.2333 | 1.005003 | 1.017784 | -0.2316 | 0.0195 | 0.0017 |
| COVE2 | 0.999425 | -0.2333 | 1.000337 | 1.003069 | -0.2316 | 0.0036 | 0.0017 |
| COWB2 | 1.004813 | -0.3440 | 0.998175 | 1.017138 | -0.3435 | 0.0123 | 0.0005 |
| COWL1J | 0.998041 | -0.2773 | 0.979243 | 1.011268 | -0.2753 | 0.0132 | 0.0020 |
| COWL1K | 0.998041 | -0.3069 | 0.994304 | 0.987784 | -0.3024 | -0.0103 | 0.0045 |
| COWL4 | 1.001699 | -0.2482 | 1.019751 | 1.000692 | -0.2456 | -0.0010 | 0.0026 |

*continued on next page*

*continued from previous page*

| | Real System | | Metered | DOLSE | | Error | |
|---|---|---|---|---|---|---|---|
| Busbar | Vm | Va | Vm | Vm | Va | Vm | Va |
| COYL1 | 0.999392 | 0.3966 | 1.003067 | 0.985982 | 0.3931 | -0.0134 | -0.0035 |
| COYL2 | 1.015371 | 0.4246 | 1.011317 | 0.984517 | 0.4155 | -0.0309 | -0.0091 |
| COYL3 | 1.001568 | 0.3756 | 1.010871 | 0.986039 | 0.3722 | -0.0155 | -0.0034 |
| COYT1T | 0.999305 | 0.3972 | 1.008538 | 0.974466 | 0.3932 | -0.0248 | -0.0040 |
| COYW2S | 1.015355 | 0.4247 | 1.034014 | 0.993595 | 0.4156 | -0.0218 | -0.0091 |
| COYW2T | 1.015354 | 0.4247 | 0.996616 | 1.002804 | 0.4156 | -0.0126 | -0.0091 |
| CRAI1 | 0.996349 | 0.6130 | 1.009718 | 0.976561 | 0.6191 | -0.0198 | 0.0061 |
| CREB1J | 0.998424 | 0.0533 | 0.977699 | 0.996367 | 0.0578 | -0.0021 | 0.0045 |
| CREB1K | 0.998424 | 0.0270 | 0.995680 | 0.995169 | 0.0326 | -0.0033 | 0.0056 |
| CREB4 | 0.997020 | 0.0836 | 0.997056 | 0.996905 | 0.0881 | -0.0001 | 0.0045 |
| CRUA2Q | 1.014790 | 0.4682 | 0.999347 | 1.017349 | 0.4591 | 0.0026 | -0.0091 |
| CRUA2R | 1.014790 | 0.4682 | 1.011808 | 1.018392 | 0.4591 | 0.0036 | -0.0091 |
| CULH3 | 1.002628 | -0.2535 | 1.022736 | 0.996516 | -0.2510 | -0.0061 | 0.0025 |
| CULH4 | 1.002628 | -0.2535 | 1.003976 | 0.995610 | -0.2510 | -0.0070 | 0.0025 |
| CULH4T | 1.002628 | -0.2535 | 1.020406 | 0.988984 | -0.2510 | -0.0136 | 0.0025 |
| CUPA1Q | 0.995739 | 0.5090 | 0.989747 | 0.969647 | 0.5040 | -0.0261 | -0.0050 |
| CUPA1R | 0.995743 | 0.5090 | 0.996389 | 0.958367 | 0.5036 | -0.0374 | -0.0054 |
| CUPA3 | 0.999335 | 0.4856 | 1.015386 | 0.972808 | 0.4806 | -0.0265 | -0.0050 |
| CURR1 | 0.999460 | 0.4356 | 0.998266 | 0.993495 | 0.4258 | -0.0060 | -0.0098 |
| CURR2 | 1.005677 | 0.4677 | 1.004764 | 1.002230 | 0.4591 | -0.0034 | -0.0086 |
| DAIN2Q | 1.000721 | -0.0631 | 1.001604 | 0.984068 | -0.0625 | -0.0167 | 0.0006 |
| DAIN4 | 0.998545 | -0.0579 | 0.990687 | 0.995682 | -0.0574 | -0.0029 | 0.0005 |
| DALL2 | 1.014714 | 0.4683 | 1.012915 | 1.012635 | 0.4591 | -0.0021 | -0.0092 |
| DALM1 | 0.999129 | 0.4297 | 0.998474 | 0.991487 | 0.4232 | -0.0076 | -0.0065 |
| DALM2Q | 1.006487 | 0.4546 | 0.991765 | 1.019944 | 0.4470 | 0.0135 | -0.0076 |
| DALM2R | 1.006493 | 0.4546 | 1.008621 | 0.986982 | 0.4469 | -0.0195 | -0.0077 |
| DEES4 | 1.004025 | -0.0799 | 1.020312 | 1.010034 | -0.0795 | 0.0060 | 0.0004 |
| DEES81 | 0.993836 | 0.0294 | 0.995790 | 1.015612 | 0.0262 | 0.0218 | -0.0032 |
| DEES82 | 0.993753 | 0.0371 | 0.996683 | 1.018343 | 0.0305 | 0.0246 | -0.0066 |
| DEVM1 | 0.999262 | 0.4217 | 1.001717 | 0.992615 | 0.4106 | -0.0066 | -0.0111 |
| DEVM4 | 1.016661 | 0.4480 | 1.005629 | 1.011276 | 0.4374 | -0.0054 | -0.0106 |
| DEVO1Q | 0.998688 | 0.4616 | 0.998943 | 0.974466 | 0.4545 | -0.0242 | -0.0071 |
| DEVO1R | 0.998659 | 0.4616 | 1.010545 | 1.004840 | 0.4551 | 0.0062 | -0.0065 |
| DEVO3 | 0.999385 | 0.4174 | 0.997701 | 1.002639 | 0.4099 | 0.0033 | -0.0075 |
| DIDC4J | 1.002080 | -0.2509 | 0.994770 | 0.994150 | -0.2482 | -0.0079 | 0.0027 |
| DIDC4K | 1.003395 | -0.2579 | 1.005886 | 0.984493 | -0.2555 | -0.0189 | 0.0024 |
| DINO4 | 1.010722 | -0.0703 | 1.010359 | 1.032241 | -0.0699 | 0.0215 | 0.0004 |
| DOUN1 | 1.000201 | 0.5797 | 0.998232 | 0.995867 | 0.5866 | -0.0043 | 0.0069 |
| DOUN2 | 0.969667 | 0.6143 | 0.988511 | 0.971243 | 0.6203 | 0.0016 | 0.0060 |
| DRAK1 | 0.998311 | -0.2317 | 1.000165 | 0.982178 | -0.2299 | -0.0161 | 0.0018 |
| DRAK2J | 1.004785 | -0.2062 | 1.013869 | 0.999874 | -0.2040 | -0.0049 | 0.0022 |
| DRAK2K | 1.002432 | -0.2035 | 1.013677 | 0.979409 | -0.2012 | -0.0230 | 0.0023 |
| DRAK2S | 0.998312 | -0.2062 | 0.994126 | 0.984837 | -0.2040 | -0.0135 | 0.0022 |
| DRAK4 | 0.999809 | -0.1752 | 0.981837 | 0.994017 | -0.1727 | -0.0058 | 0.0025 |
| DRAX1 | 0.999469 | 0.0540 | 1.010776 | 1.008216 | 0.0551 | 0.0087 | 0.0011 |
| DRAX4J | 0.999412 | 0.0786 | 0.984602 | 0.988759 | 0.0832 | -0.0107 | 0.0046 |
| DRAX4K | 0.999466 | 0.0908 | 1.017231 | 0.997257 | 0.0942 | -0.0022 | 0.0034 |
| DRAX4R | 0.999521 | 0.0975 | 0.987297 | 0.984206 | 0.1012 | -0.0153 | 0.0037 |
| DRAX81 | 1.000001 | 0.2017 | 0.983130 | 0.995948 | 0.2064 | -0.0041 | 0.0047 |

*continued on next page*

*continued from previous page*

| | Real System | | Metered | DOLSE | | Error | |
|---|---|---|---|---|---|---|---|
| Busbar | Vm | Va | Vm | Vm | Va | Vm | Va |
| DRAX82 | 0.999982 | 0.2151 | 1.000775 | 0.997189 | 0.2154 | -0.0028 | 0.0003 |
| DUBR4Q | 1.003153 | 0.0225 | 0.983967 | 0.977323 | 0.0256 | -0.0258 | 0.0031 |
| DUBR4R | 1.004650 | -0.0131 | 1.012428 | 1.004452 | -0.0112 | -0.0002 | 0.0019 |
| DUMF1 | 1.001173 | 0.4081 | 0.997274 | 0.982154 | 0.4134 | -0.0190 | 0.0053 |
| DUNF1 | 0.993644 | 0.4540 | 0.996868 | 0.985901 | 0.4469 | -0.0077 | -0.0071 |
| DUNG2 | 0.998694 | -0.1322 | 0.989113 | 1.000846 | -0.1280 | 0.0022 | 0.0042 |
| DUNG4 | 0.998571 | -0.1487 | 1.008279 | 0.994743 | -0.1449 | -0.0038 | 0.0038 |
| DUNG81 | 0.999352 | -0.0395 | 0.986594 | 0.995485 | -0.0355 | -0.0039 | 0.0040 |
| DUNG82 | 0.999383 | -0.0300 | 1.002502 | 1.007974 | -0.0267 | 0.0086 | 0.0033 |
| DUNO1Q | 0.993213 | 0.4298 | 0.995833 | 1.013594 | 0.4190 | 0.0204 | -0.0108 |
| DUNO1R | 0.993202 | 0.4298 | 0.973376 | 0.998046 | 0.4211 | 0.0048 | -0.0087 |
| DUNO3 | 0.999576 | 0.4216 | 1.004359 | 1.010032 | 0.4120 | 0.0105 | -0.0096 |
| EALI2 | 1.020419 | -0.2884 | 1.032188 | 1.026792 | -0.2870 | 0.0064 | 0.0014 |
| EALI6 | 0.998062 | -0.3226 | 1.010797 | 1.008677 | -0.3223 | 0.0106 | 0.0003 |
| EALI6Z | 0.998067 | -0.2884 | 0.994753 | 0.992752 | -0.2870 | -0.0053 | 0.0014 |
| EASO1 | 0.996984 | -0.1531 | 0.996013 | 0.982127 | -0.1507 | -0.0149 | 0.0024 |
| EASO4 | 0.996568 | -0.0923 | 1.005026 | 0.990104 | -0.0897 | -0.0065 | 0.0026 |
| EASO4Q | 0.996568 | -0.0923 | 0.999240 | 1.003824 | -0.0897 | 0.0073 | 0.0026 |
| EASO4R | 0.996446 | -0.1227 | 1.000704 | 0.978669 | -0.1202 | -0.0178 | 0.0025 |
| ECCL1 | 0.999718 | 0.4290 | 0.993660 | 0.992713 | 0.4205 | -0.0070 | -0.0085 |
| ECCL4 | 1.003945 | 0.4532 | 0.994847 | 1.016086 | 0.4434 | 0.0121 | -0.0098 |
| ECLA1 | 0.997906 | -0.2595 | 0.983576 | 1.004670 | -0.2577 | 0.0068 | 0.0018 |
| ECLA1Z | 0.997905 | -0.2134 | 1.011945 | 0.996935 | -0.2112 | -0.0010 | 0.0022 |
| ECLA4 | 1.000077 | -0.2134 | 0.984572 | 1.000287 | -0.2112 | 0.0002 | 0.0022 |
| EERH2 | 1.005745 | 0.4628 | 0.996681 | 1.011611 | 0.4554 | 0.0059 | -0.0074 |
| EGGB4J | 0.998796 | 0.0530 | 1.014052 | 0.981328 | 0.0568 | -0.0175 | 0.0038 |
| EGGB4K | 0.999811 | 0.0695 | 1.000930 | 0.989793 | 0.0726 | -0.0100 | 0.0031 |
| EKIS2 | 1.007705 | 0.4449 | 0.990053 | 1.025102 | 0.4365 | 0.0174 | -0.0084 |
| ELLA1J | 0.998995 | -0.0765 | 1.013689 | 0.970318 | -0.0743 | -0.0287 | 0.0022 |
| ELLA1K | 0.998994 | -0.0778 | 0.996056 | 0.969185 | -0.0739 | -0.0298 | 0.0039 |
| ELLA2 | 0.993030 | -0.0471 | 0.999636 | 0.958772 | -0.0441 | -0.0343 | 0.0030 |
| ELST1J | 0.997844 | -0.2468 | 0.982046 | 0.986128 | -0.2451 | -0.0117 | 0.0017 |
| ELST1K | 0.997850 | -0.2702 | 1.005490 | 0.992050 | -0.2689 | -0.0058 | 0.0013 |
| ELST1N | 0.997843 | -0.2511 | 1.011510 | 1.000788 | -0.2497 | 0.0029 | 0.0014 |
| ELST2J | 0.999517 | -0.2252 | 0.980708 | 0.986849 | -0.2229 | -0.0127 | 0.0023 |
| ELST2K | 1.000184 | -0.2325 | 1.008112 | 1.000347 | -0.2306 | 0.0002 | 0.0019 |
| ELST2S | 0.997312 | -0.1897 | 1.008831 | 0.976304 | -0.1876 | -0.0210 | 0.0021 |
| ELST4Q | 0.996843 | -0.1921 | 0.995630 | 1.006839 | -0.1900 | 0.0100 | 0.0021 |
| ELST4T | 0.996930 | -0.1897 | 0.992200 | 0.988974 | -0.1876 | -0.0080 | 0.0021 |
| ELVA2 | 0.999820 | 0.3628 | 0.983199 | 1.007535 | 0.3572 | 0.0077 | -0.0056 |
| ENDE1 | 0.998072 | -0.2336 | 0.981831 | 0.999282 | -0.2338 | 0.0012 | -0.0002 |
| ENDE4 | 0.998912 | -0.1803 | 0.998055 | 0.991255 | -0.1776 | -0.0077 | 0.0027 |
| ERRO1J | 0.997555 | 0.4852 | 0.993071 | 0.990806 | 0.4815 | -0.0067 | -0.0037 |
| ERRO1K | 0.996255 | 0.4993 | 0.999810 | 0.992573 | 0.4972 | -0.0037 | -0.0021 |
| ERRO81 | 0.999899 | 0.5648 | 0.981712 | 1.002756 | 0.5612 | 0.0029 | -0.0036 |
| ERRO82 | 0.999904 | 0.5788 | 0.985625 | 1.009502 | 0.5748 | 0.0096 | -0.0040 |
| ERSK1Q | 1.001792 | 0.4084 | 1.019940 | 0.996417 | 0.3966 | -0.0054 | -0.0118 |
| ERSK1R | 1.002166 | 0.4039 | 1.002368 | 1.029307 | 0.3930 | 0.0271 | -0.0109 |
| ERSK3 | 0.999293 | 0.3927 | 1.018955 | 1.014367 | 0.3815 | 0.0151 | -0.0112 |

*continued on next page*

*continued from previous page*

| Busbar | Real System Vm | Real System Va | Metered Vm | DOLSE Vm | DOLSE Va | Error Vm | Error Va |
|---|---|---|---|---|---|---|---|
| EXET1 | 0.998456 | -0.3446 | 0.988901 | 0.998119 | -0.3401 | -0.0003 | 0.0045 |
| EXET4 | 1.001295 | -0.2897 | 0.999699 | 1.003751 | -0.2857 | 0.0025 | 0.0040 |
| FASN1 | 0.997786 | 0.5664 | 0.979234 | 0.990811 | 0.5695 | -0.0070 | 0.0031 |
| FASN81 | 0.999981 | 0.6726 | 0.982118 | 0.998875 | 0.6763 | -0.0011 | 0.0037 |
| FAUG1 | 0.993596 | 0.5434 | 1.005913 | 0.981408 | 0.5447 | -0.0122 | 0.0013 |
| FAUG81 | 0.999970 | 0.6362 | 0.998829 | 1.001263 | 0.6371 | 0.0013 | 0.0009 |
| FAWL1 | 0.998328 | -0.3360 | 1.007080 | 1.002383 | -0.3336 | 0.0041 | 0.0024 |
| FAWL4 | 1.002388 | -0.2916 | 0.987564 | 1.002073 | -0.2890 | -0.0003 | 0.0026 |
| FECK2 | 0.999251 | -0.2408 | 0.980379 | 1.009547 | -0.2387 | 0.0103 | 0.0021 |
| FECK4 | 1.004985 | -0.2324 | 1.004434 | 1.008384 | -0.2307 | 0.0034 | 0.0017 |
| FECK6 | 0.998433 | -0.2936 | 1.009109 | 1.017109 | -0.2915 | 0.0187 | 0.0021 |
| FERR1J | 0.999169 | -0.0033 | 0.993891 | 0.973988 | -0.0002 | -0.0252 | 0.0031 |
| FERR1K | 0.999185 | -0.0058 | 1.003793 | 0.968861 | -0.0013 | -0.0303 | 0.0045 |
| FERR2J | 0.999611 | 0.0221 | 0.979549 | 0.978802 | 0.0251 | -0.0208 | 0.0030 |
| FERR2K | 0.998605 | 0.0089 | 0.993652 | 0.967473 | 0.0126 | -0.0311 | 0.0037 |
| FERR4T | 0.998479 | 0.0445 | 1.011405 | 0.965838 | 0.0480 | -0.0326 | 0.0035 |
| FERR6 | 0.999193 | -0.0146 | 0.992167 | 0.972808 | -0.0103 | -0.0264 | 0.0043 |
| FFES2Q | 1.016513 | -0.0934 | 1.032759 | 1.010902 | -0.0927 | -0.0056 | 0.0007 |
| FFES2R | 1.016527 | -0.0934 | 0.997456 | 1.022776 | -0.0927 | 0.0062 | 0.0007 |
| FIDF1J | 0.998219 | -0.0974 | 0.979774 | 0.964618 | -0.0960 | -0.0336 | 0.0014 |
| FIDF1K | 0.998247 | -0.0904 | 1.001606 | 0.971246 | -0.0889 | -0.0270 | 0.0015 |
| FIDF1L | 0.998330 | -0.1247 | 1.013100 | 0.968253 | -0.1244 | -0.0301 | 0.0003 |
| FIDF1M | 0.998286 | -0.1284 | 1.008825 | 0.970311 | -0.1275 | -0.0280 | 0.0009 |
| FIDF2J | 1.004749 | -0.0980 | 1.009239 | 0.977732 | -0.0966 | -0.0270 | 0.0014 |
| FIDF2K | 1.006061 | -0.0899 | 0.988374 | 0.967593 | -0.0884 | -0.0385 | 0.0015 |
| FIDF2L | 1.004739 | -0.0979 | 1.024201 | 0.972137 | -0.0964 | -0.0326 | 0.0015 |
| FIDF2M | 1.005983 | -0.0898 | 1.016482 | 0.979547 | -0.0884 | -0.0264 | 0.0014 |
| FLEE1J | 0.998234 | -0.3544 | 0.990680 | 0.993757 | -0.3502 | -0.0045 | 0.0042 |
| FLEE1K | 0.998234 | -0.3542 | 1.002498 | 0.994189 | -0.3514 | -0.0040 | 0.0028 |
| FLEE1L | 0.998234 | -0.3525 | 1.011409 | 0.985232 | -0.3486 | -0.0130 | 0.0039 |
| FLEE1M | 0.998234 | -0.3520 | 0.994784 | 0.982842 | -0.3493 | -0.0154 | 0.0027 |
| FLEE1Y | 0.998235 | -0.2861 | 0.979028 | 0.993960 | -0.2840 | -0.0043 | 0.0021 |
| FLEE1Z | 0.998235 | -0.2861 | 0.980860 | 1.004848 | -0.2840 | 0.0066 | 0.0021 |
| FLEE4 | 1.002932 | -0.2861 | 1.021110 | 1.001835 | -0.2840 | -0.0011 | 0.0021 |
| FORD4Q | 1.003015 | 0.0214 | 1.020559 | 0.971542 | 0.0245 | -0.0315 | 0.0031 |
| FORD4R | 1.004447 | -0.0153 | 0.993850 | 1.007347 | -0.0134 | 0.0029 | 0.0019 |
| FOYE2 | 1.000907 | 0.6496 | 1.001312 | 1.003647 | 0.6554 | 0.0027 | 0.0058 |
| FROD1J | 0.998200 | -0.1298 | 0.991284 | 0.968628 | -0.1284 | -0.0296 | 0.0014 |
| FROD1K | 0.998197 | -0.1296 | 0.987439 | 0.961732 | -0.1290 | -0.0365 | 0.0006 |
| FROD2 | 1.004837 | -0.0994 | 0.993729 | 0.971076 | -0.0980 | -0.0338 | 0.0014 |
| GALA1 | 0.998888 | 0.4199 | 1.000373 | 0.994572 | 0.4149 | -0.0043 | -0.0050 |
| GARB1Q | 0.995106 | 0.4327 | 1.010412 | 0.986782 | 0.4230 | -0.0083 | -0.0097 |
| GARB1R | 0.994586 | 0.4333 | 0.977933 | 0.981005 | 0.4235 | -0.0136 | -0.0098 |
| GARB1S | 0.994467 | 0.4325 | 1.005964 | 0.999119 | 0.4224 | 0.0047 | -0.0101 |
| GARB1T | 0.994450 | 0.4325 | 0.994474 | 1.011608 | 0.4233 | 0.0172 | -0.0092 |
| GARE1S | 0.994555 | 0.4317 | 1.005859 | 0.997464 | 0.4213 | 0.0029 | -0.0104 |
| GARE1T | 0.994534 | 0.4317 | 1.007026 | 0.994835 | 0.4225 | 0.0003 | -0.0092 |
| GLLE1 | 0.999409 | 0.3900 | 1.004109 | 1.016736 | 0.3902 | 0.0173 | 0.0002 |
| GLLE81 | 0.999847 | 0.5553 | 1.002487 | 0.987364 | 0.5584 | -0.0125 | 0.0031 |

*continued on next page*

*continued from previous page*

| | Real System | | Metered | DOLSE | | Error | |
|---|---|---|---|---|---|---|---|
| Busbar | Vm | Va | Vm | Vm | Va | Vm | Va |
| GLNI1 | 0.999175 | 0.5108 | 0.983112 | 1.013145 | 0.5048 | 0.0140 | -0.0060 |
| GLRB2 | 0.995643 | 0.5491 | 0.998342 | 0.991561 | 0.5459 | -0.0041 | -0.0032 |
| GLRO2 | 0.996203 | 0.5419 | 1.010505 | 0.990695 | 0.5379 | -0.0055 | -0.0040 |
| GRAI4J | 0.997705 | -0.2001 | 0.989648 | 0.992198 | -0.1968 | -0.0055 | 0.0033 |
| GRAI4K | 0.996531 | -0.2099 | 0.986503 | 0.987635 | -0.2072 | -0.0089 | 0.0027 |
| GREN1 | 0.997620 | -0.1076 | 0.989105 | 0.996293 | -0.1055 | -0.0013 | 0.0021 |
| GREN4 | 0.997706 | -0.1375 | 0.983854 | 0.990505 | -0.1351 | -0.0072 | 0.0024 |
| GRIW1 | 0.996384 | 0.0555 | 0.996425 | 0.994268 | 0.0634 | -0.0021 | 0.0079 |
| GRIW4 | 0.995750 | 0.0878 | 1.002849 | 0.998709 | 0.0940 | 0.0030 | 0.0062 |
| GRMO2 | 1.002825 | 0.4957 | 0.983704 | 1.000445 | 0.4883 | -0.0024 | -0.0074 |
| GRST2A | 1.000422 | 0.3122 | 0.988709 | 1.011273 | 0.3088 | 0.0109 | -0.0034 |
| GRST2B | 1.013824 | 0.3757 | 0.980332 | 1.016838 | 0.3706 | 0.0030 | -0.0051 |
| GRST81 | 0.994646 | 0.4701 | 0.983976 | 0.988751 | 0.4640 | -0.0059 | -0.0061 |
| GRST82 | 0.994542 | 0.4555 | 1.011282 | 1.001509 | 0.4473 | 0.0070 | -0.0082 |
| GRST83 | 1.038680 | 0.5252 | 0.997573 | 1.001533 | 0.5256 | -0.0371 | 0.0004 |
| GRST84 | 1.033730 | 0.5119 | 0.986045 | 0.989511 | 0.5132 | -0.0442 | 0.0013 |
| GRTO2S | 1.013339 | 0.3746 | 0.993385 | 1.002614 | 0.3694 | -0.0107 | -0.0052 |
| GRTO2T | 1.013339 | 0.3746 | 0.999651 | 1.017981 | 0.3695 | 0.0046 | -0.0051 |
| GRTO6 | 1.012914 | 0.3699 | 0.977396 | 0.990713 | 0.3642 | -0.0222 | -0.0057 |
| HACK2Q | 1.004753 | -0.2302 | 1.015172 | 1.009058 | -0.2272 | 0.0043 | 0.0030 |
| HACK2R | 1.004396 | -0.2302 | 1.002097 | 0.996017 | -0.2276 | -0.0084 | 0.0026 |
| HACK6 | 0.997844 | -0.2759 | 0.982798 | 0.997842 | -0.2726 | -0.0000 | 0.0033 |
| HAKB1 | 1.000682 | 0.3792 | 0.989464 | 0.992006 | 0.3817 | -0.0087 | 0.0025 |
| HAKB2 | 0.995562 | 0.2864 | 0.977603 | 0.996713 | 0.2825 | 0.0012 | -0.0039 |
| HAKB4 | 0.996971 | 0.2498 | 0.999750 | 0.998798 | 0.2469 | 0.0018 | -0.0029 |
| HAMB4T | 0.997118 | 0.0585 | 0.982866 | 0.985232 | 0.0591 | -0.0119 | 0.0006 |
| HAMB4U | 0.997125 | 0.0585 | 0.999182 | 0.992727 | 0.0587 | -0.0044 | 0.0002 |
| HAMH1J | 0.998321 | -0.2589 | 1.009004 | 1.003486 | -0.2570 | 0.0052 | 0.0019 |
| HAMH1K | 0.998307 | -0.2370 | 0.985733 | 0.985833 | -0.2340 | -0.0125 | 0.0030 |
| HAMH2 | 1.003956 | -0.2331 | 1.022214 | 1.001140 | -0.2313 | -0.0028 | 0.0018 |
| HAMH2P | 1.000496 | -0.2255 | 0.991378 | 1.002900 | -0.2239 | 0.0024 | 0.0016 |
| HAMH2Q | 1.007920 | -0.2254 | 1.009888 | 1.011214 | -0.2234 | 0.0033 | 0.0020 |
| HAMH4 | 1.001702 | -0.2079 | 0.989835 | 0.994085 | -0.2056 | -0.0076 | 0.0023 |
| HARK1J | 0.999314 | 0.2566 | 0.986078 | 0.996583 | 0.2527 | -0.0027 | -0.0039 |
| HARK1K | 0.999243 | 0.2514 | 1.007497 | 0.993255 | 0.2462 | -0.0060 | -0.0052 |
| HARK1M | 0.999178 | 0.3533 | 1.007833 | 0.987697 | 0.3534 | -0.0115 | 0.0001 |
| HARK2J | 0.994997 | 0.2745 | 0.988909 | 0.988939 | 0.2707 | -0.0061 | -0.0038 |
| HARK2K | 0.992745 | 0.2587 | 1.007565 | 0.990279 | 0.2558 | -0.0025 | -0.0029 |
| HARK4 | 0.996368 | 0.2349 | 1.003373 | 0.993201 | 0.2326 | -0.0032 | -0.0023 |
| HARM2 | 0.999258 | 0.2955 | 0.980897 | 1.007879 | 0.2887 | 0.0086 | -0.0068 |
| HARM6 | 1.001413 | 0.2712 | 1.008422 | 0.997433 | 0.2637 | -0.0040 | -0.0075 |
| HATL2J | 1.001174 | 0.3065 | 0.983313 | 1.010982 | 0.2990 | 0.0098 | -0.0075 |
| HATL2K | 1.007885 | 0.3920 | 0.984404 | 1.000259 | 0.3851 | -0.0076 | -0.0069 |
| HATL81 | 0.999775 | 0.4437 | 1.007571 | 1.013669 | 0.4271 | 0.0139 | -0.0166 |
| HATL82 | 1.000025 | 0.5267 | 0.998670 | 1.005666 | 0.5184 | 0.0056 | -0.0083 |
| HAVH4J | 1.000632 | 0.2322 | 1.006899 | 1.023066 | 0.2305 | 0.0224 | -0.0017 |
| HAVH4K | 1.000632 | 0.2322 | 1.003563 | 1.000206 | 0.2305 | -0.0004 | -0.0017 |
| HAWI1 | 0.998741 | 0.4160 | 0.997801 | 0.994941 | 0.4136 | -0.0038 | -0.0024 |
| HAWP2 | 0.997125 | 0.2842 | 0.995429 | 1.014681 | 0.2785 | 0.0176 | -0.0057 |

*continued on next page*

*continued from previous page*

| | Real System | | Metered | DOLSE | | Error | |
|---|---|---|---|---|---|---|---|
| Busbar | Vm | Va | Vm | Vm | Va | Vm | Va |
| HAWP4Q | 0.999947 | 0.2366 | 1.012340 | 1.023515 | 0.2344 | 0.0236 | -0.0022 |
| HAWP6 | 1.001695 | 0.2544 | 0.981129 | 1.020370 | 0.2482 | 0.0187 | -0.0062 |
| HELE1 | 0.995802 | 0.4304 | 0.997230 | 0.990740 | 0.4203 | -0.0051 | -0.0101 |
| HEYS1 | 0.998674 | 0.0626 | 0.985383 | 0.973768 | 0.0621 | -0.0249 | -0.0005 |
| HEYS4 | 0.998678 | 0.0865 | 0.978387 | 0.987434 | 0.0862 | -0.0112 | -0.0003 |
| HEYS81 | 0.999493 | 0.2095 | 1.014578 | 1.006769 | 0.2056 | 0.0073 | -0.0039 |
| HIGM2J | 0.996619 | -0.0293 | 0.982766 | 0.976321 | -0.0273 | -0.0203 | 0.0020 |
| HIGM2K | 0.995025 | -0.0265 | 1.004913 | 0.978494 | -0.0245 | -0.0165 | 0.0020 |
| HIGM2Q | 0.996314 | -0.0341 | 0.992667 | 0.978283 | -0.0320 | -0.0180 | 0.0021 |
| HIGM4 | 0.995264 | -0.0456 | 0.979197 | 1.003251 | -0.0427 | 0.0080 | 0.0029 |
| HINP2J | 0.998738 | -0.2438 | 1.003145 | 0.983689 | -0.2404 | -0.0150 | 0.0034 |
| HINP2K | 0.998737 | -0.2437 | 0.987525 | 0.986158 | -0.2402 | -0.0126 | 0.0035 |
| HINP4 | 0.998648 | -0.2514 | 1.018652 | 0.991834 | -0.2481 | -0.0068 | 0.0033 |
| HINP81 | 0.999424 | -0.0980 | 0.985230 | 1.000237 | -0.0954 | 0.0008 | 0.0026 |
| HINP82 | 0.999425 | -0.0977 | 0.994944 | 1.008608 | -0.0976 | 0.0092 | 0.0001 |
| HINP83 | 0.999330 | -0.1359 | 0.996259 | 0.992649 | -0.1300 | -0.0067 | 0.0059 |
| HUER1 | 0.000000 | 0.5888 | 0.000000 | 1.014710 | 0.4151 | 1.0147 | -0.1737 |
| HUER4 | 1.014332 | 0.4650 | 1.003124 | 1.008845 | 0.4520 | -0.0055 | -0.0130 |
| HUER81 | 1.000039 | 0.5819 | 1.003467 | 0.982473 | 0.5743 | -0.0176 | -0.0076 |
| HURS1J | 0.998102 | -0.3212 | 1.010689 | 0.985477 | -0.3185 | -0.0126 | 0.0027 |
| HURS1K | 0.998096 | -0.3246 | 1.013218 | 0.987403 | -0.3232 | -0.0107 | 0.0014 |
| HURS1L | 0.998100 | -0.3195 | 0.997776 | 0.982847 | -0.3172 | -0.0153 | 0.0023 |
| HURS2 | 0.999672 | -0.2867 | 1.003345 | 0.986459 | -0.2837 | -0.0132 | 0.0030 |
| HUTT1 | 0.998711 | 0.1731 | 0.985125 | 0.989495 | 0.1693 | -0.0092 | -0.0038 |
| HUTT4M | 0.996185 | 0.1321 | 0.984326 | 0.982646 | 0.1316 | -0.0135 | -0.0005 |
| HUTT4N | 0.995681 | 0.1311 | 1.002491 | 0.994091 | 0.1297 | -0.0016 | -0.0014 |
| INCE2J | 1.005498 | -0.0815 | 0.990265 | 1.017960 | -0.0809 | 0.0125 | 0.0006 |
| INCE2K | 1.009471 | -0.1013 | 1.028211 | 0.998562 | -0.1001 | -0.0109 | 0.0012 |
| INDQ1 | 0.998500 | -0.3436 | 0.991680 | 0.991207 | -0.3389 | -0.0073 | 0.0047 |
| INDQ4 | 1.000928 | -0.3038 | 0.984758 | 0.993395 | -0.2997 | -0.0075 | 0.0041 |
| INKI4 | 1.016707 | 0.4471 | 1.017734 | 1.018996 | 0.4364 | 0.0023 | -0.0107 |
| IROA1J | 0.998315 | -0.3163 | 0.997137 | 1.009092 | -0.3137 | 0.0108 | 0.0026 |
| IROA1K | 0.998314 | -0.3475 | 1.014680 | 1.004454 | -0.3474 | 0.0061 | 0.0001 |
| IROA2 | 1.010990 | -0.3222 | 1.021247 | 1.018816 | -0.3213 | 0.0078 | 0.0009 |
| IRON1 | 0.998228 | -0.2387 | 0.991487 | 0.977517 | -0.2339 | -0.0207 | 0.0048 |
| IRON1Z | 0.998225 | -0.1826 | 1.004099 | 0.997774 | -0.1795 | -0.0005 | 0.0031 |
| IRON4 | 1.003065 | -0.1826 | 1.013692 | 0.996110 | -0.1795 | -0.0070 | 0.0031 |
| IVER1 | 0.997977 | -0.2959 | 0.981603 | 1.005462 | -0.2961 | 0.0075 | -0.0002 |
| IVER2J | 1.006528 | -0.2712 | 0.992794 | 1.012774 | -0.2694 | 0.0062 | 0.0018 |
| IVER2K | 1.000676 | -0.2349 | 1.003144 | 0.991293 | -0.2327 | -0.0094 | 0.0022 |
| IVER2P | 1.012346 | -0.2770 | 1.028519 | 1.002829 | -0.2755 | -0.0095 | 0.0015 |
| IVER4T | 1.002450 | -0.2332 | 1.018222 | 0.992149 | -0.2315 | -0.0103 | 0.0017 |
| IVER4U | 1.004580 | -0.2429 | 0.990085 | 1.009682 | -0.2409 | 0.0051 | 0.0020 |
| IVER6J | 0.997988 | -0.2932 | 1.012710 | 0.995473 | -0.2915 | -0.0025 | 0.0017 |
| IVER6K | 0.997961 | -0.2837 | 0.999368 | 0.999411 | -0.2821 | 0.0015 | 0.0016 |
| JORD2 | 1.001992 | -0.0131 | 1.006099 | 0.993406 | -0.0107 | -0.0086 | 0.0024 |
| JORD3 | 0.998880 | -0.0318 | 0.982101 | 0.988489 | -0.0295 | -0.0104 | 0.0023 |
| JUNB1 | 1.004502 | 0.4215 | 1.015308 | 0.980215 | 0.4253 | -0.0243 | 0.0038 |
| KAIM2 | 1.006378 | 0.4620 | 1.014279 | 1.012879 | 0.4532 | 0.0065 | -0.0088 |

*continued on next page*

*continued from previous page*

| | Real System | | Metered | DOLSE | | Error | |
|---|---|---|---|---|---|---|---|
| Busbar | Vm | Va | Vm | Vm | Va | Vm | Va |
| KEAD1 | 0.997144 | 0.0849 | 0.998325 | 0.988005 | 0.0933 | -0.0091 | 0.0084 |
| KEAD4J | 0.997042 | 0.0530 | 0.985846 | 0.983007 | 0.0583 | -0.0140 | 0.0053 |
| KEAD4K | 0.995325 | 0.0445 | 1.011218 | 0.992336 | 0.0499 | -0.0030 | 0.0054 |
| KEAD4P | 0.996780 | 0.0228 | 1.006363 | 1.002350 | 0.0279 | 0.0056 | 0.0051 |
| KEAD4Q | 0.996780 | 0.0228 | 0.995157 | 0.990039 | 0.0279 | -0.0067 | 0.0051 |
| KEAD4R | 0.997017 | 0.0611 | 1.015744 | 0.998823 | 0.0665 | 0.0018 | 0.0054 |
| KEAD4S | 0.995621 | 0.0544 | 1.003519 | 0.995067 | 0.0599 | -0.0006 | 0.0055 |
| KEAD4T | 1.000213 | 0.0908 | 0.980988 | 0.980336 | 0.0942 | -0.0199 | 0.0034 |
| KEAD81 | 0.994244 | 0.1904 | 0.980999 | 0.997198 | 0.2005 | 0.0030 | 0.0101 |
| KEAD82 | 0.994169 | 0.2061 | 1.005550 | 1.001672 | 0.2133 | 0.0075 | 0.0072 |
| KEAR1J | 0.998666 | -0.0884 | 0.992849 | 1.004188 | -0.0861 | 0.0055 | 0.0023 |
| KEAR1K | 0.998667 | -0.0907 | 0.978842 | 0.998700 | -0.0904 | 0.0000 | 0.0003 |
| KEAR2 | 0.993314 | -0.0476 | 1.003813 | 0.997147 | -0.0466 | 0.0038 | 0.0010 |
| KEAR3 | 0.998670 | -0.0990 | 0.993001 | 0.992564 | -0.0985 | -0.0061 | 0.0005 |
| KEAR4Q | 0.997169 | -0.0439 | 0.982676 | 1.009518 | -0.0429 | 0.0123 | 0.0010 |
| KEAR4R | 0.996793 | -0.0340 | 1.009788 | 0.988081 | -0.0340 | -0.0087 | 0.0000 |
| KEIT1 | 1.000197 | 0.6160 | 0.990040 | 0.994672 | 0.6219 | -0.0055 | 0.0059 |
| KEMS1J | 0.998177 | -0.2602 | 0.985857 | 0.999761 | -0.2603 | 0.0016 | -0.0001 |
| KEMS1L | 0.998177 | -0.2275 | 1.007127 | 0.987816 | -0.2252 | -0.0104 | 0.0023 |
| KEMS4J | 0.998389 | -0.2002 | 1.000993 | 1.007649 | -0.1968 | 0.0093 | 0.0034 |
| KEMS4K | 0.996964 | -0.2074 | 1.012863 | 0.976712 | -0.2045 | -0.0203 | 0.0029 |
| KEOO1 | 0.999483 | 0.3907 | 0.982807 | 1.004327 | 0.3904 | 0.0048 | -0.0003 |
| KIBY1J | 0.998285 | -0.1151 | 1.000207 | 0.968085 | -0.1131 | -0.0302 | 0.0020 |
| KIBY1K | 0.998295 | -0.0978 | 0.989953 | 0.959460 | -0.0953 | -0.0388 | 0.0025 |
| KIBY2J | 1.007223 | -0.0798 | 1.010280 | 0.969740 | -0.0779 | -0.0375 | 0.0019 |
| KIBY2K | 1.007231 | -0.0798 | 1.011229 | 0.971362 | -0.0781 | -0.0359 | 0.0017 |
| KIIN1 | 0.996986 | 0.4574 | 0.991274 | 0.998462 | 0.4503 | 0.0015 | -0.0071 |
| KIIN81 | 0.999877 | 0.5436 | 1.007611 | 1.008047 | 0.5349 | 0.0082 | -0.0087 |
| KILL4 | 0.996348 | 0.0969 | 1.005218 | 0.993390 | 0.1031 | -0.0030 | 0.0062 |
| KILL81 | 0.993689 | 0.2316 | 1.010982 | 0.983230 | 0.2472 | -0.0105 | 0.0156 |
| KILL82 | 0.993701 | 0.2260 | 0.979096 | 0.998104 | 0.2297 | 0.0044 | 0.0037 |
| KILL83 | 0.994226 | 0.2296 | 1.013086 | 0.983512 | 0.2371 | -0.0107 | 0.0075 |
| KILL84 | 0.993779 | 0.3155 | 0.993614 | 1.019387 | 0.3163 | 0.0256 | 0.0008 |
| KILS2 | 1.015105 | 0.4259 | 1.009433 | 1.015384 | 0.4167 | 0.0003 | -0.0092 |
| KILS4 | 1.013920 | 0.4332 | 1.012428 | 1.024038 | 0.4233 | 0.0101 | -0.0099 |
| KINB2J | 1.002500 | 0.5176 | 1.018855 | 0.985816 | 0.5114 | -0.0167 | -0.0062 |
| KINB2K | 1.001851 | 0.5151 | 0.994248 | 0.976382 | 0.5087 | -0.0255 | -0.0064 |
| KINC1 | 0.999385 | 0.4662 | 0.999589 | 0.986567 | 0.4593 | -0.0128 | -0.0069 |
| KINC2 | 1.002515 | 0.5086 | 0.987476 | 0.995132 | 0.5019 | -0.0074 | -0.0067 |
| KINO1 | 0.998091 | -0.2600 | 1.016064 | 0.994922 | -0.2584 | -0.0032 | 0.0016 |
| KINO4 | 0.996790 | -0.2161 | 1.010269 | 0.998244 | -0.2134 | 0.0015 | 0.0027 |
| KINT1 | 1.000186 | 0.6249 | 1.004364 | 0.984923 | 0.6311 | -0.0153 | 0.0062 |
| KINT2 | 0.996302 | 0.6749 | 1.011604 | 0.986271 | 0.6806 | -0.0100 | 0.0057 |
| KIRK1 | 0.999009 | -0.1213 | 1.008346 | 0.983283 | -0.1210 | -0.0157 | 0.0003 |
| KIRK2 | 0.985767 | -0.0808 | 0.970364 | 0.955746 | -0.0783 | -0.0300 | 0.0025 |
| KIRK2Q | 1.002814 | 0.0466 | 0.990065 | 0.980738 | 0.0487 | -0.0221 | 0.0021 |
| KITW1 | 0.998323 | -0.2943 | 0.982800 | 1.002761 | -0.2904 | 0.0044 | 0.0039 |
| KITW1Z | 0.998335 | -0.2383 | 1.010972 | 0.989750 | -0.2362 | -0.0086 | 0.0021 |
| KITW2 | 1.000754 | -0.2383 | 1.020173 | 1.005392 | -0.2362 | 0.0046 | 0.0021 |

*continued on next page*

*continued from previous page*

| | Real System | | Metered | DOLSE | | Error | |
|---|---|---|---|---|---|---|---|
| Busbar | Vm | Va | Vm | Vm | Va | Vm | Va |
| KNAR1 | 0.999192 | -0.0244 | 1.012719 | 0.966971 | -0.0213 | -0.0322 | 0.0031 |
| KNAR2 | 0.996938 | -0.0005 | 0.982949 | 0.970493 | 0.0032 | -0.0264 | 0.0037 |
| LACK2 | 1.013356 | 0.3746 | 1.004787 | 1.015198 | 0.3694 | 0.0018 | -0.0052 |
| LACK2Q | 1.000185 | 0.3102 | 0.984540 | 1.019471 | 0.3069 | 0.0193 | -0.0033 |
| LACK2R | 1.000185 | 0.3102 | 1.008234 | 0.994736 | 0.3068 | -0.0054 | -0.0034 |
| LACK4 | 1.001219 | 0.2381 | 1.005662 | 1.013123 | 0.2367 | 0.0119 | -0.0014 |
| LACK6 | 1.013625 | 0.3276 | 1.003626 | 1.008273 | 0.3233 | -0.0054 | -0.0043 |
| LALE1J | 0.998064 | -0.3085 | 0.987368 | 1.013798 | -0.3075 | 0.0157 | 0.0010 |
| LALE1K | 0.998064 | -0.3085 | 1.009584 | 0.987490 | -0.3060 | -0.0106 | 0.0025 |
| LALE2 | 1.017682 | -0.2871 | 1.020501 | 1.023466 | -0.2855 | 0.0058 | 0.0016 |
| LAMB2 | 1.007830 | 0.4786 | 0.991831 | 1.003909 | 0.4703 | -0.0039 | -0.0083 |
| LAND1 | 0.998483 | -0.3498 | 0.986255 | 1.002989 | -0.3448 | 0.0045 | 0.0050 |
| LAND4 | 0.999874 | -0.3074 | 0.988837 | 1.003567 | -0.3030 | 0.0037 | 0.0044 |
| LEGA1J | 0.998043 | -0.1590 | 0.980009 | 1.020156 | -0.1576 | 0.0221 | 0.0014 |
| LEGA1K | 0.998041 | -0.1590 | 0.987504 | 1.015514 | -0.1577 | 0.0175 | 0.0013 |
| LEGA1L | 0.998205 | -0.1424 | 1.004862 | 0.999482 | -0.1406 | 0.0013 | 0.0018 |
| LEGA1M | 0.998204 | -0.1424 | 0.983423 | 0.986052 | -0.1407 | -0.0122 | 0.0017 |
| LEGA4J | 1.001321 | -0.1118 | 0.982457 | 1.020137 | -0.1105 | 0.0188 | 0.0013 |
| LEGA4K | 1.009256 | -0.1424 | 1.024956 | 1.010742 | -0.1406 | 0.0015 | 0.0018 |
| LEGA4R | 1.008929 | -0.1441 | 1.001826 | 1.020909 | -0.1422 | 0.0120 | 0.0019 |
| LEGA4T | 1.002945 | -0.1206 | 0.983231 | 1.027984 | -0.1190 | 0.0250 | 0.0016 |
| LETC1J | 0.997487 | -0.1900 | 1.010481 | 0.999323 | -0.1871 | 0.0018 | 0.0029 |
| LETC1K | 0.997487 | -0.1900 | 0.991763 | 1.007183 | -0.1871 | 0.0097 | 0.0029 |
| LEVE1Q | 0.998438 | 0.5131 | 1.000232 | 0.966100 | 0.5080 | -0.0323 | -0.0051 |
| LEVE1R | 0.998442 | 0.5131 | 0.997422 | 0.960800 | 0.5075 | -0.0376 | -0.0056 |
| LEVE3 | 0.999597 | 0.5690 | 1.003567 | 0.981851 | 0.5676 | -0.0177 | -0.0014 |
| LEVE81 | 0.999892 | 0.6735 | 1.013537 | 0.993171 | 0.6738 | -0.0067 | 0.0003 |
| LEVT1Q | 0.998115 | 0.5123 | 1.005515 | 0.982460 | 0.5071 | -0.0157 | -0.0052 |
| LEVT1R | 0.998118 | 0.5123 | 1.006970 | 0.977521 | 0.5067 | -0.0206 | -0.0056 |
| LINM2 | 1.003353 | 0.4063 | 1.006236 | 1.006772 | 0.3992 | 0.0034 | -0.0071 |
| LISD1 | 0.998264 | -0.1161 | 1.014135 | 0.954098 | -0.1135 | -0.0442 | 0.0026 |
| LISD2 | 1.007945 | -0.0819 | 1.008649 | 0.968013 | -0.0801 | -0.0399 | 0.0018 |
| LISD2Q | 1.015996 | -0.0947 | 1.029126 | 0.984192 | -0.0936 | -0.0318 | 0.0011 |
| LITB4 | 0.996559 | -0.0902 | 1.017078 | 0.980302 | -0.0876 | -0.0163 | 0.0026 |
| LITB81 | 0.993735 | 0.0233 | 1.006525 | 0.982938 | 0.0292 | -0.0108 | 0.0059 |
| LITB82 | 0.993790 | 0.0223 | 0.986232 | 1.015509 | 0.0216 | 0.0217 | -0.0007 |
| LITT1J | 0.998098 | -0.2760 | 0.986464 | 0.996784 | -0.2732 | -0.0013 | 0.0028 |
| LITT1K | 0.998082 | -0.2842 | 0.999217 | 1.004677 | -0.2811 | 0.0066 | 0.0031 |
| LITT1L | 0.998098 | -0.2755 | 0.980580 | 1.006570 | -0.2729 | 0.0085 | 0.0026 |
| LITT1Q | 0.998082 | -0.2842 | 1.008454 | 1.023254 | -0.2811 | 0.0252 | 0.0031 |
| LITT2Q | 1.006123 | -0.2378 | 1.024303 | 1.024305 | -0.2344 | 0.0182 | 0.0034 |
| LITT2R | 1.005728 | -0.2377 | 1.005156 | 1.010072 | -0.2347 | 0.0043 | 0.0030 |
| LITT2S | 1.000606 | -0.2824 | 1.004722 | 1.001749 | -0.2793 | 0.0011 | 0.0031 |
| LITT2V | 1.000608 | -0.2825 | 1.012539 | 1.004910 | -0.2794 | 0.0043 | 0.0031 |
| LITT4 | 1.002922 | -0.2397 | 0.998793 | 0.999578 | -0.2368 | -0.0033 | 0.0029 |
| LITT4T | 1.001940 | -0.2374 | 0.991730 | 0.998621 | -0.2345 | -0.0033 | 0.0029 |
| LITT4U | 1.004477 | -0.2350 | 0.994931 | 0.998817 | -0.2319 | -0.0057 | 0.0031 |
| LOAN2 | 0.998998 | 0.5246 | 0.996646 | 0.999444 | 0.5186 | 0.0004 | -0.0060 |
| LOAN81 | 0.994258 | 0.6929 | 0.992633 | 0.985698 | 0.6966 | -0.0086 | 0.0037 |

*continued on next page*

*continued from previous page*

| | Real System | | Metered | DOLSE | | Error | |
|---|---|---|---|---|---|---|---|
| Busbar | Vm | Va | Vm | Vm | Va | Vm | Va |
| LOAN82 | 1.000119 | 0.6936 | 0.992539 | 0.996445 | 0.6919 | -0.0037 | -0.0017 |
| LOVE1J | 0.998328 | -0.3250 | 0.981834 | 1.003350 | -0.3238 | 0.0050 | 0.0012 |
| LOVE1K | 0.998327 | -0.3369 | 1.008756 | 0.993418 | -0.3345 | -0.0049 | 0.0024 |
| LOVE4 | 1.000604 | -0.2856 | 1.014189 | 0.996301 | -0.2831 | -0.0043 | 0.0025 |
| MACC2 | 0.999304 | -0.0656 | 0.991379 | 0.990166 | -0.0646 | -0.0091 | 0.0010 |
| MACC3 | 0.998682 | -0.0941 | 0.982434 | 0.996616 | -0.0925 | -0.0021 | 0.0016 |
| MACC4 | 0.999057 | -0.0717 | 1.009664 | 1.007877 | -0.0702 | 0.0088 | 0.0015 |
| MAGA2 | 1.003699 | -0.3469 | 1.005591 | 1.015162 | -0.3459 | 0.0115 | 0.0010 |
| MAGA6 | 0.998290 | -0.3661 | 1.015502 | 1.001029 | -0.3646 | 0.0027 | 0.0015 |
| MANN1 | 0.998330 | -0.3566 | 0.998090 | 0.993765 | -0.3519 | -0.0046 | 0.0047 |
| MANN4 | 1.000571 | -0.3010 | 1.020612 | 0.996347 | -0.2977 | -0.0042 | 0.0033 |
| MAYB1 | 0.998305 | 0.3944 | 1.010141 | 0.973436 | 0.3909 | -0.0249 | -0.0035 |
| MAYT1T | 0.999156 | 0.3949 | 0.983720 | 0.985782 | 0.3919 | -0.0134 | -0.0030 |
| MEDW4 | 0.997708 | -0.2001 | 0.989116 | 0.974189 | -0.1968 | -0.0235 | 0.0033 |
| MELK1 | 0.998323 | -0.3497 | 1.007947 | 1.007385 | -0.3514 | 0.0091 | -0.0017 |
| MELK2J | 1.009065 | -0.3086 | 1.010668 | 1.009905 | -0.3071 | 0.0008 | 0.0015 |
| MELK2K | 1.008819 | -0.3096 | 1.004885 | 1.005285 | -0.3090 | -0.0035 | 0.0006 |
| MELK4 | 1.004470 | -0.2838 | 1.006072 | 1.002171 | -0.2818 | -0.0023 | 0.0020 |
| MILH1 | 0.997880 | -0.2645 | 0.979689 | 1.009205 | -0.2630 | 0.0113 | 0.0015 |
| MILH2T | 0.999492 | -0.2351 | 0.992400 | 1.009133 | -0.2331 | 0.0096 | 0.0020 |
| MILH2U | 0.999483 | -0.2351 | 0.999443 | 1.017976 | -0.2331 | 0.0185 | 0.0020 |
| MITY1 | 0.998279 | -0.3095 | 1.018663 | 1.011278 | -0.3084 | 0.0130 | 0.0011 |
| MITY4 | 1.004977 | -0.2788 | 1.000322 | 1.011751 | -0.2767 | 0.0068 | 0.0021 |
| MITY4T | 1.005035 | -0.2718 | 0.999124 | 1.011708 | -0.2699 | 0.0067 | 0.0019 |
| MONF2 | 0.998394 | 0.0078 | 0.990239 | 0.975915 | 0.0115 | -0.0225 | 0.0037 |
| MONF4Q | 0.998506 | 0.0486 | 1.008913 | 0.986241 | 0.0525 | -0.0123 | 0.0039 |
| MOSM1 | 0.999302 | 0.5109 | 1.000360 | 1.006182 | 0.5048 | 0.0069 | -0.0061 |
| MOSM2Q | 0.996781 | 0.5342 | 0.987725 | 1.011047 | 0.5295 | 0.0143 | -0.0047 |
| MOSM2T | 0.997077 | 0.5348 | 0.993797 | 0.996952 | 0.5300 | -0.0001 | -0.0048 |
| MOTH1 | 0.997542 | 0.4268 | 0.988109 | 1.001019 | 0.4181 | 0.0035 | -0.0087 |
| NECH1 | 0.998302 | -0.2732 | 1.015483 | 1.000578 | -0.2711 | 0.0023 | 0.0021 |
| NECH1Z | 0.998313 | -0.2294 | 1.008866 | 0.985180 | -0.2275 | -0.0131 | 0.0019 |
| NECH2 | 1.009105 | -0.2294 | 1.006004 | 1.005567 | -0.2275 | -0.0035 | 0.0019 |
| NEEP2 | 1.003014 | -0.0119 | 0.983938 | 1.002073 | -0.0092 | -0.0009 | 0.0027 |
| NEEP3 | 0.998893 | -0.0483 | 1.009593 | 0.997205 | -0.0466 | -0.0017 | 0.0017 |
| NEEP4Q | 1.001395 | 0.0092 | 0.984438 | 1.004793 | 0.0115 | 0.0034 | 0.0023 |
| NEIL1 | 0.999312 | 0.4114 | 1.013180 | 0.996021 | 0.4000 | -0.0033 | -0.0114 |
| NEIL2 | 1.009888 | 0.4448 | 1.024212 | 1.020944 | 0.4350 | 0.0111 | -0.0098 |
| NEIL4Q | 1.012243 | 0.4574 | 1.019193 | 1.019720 | 0.4457 | 0.0075 | -0.0117 |
| NEIL4R | 1.015446 | 0.4466 | 1.026187 | 1.010132 | 0.4360 | -0.0053 | -0.0106 |
| NETS1 | 0.995250 | 0.3823 | 0.986997 | 1.003110 | 0.3832 | 0.0079 | 0.0009 |
| NEWX2 | 1.003436 | -0.2920 | 0.995445 | 0.985937 | -0.2894 | -0.0175 | 0.0026 |
| NEWX6J | 0.998097 | -0.3387 | 0.998088 | 0.978413 | -0.3353 | -0.0197 | 0.0034 |
| NEWX6K | 0.998098 | -0.3273 | 0.982701 | 0.969221 | -0.3252 | -0.0289 | 0.0021 |
| NFLE1 | 0.997375 | -0.2886 | 1.003666 | 1.007750 | -0.2849 | 0.0104 | 0.0037 |
| NFLE1Q | 0.998110 | -0.2776 | 1.003910 | 1.009088 | -0.2743 | 0.0110 | 0.0033 |
| NFLW1J | 0.998078 | -0.2887 | 1.013512 | 1.013453 | -0.2848 | 0.0154 | 0.0039 |
| NFLW1K | 0.998095 | -0.2776 | 0.998787 | 0.996930 | -0.2743 | -0.0012 | 0.0033 |
| NFLW1L | 0.998078 | -0.2878 | 0.985126 | 0.988637 | -0.2841 | -0.0094 | 0.0037 |

*continued on next page*

*continued from previous page*

| | Real System | | Metered | DOLSE | | Error | |
|---|---|---|---|---|---|---|---|
| Busbar | Vm | Va | Vm | Vm | Va | Vm | Va |
| NFLW1M | 0.998078 | -0.2873 | 0.979076 | 0.992821 | -0.2839 | -0.0053 | 0.0034 |
| NFLW2 | 0.982808 | -0.2465 | 0.988227 | 0.975916 | -0.2435 | -0.0069 | 0.0030 |
| NFLW4T | 0.997056 | -0.2284 | 1.013785 | 0.999579 | -0.2257 | 0.0025 | 0.0027 |
| NFLW4U | 0.997065 | -0.2284 | 1.016863 | 0.985506 | -0.2258 | -0.0116 | 0.0026 |
| NHYD2Q | 1.007820 | -0.2721 | 1.010214 | 1.013973 | -0.2702 | 0.0062 | 0.0019 |
| NHYD2R | 1.001948 | -0.2368 | 1.011773 | 0.990250 | -0.2346 | -0.0117 | 0.0022 |
| NHYD6 | 1.032868 | -0.2952 | 1.037060 | 1.020905 | -0.2931 | -0.0120 | 0.0021 |
| NINF1J | 0.998506 | -0.2615 | 1.014514 | 1.001344 | -0.2583 | 0.0028 | 0.0032 |
| NINF1K | 0.998518 | -0.2082 | 1.018534 | 0.998433 | -0.2050 | -0.0001 | 0.0032 |
| NINF4 | 0.994967 | -0.1955 | 0.988688 | 0.986504 | -0.1923 | -0.0085 | 0.0032 |
| NORL2T | 1.003215 | -0.0127 | 0.996182 | 0.970951 | -0.0100 | -0.0323 | 0.0027 |
| NORL2U | 1.002305 | -0.0131 | 0.987453 | 1.008360 | -0.0106 | 0.0061 | 0.0025 |
| NORL3 | 0.998883 | -0.0391 | 0.988467 | 0.994035 | -0.0370 | -0.0048 | 0.0021 |
| NORM4 | 0.991324 | -0.1002 | 0.982162 | 0.985967 | -0.0968 | -0.0054 | 0.0034 |
| NORT1J | 1.001232 | 0.2316 | 1.014674 | 1.001441 | 0.2279 | 0.0002 | -0.0037 |
| NORT1K | 1.001230 | 0.2311 | 0.979559 | 1.017619 | 0.2266 | 0.0164 | -0.0045 |
| NORT2 | 0.994797 | 0.2718 | 1.001222 | 1.008396 | 0.2669 | 0.0136 | -0.0049 |
| NORT4 | 0.999944 | 0.2236 | 0.982311 | 1.012049 | 0.2221 | 0.0121 | -0.0015 |
| NORW1 | 1.007995 | -0.1523 | 0.992676 | 1.004263 | -0.1480 | -0.0037 | 0.0043 |
| NURS1 | 0.998330 | -0.3533 | 0.992038 | 0.981299 | -0.3521 | -0.0170 | 0.0012 |
| NURS4 | 1.001073 | -0.2927 | 0.996081 | 0.986656 | -0.2903 | -0.0144 | 0.0024 |
| OCKH1 | 0.998323 | -0.2559 | 0.993336 | 0.986648 | -0.2532 | -0.0117 | 0.0027 |
| OCKH1Z | 0.998322 | -0.2346 | 1.003163 | 0.978827 | -0.2326 | -0.0195 | 0.0020 |
| OCKH2 | 0.999684 | -0.2346 | 0.990173 | 0.993079 | -0.2326 | -0.0066 | 0.0020 |
| OFFE2 | 0.998342 | 0.2956 | 0.981415 | 1.014216 | 0.2895 | 0.0159 | -0.0061 |
| OFFE3 | 1.002102 | 0.2787 | 0.992430 | 1.031141 | 0.2723 | 0.0290 | -0.0064 |
| OLDB1 | 0.998331 | -0.2512 | 0.993431 | 1.005844 | -0.2492 | 0.0075 | 0.0020 |
| OLDB1J | 0.998315 | -0.3163 | 1.014266 | 0.998717 | -0.3137 | 0.0004 | 0.0026 |
| OLDB1K | 0.998314 | -0.3475 | 0.991859 | 1.023217 | -0.3474 | 0.0249 | 0.0001 |
| OLDB2 | 1.000880 | -0.2323 | 1.014102 | 1.003316 | -0.2300 | 0.0024 | 0.0023 |
| OLDB4Q | 0.999694 | -0.1962 | 0.981660 | 1.010100 | -0.1937 | 0.0104 | 0.0025 |
| OSBA1 | 0.999827 | 0.0797 | 0.981445 | 1.016393 | 0.0847 | 0.0166 | 0.0050 |
| OSBA4 | 0.997586 | 0.1243 | 0.995056 | 1.016856 | 0.1280 | 0.0193 | 0.0037 |
| PADI1J | 0.998734 | -0.0482 | 0.993115 | 1.005106 | -0.0470 | 0.0064 | 0.0012 |
| PADI1K | 0.998735 | -0.0486 | 0.997062 | 1.001355 | -0.0486 | 0.0026 | 0.0000 |
| PADI4 | 0.996628 | 0.0002 | 1.007253 | 0.989855 | 0.0009 | -0.0068 | 0.0007 |
| PAIS1Q | 1.000569 | 0.4071 | 1.017592 | 1.000715 | 0.3957 | 0.0001 | -0.0114 |
| PAIS1R | 1.000596 | 0.4071 | 1.014717 | 1.020002 | 0.3956 | 0.0194 | -0.0115 |
| PAIS1S | 1.000446 | 0.4068 | 0.995020 | 0.991175 | 0.3953 | -0.0093 | -0.0115 |
| PAIS1T | 1.000471 | 0.4067 | 1.003129 | 1.022506 | 0.3953 | 0.0220 | -0.0114 |
| PAIS3 | 0.999303 | 0.3879 | 0.993840 | 1.005434 | 0.3763 | 0.0061 | -0.0116 |
| PEHE1 | 1.000417 | 0.7445 | 0.995487 | 1.002129 | 0.7525 | 0.0017 | 0.0080 |
| PEHE2 | 1.000417 | 0.7640 | 1.010250 | 0.998664 | 0.7725 | -0.0018 | 0.0085 |
| PEHE81 | 1.000424 | 0.8869 | 1.008155 | 1.007833 | 0.8959 | 0.0074 | 0.0090 |
| PELH1J | 0.997521 | -0.1903 | 1.010585 | 0.984545 | -0.1872 | -0.0130 | 0.0031 |
| PELH1K | 0.997521 | -0.1903 | 0.978514 | 1.007121 | -0.1874 | 0.0096 | 0.0029 |
| PELH4 | 0.996454 | -0.1509 | 0.980328 | 1.001170 | -0.1483 | 0.0047 | 0.0026 |
| PEMB1 | 0.998277 | -0.3433 | 1.005455 | 0.998779 | -0.3410 | 0.0005 | 0.0023 |
| PEMB4 | 1.015094 | -0.3187 | 1.025459 | 1.017324 | -0.3172 | 0.0022 | 0.0015 |

*continued on next page*

*continued from previous page*

| | Real System | | Metered | DOLSE | | Error | |
|---|---|---|---|---|---|---|---|
| Busbar | Vm | Va | Vm | Vm | Va | Vm | Va |
| PENE1J | 0.998409 | -0.0603 | 0.994125 | 0.982563 | -0.0582 | -0.0158 | 0.0021 |
| PENE1K | 0.998415 | -0.0558 | 1.008622 | 0.977475 | -0.0544 | -0.0209 | 0.0014 |
| PENN1J | 0.998294 | -0.2503 | 0.982826 | 0.985552 | -0.2473 | -0.0127 | 0.0030 |
| PENN1K | 0.998296 | -0.2504 | 1.009552 | 0.978428 | -0.2476 | -0.0199 | 0.0028 |
| PENN2 | 1.001238 | -0.2213 | 1.015819 | 0.982503 | -0.2189 | -0.0187 | 0.0024 |
| PENN4Q | 1.002097 | -0.1915 | 1.003139 | 0.977246 | -0.1883 | -0.0249 | 0.0032 |
| PENN4R | 1.002068 | -0.1923 | 1.015874 | 0.983520 | -0.1896 | -0.0185 | 0.0027 |
| PENT1 | 0.998264 | -0.0938 | 1.013620 | 1.007691 | -0.0941 | 0.0094 | -0.0003 |
| PENT4 | 1.009580 | -0.0702 | 0.997422 | 1.016575 | -0.0699 | 0.0070 | 0.0003 |
| PENW1J | 0.998452 | -0.0325 | 0.978745 | 0.988227 | -0.0303 | -0.0102 | 0.0022 |
| PENW1K | 0.998448 | -0.0393 | 0.988968 | 0.971712 | -0.0371 | -0.0267 | 0.0022 |
| PERS2 | 0.996437 | 0.7035 | 1.003461 | 0.996853 | 0.7099 | 0.0004 | 0.0064 |
| PEWO2 | 1.000571 | -0.0294 | 1.004067 | 0.980779 | -0.0276 | -0.0198 | 0.0018 |
| PEWO4 | 0.996326 | 0.0408 | 1.002957 | 0.977562 | 0.0413 | -0.0188 | 0.0005 |
| PITS2 | 1.002599 | -0.0125 | 1.013016 | 1.005131 | -0.0098 | 0.0025 | 0.0027 |
| PITS3 | 0.998885 | -0.0219 | 0.979619 | 0.992731 | -0.0194 | -0.0062 | 0.0025 |
| POOB2Q | 1.005488 | 0.4616 | 1.019292 | 1.011295 | 0.4528 | 0.0058 | -0.0088 |
| POOB2R | 1.005488 | 0.4616 | 1.017486 | 1.007942 | 0.4527 | 0.0025 | -0.0089 |
| POOB3 | 0.999494 | 0.4246 | 0.997703 | 0.998609 | 0.4170 | -0.0009 | -0.0076 |
| POPP2 | 0.997983 | 0.0021 | 1.017026 | 0.988859 | 0.0058 | -0.0091 | 0.0037 |
| POPP3 | 0.999189 | -0.0194 | 1.017115 | 0.980002 | -0.0156 | -0.0192 | 0.0038 |
| PYLE1 | 0.998287 | -0.3704 | 1.001787 | 0.998969 | -0.3698 | 0.0007 | 0.0006 |
| PYLE2 | 1.003623 | -0.3467 | 1.002864 | 1.001426 | -0.3458 | -0.0022 | 0.0009 |
| QUER4T | 0.997491 | 0.0855 | 0.988334 | 0.973353 | 0.0854 | -0.0241 | -0.0001 |
| QUER4U | 0.997532 | 0.0856 | 0.997196 | 0.998780 | 0.0852 | 0.0012 | -0.0004 |
| RAIN1J | 0.998270 | -0.1170 | 0.984150 | 0.954926 | -0.1161 | -0.0433 | 0.0009 |
| RAIN1K | 0.998260 | -0.1363 | 1.016649 | 0.962656 | -0.1364 | -0.0356 | -0.0001 |
| RAIN2 | 1.006420 | -0.0877 | 0.995314 | 0.970124 | -0.0862 | -0.0363 | 0.0015 |
| RASS1 | 0.998267 | -0.3371 | 1.009440 | 0.995498 | -0.3341 | -0.0028 | 0.0030 |
| RASS4 | 1.009554 | -0.3080 | 0.991843 | 1.012133 | -0.3062 | 0.0026 | 0.0018 |
| RATS1 | 0.998143 | -0.2098 | 0.979297 | 0.986088 | -0.2078 | -0.0121 | 0.0020 |
| RATS1Z | 0.998129 | -0.1571 | 0.999740 | 1.011178 | -0.1541 | 0.0130 | 0.0030 |
| RATS2S | 0.998940 | -0.1883 | 0.989121 | 0.991705 | -0.1856 | -0.0072 | 0.0027 |
| RATS4J | 0.997366 | -0.1571 | 1.012215 | 1.006404 | -0.1541 | 0.0090 | 0.0030 |
| RATS4K | 0.999068 | -0.1663 | 1.006893 | 0.997732 | -0.1637 | -0.0013 | 0.0026 |
| RAYL1J | 0.998092 | -0.2315 | 0.998466 | 0.998018 | -0.2280 | -0.0001 | 0.0035 |
| RAYL1K | 0.998068 | -0.1886 | 0.983249 | 0.977913 | -0.1819 | -0.0202 | 0.0067 |
| RAYL1L | 0.998070 | -0.1936 | 0.990392 | 0.969728 | -0.1887 | -0.0283 | 0.0049 |
| RAYL4 | 0.997836 | -0.1859 | 0.980350 | 0.980731 | -0.1831 | -0.0171 | 0.0028 |
| REBR2M | 1.005968 | -0.2316 | 1.001753 | 0.999830 | -0.2285 | -0.0061 | 0.0031 |
| REBR2N | 1.005540 | -0.2315 | 0.994076 | 1.003243 | -0.2288 | -0.0023 | 0.0027 |
| REBR3 | 0.997857 | -0.2945 | 0.980206 | 1.001667 | -0.2942 | 0.0038 | 0.0003 |
| REDH1 | 0.998277 | 0.5111 | 1.016844 | 0.996196 | 0.5058 | -0.0021 | -0.0053 |
| RICH1J | 1.028279 | -0.2041 | 1.019923 | 1.014757 | -0.2014 | -0.0135 | 0.0027 |
| RICH1K | 1.028282 | -0.2024 | 1.035210 | 0.995837 | -0.1971 | -0.0324 | 0.0053 |
| ROCH1J | 0.998768 | -0.0612 | 0.992896 | 0.982040 | -0.0594 | -0.0167 | 0.0018 |
| ROCH1K | 0.998766 | -0.0613 | 1.003469 | 0.996163 | -0.0606 | -0.0026 | 0.0007 |
| ROCH2 | 0.994392 | -0.0388 | 1.002215 | 0.980617 | -0.0376 | -0.0138 | 0.0012 |
| ROCH4Q | 0.995496 | 0.0178 | 0.992741 | 0.973748 | 0.0205 | -0.0217 | 0.0027 |

*continued on next page*

*continued from previous page*

| | Real System | | Metered | DOLSE | | Error | |
|---|---|---|---|---|---|---|---|
| Busbar | Vm | Va | Vm | Vm | Va | Vm | Va |
| ROOS1 | 1.010206 | 0.2401 | 1.012575 | 0.984834 | 0.2328 | -0.0254 | -0.0073 |
| ROWD2Q | 1.000851 | -0.2859 | 1.001080 | 0.995056 | -0.2839 | -0.0058 | 0.0020 |
| ROWD2R | 1.004707 | -0.2886 | 0.992283 | 1.005234 | -0.2864 | 0.0005 | 0.0022 |
| ROWD4T | 1.001191 | -0.2514 | 0.987588 | 1.002998 | -0.2481 | 0.0018 | 0.0033 |
| RUGE1 | 0.998287 | -0.2105 | 1.011039 | 0.976024 | -0.2081 | -0.0223 | 0.0024 |
| RUGE1M | 0.998544 | -0.1939 | 1.008697 | 1.009571 | -0.1933 | 0.0110 | 0.0006 |
| RUGE4 | 1.000733 | -0.1792 | 0.985086 | 0.987091 | -0.1765 | -0.0136 | 0.0027 |
| RYEH1 | 0.997328 | -0.2300 | 0.991838 | 1.013257 | -0.2250 | 0.0159 | 0.0050 |
| RYEH4 | 0.997019 | -0.1535 | 1.013219 | 1.019700 | -0.1511 | 0.0227 | 0.0024 |
| RYEH4T | 0.997002 | -0.1535 | 0.999871 | 1.014728 | -0.1511 | 0.0177 | 0.0024 |
| RYEH4U | 0.996466 | -0.1714 | 0.984147 | 1.001704 | -0.1688 | 0.0052 | 0.0026 |
| RYEH81 | 0.993207 | -0.0438 | 0.995780 | 1.008507 | -0.0437 | 0.0153 | 0.0001 |
| RYEH82 | 0.993199 | -0.0375 | 0.983295 | 1.020841 | -0.0432 | 0.0276 | -0.0057 |
| SALH1 | 1.001253 | 0.2691 | 0.988132 | 0.996862 | 0.2622 | -0.0044 | -0.0069 |
| SALH2 | 0.999576 | 0.2912 | 0.975888 | 0.999649 | 0.2844 | 0.0001 | -0.0068 |
| SALH4 | 1.000627 | 0.2322 | 0.975192 | 1.013062 | 0.2305 | 0.0124 | -0.0017 |
| SEAB1 | 0.998314 | -0.3392 | 1.009450 | 1.008882 | -0.3376 | 0.0106 | 0.0016 |
| SEAB4 | 1.006341 | -0.3055 | 1.005928 | 1.002680 | -0.3041 | -0.0037 | 0.0014 |
| SEAL4 | 1.000772 | 0.2335 | 0.981983 | 1.021981 | 0.2320 | 0.0212 | -0.0015 |
| SEFI1 | 1.041060 | 0.3168 | 1.040763 | 1.003451 | 0.3066 | -0.0376 | -0.0102 |
| SELL1J | 0.998480 | -0.1805 | 0.985356 | 0.995883 | -0.1782 | -0.0026 | 0.0023 |
| SELL1K | 0.998478 | -0.1408 | 1.009484 | 0.999087 | -0.1372 | 0.0006 | 0.0036 |
| SELL4 | 0.996527 | -0.1357 | 0.977926 | 0.996655 | -0.1319 | 0.0001 | 0.0038 |
| SHBA4 | 0.996146 | 0.1023 | 0.982044 | 0.985963 | 0.1089 | -0.0102 | 0.0066 |
| SHBA81 | 0.993832 | 0.2035 | 1.014798 | 0.985573 | 0.2172 | -0.0083 | 0.0137 |
| SHBA82 | 0.993844 | 0.2253 | 0.985585 | 0.990748 | 0.2330 | -0.0031 | 0.0077 |
| SHEC2 | 1.003239 | -0.0126 | 1.008856 | 0.986264 | -0.0098 | -0.0170 | 0.0028 |
| SHEC3 | 0.998889 | -0.0413 | 1.001572 | 0.986329 | -0.0383 | -0.0126 | 0.0030 |
| SHIN1 | 0.999285 | 0.5702 | 0.987456 | 0.992936 | 0.5755 | -0.0063 | 0.0053 |
| SHRU2Q | 1.005227 | 0.4615 | 1.002797 | 1.019247 | 0.4527 | 0.0140 | -0.0088 |
| SHRU2R | 1.005226 | 0.4615 | 1.006820 | 1.009166 | 0.4526 | 0.0039 | -0.0089 |
| SHRU3 | 0.999493 | 0.4334 | 0.991649 | 1.010113 | 0.4237 | 0.0106 | -0.0097 |
| SIZE1J | 0.998431 | 0.0241 | 0.987845 | 0.993290 | 0.0309 | -0.0051 | 0.0068 |
| SIZE1K | 0.998431 | 0.0241 | 1.007000 | 0.989817 | 0.0288 | -0.0086 | 0.0047 |
| SIZE4 | 0.998432 | -0.0633 | 1.016834 | 0.991401 | -0.0595 | -0.0070 | 0.0038 |
| SIZE81 | 0.999461 | 0.0560 | 1.016244 | 1.008790 | 0.0580 | 0.0093 | 0.0020 |
| SJOW1J | 0.998008 | -0.2811 | 0.991280 | 1.001978 | -0.2785 | 0.0040 | 0.0026 |
| SJOW1K | 0.997887 | -0.2672 | 1.004165 | 1.020409 | -0.2650 | 0.0225 | 0.0022 |
| SJOW2 | 1.004308 | -0.2359 | 0.990883 | 1.003119 | -0.2330 | -0.0012 | 0.0029 |
| SJOW2Q | 1.012547 | -0.2825 | 1.000436 | 1.005158 | -0.2806 | -0.0074 | 0.0019 |
| SJOW2R | 1.012484 | -0.2825 | 1.012872 | 1.013572 | -0.2807 | 0.0011 | 0.0018 |
| SJOW4Q | 1.000397 | -0.2436 | 0.990514 | 1.007415 | -0.2410 | 0.0070 | 0.0026 |
| SJOW4R | 0.999312 | -0.2435 | 1.015876 | 0.996150 | -0.2408 | -0.0032 | 0.0027 |
| SJOW6J | 0.998007 | -0.2764 | 0.991951 | 0.996463 | -0.2749 | -0.0015 | 0.0015 |
| SJOW6K | 0.998009 | -0.2889 | 0.997329 | 1.007720 | -0.2842 | 0.0097 | 0.0047 |
| SKLG1J | 0.999079 | -0.0087 | 0.978605 | 0.988293 | -0.0070 | -0.0108 | 0.0017 |
| SKLG1K | 0.999079 | -0.0093 | 0.985878 | 0.992541 | -0.0052 | -0.0065 | 0.0041 |
| SKLG2 | 1.001042 | 0.0350 | 0.992201 | 0.993834 | 0.0374 | -0.0072 | 0.0024 |
| SLOY1 | 0.993918 | 0.4358 | 0.997369 | 0.993362 | 0.4264 | -0.0006 | -0.0094 |

*continued on next page*

*continued from previous page*

| | Real System | | Metered | DOLSE | | Error | |
|---|---|---|---|---|---|---|---|
| Busbar | Vm | Va | Vm | Vm | Va | Vm | Va |
| SLOY81 | 0.999848 | 0.5153 | 0.993023 | 0.986468 | 0.5078 | -0.0134 | -0.0075 |
| SMAN1 | 0.998640 | -0.1034 | 0.997874 | 0.988770 | -0.1019 | -0.0099 | 0.0015 |
| SMAN2 | 1.001038 | -0.0643 | 0.982550 | 0.989788 | -0.0635 | -0.0113 | 0.0008 |
| SMEA2 | 1.005874 | 0.4627 | 0.990751 | 1.011427 | 0.4539 | 0.0056 | -0.0088 |
| SMEA4R | 1.004047 | 0.4747 | 0.985459 | 1.011769 | 0.4648 | 0.0077 | -0.0099 |
| SPEN1 | 1.001161 | 0.2612 | 1.012715 | 1.027976 | 0.2542 | 0.0268 | -0.0070 |
| SPEN2M | 0.997137 | 0.2877 | 0.984903 | 1.018930 | 0.2816 | 0.0218 | -0.0061 |
| SPEN2N | 0.997905 | 0.2892 | 1.013818 | 1.003505 | 0.2832 | 0.0056 | -0.0060 |
| SSHI2 | 0.999869 | 0.3065 | 1.004188 | 1.005216 | 0.3002 | 0.0053 | -0.0063 |
| SSHI3 | 1.002297 | 0.2868 | 0.981933 | 1.004447 | 0.2801 | 0.0022 | -0.0067 |
| STAH1 | 0.998504 | -0.0089 | 0.984714 | 0.987764 | -0.0072 | -0.0107 | 0.0017 |
| STAH4Q | 0.996991 | 0.0579 | 1.008972 | 0.992821 | 0.0585 | -0.0042 | 0.0006 |
| STAH4R | 0.997003 | 0.0579 | 0.981043 | 0.988700 | 0.0581 | -0.0083 | 0.0002 |
| STAL1J | 0.998846 | -0.0741 | 1.005350 | 0.963083 | -0.0714 | -0.0358 | 0.0027 |
| STAL1K | 0.998848 | -0.0733 | 1.000178 | 0.968577 | -0.0713 | -0.0303 | 0.0020 |
| STAL2 | 0.997625 | -0.0450 | 0.988584 | 0.972124 | -0.0434 | -0.0255 | 0.0016 |
| STAL4Q | 1.001627 | 0.0119 | 0.984013 | 0.969695 | 0.0147 | -0.0319 | 0.0028 |
| STAY1 | 0.997463 | -0.1025 | 0.993655 | 0.983452 | -0.0985 | -0.0140 | 0.0040 |
| STAY4 | 0.995360 | -0.0624 | 0.998664 | 0.986134 | -0.0585 | -0.0092 | 0.0039 |
| STAY4R | 0.998752 | -0.1141 | 0.991842 | 0.999879 | -0.1108 | 0.0011 | 0.0033 |
| STEN1 | 1.000862 | 0.2856 | 1.012312 | 1.010837 | 0.2782 | 0.0100 | -0.0074 |
| STES1 | 1.000861 | 0.2917 | 0.988701 | 1.002286 | 0.2864 | 0.0014 | -0.0053 |
| STEW2 | 0.999231 | 0.3257 | 1.007322 | 1.007415 | 0.3189 | 0.0082 | -0.0068 |
| STEW4Q | 0.997698 | 0.3621 | 0.978357 | 1.010809 | 0.3560 | 0.0131 | -0.0061 |
| STEW4R | 0.997698 | 0.3621 | 0.979977 | 0.999067 | 0.3536 | 0.0014 | -0.0085 |
| STHA2 | 1.007143 | 0.4453 | 0.988817 | 1.007321 | 0.4372 | 0.0002 | -0.0081 |
| STHA4 | 1.011411 | 0.4196 | 1.013428 | 1.007006 | 0.4107 | -0.0044 | -0.0089 |
| STIR1Q | 0.999074 | 0.4609 | 0.995607 | 1.003385 | 0.4533 | 0.0043 | -0.0076 |
| STIR1R | 0.999160 | 0.4609 | 1.018832 | 1.003050 | 0.4533 | 0.0039 | -0.0076 |
| STIR1S | 0.998917 | 0.4602 | 1.004148 | 1.021943 | 0.4527 | 0.0230 | -0.0075 |
| STIR1T | 0.999007 | 0.4603 | 1.012748 | 0.991352 | 0.4527 | -0.0077 | -0.0076 |
| STIR3 | 0.999401 | 0.4242 | 1.002024 | 1.001845 | 0.4179 | 0.0024 | -0.0063 |
| STLB3 | 0.999538 | 0.4067 | 1.008477 | 1.005715 | 0.3959 | 0.0062 | -0.0108 |
| STLE1 | 0.994877 | 0.4302 | 0.977855 | 1.000740 | 0.4198 | 0.0059 | -0.0104 |
| STLE3N | 0.999538 | 0.4067 | 1.008886 | 1.010904 | 0.3959 | 0.0114 | -0.0108 |
| STLE3S | 0.999538 | 0.4067 | 0.988001 | 0.992201 | 0.3959 | -0.0073 | -0.0108 |
| STSB4 | 1.001404 | 0.0124 | 1.006912 | 1.003277 | 0.0147 | 0.0019 | 0.0023 |
| STSB4R | 1.003912 | 0.0002 | 0.988669 | 1.008012 | 0.0023 | 0.0041 | 0.0021 |
| STSB6 | 0.999088 | 0.0124 | 1.012657 | 1.008952 | 0.0147 | 0.0099 | 0.0023 |
| STWB4Q | 1.002884 | 0.4319 | 0.983838 | 1.026060 | 0.4236 | 0.0232 | -0.0083 |
| STWB4R | 1.002884 | 0.4319 | 1.013647 | 1.001565 | 0.4221 | -0.0013 | -0.0098 |
| SUND1J | 0.997663 | -0.2293 | 0.978984 | 0.989880 | -0.2275 | -0.0078 | 0.0018 |
| SUND1K | 0.997664 | -0.2154 | 1.013476 | 0.992903 | -0.2114 | -0.0048 | 0.0040 |
| SUND4 | 0.996810 | -0.1737 | 1.016641 | 0.992684 | -0.1715 | -0.0041 | 0.0022 |
| SWAN1J | 0.998288 | -0.3800 | 1.008544 | 1.006235 | -0.3813 | 0.0079 | -0.0013 |
| SWAN1K | 0.998287 | -0.3800 | 1.003152 | 1.010155 | -0.3795 | 0.0119 | 0.0005 |
| SWAN2 | 1.005097 | -0.3444 | 1.017617 | 1.013499 | -0.3436 | 0.0084 | 0.0008 |
| SWAN4 | 1.009768 | -0.3283 | 1.017355 | 1.003461 | -0.3273 | -0.0063 | 0.0010 |
| TAUN1 | 0.998662 | -0.2951 | 1.017779 | 0.995783 | -0.2911 | -0.0029 | 0.0040 |

*continued on next page*

*continued from previous page*

| | Real System | | Metered | DOLSE | | Error | |
|---|---|---|---|---|---|---|---|
| Busbar | Vm | Va | Vm | Vm | Va | Vm | Va |
| TAUN4Q | 1.001278 | -0.2708 | 0.999423 | 0.997971 | -0.2672 | -0.0033 | 0.0036 |
| TAUN4R | 1.000575 | -0.2716 | 0.981632 | 0.993839 | -0.2679 | -0.0067 | 0.0037 |
| TEAL1 | 0.999798 | 0.5106 | 0.991781 | 0.984800 | 0.5111 | -0.0150 | 0.0005 |
| TEAL2 | 0.993112 | 0.5722 | 0.990159 | 0.981665 | 0.5711 | -0.0114 | -0.0011 |
| TEMP2J | 1.001765 | -0.0126 | 0.994958 | 1.005941 | -0.0098 | 0.0042 | 0.0028 |
| TEMP2K | 1.002254 | -0.0126 | 1.002915 | 0.988795 | -0.0097 | -0.0135 | 0.0029 |
| TEMP3F | 0.998875 | -0.0126 | 0.990882 | 1.005102 | -0.0098 | 0.0062 | 0.0028 |
| TEMP3G | 0.998872 | -0.0263 | 1.006521 | 0.981891 | -0.0235 | -0.0170 | 0.0028 |
| THOM2J | 0.998354 | 0.0065 | 1.005214 | 0.997536 | 0.0091 | -0.0008 | 0.0026 |
| THOM2K | 0.998766 | 0.0202 | 0.994936 | 0.976784 | 0.0221 | -0.0220 | 0.0019 |
| THOM4 | 0.999712 | 0.0543 | 0.985211 | 0.972387 | 0.0577 | -0.0273 | 0.0034 |
| THOM6 | 0.999001 | -0.0507 | 0.986294 | 0.992476 | -0.0482 | -0.0065 | 0.0025 |
| THTO4J | 0.998092 | 0.1082 | 0.982791 | 0.998236 | 0.1120 | 0.0001 | 0.0038 |
| THTO4K | 0.998543 | 0.1153 | 1.008768 | 1.012844 | 0.1179 | 0.0143 | 0.0026 |
| THUR2 | 0.995377 | -0.0088 | 1.010598 | 0.985574 | -0.0063 | -0.0098 | 0.0025 |
| THUR2T | 0.995767 | -0.0087 | 0.976376 | 0.971964 | -0.0062 | -0.0238 | 0.0025 |
| THUR6 | 0.998824 | -0.0486 | 1.002430 | 0.996913 | -0.0448 | -0.0019 | 0.0038 |
| TILB1J | 0.997999 | -0.2478 | 0.997981 | 1.002087 | -0.2471 | 0.0041 | 0.0007 |
| TILB1K | 0.998002 | -0.2476 | 0.988689 | 0.987842 | -0.2455 | -0.0102 | 0.0021 |
| TILB2J | 0.996407 | -0.2182 | 1.000015 | 0.982733 | -0.2165 | -0.0137 | 0.0017 |
| TILB2K | 0.996127 | -0.2205 | 0.996459 | 0.985373 | -0.2183 | -0.0108 | 0.0022 |
| TILB4T | 0.997156 | -0.2054 | 1.004963 | 0.997454 | -0.2028 | 0.0003 | 0.0026 |
| TILB4U | 0.997978 | -0.1955 | 1.012896 | 0.990445 | -0.1923 | -0.0075 | 0.0032 |
| TINP2T | 0.996113 | -0.0072 | 1.000493 | 0.988808 | -0.0048 | -0.0073 | 0.0024 |
| TINP2U | 0.996113 | -0.0072 | 1.000857 | 0.986100 | -0.0048 | -0.0100 | 0.0024 |
| TINP3F | 0.998832 | -0.0072 | 1.007263 | 0.985590 | -0.0048 | -0.0132 | 0.0024 |
| TINP3G | 0.998831 | -0.0138 | 0.983734 | 0.984697 | -0.0114 | -0.0141 | 0.0024 |
| TODP2 | 1.012068 | 0.3788 | 0.998613 | 0.999756 | 0.3733 | -0.0123 | -0.0055 |
| TODP6 | 1.012884 | 0.3705 | 0.998239 | 1.006803 | 0.3657 | -0.0061 | -0.0048 |
| TONG1 | 0.997837 | 0.3885 | 0.992365 | 0.993792 | 0.3904 | -0.0040 | 0.0019 |
| TORN1 | 0.999728 | 0.4702 | 0.989279 | 0.999578 | 0.4595 | -0.0001 | -0.0107 |
| TORN4 | 0.999728 | 0.4826 | 1.012292 | 1.003391 | 0.4722 | 0.0037 | -0.0104 |
| TORN81 | 0.999879 | 0.6020 | 0.980023 | 1.004075 | 0.5900 | 0.0042 | -0.0120 |
| TOTE2J | 1.005369 | -0.2286 | 1.025456 | 1.011997 | -0.2255 | 0.0066 | 0.0031 |
| TOTE2K | 1.004979 | -0.2285 | 1.024271 | 0.996900 | -0.2257 | -0.0081 | 0.0028 |
| TOTT1J | 0.997903 | -0.2619 | 0.992664 | 0.986478 | -0.2601 | -0.0114 | 0.0018 |
| TOTT1K | 0.997828 | -0.2446 | 1.010861 | 0.980958 | -0.2413 | -0.0169 | 0.0033 |
| TOTW2J | 1.003624 | -0.2279 | 0.992883 | 0.999826 | -0.2251 | -0.0038 | 0.0028 |
| TOTW2K | 1.003543 | -0.2280 | 1.016672 | 0.988050 | -0.2247 | -0.0155 | 0.0033 |
| TRAW1 | 0.998214 | -0.0967 | 0.992253 | 0.999379 | -0.0960 | 0.0012 | 0.0007 |
| TRAW2 | 1.016483 | -0.0934 | 1.018800 | 1.025304 | -0.0927 | 0.0088 | 0.0007 |
| TRAW4 | 1.014576 | -0.0929 | 1.026396 | 1.021451 | -0.0923 | 0.0069 | 0.0006 |
| TREM2T | 1.007160 | -0.3374 | 1.009253 | 1.022517 | -0.3368 | 0.0154 | 0.0006 |
| TREM3 | 0.998298 | -0.3374 | 0.979664 | 1.021484 | -0.3368 | 0.0232 | 0.0006 |
| TYNE1 | 1.002047 | 0.2685 | 1.009038 | 0.997713 | 0.2621 | -0.0043 | -0.0064 |
| TYNE2 | 1.000336 | 0.3039 | 0.976879 | 1.004691 | 0.2976 | 0.0044 | -0.0063 |
| UPPB1 | 0.998288 | -0.3574 | 1.012425 | 0.987158 | -0.3556 | -0.0111 | 0.0018 |
| UPPB2M | 1.000572 | -0.3351 | 1.015746 | 1.002138 | -0.3342 | 0.0016 | 0.0009 |
| UPPB2N | 1.001734 | -0.3353 | 1.007638 | 1.012096 | -0.3349 | 0.0104 | 0.0004 |

*continued on next page*

*continued from previous page*

| | Real System | | Metered | DOLSE | | Error | |
|---|---|---|---|---|---|---|---|
| Busbar | Vm | Va | Vm | Vm | Va | Vm | Va |
| UPPB3 | 0.998292 | -0.3713 | 0.995139 | 0.995354 | -0.3709 | -0.0029 | 0.0004 |
| USKM1J | 0.998304 | -0.3743 | 0.994494 | 1.016479 | -0.3730 | 0.0182 | 0.0013 |
| USKM1K | 0.998304 | -0.3743 | 0.983226 | 1.024577 | -0.3746 | 0.0263 | -0.0003 |
| USKM2Q | 1.007568 | -0.3344 | 1.007097 | 1.005463 | -0.3342 | -0.0021 | 0.0002 |
| USKM2R | 1.007703 | -0.3345 | 1.006968 | 1.032061 | -0.3344 | 0.0244 | 0.0001 |
| USKM2T | 1.007561 | -0.3354 | 0.991986 | 1.039118 | -0.3350 | 0.0316 | 0.0004 |
| USKM2U | 1.008065 | -0.3368 | 1.015089 | 1.036069 | -0.3365 | 0.0280 | 0.0003 |
| USKM3 | 0.998303 | -0.3436 | 1.006129 | 1.019722 | -0.3432 | 0.0214 | 0.0004 |
| WALH1J | 0.998213 | -0.3308 | 0.996835 | 1.001793 | -0.3274 | 0.0036 | 0.0034 |
| WALH1K | 0.998211 | -0.3238 | 1.006112 | 0.998745 | -0.3209 | 0.0005 | 0.0029 |
| WALH4 | 1.010691 | -0.2795 | 1.022750 | 1.013435 | -0.2773 | 0.0027 | 0.0022 |
| WALL4 | 0.996578 | -0.2106 | 0.988905 | 0.997968 | -0.2078 | 0.0014 | 0.0028 |
| WALP1J | 0.997664 | -0.1630 | 0.998719 | 0.987003 | -0.1574 | -0.0107 | 0.0056 |
| WALP1K | 0.997661 | -0.1634 | 1.004410 | 0.992079 | -0.1577 | -0.0056 | 0.0057 |
| WALP4 | 0.990311 | -0.0968 | 0.986240 | 0.989095 | -0.0937 | -0.0012 | 0.0031 |
| WALX2J | 1.003212 | -0.2134 | 1.002756 | 1.010350 | -0.2107 | 0.0071 | 0.0027 |
| WALX2K | 1.003034 | -0.2134 | 0.996606 | 1.015318 | -0.2101 | 0.0123 | 0.0033 |
| WALX4T | 0.997194 | -0.1595 | 1.001524 | 1.000945 | -0.1570 | 0.0038 | 0.0025 |
| WALX4U | 0.996889 | -0.1759 | 1.013025 | 1.017747 | -0.1731 | 0.0209 | 0.0028 |
| WARL1 | 0.997971 | -0.2692 | 1.015159 | 1.015426 | -0.2683 | 0.0175 | 0.0009 |
| WARL1Z | 0.997973 | -0.2235 | 0.979717 | 1.006081 | -0.2215 | 0.0081 | 0.0020 |
| WARL2 | 0.996588 | -0.2235 | 1.009578 | 0.996860 | -0.2215 | 0.0003 | 0.0020 |
| WASF1 | 0.998324 | -0.0896 | 0.983938 | 0.977785 | -0.0884 | -0.0205 | 0.0012 |
| WASF2T | 1.004476 | -0.0647 | 1.004608 | 0.983078 | -0.0628 | -0.0214 | 0.0019 |
| WASF2U | 1.004493 | -0.0647 | 0.995352 | 0.969381 | -0.0630 | -0.0351 | 0.0017 |
| WATF1J | 0.997852 | -0.2713 | 1.005387 | 0.987880 | -0.2699 | -0.0100 | 0.0014 |
| WATF1K | 0.997846 | -0.2476 | 0.995391 | 0.995926 | -0.2460 | -0.0019 | 0.0016 |
| WATF1Z | 0.997848 | -0.2283 | 0.992712 | 1.014823 | -0.2260 | 0.0170 | 0.0023 |
| WATS2M | 0.999760 | -0.2283 | 0.981730 | 0.997193 | -0.2260 | -0.0026 | 0.0023 |
| WATS2N | 0.999764 | -0.2345 | 1.019606 | 0.984958 | -0.2325 | -0.0148 | 0.0020 |
| WBOL2 | 0.999656 | 0.3060 | 1.003491 | 1.010347 | 0.2997 | 0.0107 | -0.0063 |
| WBOL6 | 1.002460 | 0.2517 | 0.998071 | 1.017714 | 0.2467 | 0.0153 | -0.0050 |
| WBUR1 | 0.997516 | -0.0638 | 1.015095 | 0.988581 | -0.0592 | -0.0089 | 0.0046 |
| WBUR4 | 0.995196 | -0.0244 | 1.009938 | 0.985740 | -0.0207 | -0.0095 | 0.0037 |
| WFIB2 | 0.995954 | 0.5491 | 1.013419 | 0.982218 | 0.5454 | -0.0137 | -0.0037 |
| WFIE1J | 0.996792 | 0.4580 | 0.986613 | 0.994328 | 0.4510 | -0.0025 | -0.0070 |
| WFIE1K | 0.999306 | 0.5120 | 0.980079 | 0.996794 | 0.5070 | -0.0025 | -0.0050 |
| WFIE2 | 0.996965 | 0.5363 | 0.987488 | 0.995647 | 0.5317 | -0.0013 | -0.0046 |
| WHAM1 | 0.998012 | -0.2658 | 0.996398 | 1.001329 | -0.2640 | 0.0033 | 0.0018 |
| WHAM2Q | 1.004108 | -0.2314 | 0.986681 | 0.995436 | -0.2284 | -0.0087 | 0.0030 |
| WHAM2R | 1.003789 | -0.2313 | 0.991891 | 0.980613 | -0.2292 | -0.0232 | 0.0021 |
| WHAM4 | 0.999632 | -0.2411 | 0.989224 | 0.997803 | -0.2385 | -0.0018 | 0.0026 |
| WHGA1 | 0.998741 | -0.0940 | 1.007081 | 0.988097 | -0.0951 | -0.0106 | -0.0011 |
| WHGA1Z | 0.998744 | -0.0444 | 1.009159 | 1.008227 | -0.0433 | 0.0095 | 0.0011 |
| WHGA2 | 0.993757 | -0.0444 | 0.978918 | 0.986375 | -0.0433 | -0.0074 | 0.0011 |
| WHSO2 | 1.008045 | -0.3336 | 1.025102 | 1.024658 | -0.3333 | 0.0166 | 0.0003 |
| WHSO2Q | 1.008393 | -0.3307 | 0.995382 | 1.024099 | -0.3302 | 0.0157 | 0.0005 |
| WHSO2R | 1.008393 | -0.3307 | 0.992624 | 1.014400 | -0.3307 | 0.0060 | 0.0000 |
| WHSO3J | 0.998304 | -0.3374 | 0.994104 | 1.011983 | -0.3370 | 0.0137 | 0.0004 |

*continued on next page*

*continued from previous page*

| | Real System | | Metered | DOLSE | | Error | |
|---|---|---|---|---|---|---|---|
| Busbar | Vm | Va | Vm | Vm | Va | Vm | Va |
| WHSO3K | 0.998305 | -0.3336 | 0.998508 | 1.002200 | -0.3333 | 0.0039 | 0.0003 |
| WHSO4T | 1.008456 | -0.3132 | 0.989003 | 1.017674 | -0.3118 | 0.0092 | 0.0014 |
| WHTB1S | 0.994205 | 0.4312 | 0.983843 | 0.998561 | 0.4207 | 0.0044 | -0.0105 |
| WHTB1T | 0.994195 | 0.4312 | 0.978943 | 0.990025 | 0.4221 | -0.0042 | -0.0091 |
| WHTL1S | 0.994280 | 0.4313 | 0.979327 | 0.988282 | 0.4208 | -0.0060 | -0.0105 |
| WHTL1T | 0.994270 | 0.4313 | 0.985228 | 0.994777 | 0.4222 | 0.0005 | -0.0091 |
| WHTL3 | 0.999576 | 0.4118 | 0.986242 | 0.994725 | 0.4019 | -0.0049 | -0.0099 |
| WIBA2 | 1.002526 | -0.0126 | 0.985789 | 0.988537 | -0.0098 | -0.0140 | 0.0028 |
| WIBA3 | 0.998881 | -0.0250 | 1.003582 | 0.989838 | -0.0221 | -0.0090 | 0.0029 |
| WIEN1 | 1.004901 | -0.2584 | 0.999152 | 1.007402 | -0.2563 | 0.0025 | 0.0021 |
| WIEN2Q | 0.997195 | -0.2348 | 1.000884 | 1.007301 | -0.2328 | 0.0101 | 0.0020 |
| WILL1 | 0.998258 | -0.2397 | 0.983084 | 1.009296 | -0.2364 | 0.0110 | 0.0033 |
| WILL2J | 0.998088 | -0.2078 | 1.015708 | 0.990279 | -0.2053 | -0.0078 | 0.0025 |
| WILL2K | 0.996464 | -0.1817 | 0.989507 | 1.015852 | -0.1793 | 0.0194 | 0.0024 |
| WILL4 | 0.998475 | -0.1704 | 0.996790 | 1.000502 | -0.1677 | 0.0020 | 0.0027 |
| WILT6 | 1.007342 | 0.3299 | 0.984976 | 1.017004 | 0.3258 | 0.0097 | -0.0041 |
| WIMB1J | 0.998096 | -0.3416 | 1.013684 | 0.989174 | -0.3405 | -0.0089 | 0.0011 |
| WIMB1K | 1.024478 | -0.3172 | 1.045447 | 1.022184 | -0.3148 | -0.0023 | 0.0024 |
| WIMB1L | 0.998095 | -0.3205 | 0.992010 | 0.972725 | -0.3179 | -0.0254 | 0.0026 |
| WIMB1M | 0.998096 | -0.3138 | 1.007341 | 0.996246 | -0.3118 | -0.0019 | 0.0020 |
| WIMB1Z | 0.998096 | -0.2928 | 1.007531 | 0.999181 | -0.2905 | 0.0011 | 0.0023 |
| WIMB2 | 1.004409 | -0.2928 | 0.985611 | 0.994794 | -0.2905 | -0.0096 | 0.0023 |
| WISD1 | 0.998067 | -0.3109 | 1.012537 | 0.992570 | -0.3089 | -0.0055 | 0.0020 |
| WISD2 | 1.012505 | -0.2848 | 1.002730 | 1.011502 | -0.2830 | -0.0010 | 0.0018 |
| WISD2Q | 1.010847 | -0.2899 | 1.000671 | 0.997617 | -0.2877 | -0.0132 | 0.0022 |
| WISD2R | 1.019500 | -0.2877 | 1.010766 | 1.022691 | -0.2864 | 0.0032 | 0.0013 |
| WISD6 | 0.998066 | -0.3214 | 0.996337 | 1.003743 | -0.3208 | 0.0057 | 0.0006 |
| WISH1 | 0.999144 | 0.4287 | 1.006464 | 0.995336 | 0.4189 | -0.0038 | -0.0098 |
| WISH2 | 1.007730 | 0.4488 | 1.024638 | 1.013705 | 0.4407 | 0.0060 | -0.0081 |
| WIYH1 | 0.999516 | 0.4346 | 0.983742 | 1.002766 | 0.4240 | 0.0033 | -0.0106 |
| WIYH2 | 1.009936 | 0.4688 | 1.005874 | 1.008752 | 0.4596 | -0.0012 | -0.0092 |
| WIYH4Q | 1.015690 | 0.4532 | 1.026781 | 1.005555 | 0.4430 | -0.0101 | -0.0102 |
| WIYH4R | 1.013855 | 0.4665 | 1.025298 | 1.010216 | 0.4550 | -0.0036 | -0.0115 |
| WMEL1J | 0.998953 | -0.0309 | 0.997642 | 0.995354 | -0.0296 | -0.0036 | 0.0013 |
| WMEL1K | 0.998954 | -0.0244 | 0.994732 | 0.988341 | -0.0213 | -0.0106 | 0.0031 |
| WMEL1L | 0.998957 | -0.0350 | 0.996777 | 0.989509 | -0.0328 | -0.0094 | 0.0022 |
| WMEL1M | 0.998955 | -0.0341 | 1.014749 | 1.001861 | -0.0316 | 0.0029 | 0.0025 |
| WMEL2 | 0.995895 | -0.0015 | 0.985024 | 0.989886 | 0.0009 | -0.0060 | 0.0024 |
| WTHU2M | 1.006087 | -0.2376 | 1.015173 | 1.014345 | -0.2343 | 0.0083 | 0.0033 |
| WTHU2N | 1.005703 | -0.2375 | 1.011642 | 1.011144 | -0.2346 | 0.0054 | 0.0029 |
| WWEY1 | 0.998097 | -0.3264 | 0.990850 | 0.985359 | -0.3245 | -0.0127 | 0.0019 |
| WWEY1X | 0.998114 | -0.2924 | 0.994186 | 0.962493 | -0.2905 | -0.0356 | 0.0019 |
| WWEY1Y | 0.998114 | -0.2924 | 1.009418 | 0.966371 | -0.2905 | -0.0317 | 0.0019 |
| WWEY1Z | 0.998092 | -0.2871 | 1.000672 | 1.019496 | -0.2851 | 0.0214 | 0.0020 |
| WWEY2J | 1.003057 | -0.2871 | 0.999729 | 1.009952 | -0.2851 | 0.0069 | 0.0020 |
| WWEY2K | 1.001602 | -0.2924 | 0.991559 | 0.985134 | -0.2905 | -0.0165 | 0.0019 |
| WWEY2P | 1.016052 | -0.2866 | 1.008527 | 1.030401 | -0.2849 | 0.0143 | 0.0017 |
| WWEY4T | 1.003729 | -0.2861 | 1.010929 | 0.999996 | -0.2839 | -0.0037 | 0.0022 |
| WWEY4U | 1.007748 | -0.2846 | 1.021333 | 1.014834 | -0.2834 | 0.0071 | 0.0012 |

*continued on next page*

*continued from previous page*

| | Real System | | Metered | DOLSE | | Error | |
|---|---|---|---|---|---|---|---|
| Busbar | Vm | Va | Vm | Vm | Va | Vm | Va |
| WYLF1 | 0.998549 | -0.0960 | 1.009701 | 1.000537 | -0.0960 | 0.0020 | 0.0000 |
| WYLF4 | 1.002834 | -0.0557 | 0.987826 | 1.007948 | -0.0555 | 0.0051 | 0.0002 |
| WYLF81 | 0.999638 | 0.0397 | 1.017079 | 1.009987 | 0.0390 | 0.0103 | -0.0007 |
| WYMO1 | 0.997487 | -0.1900 | 0.979735 | 0.994916 | -0.1871 | -0.0026 | 0.0029 |
| WYMO4 | 0.996235 | -0.1445 | 0.982964 | 0.992201 | -0.1419 | -0.0040 | 0.0026 |
| YGAR4Q | 1.015023 | -0.0885 | 1.013768 | 1.024882 | -0.0879 | 0.0099 | 0.0006 |
| YWER4Q | 1.014763 | -0.0862 | 0.994742 | 1.012376 | -0.0858 | -0.0024 | 0.0004 |

Appendix F

# Global Positioning System

## F.1 Background

The Global Positioning System is a constellation of satellites launched by the United States Military costing approximately US$12 billion. Technically known as the *Navstar Global Positioning System* the main purpose envisaged was to allow a GPS receiver to calculate its exact geographic location. The military uses for this information are clear - the exact location on the battlefield would be immediately known, knowledge of the exact location of a missile could be used to remotely direct it, and with most of the US nuclear arsenal on board submarines exact co-ordinates at sea were useful. Fortunately as technology so often developed for military or *defence* purposes matures, it is often put to more peaceful applications.

### F.1.1 Tolerances

So it has been with peaceful application of the Global Positioning System. GPS operates in two levels of accuracy; civilian (Coarse Acquisition (CA) Pseudo Random Code (PRC)) and military (Precise (P) PRC). They are carried on two radio frequencies level 1 (termed L1, 1575MHz), and level 2 (L2, 1227.6MHz) respectively. The system was designed so that only military personnel with special receivers pre-programmed with the required almanac could obtain the higher resolution information carried on L2. Also this may be encrypted, the

P-code in this instance is then termed Y-code. The L1 and L2 signals consist of a pseudo-random code sequence, which alters subtly each time it transmitted. Timing errors are deliberately added to the sequence to control the accuracy achievable.

The United States Department of Defence monitors the GPS satellites to reach acceptable precision by using radar monitoring stations to measure each satellite's altitude, position, and velocity. Although the satellites are higher than the earth's atmosphere and thus free from its effects, their orbits are disrupted by gravitational pull from the moon and the sun. Solar radiation also exerts a force on the satellites, thus causing errors.

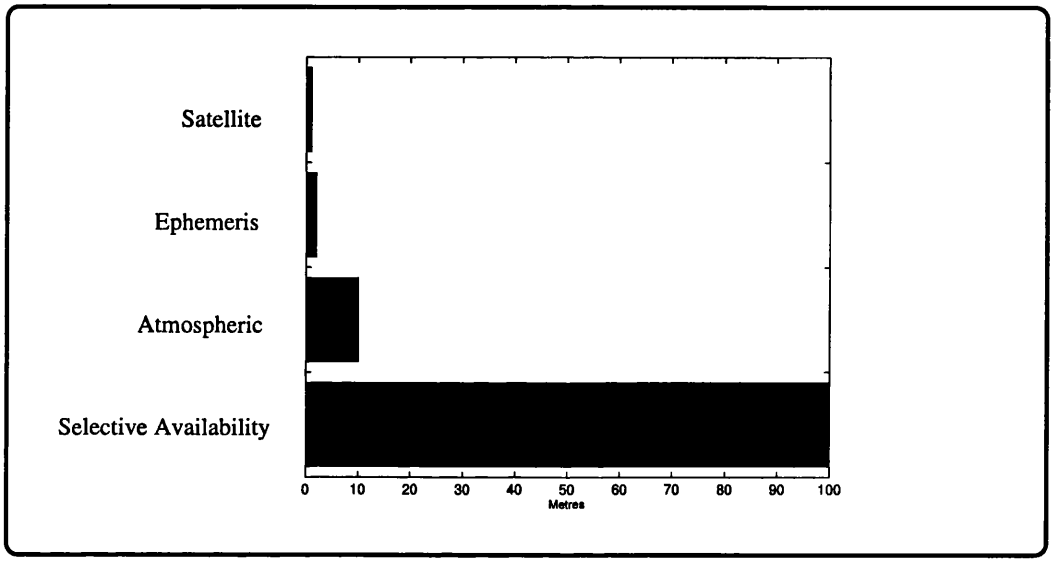


Figure F.1: System-wide GPS sources of error

It was soon realised by the academic community that if the exact geographical location is known, it is possible to back-work the GPS equations and calculate the artificially injected timing errors. Initially these were then transmitted by other means to provide a GPS error correction facility. In the UK this is available to subscribers via a commercial radio station, which has a network of 20 GPS reference stations in the UK. The location of each site was determined using a Trimble 4000 SSe/SSi GPS device giving an accuracy of +/- 2 centimetres. Subscribers to the radio service can expect an accuracy of 1 metre

anywhere within the British Isles. A power system intrinsically has communications channels available. The correction signals could easily be calculated by the transmission utility, used for internal applications, but also sold to other commercial users.

Economically it is possible to obtain a timing accuracy of 1micro second. On a 50Hz system this gives an accuracy of:

$$1/50Hz = 20ms \tag{F.1}$$

$$20ms/1\mu s = 20,000 \; samples \; per \; cycle \tag{F.2}$$

$$1/20,000 = 0.018 \; degrees \tag{F.3}$$

Figure F.2 shows the peak of a sine curve, zoomed in many times to view the peak of the waveform. The solid line is a plot of $\sin(x)$, the dashed line is the sin curve lagging by one resolution, and the dotted line is the sin curve lagging by 10 resolutions. This shows the high accuracy available.

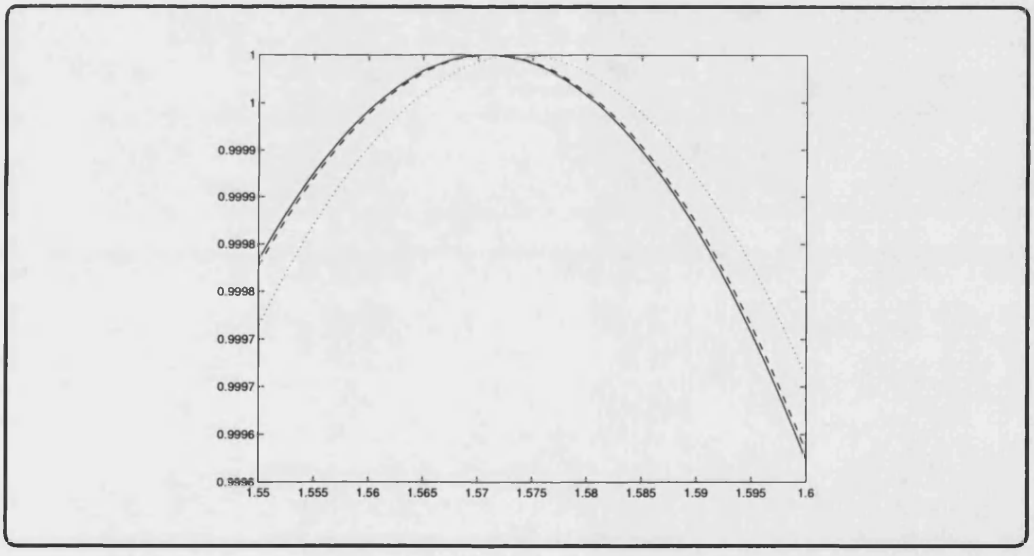


Figure F.2: Sine curve peak showing GPS resolution

## F.1.2 Implementation in Power Systems

The system could be implemented in the manner postulated in the Suggestions for Further Work Chapter. Accurate GPS devices could be used to find the

geographic location of each substation. With this information less expensive GPS equipment could be installed at each substation to calculate UTC time continuously in order to time-synchronise or time-stamp measurements.

## F.2 A Planning Tool to Aid Initial Placement of GPS Facilities

The SCADA emulator and Dynamic On-Line State Estimator could be set up to evaluate the optimal locations for initial installation of GPS facilities.

## F.3 Modes of DOLSE operation with GPS

It is important that DOLSE is able to operate with or without input from GPS enabled RTUs. It should not be presumed that the Navstar GPS facility would be available say during periods of military alert in the United States of America. For this reason DOLSE should never be modified to ever assume that GPS is always going to be available, it should never become dependant upon it. However if it is available, it does enrich the data set from the power system. Immediately the voltage angle and another measure of the apparent power angle at the busbar become available. Thus the measurement set is enlarged and the observability of the system increased in order to obtain a more accurate solution in any circumstance.

Appendix G

# Published Work

This appendix contains reproductions of the author's papers published during the course of the research work.

- Dynamic On-Line State Estimation.
  A.C. Bennett, J.E. Hodgson, R.W. Dunn and M.E. Bradley. *Proceedings of the 31st Universities Power Engineering Conference,* Vol 1, pp 338-341, September 1996.

- State Estimation: A Novel Approach.
  A.C. Bennett, R.W. Dunn and M.E. Bradley. *Proceedings of the International Power Engineering Conference,* Vol 1, pp 398-403, May 1999.

# Dynamic On Line State Estimation

A.C. Bennett, J.E.Hodgson, R.W.Dunn, M.E.Bradley *

Power and Energy Systems Group, School of Electronic and Electrical Engineering, University of Bath, UK

## Abstract

The ability of an EMS to find a consistent set of states that describes the current condition of the power system from a static set of SCADA data is crucial to its entire function. The state estimation task is the basic building block upon which all other EMS functions are based.

This paper describes the telemetry aspects of the SCADA system, briefly outlines present techniques for state estimation, and investigates a new technique termed Dynamic On Line State Estimation.

keywords: power system state estimation, power system real time modelling, power system monitoring

## 1 INTRODUCTION

The increasing complexity of interconnected power systems means that management of a network in an economic and stable manner, has become more and more important. This is achieved through the application of an *energy management system* (EMS). An EMS depends on accurate status data being quickly available from a power system. In practice, this data may be inconsistent or incomplete. Causes include analogue and digital metering errors, transients, communication failures, and data time skew.

Traditionally, it has been necessary to process a whole static set of telemetered data to find a consistent set of states that best describes the current condition of the power system. This process is called state estimation, and is used as the basic input for further EMS functions.

This paper presents a new approach for the conversion of telemetered power system data from the transducers on a transmission network, into a reliable, coherent set of values that more accurately portray the state of the power system. This technique is known as *dynamic state estimation* (DSE), and involves the passing of system data to a dynamic time domain simulation of the power system in order to update a real time model of the actual system. This model then allows the rapid computation of an approximation to the real system state, without the need for a complete update of the entire metered system data set.

The method presented attempts to provide an estimation which is more consistent with the actual system state than is achieved by current techniques, particularly following fault conditions and topology changes. The proposed solution also achieves the required results with significantly less computational effort.

## 2 SCADA SYSTEM

### 2.1 The Need for Information and Control

A large integrated power system is generally co-ordinated from a central location, namely a control centre. In the case of the National Grid Company (NGC) this function is performed by four Area Control Centres (ACCs) and the National Grid Control Centre (NGCC). The function is presently being rationalised to form one central control centre at NGCC. The control centres need the ability to receive information from remote parts of the network, and the ability to effect remote changes. In order to do this there is a need for a system which allows the flow of all the relevant information and control signals to the appropriate locations. Facilities required by a control centre include the functions of monitoring and control. Typically, circuit breakers, isolators, busbar voltages, current and power flows, transformer tap positions, FACTS devices, and substation alarms must all be monitored and controlled.

*The author is with the Technology and Science Division, National Grid Company plc., UK. The authors may be contacted by e-mail via andrew@ee.bath.ac.uk

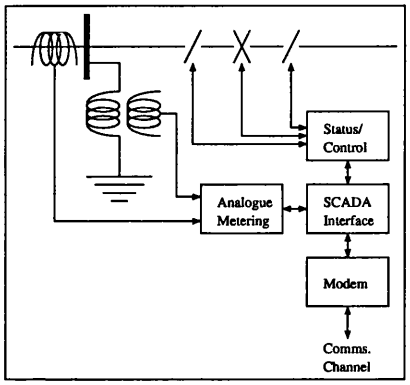


Figure 1: A diagrammatic representation of a Remote Terminal Unit

In NGC the above facilities are provided by a *supervisory control and data acquisition* (SCADA) system implemented using a communications network, a diagrammatic representation of which is shown in figure 1. This network contains channels of different forms, such as telephone lines, HV transmission line carrier waves, optical fibre, radio and microwave links. It is used for telecommand/telecontrol and for telemetry. Data travels from both unstaffed and staffed substations to *remote terminal units* (RTUs), and is passed from there to the ACCs and then to NGCC. As state estimation involves processing power system data into a coherent and complete form, the remainder of section 2 will focus on the telemetry aspect of SCADA operation, i.e. obtaining information from the power system. In particular, the various errors inherent in the telemetered data will be be discussed.

### 2.2 Transducer Errors

Measurement of system variables is made by various power system transducers. Voltage and current transformers provide basic input to metering systems, known as *analogues*. Devices which register the status of plant such as switchgear are termed *digitals*.

It should be noted that some of the metering equipment on the NGC system was installed during construction in the 1960s. This metering is generally not as accurate as say that of the United States systems where most of the metering equipment was installed in the 1970s and the quality of metering had increased substantially by that time. With the advent of NGC's IONA project to install more accurate metering, and to calibrate existing metering the situation is becoming somewhat better.

Electrical power enters the network at generator bus bars, and exits the network at locations called *grid supply points* (GSPs). Voltage levels and power flows at the injection buses and GSPs are measured by 'tariff' metering, the specified accuracy of which is maintained up to a power factor of about 0.86. Meters which measure the power flows on the transmission circuits tend to be less accurate as they are not calibrated as often.

The status of circuit breakers and isolators on the power system are also monitored. This enables the correct topology of the network to be established. This is safety critical information - peoples lives may

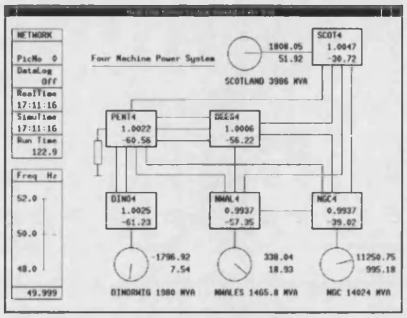


Figure 2: A diagrammatic representation of the Network

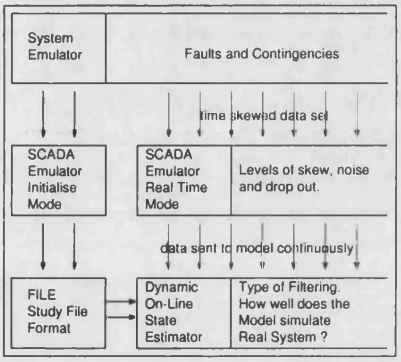


Figure 3: A diagrammatic representation of the Software Implementation

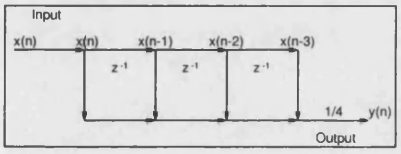


Figure 4: A Four Stage Moving Average Filter

be in danger if this information is incorrect as permits to work could be issued inappropriately. For these reasons it is ensured that topological data is rarely incorrect.

### 2.3 Digitisation and Communication Errors

The NGC SCADA communication network is digital. Analogues are converted to digital signals by analogue to digital (A/D) converters. Switch positions are inherently digital already. Readings may be inaccurate and noisy, with additional errors introduced by the quantisation in the A/D process.

Older power flow metering, such as that found monitoring supergrid circuit flows has a resolution of seven data bits. A full scale deflection (FSD) of 2000 MW gives a resolution of 16 MW. Injection points and GSPs have a resolution of 10 bits.

Voltage measurements are mainly 7 bit at present, with A/D converters being upgraded to provide a resolution of 10 bits for *wound* voltage transformers. These have a range of 340-440kV and it is usual to index the values to this range rather than sending absolute values on the communication path to the control centre. This gives a quanta resolution of 0.8kV for 7 bit, and 0.1 kV for 10 bit A/D systems.

Measurement inaccuracy is not a significant problem due to the comparatively low resolution, although it is most pronounced if the values measured are directly on the break point between quanta.

Signals on the communication channel may also be subjected to noise and interference. The noise may be white, i.e. the amplitude of the interference being equal over the frequency spectrum, or more usually on a power system, the interference may be of the burst noise type - due to system switching transients, for example. Generally, however, due to coding and error detection built into the digital signal processing, corruption is detectable at the receiving end of the communications channel. Values will be classified as correct, or wrong - whereby a NULL value will be put into the set of system data. Occasionally, corruption can occur to such an extent that, by chance, error checking can be defeated. Such corruption is rare, but provision needs to be made for its occurrence.

### 2.4 Operation of SCADA

The final attributes of the NGC SCADA system which need to be understood are the time skewing of data, and the marshalling of analogue and digital information.

Information is sent from transducers, via A/D converters along communication channels to the control centres. All the information is not measured at the same instant in time, nor does it arrive at the control centre at the same time. The process of information gathering is cyclic, with a 15 second period over which a complete set of system data is received at the control centre.

Marshalling of the data may be thought of as the priority given to the data on its way from a meter to the control centre. Measurements are marshalled to the RTU, where they are sent via a communications link to an area SCADA database. The national EMS computer reads all four area data bases every ten seconds. In the marshalling process digitals are counted as priority and the position of switches is sent immediately to the SCADA database.

### 2.5 Summary

It may be seen from the above discussion that there are three main forms of error on the SCADA system: metering, communications and time skew. Each has different causes and affects the data received at the control centre in different ways. There may even be an information blackout from an RTU at any time, lasting up to ninety minutes.

For DSE to be effective, algorithms must be formulated to negotiate the sort of errors described. A SCADA emulation is used for the work in this paper to test the DSE developed. This emulation is designed to produce the errors described in this section.

## 3 CONVENTIONAL STATE ESTIMATION

### 3.1 Objectives of State Estimation

The information that is received at NGCC needs to be processed into a coherent power system state. Errors that may have been introduced to SCADA data cannot be quantified or corrected for on an individual basis at present. However, on a global basis, by looking at all of the data together and assuming that it is generally 'good', a more accurate picture of system conditions may be formed.

State estimation is the process by which telemetered data on bus-

| | System Voltages | | | | | |
|---|---|---|---|---|---|---|
| BusBar | DINO4 | DEES4 | NGC4 | NWAL4 | SCOT4 | PENT4 |
| System Emulator | 1.002 | 1.000 | 0.994 | 0.994 | 1.005 | 1.002 |
| SCADA Emulator | 0.995 | (null) | 1.006 | 0.982 | 1.010 | 0.990 |
| DOLSE Output | 1.005 | 0.999 | 1.006 | 0.982 | 1.011 | 0.998 |

Table 1: A Table showing the System Voltages as given by the Emulators and by DOLSE

| | Generator Real Power Output | | | |
|---|---|---|---|---|
| BusBar | DINORWIG | NGC | NWALES | SCOTLAND |
| System Emulator | -1797 | 11250 | 338 | 1807 |
| SCADA Emulator | -1818 | 11230 | 334 | 1785 |
| DOLSE Output | -1814 | 11266 | 338 | 1795 |

Table 2: A Table showing the values of Generator Real Power Output as given by the Emulators and by DOLSE

bar voltage magnitudes, and details of real and reactive power flows within, to, and from the Grid system are assembled into an estimate of the current system state. The algorithms must be able to recognise items of data that are incorrect due to meter or communication failure or due to the existence of transients on the system. They must also be able to recognise whether there is enough metered information available to be able to formulate an estimation of the system states.

Conventional state estimation operates in a 'batch processing' mode; a set of power system measurements are collected and are then processed in a single pass to find a best-fit estimate of actual power system conditions. This slows down the state estimation process for the following reason; when an event has occurred, such as a line trip, new analogue data must be received from all outstations before estimation can commence. The state estimator must then start 'from scratch'.

Information from the RTUs at sub-stations needs to be processed quickly, and correctly. Presently NGC uses their own EMS state estimator which is periodically run with a 'snap shot' of the system obtained via SCADA. The problem with this technique is the comparatively large lag time from system changes occurring, until details of these changes reach the control engineers. These engineers effectively form the closed part of the power system control loop. It is essential that the aforementioned lag time is kept to an absolute minimum so that control engineers can respond rapidly to system state changes.

### 3.2 Static State Estimation

The classical approach for Static State Estimation (SSE) is the *normal equations* approach [1]. In this method different types of measurements are differentiated by the use of different weighting factors in the solution formulation.

Methods proposed to improve this method in terms of both numerical robustness and computational speed include the 'orthogonal transformation' method [2], the 'hybrid' method [3], and Hachtel's 'augmented matrix method' [4].

### 3.3 Cycle-time State Estimation

Rather than static state estimation, elsewhere research is going on to develop what is known as *cycle-time* state estimation. With this method the previously estimated solution is re-used to help to form the present solution. Ultimately the estimate could be up-dated each time a new analogue or digital dataset is received at the control centre. This will increase accuracy and decrease the lag time of solution when the system is in a steady state, but when there are significant system changes then this method is unlikely to be able to respond quickly enough and the estimator will once again have to wait for a complete data update from the whole system and then start from scratch.

## 4 DYNAMIC STATE ESTIMATION

The problem of the lag in the cycle time can be approached in two ways. The first method is to maintain the same processing structure of static state estimation, but reduce the time taken by using faster algorithms. The second method, and that which is presented in this paper, is to utilise a dynamic model of the system to perform state estimation.

A real time dynamic model is linked to and 'locked' in synchronism with the actual power system being modelled. Analogues and digitals are passed to the model as soon as they are received at the control centre. If, for example, a switch opens, the real time model will respond in the same way as the real system in reaching a new state. Incoming system measurements can then be compared against the DSE's estimate of where the system 'should' be.

The key concept of DSE is the conversion of measured values from the system into suitable quantities for the dynamic model, i.e. quantities which are largely invariant under fault conditions. When there is a change in the system topology, the line flows in almost every part of the interconnected network change and a conventional state estimator must wait for a whole set of system variables before it can begin it's estimate of the current system state. However, DSE relies mainly on the tariff metering at GSPs and at generator buses as these are largely unchanged when a major circuit trips. The values of the line flows are calculated by the dynamic model.

Real and reactive flows into a GSP are converted to an estimate of the real and reactive loads at that point. This ensures that the model is relatively insensitive to LV busbar topology errors caused by 'hand dressing' errors. Voltage measurements at the GSP are used to compute tap positions. At points of injection, power flows give an estimate of the real power output of the generator with reactive flows and voltages used to estimate tap positions of the generator transformer. This data is then fed to the PowSim model and line flows and system voltages are calculated. This provides a reference to error check the line flow and system voltage readings actually received via SCADA. If deemed correct these may then be incorporated into the model also.

## 5 DYNAMIC ON LINE STATE ESTIMATOR

The dynamic on line state estimator (DOLSE) described in this paper realises the method described above in section 4. A diagrammatic representation of the software implementation of DOLSE is shown in figure 3.

| | Significant Line Flows | | | | | |
|---|---|---|---|---|---|---|
| BusBar | DEES4-PENT4 | DINO4-PENT4 | DEES4-NGC4 | PENT4-NGC4 | NGC4-NWAL4 | NGC4-SCOT4 |
| System Emulator | 598 | -960 | -4346 | -189 | 37 | -312 |
| SCADA Emulator | 609 | -972 | -4266 | -188 | 35 | -296 |
| DOLSE Output | 588 | -972 | -4410 | -184 | 38 | -313 |

Table 3: A Table showing Significant Line Flows as given by the Emulators and by DOLSE

### 5.1 System and SCADA emulator

A real-time transient stability simulator previously developed at the University of Bath known as *PowSim* [5] is used to model the real system. This allows a great deal of flexibility when testing state estimator algorithms as system conditions may be changed easily and interactively. For example, generator settings and plant status may be altered while the simulator is running. This copy of PowSim will be known as the *system emulator* from now on.

The output of system emulator is then fed to a second program known as the *SCADA emulator*. This attempts to model all the characteristics of the output of the actual SCADA system. Data values may be subjected to noise, the levels of which can be varied so as to correctly represent errors on the signals due to the type of metering. Sets of data from an RTU (mainly analogues), or individual switch positions (digitals) may be lost or 'dropped out' at a rate that would be experienced on the real system due to communications errors or failures. The data may also be time skewed so as to properly represent the effects of the SCADA network on the timing of the arrival of the data at the PSM computer.

When the state estimator is finally used on the real system, both the system emulator and SCADA emulator would be replaced by the output of the actual SCADA system.

### 5.2 State Estimator

DOLSE is implemented using a modified version of PowSim. This takes input from either the SCADA emulator or the real SCADA system. The various items of SCADA data are processed so that GSP data and 'reliable' digitals are extracted as the primary data inputs. Basic analogue data validation is performed using a four stage moving average filter as shown in figure 4. This involves storing the previous four system data snap-shots.

As soon as new digitals are received, they may be passed to DOLSE. PowSim then follows the same transient response as the real system in reaching a new state. Values of loads and line flows are automatically calculated by the simulator's solution algorithm. Comparison with the real system then enables a second level of data validation to be performed. Any disparity may enable faulty metering and communications to be identified.

When DOLSE is first started, it must be given an entire set of SCADA data at once. This is achieved using an IEEE standard format input file built from SCADA data. When using the SCADA emulator, the initialisation data set is subject to the same form of corruption as the continuous data stream.

## 6 RESULTS

The SCADA information stream has been implemented with error levels as close to the real system as possible, based on data provided by NGC.

The use of the state estimator is illustrated in this section using a four machine, six busbar reduction of the UK Supergrid system shown in figure 2. Busbars are represented by boxes enclosing voltage magnitudes and angles, while machine groups are represented by a load angle vector inside a circle. Real and reactive power generation are shown alongside.

Table 1 shows the values of the system voltages at various stages of the flow of data from system emulator to state estimator. Table 2 gives the active power output by the four generating sets connected to the system, and table 3 shows a selection of the most significant line flows of the system. Note that the 'null' field in the SCADA busbar voltage data indicates that this item of data has been dropped out.

The tables show that the dynamic state estimator follows a solution closer to the real system data than data from the SCADA emulator. Both the mean system voltage error and real power output error have been reduced by about 40%. The corresponding line flows calculated by the state estimator are also shown to be significantly more accurate than the output of the SCADA emulator.

Most importantly, the state estimator data set is consistent and closely related to the real system. This makes it output suitable for other EMS functions, such as dynamic security assessment and dispatch.

## 7 CONCLUSIONS

This paper has compiled a comprehensive review of the NGC SCADA system with a view to defining the requirements of a dynamic on line state estimator. Sources of error and uncertainty been identified, the operation of the SCADA system has been analysed, and the effects of errors have been discussed.

DSE is presented in this paper as a means of providing rapid and accurate state estimation which is crucial to an efficient EMS. A basic form of DSE has been implemented using a real time transient power system simulator and straight forward filtering techniques. Results demonstrate the feasibility of the method outlined and further work is aimed at extending these so that DOLSE may be used on line in the future.

## References

[1] F.C. Schweppe and E.J. Handschin. Static State Estimation in Electric Power Systems. *Proceedings of the IEEE*, 62(7):972–982, July 1974.

[2] J.W. Gu, K.A. Clements, G.R. Krumpholz, and P.W. Davis. The solution of Ill-Conditioned Power System State Estimation Problems via the Method of Peters and Wilkinson. In *PICA Conference Proceedings*, pages 239–246, May 1983.

[3] A. Monticelli, C.A.F. Murari, and F.F. Wu. A Hybrid State Estimator: Solving Normal Equations by Orthogonal Transformations. In *IEEE Transactions on Power Apparatus and Systems*, volume 105, pages 3460–3468, December 1985.

[4] K. Bell. *Artificial Intelligence and Uncertainty in Power System Operation*. PhD thesis, School of Electronic and Electrical Engineering, University of Bath, 1995.

[5] K.W. Chan, A.R. Edwards, R.W. Dunn, and A.R. Daniels. Real Time Electro-mechanical Transient Simulator for On-Line Applications. *International Conference on Digital Power System Simulators*, page 259, April 1995.

# STATE ESTIMATION: A NOVEL APPROACH

**A.C. Bennett, R.W. Dunn***
University of Bath
UK

**M.E. Bradley**†
National Grid Company
UK

## Abstract

Information from an Electrical Power System is necessary for direct use by control engineers and in the processing performed by the *Real Time Network Analysis* (RTNA) software installed on the *Energy Management System* (EMS). Conventional State Estimators are used to improve the reliability of the data, but generally provide only enough information to reconstruct a load-flow solution of the network.

If dynamic stability is to be investigated, a dynamic system model is built at a later stage within the EMS, and then a *Dynamic Security Assessor* (DSA) can be used. Using *Dynamic On Line State Estimation* (DOLSE) developed in this paper, the dynamics of the power system can be more accurately followed. Clean data is available continuously to the RTNA tools.

## Keywords

State Estimation, Time Domain Simulation, Real Time Network Analysis, On-line Dynamic Security Assessment

## 1 INTRODUCTION

The state of a system represents the minimum amount of information about the system at any instant in time that is necessary so that its future behaviour can be determined without reference to the input prior to that time.

### 1.1 Static State Estimation

The states of the power system may be considered to be a vector of complex voltages - ie voltage magnitude and angle at every bus-bar on the power system:

$$x = [V_1, ...V_b, \theta_1, ..., \theta_{b-1}] \quad (1)$$

where $\theta_b$ is the voltage angle of reference.

In equation (1) above the state vector $x$ has been defined. The measurement of $x$ may be considered to be a non-linear function $h(x)$. When the measurement error $\omega$ is taken into account, the vector of measured quantities $z$ is:

$$z = h(x) + \omega \quad (2)$$

Now if the residual vector $r$ is minimised, the best estimate of the state vector $x$ is obtained, where:

$$r = z - h(x) \quad (3)$$

*psmac@ee.bath.ac.uk
†martin.bradley@ngc.co.uk

*Static State Estimation* (SSE) was first applied to electrical power systems by Schweppe [1, 2, 3]. There are a number of methods to minimise $r$, the first tried by Schweppe was the *Weighted Least Squares* criteria. If $W$ is a diagonal matrix of weightings and the estimate of the state vector $x$ is denoted as $\hat{x}$, with the cost function being $J(x)$, then:

$$J(x) = \frac{1}{2}[z - h(x)]^T W^{-1}[z - h(x)] \quad (4)$$

In order to achieve this minimisation, $J(x)$ must be differentiated with respect to $x$, and this be set equal to 0:

$$\left.\frac{\partial J(x)}{\partial x}\right|_{x=\hat{x}} = -H(\hat{x})^T W^{-1}[z - h(\hat{x})] = 0 \quad (5)$$

where $H(\hat{x})$ is the measurement Jacobian matrix such that:

$$H(\hat{x}) = \left.\frac{\partial h(x)}{\partial x}\right|_{x=\hat{x}} \quad (6)$$

Since the normal output is non-linear, to find a solution, iterative methods must be employed based on the approximation of:

$$h(\hat{x}_{k+1}) = h(\hat{x}_k) + H(\hat{x}_k)\Delta\hat{x} \quad (7)$$

Approximating further, if $H(\hat{x}_{k+1})$ is assumed to be $H(\hat{x}_k)$, equation (8) is obtained:

$$H(\hat{x}_k)^T W^{-1} H(\hat{x}_k)\Delta\hat{x} = H(\hat{x}_k)^T W^{-1} H(\hat{x}_k)[z - h(\hat{x}_k)] \quad (8)$$

$$\hat{x}_{k+1} = \hat{x}_k + \Delta\hat{x} \quad (9)$$

The weighting matrix $W$ has often been composed with the diagonal elements $\sigma_{ii}$ chosen as measurement error variances. On the electric power system, however, some buses have exactly zero injections as they are neither load nor generation buses. These are perfect measurements, but may only be treated as very accurate measurements. Even a low weight in $W^{-1}$ leads to ill-conditioning and non-convergence of the SSE in certain conditions.

### 1.2 Dynamic State Estimation

Debs proposed a *dynamic state estimator* [4] in 1970. This uses the present state to predict the future state of the system. This may be used to increase the redundancy of information, and hence improve the solution.

Both Nishiya [5] and Sakr [6] provide methods for Dynamic State Estimation (DSE), with the detection and identification of anomalies. Sakr also proposed a method for correction of these anomalies.

Leite da Silva [7] compared dynamic and *tracking estimators*, and proposed a new form of DSE based on the advantages of these two types of estimator.

A common technique used in DSE is the *kalman filter*. This is a recursive procedure for computing the optimal estimate of the state vector at time $t$, based on the information available at time $t$. The filter allows the estimate of the state vector to be continually updated as new observations become available. See Harvey [8].

Mandal [9] incorporated the non-linearities of the measurement function into a DSE. As well as multiplying the present state vector by a dynamic model parameter matrix, Mandal also added a matrix which accounts for the known control actions on the system. This is termed the *Extended Kalman Filter* (EKF) approach.

## 2 TIME DOMAIN SIMULATION

Power systems must withstand credible disturbances. To ensure that they are capable of doing so, stability simulations are essential. Simulators in the late 1920s, called A.C. network analysers, were analogue models of the electrical power system. In the 1950s digital computers began to be applied to this simulation task. Since that time computers have become faster and their use has increased as they have become cheaper.

Due to the large amount of computing power necessary, power system models of varying levels of detail were developed. In general for transient stability studies, system dynamics must be modelled to include effects at the 10ms time frame. System states are required to be evaluated at intervals of 10ms to 100ms over a time period of 30 seconds.

With the advent of fast time domain electromechanical transient simulators, it is now possible to accurately model the power system at real time speeds or faster.

The simulator used in this work was originally developed by Dale [10], Berry [11], and Chan [12].

## 3 DYNAMIC ON LINE STATE ESTIMATION

The Dynamic On Line State Estimation method uses a time domain power system simulator as the main core of the DOLSE algorithm to process incoming Supervisory Control And Data Acquisition (SCADA) information [13]. Rather than using a state space model of the electrical power network to aid in state estimation, the method uses a real time, time domain transient stability simulator as described in section 2. This is a more accurate model of the power system than the traditional models used, say, for DSE which only utilise state trajectories, rather than the detailed models of the specific power system apparatus and plant. The simulator used is the University of Bath's *PowSim* [14]. Figure 1 shows the differences in data flow between SSE, DSE and DOLSE.

DOLSE processing removes gross measurement errors, enhances the reliability and improves the accuracy of the data. With the ability to apply a topology change directly to the time domain model, a smooth transition in data processing during network switching events is possible. This leads to quicker and better identification of system topology immediately after a transient. Smaller errors in the data are minimised by comparing the incoming data with the values in the time domain model. This information is used to update both the real-time model's parameters and states, so that it provides a good estimate of the actual behaviour of the power system.

The errors between the incoming power system data and the states of the time domain model are minimised. As the metering on generator outputs and at grid supply points is calibrated to satisfy the requirements of accuracy for billing purposes, these bus injections are given higher confidence values. Unlike SSE, with DOLSE the zero injection buses may be treated as being perfect measurements without causing ill conditioning. The states in the simulator may be held at the appropriate value without causing non-convergence.

Although known control actions are applied to a load-flow solution, DSE methods provide no indication of the expected magnitude or duration of oscillations in the measured system variables. DOLSE is able to spawn a simulation on another available workstation in order to model the transient phenomena associated with the switching action. The information derived from this can be used to screen incoming system data. Data from areas of the system which are unaffected by the topology change can continue to be injected into the time domain model, whereas data from parts of the system affected by the topology change can be used once the transient has died away. The spawned simulation estimates the duration of transient conditions on a per metered variable basis, ensuring that only quasi-steady state data will be passed to the time domain model from the SCADA data once the transient has finished.

With DSE methods as outlined in subsection 1.2, data sets could be used for processing which were from a period of system oscillation. This would corrupt the solution, causing problems in both the present and the next DSE iteration. DOLSE will not allow this corruption to occur.

Any gross data errors are screened and rejected using a novel technique involving tolerance ranges calculated by monitoring the rate of change of kinetic energy in the power system. This is achieved by monitoring the actual power system frequency and its rate of change to detect

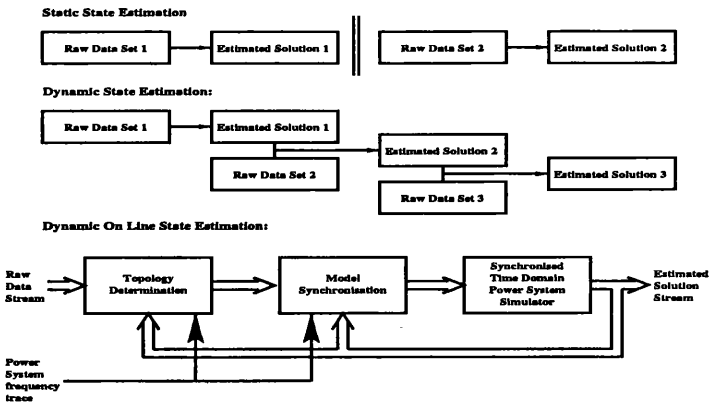


Figure 1: State Estimation Methodology Explained

an imbalance between electrical supply and demand (see section 5).

The metering from the grid system generally provides enough data so that under normal circumstances the network is completely observable. Presently Automatic Voltage Regulator (AVR) and power system stabiliser (PSS) parameters on the NGC system are not tuned in an on line mode. Potential errors in the modelling of devices with fast time constants can be flagged, to be specifically studied by the software over a longer period. Data logs of significantly different responses can be stored for analysis off-line. Network parameters can be estimated in on-line time scales.

## 4 TOPOLOGY DETERMINATION

Analogue data received from the NGC power system is not time stamped at source, and is subject to the vagaries of the SCADA marshalling process. If the system has been subject to a transient there is no way of ascertaining which point on the transient oscillation a particular analogue data value is from.

Digital data, such as switch state changes, is marshalled ahead of analogue data values over SCADA channels. Therefore if a system event occurs and a circuit breaker is tripped, the control centre should receive the information of the switch before any other corroborative data.

Precautions have been taken to ensure that the DOLSE time domain model is not corrupted with bad data, as described at the end of sub-section 1.2. These still need to be refined and optimised for use in a time domain model.

When notified of a digital switch change the simulator outputs a study file to disk. This is a fail safe mechanism, so that should the switch change prove to be incorrect, DOLSE may recover itself. The states of the simulator can be set to the data held in this buffer immediately prior to the time-stamp on the switch status data. It may then be fast forwarded to the instant of the time stamp, and the fault applied. It can then be run in fast forward mode again to catch up with the present system time. DOLSE now presents an accurate model of the power system.

Within the period indicated by the spawned simulator DOLSE is able to check the analogues against its estimate of where the system is. If the incoming analogues match those in DOLSE then it may be assumed that the original topology change information was correct. Winding the simulator back to the end of the transient (determined from the spawned time domain model) and injecting the analogue data from that point to the present time, with the simulator running faster than real time, means that DOLSE will be back in synchronisation with the power system post fault quickly and with all digital switch status and analogue data validated.

## 5 SYSTEM STIFFNESS

The ratio of the change in real power, $\Delta P$, to a given change of frequency, $\Delta f$, of an interconnected power system is termed the system *stiffness*, $K$:

$$K = \frac{\Delta P}{\Delta f} \tag{10}$$

Figure 2 shows the steady state post fault system frequency for loss of loads at all substations in arbitrary areas *I* and *II* of a time domain electro-mechanical model of the NGC System (*PowSim*). The two lines of best-fit show that the stiffness is not uniform for loss of busbar loads of the same magnitude in different areas of the sys-

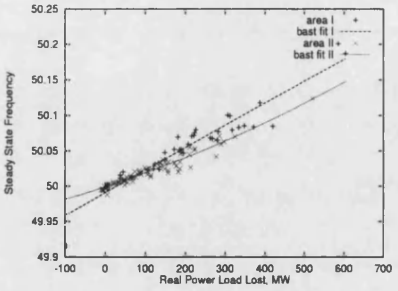


Figure 2: Change in Frequency for a change in Real Power post-Transient

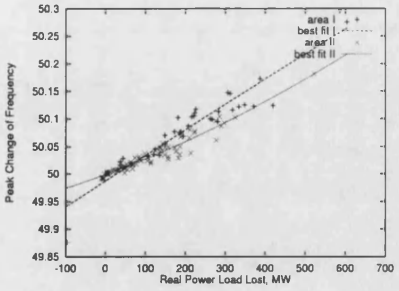


Figure 3: Peak of Change in Frequency for a change in Real Power

tem. To ensure that steady state was achieved the simulations were run for a duration of 30 seconds post-transient before the measurement of frequency was taken.

Figure 3 shows a plot of the peak system frequency against the loss of real power load at bus bars in the same two areas of the power system. This peak in frequency occurs on average 11 seconds after the loss of the load. The similarity of the two plots shows that there is a strong relationship between the system peak frequency and the steady state frequency after 30 seconds.

The gradient of the the lines of best fit in figure 3 may now be termed $K_{transient}$, and may be calculated by the ratio of $\Delta P$ to $\Delta f_{max}$:

$$K_{transient} = \frac{\Delta P}{\Delta f_{max}} \tag{11}$$

If system stiffness is calculated off-line by running power system studies, this may be used on-line with frequency information to estimate the rate of change of real power imbalance. Use of the frequency data in this manner aids the estimator to track the power system.

The calculation of the $K_{transient}$ characteristic off-line may be achieved three times more quickly than the calculation of the original $K$ stiffness characteristic. It should be noted that once an increase in frequency has been detected from the frequency trace, with pre-calculated estimation of $K_{transient}$ it is possible to ascertain the changes in the real load imbalance of the system within approximately 12 seconds (dependent on governor characteristic), rather than having to wait for the system to settle into steady state (minimum of 30 seconds). This makes $K_{transient}$ immediately more useful than $K$.

## 6 MODEL SYNCHRONISATION

Once the model is known to be topologically correct the analogue data of voltage magnitudes, real and reactive injections and line flows must be synchronised in the model to represent the actual power network.

Firstly, consider the real power balance of injections to the system. At the normal power system operating frequency:

$$P_g = P_l + P_n \tag{12}$$

where $P_g$ is the real power generated, $P_l$ is the real power load demand, and $P_n$ is the network/system losses. Any imbalance between the LHS and RHS of equation (12) causes a change in the system frequency. If more power is generated than is demanded system frequency rises, and if more power is demanded than generated, system frequency falls. Representing this relationship as a function of frequency, $F(f)$, we obtain:

$$P_g = P_l + P_n + F(f) \tag{13}$$

By knowing previous recent real power magnitudes at the known previous frequency, information of the change in frequency since that data was calculated gives an indication of the magnitude of $F(f)$. This may be used on-line to indicate the imbalance between $P_g$ and $P_l$ on a system wide basis. Changes in line flows may be used to calculate the imbalance of $P_g$ and $P_l$ on a local basis.

The electrical power generated at generating busbars, and the real power load at a grid supply points are estimated by considering the sum of injections at the bus bar. This value of $P_g$ is then back worked through the machine equations to provide an estimate of the mechanical output torque of the generator $T_{mo}$. Loads at a busbar are set to the appropriate level of real power demand.

Similar analogies may be constructed for the system's reactive power balance. As the reactive power losses ($I^2X$) on an overhead transmission network are typically 10 times greater than the real power losses ($I^2R$), reactive power imbalance is much more of a local phenomenon. This is manifested as bus bar voltages which

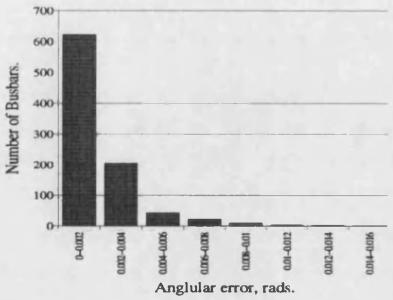


Figure 4: Histogram of DOLSE busbar voltage angle error

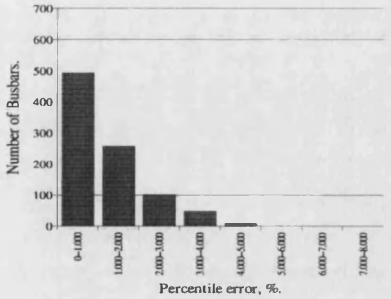


Figure 5: Histogram of DOLSE busbar voltage magnitude error

are not at their nominal value. With a knowledge of the terminal voltage of the generator (bus bar voltage referred through the generator's transformer), the automatic voltage regulator equations may be back worked to give the voltage reference to the AVR.

By decoupling the real and reactive power data processing, errors may be minimised on the appropriate system wide or local area basis. The machine and AVR equations may then be back worked to yield accurate information of the internal states of the machine, thus providing the correct dynamic response should a transient occur.

## 7 RESULTS

A test bench has been constructed to test the Dynamic On Line State Estimator. A power system simulator has been adapted so that it outputs data with the same errors and characteristics as a SCADA data stream. This stream of data is then passed to DOLSE.

The system model used for these simulations, to construct the SCADA data stream and within DOLSE, is a representation of the UK England and Wales National Grid System, owned and maintained by the National Grid Company, UK. It contains 46 machines, approximately 900 busbars, and 1500 lines. Generator models are $6^{th}$ order voltage behind sub-transient reactance, with AVRs and governors being non-linear differential equation models up to $10^{th}$ order.

Within DOLSE, providing enough processing power is available, the time domain model equations may be solved within the simulated time-step. On a Pentium II 300 MHz, the University of Bath's Power System simulator can model the system accurately for every 10ms at 3 times faster than real time. This means that with a processor dedicated to dynamic on-line state estimation in real time, the processor is free for 66% of the time to perform data processing and filtering.

Currently DOLSE has been optimised to minimise the errors of real power flows, generator outputs and loads. Figure 4 shows a histogram of the errors between the SCADA model of the power system and the output of DOLSE. It may be seen that the angular error is mostly less than 0.002 radians.

Further work is in progress to minimise the reactive power and voltage magnitude errors. Figure 5 shows a histogram of the percentile error of the busbar voltage magnitudes.

## 8 ADVANTAGES

Present dynamic state estimation techniques suffer problems when there is a topology change. Using basic linear models there is no way to forecast the effect of a switching operation. A higher order model of the transient stability simulator is designed to accurately model these events. So if the event sequence is applied to the power system model, the resultant state of the power system may be easily forecast. This can then be used to filter the incoming data for errors.

EMS software generally operates in a batch mode, and may be set to start analysis using a periodic trigger or an event trigger. With DOLSE, data is continuously available, hence conventional RTNA software may be started to perform the analysis, post transient, virtually immediately - as soon as the network event has been effected in the simulator and the system has settled down to steady state. The results of the analysis will not be flagged as valid unless DOLSE is able to validate that the topology has actually changed on the power system as it had been informed. If subsequently it is found that the topology change as previously notified did not actually occur the RTNA analysis can be immediately re-triggered with a correct data set.

The amount of data which is available off the power system is immense. For this reason it is not possible to

archive all of the data. Techniques can be developed within the scope of this project to look at ways of storing system data. This will need to be done so that profiling of loads and of generators can be obtained easily, but also so that the power system model may be more finely tuned. Maximum and mean errors in voltages at bus bars and in other parameters may be stored. More data can be stored about bus bars where the topology is suspect. The complete data set can then be used to ascertain the exact nature of the problem at the end of a 24 hour period.

## 9 CONCLUSION

DOLSE allows power system data processing to move from a batch-processing mode of state estimation and RTNA. There is no longer a need for a synchronised system wide data set. Real time estimation of a wider set of system states allows better tracking of the power system during disturbances.

The ultimate aim of the DOLSE software developed during the course of this research is to speed up the provision of state estimated data to the RTNA tools and the control engineer.

DOLSE would enable this to be achieved without costly investment in the metering and telecommunications channels.

## ACKNOWLEDGEMENTS

The authors gratefully acknowledge the financial and technical contributions of the National Grid Company plc, UK. They also acknowledge the financial support of the Engineering and Physical Sciences Research Council.

## References

[1] F.C. Schweppe and J. Wildes. Power System Static State Estimation Part 1: Exact Model. *IEEE Transactions on Power Apparatus and Systems*, 89(1):120–125, January 1970.

[2] F.C. Schweppe and D.B. Rom. Power System Static State Estimation Part 2: Approximate Model. *IEEE Transactions on Power Apparatus and Systems*, 89(1):125–130, January 1970.

[3] F.C. Schweppe. Power System Static State Estimation Part 3: Implementation. *IEEE Transactions on Power Apparatus and Systems*, 89(1):130–135, January 1970.

[4] A.S. Debs and R.E. Larson. A Dynamic Estimator for tracking the State of a Power System. *IEEE Transactions on Power Apparatus and Systems*, 89(7):1670–1678, September 1970.

[5] K. Nishiya, J. Hasegawa, and T. Koike. Dynamic State Estimation including anaomaly detection and identification for power systems. *IEE Proc. part C: Generation, Transmission and Distribution*, 129(5):192–198, September 1982.

[6] M.M.F. Sakr, A. Bahgat, and A.R. El-Shafei. Dynamic State Estimation in Power Systems with abnormalities detection , identification and correction. In *IEE Control'85 Conference*, 252, pages 245–251, Cambridge, July 1985. IEE.

[7] A.M. Leite da Silva, M.B. Do Coutto Filho, and J.M.C. Cantera. An Efficient Dynamic State Estimation Algorithm including bad data processing. *IEEE Transactions on Power Systems*, 2(4):1050–1058, November 1987.

[8] A.C. Harvey. *Forecasting, structural time series models and the Kalman filter*. Cambridge University Press, Cambridge, 1989.

[9] J.K. Mandal, A.K. Sinha, and L. Roy. Incorporating nonlinearities of measurement function in power system dynamic state estimation. *IEE Proc. Generation, Transmission and Distribution*, 142(3):289–296, May 1995.

[10] L.A. Dale, T. Berry, A.R. Daniels, and R.W. Dunn. Realtime Modelling of multi-machine power systems. *IEE Proc on Generation, Transmission and Distribution*, 140(4):241–248, Jul 1993.

[11] T. Berry, A.R. Daniels, R.W. Dunn, and S. Geeves. Real-Time Power System Dynamics Simulation. *CIGRE, Proc Group 38, paper 201*, September 1990.

[12] K.W. Chan. *A Power System Simulator to Model the Transient Mode of Operation of the (UK) National Super Grid in Real Time*. PhD thesis, Department of Electronic and Electrical Engineering, University of Bath, 1992.

[13] A.C. Bennett, J.E. Hodgson, R.W. Dunn, and M.E. Bradley. Dynamic On Line State Estimation. In *Proceedings of the Universities Power Engineering Conference*, volume 1, pages 338–341, Iraklio Greece, September 1996. Technological Educational Institute.

[14] K.W. Chan, R.W. Dunn, and A.R. Daniels. Efficient Heuristic Partitioning Algorithm for Parallel Processing of Large Power Systems Network Equations. *IEE Proceedings on Generation, Transmission, and Distribution*, 142(6):625–631, November 1995.

# References


[1] F.C. Schweppe and J. Wildes. "Power System Static State Estimation Part 1: Exact Model". *IEEE Transactions on Power Apparatus and Systems*, 89(1), 120–125, January 1970.

[2] F.C. Schweppe and D.B. Rom. "Power System Static State Estimation Part 2: Approximate Model". *IEEE Transactions on Power Apparatus and Systems*, 89(1), 125–130, January 1970.

[3] F.C. Schweppe. "Power System Static State Estimation Part 3: Implementation". *IEEE Transactions on Power Apparatus and Systems*, 89(1), 130–135, January 1970.

[4] R.E. Larson, W.F. Tinney and J. Peschon. "State estimation in electric power systems, pt i: theory and feasibility". *IEEE Transactions on Power Apparatus and Systems*, 89, 345–352, Mar 1970.

[5] R.E. Larson, W.F. Tinney, L.P. Hajdu and D.S. Piercy. "State estimation in electric power systems, pt ii: implementation and applications". *IEEE Transactions on Power Apparatus and Systems*, 89, 353–363, Mar 1970.

[6] M.B. Do Coutto Filho, A.M. Leite da Silva and D.M. Falcao. "Bibliography on Power System State Estimation (1968-1989)". *IEEE Transactions on Power Systems*, 5(3), 950–957, August 1990.

[7] R.E. Larson and L.P. Hajdu. "Potential applications and on-line implementation of power system state estimation". Tech. rep., Wolf Management Services, Palo Alto, California, Jan 1969. Final Report.

[8] F.C. Schweppe. "Power system static state estimation". presented at the Minnesota Power Conference.

[9] S.O. Orero and M.R Irving. "A genetic algorithm for network partitioning in power system state estimation". In *Proceedings of International Conference on Control*, vol. 1, pp. 162–165, London, UK, Sept 1996. UKACC, IEE.

[10] K. Bell. *Artificial Intelligence and Uncertainty in Power System Operation.* Ph.D. thesis, Department of Electronic and Electrical Engineering, University of Bath, 1995.

[11] D.M. Vinod Kumar, S.C. Srivastava, S. Shah and S. Mathur. "Topology processing and static state estimation using artificial neural networks". *IEE Proceedings of Generation, Transmission and Distribution*, 143(1), 99–105, Jan 1996.

[12] B Stott. "Review of load-flow calculation methods". *Proceedings of the IEEE*, 62(7), 916–929, Jul 1974.

[13] H Modir and R.A. Schleuter. "A dynamic state estimator for dynamic security assessment". *IEEE Transactions on Power Apparatus and Systems*, 100(11), 4644–4652, Nov 1981.

[14] M. La Scala, R. Sbrizzai, F. Torelli and P. Scarpellini. "A tracking time domain simulator for real-time transient stability analysis". *IEEE Transactions on Power Systems*, 13(3), 992–998, Aug 1998.

[15] M. Moghavvemi and F.M. Omar. "Technique for contingency monitoring and voltage collapse prediction.". *IEE Proceedings of Generation, Transmission and Distribution*, 145(6), 634–640, Nov 1998.

[16] R.C. Dorf. *Modern Control Systems.* Addison Wesley, 5th edn., 1989.

[17] F.C. Schweppe and E.J. Handschin. "Static State Estimation in Electric Power Systems". *Proceedings of the IEEE*, 62(7), 972–982, July 1974.

[18] L. Holten. "Comparison of Different Methods for State Estimation". *IEEE Transactions on Power Systems*, 3(4), 1798–1806, November 1988.

[19] K.O. Lo, M.M. Salem, R.R. McColl and A.M. Moffatt. "Two-level State Estimation for Large Power System, Part 1: Algorithms". *IEE Proceedings, Generation Transmission and Distribution*, 135(C-4), 299–308, July 1988.

[20] K.O. Lo, M.M. Salem, R.R. McColl and A.M. Moffatt. "Two-level State Estimation for Large Power System, Part 2: Computational Experience". *IEE Proceedings, Generation Transmission and Distribution*, 135(C-4), 309–318, July 1988.

[21] O. Alsaç, N. Vempati, B Stott and A. Monticelli. "Generalised state estimation". *IEEE Transactions on Power Systems*, 13(3), 1069–1075, Aug 1998.

[22] A. Monticelli. *State Estimation in Electric Power Systems (A Generalised Approach)*. Kluwer Academic Publishers, 1999.

[23] A.S. Debs and R.E. Larson. "A Dynamic Estimator for tracking the State of a Power System". *IEEE Transactions on Power Apparatus and Systems*, 89(7), 1670–1678, September 1970.

[24] A.M. Leite da Silva, M.B. Do Coutto Filho and J.M.C. Cantera. "An Efficient Dynamic State Estimation Algorithm including bad data processing". *IEEE Transactions on Power Systems*, 2(4), 1050–1058, November 1987.

[25] K. Nishiya, J. Hasegawa and T. Koike. "Dynamic State Estimation including anaomaly detection and identification for power systems". *IEE Proc. part C: Generation, Transmission and Distribution*, 129(5), 192–198, September 1982.

[26] J.K. Mandal, A.K. Sinha and L. Roy. "Incorporating nonlinearities of measurement function in power system dynamic state estimation". *IEE Proc. Generation, Transmission and Distribution*, 142(3), 289–296, May 1995.

[27] I.W. Slutsker, S. Mokhtari and K.A. Clements. "Real time recursive parameter estimation in energy management systems". *IEEE Transactions on Power Systems*, 11(3), 1393–1399, August 1996.

[28] C.W. Hansen and A.S. Debs. "Power system state estimation using three-phase models". *IEEE Transactions on Power Systems*, 10(2), 818–824, May 1995.

[29] S. Hamilton. "Taking moore's law into the next century". *IEEE Computing Society, Computer*, 32(1), 43–48, Jan 1999.

[30] M.E. Bradley, A.O. Ekwue, F. Li, K.W. Chan, R.W. Dunn and A.R. Daniels. "On-line stability analysis for an operational tripping scheme monitor". In *Fourth International Conference on Power System Control and Management*, no. Conf. Publ. No. 421, pp. 71–75, London, UK, 1996. IEE.

[31] L.A. Dale. *Real-Time Modelling of Multimachine Power System*. Ph.D. thesis, Department of Electronic and Electrical Engineering, University of Bath, 1986.

[32] T. Berry. *Real Time Simulation of Complex Systems Using Parallel Processors*. Ph.D. thesis, Department of Electronic and Electrical Engineering, University of Bath, 1989.

[33] K.W. Chan. *A Power System Simulator to Model the Transient Mode of Operation of the (UK) National Super Grid in Real Time*. Ph.D. thesis, Department of Electronic and Electrical Engineering, University of Bath, 1992.

[34] J Machowski, J.W. Bialek and J.R. Bumby. *Power System Dynamics and Stability*. John Wiley and Sons, 1997.

[35] J.E. Hodgson. *A Comprehensive Method to Estimate Power System Stability Constraint Costs*. Ph.D. thesis, Department of Electronic and Electrical Engineering, University of Bath, 1997.

[36] J. Toal. "Learning to live with power system oscillations". In *Colloquium on Power system dynamic stabilisation*, pp. 7/1–7/8. IEE, Savoy Place, London, Feb 1998.

[37] IEEE Committee Report. "Excitation system models for power system stability studies". *IEEE Transactions on Power Apparatus and Systems*, 100, 494–510, 1981.

[38] IEEE Committee Report. "Dynamic models for steam and hydro turbines in power system studies". *IEEE Transactions on Power Apparatus and Systems*, 92, 1904–1915, 1973.

[39] IEEE Committee Report. "Computer representations of excitation systems". *IEEE Transactions on Power Apparatus and Systems*, 87, 1460–1464, 1968.

[40] N. Singh and H. Glavitsch. "Detection and identification of topological errors in online power system analysis". *IEEE Transactions on Power Systems*, 6(1), 324–331, Feb 1991.

[41] M. Prais and A. Bose. "A topology processor that tracks network modifications". *IEEE Transactions on Power Systems*, 3(3), 992–998, Aug 1998.

[42] J.C.S. Souza, A.M. Leite da Silva and A.P. Alves da Silva. "Online topology determination and bad data suppression in power system operation using artificial neural networks". *IEEE Transactions on Power Systems*, 13(3), 796–803, Aug 1998.

[43] M.R. Irving and M.J.H. Sterling. "Substation data validation". *IEE Proc. part C: Generation, Transmission and Distribution*, (3), 119–122, May 1982.

[44] P.J. Moore and R.D. Carranza. "Power system frequency measurement under dynamic conditions". In *Proceedings of 11th International Conference on Power System Protection*, pp. 47–52, Sep 1998.

[45] D.R. Butenhof. *Programming with POSIX THreads*. Addison Wesley, 1997.

[46] J.D. Martin. *Signals and Processes*. UCL Press Ltd., 1991. ISBN 0-273-03256.

[47] W.H Press, B.P. Flannery, S.A. Teukolsky and W.T. Vetterling. *Numerical Recipes in C: The Art of Scientific Computing*. Cambridge University Press, 1990. ISBN 0-521-35465-X.

[48] S.N. Ironmonger, M.J. Bushnell, R. Patel, M.E. Bradley and B.W. Vaughan. "An object-oriented power system model and graphical information display system for control engineers". In *Fourth International Conference on Power System Control and Management*, no. Conf. Publ. No. 421, pp. 120–124, London, UK, 1996. IEE.

[49] A.R. Edwards. *Detection of Instability in Power Systems using Connectionism*. Ph.D. thesis, Department of Electronic and Electrical Engineering, University of Bath, 1995.

[50] A.G. Phadke. "Synchronised power measurements". *IEEE Computer Applications in Power*, pp. 10–15, Apr 1993.